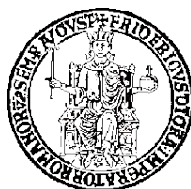


UNIVERSITY OF NAPLES FEDERICO II
School of Polytechnic and Basic Sciences

Department of Structures for Engineering and Architecture



PH.D. PROGRAMME IN MATERIALS AND STRUCTURES
COORDINATOR: PROF. GIUSEPPE MENSITIERI
XXVIII Cycle



ANNA BOZZA
Ph.D. Thesis

**Ecosystems And Engineering:
A Working Synergy Towards City
Resilience To Natural Disasters**

TUTOR PROF. ENG. GAETANO MANFREDI
CO-TUTORS PROF. ENG. ANDREA PROTA
 DR. ENG. DOMENICO ASPRONE

2016

Acknowledgements

Words are powerless to express my gratitude ... actually they are the only means I have available now to do it.

Before all, I would like to particularly thank Domenico Asprone, for his great patience and his precious teachings. Thank you for driving me through this course of research, for encouraging me to persist good ideas, as well as to give up the bad ones, always supporting me with your valuable instructions and help.

Special thanks go to Prof. Andrea Prota and Prof. Gaetano Manfredi that gave me the chance to start this exciting journey. They made this PhD possible giving me the opportunity to learn so many things and, above all, to work in such an outstanding team, as DiSt is!

I would like to thank the people, who valuable contributed to my thesis, helping me to deepen my knowledge in specific fields and also supporting me when I was doubtful and enabling me to open my mind: thank you Vito Latora and Fatemeh Jalayer.

I would like to acknowledge all my colleagues and particularly my present and past office mates, who bear with me every day: Giancarlo Ramaglia, Claudio D'Ambra, Nunzia Iuliano, Iolanda Nuzzo, Vincenzo Giamundo, Loredana Napolano, Angela Cacciapuoti, Houman Hadad, Claudio Balestrieri, Umberto Vitiello. Thank you guys, you have been so precious to me!

I cannot forget my friends, for helping me during this period in the most disparate ways and in the most different places, also during my abroad experiences. Particularly, I want to thank Bruna, Ileana and Federica. Thank you girls!

Last but not least, my amazing family. My little nephew and nieces, Lorenzo, Matteo, Filippo and Flavia, for driving me crazy in my days off too. My sister Lia, and mummy and daddy: thank you for never stop rocking me in your arms. Finally Eugenio, my best friend, always being the one believing in me the most.

INDEX

LIST OF FIGURES	8
LIST OF TABLES	13
INTRODUCTION	16
CHAPTER 1	
OPPORTUNITIES AND CHALLENGES OF RESILIENCE	22
1.1 THE CONCEPT OF RESILIENCE, UNDERSTANDINGS AND PERSPECTIVES	22
1.1.1 Defining resilience.....	24
1.1.2 A novel understanding of resilience: engineering resilience in the sense of the ecosystems theory.....	35
1.1.3 Closing the loop between resilience and sustainability.....	36
1.1.4 Measuring resilience.....	38
1.1.4.1 Approaches to physical resilience assessment.....	39
1.1.4.2 Resilience assessment according to social-economics approaches	54
1.1.4.3 Resilience assessment according to the graph theory.....	62
1.2 FROM SOCIAL ACTORS TO CITIES: THE SCALE OF RESILIENCE	74
1.3 OPPORTUNITIES AND CHALLENGES AROUND RESILIENCE	78
1.3.1 Opportunities	79
1.3.2 Challenges	80
1.3.3 Integration.....	81
1.4 CURRENT FRAMEWORKS AND ACTIONS ON RESILIENCE	81

CHAPTER 2***ECONOMIC RESILIENCE OF URBAN SYSTEMS:******PROPOSAL OF A SEISMIC INSURANCE MODEL FOR******THE ITALIAN BUILDING STOCK 88***

<i>2.1 MERGING ECOSYSTEMS ENGINEERING AND ECONOMICS FOR RESILIENCE</i>	<i>89</i>
<i>2.2 A SEISMIC INSURANCE MODEL AS AN INSTRUMENT FOR RESILIENCE AT THE SUPERURBAN SCALE</i>	<i>91</i>
<i>2.3 SEISMIC LOSS ESTIMATION</i>	<i>95</i>
<i>2.4 SEISMIC RISK ASSESSMENT</i>	<i>98</i>
2.4.1 Seismic hazard.....	98
2.4.2 Seismic fragility	98
2.4.3 Exposed value	101
<i>2.5 LOSS ESTIMATION ACCORDING TO A PBEE APPROACH</i>	<i>102</i>
<i>2.6 A BACK-ANALYSIS ON L'AQUILA 2009 AND MOLISE 2012 EARTHQUAKES</i>	<i>105</i>
<i>2.7 THE INSURANCE MODEL</i>	<i>108</i>
<i>2.8 A REAL APPLICATION: THE ITALIAN RESIDENTIAL BUILDING STOCK.....</i>	<i>112</i>
2.8.1 Discussion on the case study	119

CHAPTER 3***INSURANCE SCENARIOS AGAINST SEISMIC******CATASTROPHES: REMARKS BASED ON HISTORICAL******CATALOGUE..... 121***

<i>3.1 SUPPORTING THE INSURANCE INDUSTRY WITH A PBEE-BASED METHODOLOGY</i>	<i>123</i>
3.1.1 What is needed to implement the methodology	125
3.1.2 Earthquake scenario analysis: accounting for seismic ground shaking correlations.....	129

3.1.3 Expected losses against spatial correlation.....	133
3.2 <i>PROCESSING ANALYSIS' RESULTS</i>	137
3.2.1 Derivation of expected loss relationships through regression analysis	138
3.2.2 Bin processing of the empirical results.....	143
3.3 <i>COMPARISONS AND RESULTS</i>	147
3.4 <i>DISCUSSION ON RESULTS</i>	153
3.5 <i>ALTERNATIVE INSURANCE PRODUCTS ENHANCING RESILIENCE OF LOCAL AUTHORITIES: THE CAT BOND MODEL</i>	
155	

CHAPTER 4

<i>DEVELOPING AN INTEGRATED FRAMEWORK TO QUANTIFY RESILIENCE OF URBAN SYSTEMS AGAINST DISASTERS</i>	159
4.1 <i>RESILIENCE AS A CATALYST TO SUSTAINABLE DEVELOPMENT</i>	160
4.2 <i>DEFINING AND MEASURING HYBRID SOCIAL-PHYSICAL NETWORKS</i>	164
4.3 <i>QUALITY OF LIFE INDICATORS ACCORDING TO A SUSTAINABLE APPROACH</i>	170
4.4 <i>LINKING ENGINEERING METRICS ON NETWORKS AND SUSTAINABILITY INDICATORS</i>	176

CHAPTER 5

<i>SEISMIC CATASTROPHE RESILIENCE AGAINST URBAN SHAPE AND SIZE</i>	185
5.1 <i>AN ENGINEERING FRAMEWORK TO QUANTIFY URBAN RESILIENCE</i>	186
5.1.1 Contemporary city ecosystems modelling.....	190
5.1.2 Scenario simulation: the citizen-citizen and citizen-school case study	194

5.1.3 A novel understanding of complex networks metrics: assessing the urban systemic damage	198
5.1.4 The quantification of urban resilience.....	204
5.1.4.1 Quantification of damage-independent resilience.....	207
5.1.4.2 Quantification of damage-dependent resilience.....	211
5.2 THE HISTORICAL CENTRE OF THE CITY OF NAPLES: THE QUARTIERI SPAGNOLI EARTHQUAKE CASE ANALYSIS.....	212
5.2.1 Modeling Quartieri Spagnoli as a complex network.....	212
5.2.2 Discussion of results.....	215
5.3 CITY RESILIENCE AGAINST URBAN SIZE AND SHAPE: CASE STUDIES.....	221
5.3.1 Numerical simulation and graph modelling.....	221
5.3.2 Discussion on analysis results.....	226

CHAPTER 6

NOVEL RESILIENCE METRICS FOR CITY ECOSYSTEMS SUBJECTED TO NATURAL HAZARDS..... 231

6.1 ASSESSING URBAN RESILIENCE TO DIVERSE HAZARD TYPOLOGIES	232
6.1.1 The methodology.....	233
6.1.2 HSPNs modeling.....	234
6.1.3 Seismic and flow-type landslide fragility.....	236
6.1.4 The systemic damage assessment	239
6.1.5 Alternative resilience metrics.....	241
6.2 A REAL CASE STUDY: THE CITY OF SARNO	246
6.2.1 Modelling Sarno as a complex network.....	249
6.2.2 Fragility of the Sarno physical network.....	251
6.2.3 Approaches to the event type and systemic damage assessment	254
6.2.4 Discussion of results.....	258
6.3 CONCLUSIONS	267

CHAPTER 7	
CONCLUSIONS.....	270
APPENDIX 2.A: SEISMIC FRAGILITY CURVES FOR REINFORCED CONCRETE BUILDINGS FROM THE LITERATURE.....	280
APPENDIX 2.B: SEISMIC FRAGILITY CURVES FOR MASONRY BUILDINGS FROM THE LITERATURE.....	293
APPENDIX 5.A: GRAPHS OF THE CITY MODELS CONFIGURATION BEFORE AND SOON AFTER THE EARTHQUAKE OCCURRENCE	299
APPENDIX 5.B: ANALYSIS RESULTS IN TERMS OF THE RESILIENCE HISTOGRAMS.....	301
REFERENCES.....	305

List of figures

Figure 1.1 Physical resilience according to Bruneau et al. (Bruneau et al. 2003)	41
Figure 1.2 Physical meaning of the resilience metrics by Bruneau et al. (Bruneau et al. 2003) and by Cimellaro et al. (Cimellaro et al. 2010), according to Bocchini and Frangopol (Bocchini and Frangopol 2011)	45
Figure 1.3 Resilience assessment with reference to the recovery curve, as proposed by Bocchini and Frangopol (Bocchini and Frangopol 2011)	46
Figure 1.4 Non-dimensional resilience assessment as proposed by Bocchini and Frangopol (Bocchini and Frangopol 2011)	47
Figure 1.5 Typical performance curve of an infrastructure system after the occurrence of a disruptive event (Ouyang and Dueñas-Osorio 2014)	50
Figure 1.6 Performance curve definition by Francis and Bekera (Francis and Bekera 2014)	52
Figure 1.7 Object-Oriented civil infrastructure model, according to Franchin and Cavalieri (Franchin and Cavalieri 2015)	64
Figure 2.1 Yearly insurance premium per square meter for seismic (a) and gravity (b) load designed RC structures in case of full insurance model	115
Figure 2.2 Yearly total insurance premium per municipality in case of full insurance model	116
Figure 3.1 World map of natural hazards, developed and updated by Munich Re (2011)	121
Figure 3.2 List of the 10 costliest events worldwide from 1980 to 2014 (Munich Re 2015)	122
Figure 3.3 The Italian historical catalogue of earthquakes from INGV (INGV 2004)	126
Figure 3.4 Map of seismic hazards for the Italian peninsula (OPCM 3519 - 2006); 10 percent probability of exceedance in 50 years	127
Figure 3.5 Error simulated (Nsim=100) for Molise 2002 (M _{sp} =5.59) for the Benevento municipality in the case of the fully uncorrelated PGA	132
Figure 3.6 Error simulated (Nsim=100) for Molise 2002 (M _{sp} =5.59) for the Benevento municipality in the case of the partially correlated PGA	133
Figure 3.7 Total expected losses for each simulated earthquake in the case of the fully completely uncorrelated PGA	135

Figure 3.8 Total expected losses for each simulated earthquake in the case of the partially correlated PGA.....	136
Figure 3.9 Expected losses for the Italian peninsula evaluated in the cases of the fully uncorrelated (left side) and the partially correlated assumptions (right side). The results refer to the historical seismic events in Messina in 1908 (9.a-9.b) and Irpinia in 1980 (9.c-9.d)	137
Figure 3.10 Expected losses data points and regression curves for the case of the fully uncorrelated PGA	139
Figure 3.11 Expected losses data points and regression curves for the case of the inter-event correlated PGA.....	141
Figure 3.12 Regression curves fitted to the median (a) and the mean (b) in the two cases	142
Figure 3.13 Frequency of historical earthquakes in terms of magnitude	144
Figure 3.14 Bin regression in the case of the fully uncorrelated assumption.....	146
Figure 3.15 Bin regression in the case of the partial correlation assumption.....	146
Figure 3.16 Regression curves for the median (a) and the mean (b) values for the two limit cases.....	148
Figure 3.17 Case of the fully uncorrelated PGA: comparison between the regression curves of the median (a) and the mean values (b) in the case of bin regression and the case of regression for each magnitude (M_{sp}) value.....	150
Figure 3.18 Case of inter-event correlated PGA: comparison between the regression curves for the median (a) and the mean values (b) in the bin regression case and the case of regression for each magnitude (M_{sp}) value	151
Figure 3.19 Typical Cat Bond model functioning.....	158
Figure 4.1 The proposed framework's conceptual scheme (Bozza et al. 2015) 161	
Figure 4.2 Modeling of a hybrid social-physical network, a case study for the city of Acerra (NA) (Cavallaro et al. 2014)	165
Figure 4.3 Typological evolving dynamical network scheme (Bozza et al. 2015)	168
Figure 4.4 Sustainability dimensions Venn diagram (Bozza et al. 2015)	173
Figure 4.5 The proposed framework, where: R_i , are the efficiency measures performed first on the punctual nodes and then on the global HSPNs; C_j , are the resilience and efficiency measures performed on the typological groups and S_k	

are indicators referring to the social-economic background (Bozza et al. 2015).	181
Figure 4.6 Methodology exploiting scheme (Bozza et al. 2015).....	183
Figure 5.1 Picture of Rome and the city map, showing analogy with the circular shape	191
Figure 5.2 Picture of Philadelphia and the city map, showing its typically rectangular shape.....	192
Figure 5.3 Picture of the city of Palmanova and its typically star shaped planimetry.....	192
Figure 5.4 Trend of the recovery function, $Y(t)$, across the recovery strategy against the time, t	205
Figure 5.5 Recovery curve in terms of the global efficiency, normalized to the pre-event efficiency value, as a function of relocated citizens in each stage of the recovery process, in turn normalized with respect to the maximum number of evacuated citizens.....	208
Figure 5.6 Perfectly linear recovery curve	210
Figure 5.7 Limit case in which recovery is almost instantaneous and resilience attains its maximum value	210
Figure 5.8 Graphical representation of the recovery path in the C - D plane.....	212
Figure 5.9 Map of Naples' historical centre (red markers represent school buildings).....	213
Figure 5.10 HSPN of the historical centre of the city of Naples (the Quartieri Spagnoli Area), where only residential buildings have been modelled	214
Figure 5.11 HSPN of the historical centre of the city of Naples (the Quartieri Spagnoli Area), where both school (red squared markers) and residential buildings (black starred dots) have been modelled	215
Figure 5.12 City shapes modelled for the 200 buildings case analysis	223
Figure 5.13 City shapes modelled for the 1250 buildings case analysis, 25 of which are considered to be schools	224
Figure 5.14 Example of scaling in the case of star-shaped city with 50, 200, 1250 and 5000 residential buildings.....	226
Figure 5.B.1 Damage-dependent resilience, R^D , in the citizen-citizen case analysis, when 15% collapsed buildings are assumed, as a function of the HSPN's shape and size.....	301

Figure 5.B.2 Damage-independent resilience, R^E , in the citizen-citizen case analysis, when 15% collapsed buildings are assumed, as a function of the HSPN's shape and size.....	301
Figure 5.B.3 Damage-dependent resilience, R^D , in the citizen-citizen case analysis, when 30% collapsed buildings are assumed, as a function of the HSPN's shape and size.....	302
Figure 5.B.4 Damage-independent resilience, R^E , in the citizen-citizen case analysis, when 30% collapsed buildings are assumed, as a function of the HSPN's shape and size.....	302
Figure 5.B.5 Damage-dependent resilience, R^D , in the citizen-school case analysis, when 15% collapsed buildings are assumed, as a function of the HSPN's shape and size.....	303
Figure 5.B.6 Damage-independent resilience, R^E , in the citizen-school case analysis, when 15% collapsed buildings are assumed, as a function of the HSPN's shape and size.....	303
Figure 5.B.7 Damage-dependent resilience, R^D , in the citizen-school case analysis, when 30% collapsed buildings are assumed, as a function of the HSPN's shape and size.....	304
Figure 5.B.8 Damage-independent resilience, R^E , in the citizen-school case analysis, when 30% collapsed buildings are assumed, as a function of the HSPN's shape and size.....	304
Figure 6.1 The framework's flow-chart	234
Figure 6.2 Normalized efficiency against the number of relocated citizens	244
Figure 6.3 Picture of Mount Saro, Italy	246
Figure 6.4 Typical flow-type landslide	247
Figure 6.5 Flow-type landslide scheme (Highland 2004).....	248
Figure 6.6 Seismic classification of the Campania region, with the low (yellow), medium (blue) and high (red) seismicity areas outlined	248
Figure 6.7 Building (black points) and street pattern (red bold lines) networks for the city of Sarno	249
Figure 6.8 Fragility curves according to Ahmad (Ahmad et al. 2011) for reinforced concrete and masonry buildings.....	251
Figure 6.9 Fragility curves according to Parisi (Parisi et al. 2015) for reinforced concrete buildings and the FP7-funded SafeLand project (2009–2012, Grant Agreement No. 226479) (Corominas et al. 2011) for masonry buildings.....	252

Figure 6.10 Travel paths of the landslides by Cascini (Cascini et al. 2011) drawn on the Sarno HSPN, May 1998, for the analysis of the run-out distance.....	255
Figure 6.11 Normalized efficiency of the residential HSPN, $E_{cc}(C) / E_{cc,pre-event}$, as a function of the number of reallocated citizens, C , for the landslide scenario with $v=10$ m/s	259
Figure 6.12 Normalized efficiency of the residential HSPN, $E_{cc}(C)/E_{cc,pre-event}$, as a function of the number of relocated citizens, C , in the earthquake scenarios with $PGA=0.25g$	260
Figure 6.13 Pre-event graph	262
Figure 6.14 Post-landslide graph.....	263
Figure 6.15 Post-earthquake graph.....	263

List of tables

Table 1.1 Main aspects contributing to resilience, according to the area of interest	26
Table 1.2 Definition of resilience from different authors for complex and infrastructural systems.....	27
Table 1.3 Definition of resilience from different authors for safety management systems	27
Table 1.4 Definition of resilience from different authors for organizational systems	28
Table 1.5 Definition of resilience from different authors for social-ecological systems	29
Table 1.6 Definition of resilience from different authors for economic systems.	30
Table 1.7 Definition of resilience from different authors for social systems	30
Table 1.8 Definition of resilience from different authors for communities	31
Table 2.1 Number of residential buildings in Italy per construction time and structural typology (ISTAT 2001).....	96
Table 2.2 Total square meters in residential buildings in Italy classified per construction time and structural typology	97
Table 2.3 Expected annual loss per square meter	104
Table 2.4 Expected annual loss per municipality	105
Table 2.5 Estimated loss caused by L'Aquila and Molise earthquakes	107
Table 2.6 Yearly insurance premium per square meter in case of full insurance model.....	113
Table 2.7 Average premium for masonry structures at different maximum coverage and insurance excess values.....	117
Table 2.8 Total annual income at different maximum coverage and insurance excess values	118

Table 2.9 Total annual profit at different maximum coverage and insurance excess values	118
Table 2.10 Total expenses per year at different maximum coverage and insurance excess values	118
Table 2.A.1 Parameters of fragility curves from the 12 literature studies, used to implement the loss assessment methodology, described in Chapter 2	280
Table 2.A.2 Methodologies used for the development of fragility curves selected from the literature for RC buildings	282
Table 2.A.3 Methodologies used for the development of fragility curves selected from the literature for mixed buildings	292
Table 2.B.1 Parameters of fragility curves from the 5 literature studies, used to implement the loss assessment methodology, described in Chapter 2	293
Table 2.B.2 Methodologies used for the development of fragility curves selected from the literature for masonry buildings.....	294
Table 3.1 Statistics on the expected losses for the Venafro seismic event.....	138
Table 3.2 Historical earthquakes for which the scenario analysis is performed, gathered in bins with a 0.10 M amplitude	145
Table 3.3 Comparison between the mean and median values calculated in the case of the scenario analysis performed according to the fully uncorrelated and inter-event correlation assumptions.....	152
Table 5.1 Analysis results and post-event graph in the case of 15% collapsed buildings, where citizen-citizen efficiency is computed (only residential buildings).....	217
Table 5.2 Analysis results and post-event graph in the case of 30% collapsed buildings, where citizen-citizen efficiency is computed (only residential buildings).....	217
Table 5.3 Analysis results and post-event graph in the case of 15% collapsed buildings and schools, where citizen-school efficiency is computed.....	218
Table 5.4 Analysis results and post-event graph in the case of 30% collapsed buildings and schools, where citizen-school efficiency is computed.....	218
Table 5.5 HSPN shapes modelled and related features in the case of citizen-citizen efficiency assessment.....	225

Table 5.6 HSPN shapes modelled and related features in the case of citizen-school efficiency assessment.....	225
Table 5.7 Analysis' results for each HSPN's shape and size for the 15% citizen-citizen case analysis	227
Table 5.8 Analysis' results for each HSPN's shape and size for the 30% citizen-citizen case analysis	227
Table 5.9 Analysis' results for each HSPN's shape and size for the 15% citizen-school case analysis.....	228
Table 5.10 Analysis' results for each HSPN's shape and size for the 30% citizen-school case analysis.....	228
Table 5.A.1 Rectangular HSPN's configuration before and after the earthquake	299
Table 5.A.2 Examples of different HSPNs' shapes subjected to 30% buildings' damage	300
Table 6.1 Parameters of the seismic fragility curves by Ahmad (Ahmad et al. 2011)	251
Table 6.2 Parameters of the landslide fragility curves from the FP7-funded SafeLand project (Corominas et al. 2011) and Parisi (Parisi et al. 2015)	252
Table 6.3 Efficiency, relocated citizens and collapsed buildings in the case of the landslide back analysis	256
Table 6.4 Efficiency, relocated citizens and collapsed buildings in the case of earthquake simulation #1	257
Table 6.5 Efficiency, relocated citizens and collapsed buildings in terms of the standard deviation of the five seismic simulations.....	257
Table 6.6 Efficiency, relocated citizens and collapsed buildings in terms of the median of the five seismic simulations	257
Table 6.7 Y(0) value in the case of an earthquake and landslide	261
Table 6.8 Resilience results with reference to an earthquake event.....	264
Table 6.9 Resilience results with reference to a landslide event.....	264

INTRODUCTION

Climate change, global warming, biodiversity loss, natural and human induced risks are a threat to the cities' development, now more than ever.

Contextually contemporary cities are getting ever more exposed in time and space, due to accelerated urbanization and high concentration of resources and activities, within the rapid socio-economic growth.

As a consequence, increasing complexity of cities along with more severe threats induced by climate change is pressing modern societies to search for new paths of prevention, preparedness and rapid recovery. Particularly, the alarming rate of occurrence and severity of natural disasters is nowadays recognized as one of the main global issues affecting human life quality and environmental safety. Hence, a feasible approach aiming at managing urban and global environment is urgently needed and, at this aim, sustainable development is the solution.

A sustainable process is, in fact, a set of actions aiming at ensuring the well-being of both actual and future generations. It is implemented in order to govern the two main complex systems constituting urban fabric: the first includes man and society, and the latter environment and natural resources, mutually interrelated by dynamic and sometimes also conflicting relationships.

Nowadays the sustainability of urban environments represents an ambitious challenge, both on a local, that is in terms of land, community and local resources management, and a global perspective, as the energy and financial use efficiency, societal development and human well-being at a planetary level. With this, a fundamental requirement for communities, being continuously threaten by natural disasters, is to cope with them by addressing mitigation, adaptation, emergency management and recovery actions in a conscientious and efficient fashion. Hence, a focal, comprehensive objective that communities can persecute, in order to

ensure for future sustainable cities to cope with risks they are exposed to, is related to the local and global cities' resilience.

Keeping with this, resilience to natural disasters represents a key issue for contemporary society, substantially contributing to sustainability. Resilience is triggering increasing interest in many scientific contexts, as the capability of cities and communities to withstand strong unexpected events and the pace of their recovery in a functional and efficient fashion. Hence, the same definition of the resilience concept implies a wide and highly diversified range of components, factors and intrinsic dynamics to be accounted for. In this context, resilience can be regarded as a fundamental prerequisite to strengthen modern societies through a multiscale approach: from the single building scale to the urban and finally the global environment scale.

Starting from a smaller-scale perspective, one has to consider that to date, a growing number of structural systems are clustered in disaster-prone areas worldwide. Keeping with this, whenever a catastrophic event occurs, buildings and infrastructures have to be not only capable to withstand it but they have to be resilient too. Particularly, a robust structural system is a key feature for a structure to be resilient, ensuring an advanced bouncing back capacity whenever extreme events occur. Once structural robustness is achieved, usually an adequate resilience level is also guaranteed. On the other hand, a resilient structure plays a critical role within the urban environment also enhancing the resilience of the local community. This is because of its capability to ensure essential services, emergency response and shelter for deallocated citizens. Furthermore, severe economic and human losses are expected from buildings' damage and collapse in the face of shocking events. Hence, designing and erecting disaster-resilient buildings and infrastructures has a positive outcome, allowing to address social and economic issues too.

Besides, structures and infrastructures within the urban environment are upstream and downstream interrelated with other components and actors,

causing uncontrollable cascade effects and consequences at different scales. Physical, geographical and societal links subsist between urban components ruling dynamics, which are peculiar to each considered system. Particularly, when focusing from the single structure to the single city scale, human behaviour reveals to be a very critical aspect. This is because of the way in which social actors act and make choices every day, in an unpredictable and non-organized way, affecting the same city functioning.

In this sense, an innovative, transdisciplinary field of study is developed around the cities' study, that is the ecosystems theory. According to a holistic view, it encounter for cities being complex systems, made of physical and human components, which are mutually correlated and interacting. Hence, cities can be understood as systems being subjected to dynamic equilibrium states and continuously exposed to external changes, just like ecosystems.

The ecosystems approach recognise citizens having a core role in culture, economics and politics within the city system. As a consequence, also when studying sustainability and resilience issues at the local level, this is a fundamental aspect to be taken into account. On the other hand, the city efficiency level is strictly related to its physical environment, hence to be modelled as a thick network of linkages between structures and infrastructures, and to be assessed according to a rigorous metrics. To this aim, a city can be modelled as a complex network, being composed of arches, representing links between urban structures and services, and nodes, representing the meeting point between them. In this context, also the city social component can be considered, by computing to each urban node and arch, all the citizens being served by it.

At this scale, resilience can be understood as the potential of the city complex system to overcome a catastrophic event, affecting its built environment and consequently citizens using it. Actually this is a perspective, enabling resilience to be defined in two different ways: the

ecosystem approach and the engineering one. The former referring to the city capability to recover from a shocking event by reaching an always new dynamic equilibrium state, and the latter referring to the evidence of such equilibrium usually converging towards a steady state.

In this thesis, the two definitions are merged and the engineering resilience according to the ecosystems theory is defined. It is the capability of a complex system to withstand an external stress and bounce back to an equilibrium state, which can be the same of the pre-event but also a new one. As a consequence, cities are understood as physical systems, being assessed through engineering metrics, but contextually being studied also according to a human-centric perspective. With this, in this thesis a rigorous methodology is presented, to model a city according to the complex network theory, accounting for both its physical and social components, defined as a hybrid social-physical network (HSPN). HSPN enables us to assess efficiency engineering metrics and contextually to quantify the physical and social urban resilience.

Nonetheless, there are still issues, which cannot be studied with this approach, influencing the development and safety of communities. The aforementioned are not only related to the local level, but need to be investigated to a broader spectrum.

It is worth notice that whenever a catastrophe occurs, political and economic dynamics are fundamental to address recovery. While on the one hand they have direct effect on the single city structure, on the other hand they arise from a higher level, from institutional and governmental choices. Hence, to understand and monitor such dynamics, scientific research should be addressed to a super-urban scale.

This is the case of mitigation and adaptation actions, being focused on ecological economics principles. Ecological economics still matters the ecosystems theory field, being an anthropocentric discipline, encompassing traditional economics and ecology. It considers humans as primary component of an overall system, hence as a part of the natural

capital, which can strike a dynamic balance between ecological constraints and economic development. According to this perspective, economics and politics are seen as keystone processes, which are essential to city ecosystem functioning and resilience. A specific focus is done on financial mitigation instruments, directly affecting economic resilience and sustainability of humans populations. This is the case of insurance models against natural hazards. These are studied, according to the novel approach of global resilience to natural hazards, from the householders and also from the insurers perspective.

The present thesis project presents, first of all, a brief overview on the resilience concept and on its understanding in view of the current exposure of urban and worldwide communities and assets.

Chapter 1 describes the existing literature concerning the definition and quantification of resilience, with particular attention to catastrophe resilience. The link between resilience and sustainability is also investigated.

Chapter 2 shows a methodology being developed for the modelling of an insurance model against seismic risk for private householders, which is based on the probabilistic assessment of seismic hazard. A real case study application is also developed for the Italian residential building stock. Expected seismic losses are evaluated for the entire national territory, being evaluated at the single municipality level. Seismic insurance premiums are also evaluated, according to the actual exposure and annual rate for each municipality, according to different models, considering diverse excess and maximum coverage levels.

In Chapter 3 a performance-based earthquake engineering (PBEE) methodology is described for the development of curves enabling to forecast economic losses, given the magnitude of the expected seismic event. Curves are obtained through regression analysis, which are performed on scenario analysis' results, based on seismic events collected

in the Italian catalogue of historical earthquakes from the National Institute of Geophysics and Volcanology (INGV).

Chapter 4 describes a methodological framework for the quantification of urban resilience. It shows the chance to model any urban environment as a hybrid social-physical network (HSPN) and to assess its performance level according to the complex network theory. The human component of the modelled HSPN is then further considered through the integration of social indicators, enabling to evaluate the life quality level and the happiness of citizens. Finally an integrated framework is described, which methodologies can be integrated in, in order to homogenize data and to compare them, to finally obtain a synthetic resilience index.

In Chapter 5 a rigorous methodology for the quantification of resilience of HSPNs is described. The trend of the scaling relationships between urban size and shape and the seismic resilience level is investigated. Furthermore, a real application is developed for case study of the Quartieri Spagnoli, the historical centre of the city of Naples (Campania, Italy). Here the connectivity level between couple of inhabitants and between inhabitants and school buildings is investigated, together with the global urban efficiency and the seismic resilience.

Finally, Chapter 6 shows a probability-based methodology for the quantification of urban resilience to diverse event typology, particularly earthquakes and flow-type landslide. Alternative resilience metrics are herein proposed, accounting for the initial state of damage level and the number of delocated citizens. A further resilience measure is also proposed, begin totally independent on the simulated event typology. The robustness of the proposed metrics is then evaluated, through the implementation of seismic and landslide scenario analysis within a real case study for the city of Sarno (Campania, Italy).

CHAPTER 1

OPPORTUNITIES AND CHALLENGES OF RESILIENCE

1.1 THE CONCEPT OF RESILIENCE, UNDERSTANDINGS AND PERSPECTIVES

The word *resilience* is derived from the Latin *resilire*, whose meaning is literally “*to bounce back*”.

To date, the concept of resilience is used in multiple scientific contexts, with its meaning being adapted to the diverse disciplines and the related fields of interest, hence being interpreted according to several different perspectives. Basically, resilience identify the capability to recover, absorb shocks, and restore equilibrium after a perturbation.

Historically, the first approach to this notion dates back to the XIX century, it was used in physics to indicate the ability of materials to withstand impulsive loads without suffering damages. Then, resilience was also used in medicine (Lotka 1924; Pfeiffer 1929), psychology (Werner 1971; Garmezy 1973) and biology (Holling 1973).

Recently, resilience is triggering increasing interest in other scientific contexts, referred to communities, urban systems and built environments, as the capability to recover from natural and human-induced disasters. This approach found its basis at the dawn of the 80’s, when Timmerman referred to this term to define “*the ability of human communities to withstand external shocks or perturbations to their infrastructure and to recover from such perturbations*” (Timmerman 1981).

It is clearly evident, that the advent of the concept of resilience in this context is the result of an increasing need for a response to new and more intense threats to modern societies. In fact, increasing interdependences,

exposure and complexity of contemporary cities along with more severe events induced by climate change is making modern societies asking for prevention, preparedness, impacts and damages reduction and rapid recovery, that is resilience. This urgent need is pushing scientific community to discuss about the best approach to resilience against disasters, first of all to define disaster resilience and then to quantify it.

On the other hand, in order to develop a unique and exhaustive definition, a comprehensive approach is needed, which primarily defines all the agents and features, being involved in the study and management of cities subjected to disasters. Contemporary cities can be interpreted as complex systems, composed of dynamic relationships between physical environment, i.e. infrastructural systems (e.g. utility and transportation networks) and more in general all lifelines, natural environment and social environment, consisting of communities and their internal relationships. Hence, according to a general definition, cities can be considered resilient if able to cope with extreme events without suffering devastating losses and damages to their physical systems or reduced quality of life for the inhabitants (Godschalk 2003). However, a comprehensive definition is still not available, given the complexity in defining the behaviour of urban systems in peacetime and whenever a shocking event occurs.

What are the real operations taking place in urban systems? What about the dynamic equilibrium at the basis of the urban system operations? What is meant by limited damages and preservation of functionality for urban systems after extreme events? Which are and how can be defined the boundaries for assessing functionality? Does the optimal response of urban systems to extreme events, i.e. the “resilient” response, depend on the type of extreme event? These are just some of the questions that make the concept of disaster resilience exploding with different and multidisciplinary meanings.

1.1.1 Defining resilience

The theoretical construct of resilience is just an innovative one, when applied to the context of urban systems. Nonetheless it is a concept, which find its basis a way back, applied to different topics. The basic general principle refers to the capacity of a system constituted by several, non-homogeneous components (a person and its body, human brain, the microstructure of a material, etc.), which interact and coexist within the same organism (material structure, ecosystems, human or animal organism, communities, cities, etc.), in order to face an extreme event and to bounce back from arising adversities. This general definition can be well adapted to diverse complex systems, such as ecosystems, economics, human body, and also to cities, as already done in many studies in literature (Zhou et al. 2010).

On the other hand, cities can be subjected to diverse event's typologies, each of which needs a specific approach to define resilience. Particularly, urban systems are exposed to four extreme event's typologies (O'Brien et al. 2006): natural events (earthquakes, floods, tsunamis, etc.), technological events or human-induced events (transport networks, industrial accidents, terrorist attacks, etc.), humanitarian emergencies (famines, epidemic, wars, etc.), and events induced by climate change, which may still be considered as natural events (flood, cyclones, etc.) or as humanitarian emergencies (drought, political refugees, etc.), but that are induced by recent climate changes and can affect unprepared populations with unexpected intensity. All of these events can be faced through the implementation of effective adaptation, mitigation and recovery actions. Nonetheless it is not easy to identify unique patterns for such processes to be shared among worldwide communities and to be applied in cities. This is because each city has got specific weaknesses and strengths and is threaten by different hazards typology. For instance, in the case of climate-related events, the most effective mitigation techniques are indirect, to be undertaken on the global scale, through the reduction of

CO₂ emissions and the environmental protection. On the other hand, when thinking at seismic events, each area in the world exhibits diverse vulnerability and exposure, hence actions have to be thought and applied at the local scale.

Disaster resilience is highly variable across the time and the territorial scale, and different strategies can be implemented to enhance city resilience, in terms of adaptation and mitigation actions, risk management, shock preparedness and recovery capability from damages.

Given the wide range of perspectives on resilience, the multidisciplinary and multidimensional understandings of it, several diverse definition of resilience can be found in the literature. Actually, none of these excludes the others, but, simply, each definition is better applied to a context rather than another one. For this reason, many authors have reviewed these definitions.

According to Francis and Bekera (Francis and Bekera 2014) some main areas of interest can be recognized, based on the specific system resilience is studied with reference to, that are: infrastructure systems, safety management systems, organizational systems, social-ecological systems, economic systems, social systems and a further category, which is indicated as “uncategorized”.

In this thesis, a similar subdivision is done, for reviewing the definition of resilience, as they are given in the literature, by accounting for a further category, that is the community disaster resilience.

Community resilience is interpreted as dependent on all the dimensions and fields of interest proposed by Francis and Bekera, hence as the merger of them, being also in line with the interpretation given by Cutter et al. (Cutter et al. 2008).

With this, many authors, particularly in the field of civil engineering, address resilience against natural disasters with a specific humanitarian perspective, which enables to account for the ability of both the physical and the social system within the urban environment to face extreme events

(Franchin and Cavalieri 2015; Miles 2015; Davis 2014; Decò et al. 2013; Frazier et al. 2010, 2013; Cimellaro et al. 2010; Cutter et al. 2008; Chang and Chamberlain 2004; Bruneau et al. 2003).

Hence, based on the literature review from Francis and Bekera (Francis and Bekera 2014) and Cutter et al. (Cutter et al. 2008) by integrating it with further investigated studies, Table 1.1, following, shows the main properties contributing to disaster resilience, according to the area of interest they are applied to and highlighting the most important aspects, which should be focused when evaluating each of them:

Table 1.1 Main aspects contributing to resilience, according to the area of interest

<i>Resilience of ecological systems</i>	Biodiversity, redundancies, response diversity, spatiality, and governance and management plans.
<i>Social resilience</i>	Communications, risk awareness, and preparedness, development and implementation of disaster plans, purchase of insurance, and sharing of information to aid in the recovery process. Some of these are a function of the demographic characteristics of the community and its access to resources.
<i>Economic resilience</i>	Loss estimation models, business disruption post-event, employment, value of property, wealth generation, municipal finance/revenues.
<i>Organizational resilience</i>	Institutions and organizations and requires assessments of the physical properties, how organizations manage or respond to disasters such as organizational structure, capacity, leadership, training, and experience.
<i>Infrastructure resilience</i>	Lifelines and critical infrastructure, transportation network, residential housing stock and age, commercial and manufacturing establishments as well as their dependence and interdependence on other infrastructure.
<i>Safety Management system</i>	Vulnerability and exposure assessment, risk management, recovery planning, adaptation and mitigation
<i>Community resilience</i>	Ecological, social, economic, institutional, infrastructure, community competence indicators being merged with population wellness,

	quality of life, and emotional health, pre- and post-disaster community functioning
--	-------------------------------------------------------------------------------------

Tables 1.2-1.8 show the main definition of resilience, according to the area of study and to the explanation given by diverse authors:

Table 1.2 Definition of resilience from different authors for complex and infrastructural systems

Complex/Infrastructure systems	
NIAC, National Infrastructure Advisory Council—a framework for establishing critical infrastructure resilience goals final report and recommendations; 2009.	Ability to anticipate, to absorb, to adapt and to recover
Commonwealth of Australia. Critical infrastructure resilience strategy. Canberra: Commonwealth of Australia; 2010.	Coordinated planning, responsiveness, flexibility, timely recovery, guarantee minimum level of service while undergoing changes
Tokgoz, B. E., & Gheorghe, A. V. Resilience quantification and its application to a residential building subject to hurricane winds. <i>International Journal of Disaster Risk Science</i> , 2013, 4(3), 105-114.	Overcome negative consequences of a disaster, getting back to normal operations as quickly as possible
McCarthy JA. From protection to resilience: injecting ‘Moxie’ into the infrastructure security continuum. Arlington, VA: Critical Infrastructure Protection Program at George Mason University School of Law; 2007.	Ability to recover back to the original state or an adjusted state, reengineering technical and social fundamental processes

Table 1.3 Definition of resilience from different authors for safety management systems

Safety Management systems	
Hale A, Heijer T. Defining resilience. In: Hollnagel E, Woods DD, Leveson N, editors. <i>Resilience engineering: concepts and precepts</i> , 3. Hampshire, UK: Ashgate; 2006. p. 35–40.	Ability to anticipate, to circumvent threats, recover rapidly, preserve identity & goals
DHS Risk Steering Committee, “U.S.	Ability to resist, to absorb, to recover, to

Department of Homeland Security Risk Lexicon,” United States Department of Homeland Security. Washington DC; 2008.	adapt to harmful events
Miletti D Disasters by design: a reassessment of natural hazards in the United States. Joseph Henry Press, Washington, 1999.	Ability to resist or adapt to stress from hazards, and to recover quickly.
Geis DE By design: the disaster resistant and quality-of-life community. Nat Hazards Rev 1(3):106–120, 2000.	
Chen SC, Ferng JW, Wang YT, Wu TY, Wang JJ Assessment of disaster resilience capacity of hillslope communities with high risk for geological hazards. Eng Geol 98(3–4):86–101, 2008.	

Table 1. 4 Definition of resilience from different authors for organizational systems

Organizational systems	
Fujita Y. Systems are ever-changing. In: Hollnagel E, Woods DD, Leveson N, editors. Resilience engineering: concepts and precepts, 3. Hampshire, UK: Ashgate; 2006. p. 20–33.	Ability to recognize unanticipated perturbations, and to adapt, evaluate existing model of competence and improve
Grote G. Rules management as source for loose coupling in high-risk systems. In: Proceedings of the second resilience engineering symposium; 2006. p. 116–24.	Balance of stability and flexibility, adaptive capacity in the face of uncertainties, self-control
Woods DHE. Resilience-the challenge of the unstable. Burlington: Ashgate Publishing Company; 1–16	Ability to efficiently adjust
DHS Risk Steering Committee, “U.S. Department of Homeland Security Risk Lexicon,” United States Department of Homeland Security. Washington DC; 2008	Capacity to recognize threats, to prepare for future protection efforts, and to reduce likely risks
Haimes YY. On the definition of resilience	Ability to withstand, sustain acceptable

in systems. <i>Risk Analysis</i> 2009;29(4):498–501.	degradation, recover quickly
Fiksel J. Sustainability and resilience: toward a systems approach. <i>Sustainability: Science Practice and Policy</i> 2006;2(2):14–21.	Capacity to tolerate and retain function & structure
Woods D, Cook R. Incidents-markers of resilience or brittleness. In: Hollnagel E, Woods DD, Leveson N, editors. <i>Resilience Engineering: Concepts and Precepts</i> . Hampshire, UK: Ashgate; 2006. p. 69–79.	Adaptive capacity
Kendra JM, Wachtendorf T. Elements of resilience after the World Trade Center disaster: reconstituting New York City's emergency operations centre. <i>Disasters</i> 2003;27(1):37–53.	Ability to sustain a shock by adapting to and bouncing back

Table 1. 5 Definition of resilience from different authors for social-ecological systems

Social-ecological systems	
Cumming GS, Barnes G, Perz S, Schmink M, Sieving KE, Southworth J, et al. An exploratory framework for the empirical measurement of resilience. <i>Ecosystems</i> 2005;8(8):975–87.	Ability to retain system identity (structure, interrelationships and functions)
Holling CS. Resilience and stability of ecological systems. <i>Annual review of ecology and systematics</i> . 1973.	Amount of disturbance that can be sustained by a system before a change in system control or structure occurs, at least persisting in its pre-disturbance state.
Holling, C. S. Engineering resilience versus ecological resilience. <i>Engineering within ecological constraints</i> , 31, 32, 1996.	Persistence to change, ability to absorb change, retain relationships between people or state variables.
Gunderson L, Holling CS, Pritchard L, Peterson G. Resilience. In: Mooney H, Canadell J, editors. <i>Encyclopedia of global environmental change</i> , 2. Scientific Committee on Problems of the Environment; 2002. p. 530–1.	Time of return to global equilibrium, amount of disturbance absorbed before change of state

Pimm (1984); Holling et al. (1995); Gunderson et al. (1997)	Ability to maintain a steady ecological state related to the functioning of the system, rather than the stability of its component populations
Kinzig AP, Ryan P, Etienne M, Allison H, Elmqvist T, Walker BH. Resilience and regime shifts: assessing cascading effects. Ecology and Society 2006;11 (1):20–42.	Ability to absorb disturbance, re-organize while undergoing change, retain the same function, structure, identity & feedbacks

Table 1.6 Definition of resilience from different authors for economic systems

Economic systems	
Rose A. Defining and measuring economic resilience to earthquakes. Buffalo, NY: University of Buffalo NSF Earthquake Engineering Research Center; 1999.	Ability to recover, resourcefulness, ability to adapt
Perrings C. Resilience and sustainable development. Environment and Development Economics 2006;11(4):417.	Ability to withstand without losing the capacity to allocate resources efficiently
Fiksel J. Sustainability and resilience: toward a systems approach. Sustainability: Science Practice and Policy 2006;2(2):14–21.	Capacity to survive and to adapt

Table 1.7 Definition of resilience from different authors for social systems

Social systems	
Adger WN. Social and ecological resilience: are they related? Progress in Human Geography 2000;24(3):347–64.	Ability to cope with stress
Allenby B, Fink J. Toward inherently secure and resilient societies. Science 2005;309(5737):1034–6.	Capability to maintain current function, structure degrade gracefully

As shown in Table 1.1, one of the most recent fields of study about resilience is related to the communities. Community resilience is mostly understood as the merger of all aspects affecting resilience in diverse disciplines. Zhou et al. (Zhou et al. 2010) provide a large literature review

in this particular field, which has been enlarged with other literature studies, as shown in Table 1.8, following:

Table 1.8 Definition of resilience from different authors for communities

Community	
Wildavsky, A. for Safety. Transaction, New Brunswick, 1991.	Capacity to cope with unanticipated dangers, learning to bounce back.
Dovers, S.R., and J.W. Handmer. Uncertainty, sustainability and change. <i>Global Environmental Change</i> 2.4 (1992): 262-276.	Re-active and pro-active resilience of society are distinguished, based on the major difference between ecosystems (that react to disturbances) and societies (that can plan in advance, due to human capacity for anticipation and learning)
Horne JF, Orr JE Assessing behaviours that create resilient organizations. <i>Employ Relat Today</i> , 24(4):29–39, 1998.	Quality of individuals, groups and organizations, and systems as a whole to respond productively to significant change that disrupts the expected pattern of events without engaging in an extended period of regressive behaviour
Mallak L Resilience in the healthcare industry. Paper presented at the seventh annual engineering research conference, Banff, Alberta, Canada, 9–10 May, 1998.	Ability to expeditiously design and implement positive adaptive behaviours, while enduring minimal stress
Miletti D Disasters by design: a reassessment of natural hazards in the United States. Joseph Henry Press, Washington, 1999.	Ability to withstand an extreme natural event without suffering devastating losses, damage, diminished productivity or quality of life and without a large amount of assistance from outside the community
Comfort L (1999) Shared risk: complex systems in seismic response. Pergamon, New York, 1999.	Capacity to adapt existing resources and skills to new systems and operating conditions
Kimhi S, Shamai M (2004) Community resilience and the impact of stress: adult response to Israel's withdrawal from Lebanon. <i>J Community Psychol</i> 32(4):439–451, 2004.	Resistance of society to withstand a disturbance and its consequences, that is the degree of disruption that can be accommodated without social entity undergoing long-term change; recovery,

	as the time taken for an entity to recover from a disruption; and creativity to adapt to new circumstances and learning from the disturbance experience
Carpenter S, Walker B, Anderies JM, Abel N From metaphor to measurement: resilience of what to what? <i>Ecosystems</i> (N Y, Print) 4(8):765–781, 2001.	The Resilience Alliance defines social-ecological systems (SES) by considering three distinct dimensions: (1) the amount of disturbance a system can absorb and still remain within the same state or domain of attraction; (2) the degree to which the system is capable of self-organization; (3) the degree to which the system can build and increase the capacity for learning and adaptation
Paton D, Smith L, Violanti J Disasters response: risk, vulnerabilities and resilience. <i>Disaster Prev Manage</i> 9(3):173–179, 2000.	Active process of self-righting, learned resourcefulness and growth: the ability to function psychologically at a level far greater than expected given the individual's capabilities and previous experiences
United Nations International Strategy for Disaster Reduction (UNISDR). <i>Global Assessment Report on Disaster Risk Reduction: Risk and Poverty in a Changing Climate</i> . UNISDR: Geneva. 2009.	The ability of a system, community or society exposed to hazards to resist, absorb, accommodate to and recover from the effects of a hazard in a timely and efficient manner, including through the preservation and restoration of its essential basic structures and functions
Bruneau M, Chang S, Eguchi R, Lee G, O'Rourke T, Reinhorn A, Shinozuka M, Tierney K, Wallace W, von Winterfeldt D A framework to quantitatively assess and enhance seismic resilience of communities. <i>Earthq Spectra</i> 19:733–752, 2003.	Robustness, Redundancy, Resourcefulness, and Rapidity. A resilient system has reduced probability of failures; reduced consequences from failures; and reduced time to recovery
Kendra MJ, Wachtendorf T Elements of resilience after the world trade center disaster: reconstructing New York city's emergency operation center. <i>Disasters</i>	The ability to respond to singular or unique events

27(1):37–53, 2003.	
Cardona OD The notions of disaster risk: conceptual framework for integrated management. Information and indicators program for disaster risk management. Inter-American Development Bank, Manizales, 2003.	The capacity of the damaged ecosystem or community to absorb negative impacts and recover from these
Pelling M The vulnerability of cities: natural disasters and social resilience. Earthscan, London, 2003.	The ability of an actor to cope with or adapt to hazard stress
Rockstrom J Resilience building and water demand management for drought mitigation. <i>Phys Chem Earth</i> 28:869–877, 2003.	Institutional development, land reform, land tenure, diversification, marketing, human capacity building, and unmanageable ones, such as relief food, cereal banks, social networks, virtual water imports.
Rose A Defining and measuring economic resilience to disasters. <i>Disaster Prev Manage</i> 13:307–314, 2004.	Inherent resilience (ability under normal circumstances) and adaptive resilience (ability in crisis situations due to ingenuity or extra effort).
Rose A Economic resilience to natural and man-made disasters: multidisciplinary origins and contextual dimensions. <i>Environ Hazards</i> 7:383–398, 2007.	
Aguirre B On the concept of resilience. Disaster Research Center, University of Delaware, Delaware, 2006.	Capacity to absorb, respond and recover from the shock; to improvise and innovate in response to disturbances
Maguire B, Hagan P Disasters and communities: understanding social resilience. <i>Aust J Emerg Manage</i> 22(2):16–20, 2007.	Capacity of a social entity (e.g., a group or community) to bounce back or respond positively to adversity
Kang B, Lee SJ, Kang DH, Kim YO A flood risk projection for Yongdam dam against future climate change. <i>J Hydro-Environ Res</i> 1(2):118–125, 2007.	Ability of the system to recover
Asprone D., Manfredi Linking disaster resilience and urban sustainability: a glocal approach for future cities. Available at	Economic, Social and Environmental Sustainability of the phase of extreme event occurrence within the urban life

SSRN 2298652, 2014.	
Bozza A, Asprone D, & Manfredi G Developing an integrated framework to quantify resilience of urban systems against disasters. <i>Natural Hazards</i> , 78(3), 1729-1748, 2015.	cycle, for all the present and future actors, directly and indirectly involved in the recovery process.
Cavallaro, M., Asprone, D., Latora, V., Manfredi, G., & Nicosia, V. Assessment of urban ecosystem resilience through hybrid social-physical complex networks. <i>Computer-Aided Civil and Infrastructure Engineering</i> , 29(8), 608-625, 2014.	
Timmerman P, Vulnerability. Resilience and the collapse of society: A review of models and possible climatic applications. <i>Environmental Monograph</i> , Institute for Environmental Studies, University of Toronto, 1, 1981.	Ability of human communities to withstand external shocks or perturbations to their infrastructure and to recover from such perturbations
Environment and Development Division, UNESCAP, Sustainability, resilience and resource efficiency, UNESCAP. Bangkok, Thailand; 2008.	Ability to absorb disturbance, retain structure & functions; re-organizing capacity, adaptive capacity to change, sustain/withstand impact, recovery back to acceptable performance
Bruneau M, Chang SE, Eguchi RT, Lee GC, O'Rourke TD, Reinhorn AM, et al. A framework to quantitatively assess and enhance the seismic resilience of communities. <i>Earthquake Spectra</i> 2003;19(4):733-52.	Ability to reduce failure chances and to absorb shocks Ability to recover quickly

1.1.2 A novel understanding of resilience: engineering resilience in the sense of the ecosystems theory

A very important issue within the modern scientific debate concerns the methodology which shall be used, in order to measure the resilience level of a system as best as possible.

When dealing with engineering and economic systems, a quantitative assessment is actually necessary, this is to quantify the effectiveness of the recovery process and to recognize synthetic indicators representing the system's wellness. In this case, resilience is the measure of the ability of the investigated system to recover from a shock event, bouncing back to the previous steady equilibrium condition. This is the so-called "*engineering resilience*" (Bruneau et al. 2003; Holling 1996; Tilman and Downing 1994; O'Neill et al. 1986; Pimm 1984). On the other hand, when we deal with systems subjected to dynamic equilibrium states, continuously exposed to external changes, the meaning of resilience is a kind of qualitative. A typical example is related to the ecosystems, where the attention shifts from the persistency of the existing relationships to the overall behaviour of the system. This is, in fact, the case of "*resilience of ecosystems*", whose measure is given by the capability of a system, subjected to external shocks, to reach a different, even new, dynamic equilibrium condition (Holling 2001, 1996, 1986, 1973).

Looking at the typical structure of a city, with its physical and social components, mutual relationships and underlying mechanisms, one can argue that a city is easily comparable to an ecosystem, hence to be assessed according to the resilience of ecosystem approach. An urban system is, in fact, constituted by three main subsystems, the infrastructural, the economic and the social one, mutually interacting through a dynamic network of relationships, therefore difficult to understand when studied in isolation (West and Bettencourt 2010). Cities' subsystems are continuously varying and well-functioning in various different configurations, being equilibrium stages as well. Moreover it

shall be considered that the resilience of an isolated urban centre itself cannot be adequate at all. It is worth notice, in fact, that copying and bouncing back capacity are given by the global context, which the city is located in. Hence, also the relationships with other cities are fundamental, when dealing with copying capacity to extreme events.

A dynamic system, as the city, can easily move to a contingent new state of equilibrium, even if it moves to a new configuration, using more or less resources, and within the short or long period, and this new post-event stage can be both better or worse than the previous one. Hence, in order to evaluate the “relative goodness” of the new configuration, an engineering approach is needed.

According to this, and to the modern transdisciplinary approach to resilience, the two different definitions of resilience can be mutually completed, and resilience of cities can be defined as the ecosystem resilience, according to an engineering perspective.

So it can be concluded that resilience of a city is its capability to absorb external shocks and to reach a dynamic equilibrium stage, which can be at least the same as the pre-event, but it can be also different from the previous one, provided that critical indicators, giving a measure of efficiency and quality of the system’s performances, have got at least the same values as in the pre-event configuration (Bozza et al. 2015; Cavallaro et al. 2014; Asprone and Manfredi 2013; Dalziell and McManus 2004).

1.1.3 Closing the loop between resilience and sustainability

Resilience is related to the ability of a system to have a positive response to external shocks. Given the great attention to the safety of people in cities and their exposure, due to the increasing urbanization and natural hazards risks, the main system, which should be considered for assessing resilience is the urban environment, e.g. the city. Nevertheless, the measure of “goodness” of the response of the city is very difficult to

determine for contemporary cities. Hence, it can be said that a response is positive when it meets the appropriate equilibrium condition between the natural and the constructed environment, e.g. the physical system and the citizens' needs, e.g. the quality of life level in the city, according to the concept of resilience as defined by Godshalk (2003). Consequently, there is a clear correlation between resilience and sustainability, as already stated by the world scientific community (UNESCAP 2008; Fiksel 2006; Perrings 2006; Adger 1997, 2000; WCED 1987; Dovers and Handmer 1992; UN 1992, 1997), emphasising the concept that a truly sustainable city also needs to be resilient (UN Climate Conference, COP21 2015; UNISDR 2009; World Summit on Sustainable Development 2002). In particular, resilience is perceived as a requirement for global and urban system sustainability (Adger 1997, Asprone and Manfredi 2014, Bozza et al. 2015), as the capability of the system to bounce back to equilibrium after an adverse event occurrence.

With this, one could think that there is only one stable optimum state for a city to achieve equilibrium, which should be the main objective of planning for infrastructure resilience when an extreme event takes place, as in the case of an earthquake. Actually, as explained by McDaniels et al. (McDaniels et al. 2008), the city infrastructural system has to be conceived as linked with social and institutional systems, and also with the economic and environmental ones that are all embedded within the urban context.

This is a perspective which cannot disregard from considering the dynamic nature of cities and of all the processes, which take place in urban contexts. Hence, actually when focusing on cities, one deals with highly unstable systems that have multiple equilibrium states. In particular, the measure of a “good” state is given by its level of sustainability within all the above mentioned systems.

Specifically, social sustainability measures can be used as key indicators in order to better evaluate the level of functionality of a urban system,

namely its resilience, assuming they represent the level of satisfaction of its citizens. An ambitious goal that requires dedicated transdisciplinary collaboration across sciences, economics and technology.

The connection between the concept of city resilience and that of city sustainability actually remains faithful to the approach addressing the complexity of sustainability. In engineering, in particular regarding industrial products and processes, sustainability assessment refers to each phase of the entire life cycle of the investigated system.

The same kind of framework can be applied to the city, too. Therefore, in dealing with the life cycle assessment of the city, one can analyse the transformations over the constructed environment. In this case, apart from the phase of construction, operation, maintenance and disposal, a further phase can be considered: the hazardous event occurrence (HEO) phase. In this phase, whose consequences because of a hazardous event take place (Bozza et al. 2015; Asprone and Manfredi 2013), both the direct (damages and losses) and indirect (due to the post-event recovery process) effects have to be evaluated in terms of economic, environmental and social burden. For instance, a structure or an infrastructure is considered truly resilient if the negative effects of an extreme event are minimised - that is, sustainability in the HEO phase is maximised. For this reason, a city is deemed resilient if it is sustainable during the HEO phase, the period in which the city suffers an extreme event and tries to reconfigure both its physical and social systems with the primary aim of reaching an equilibrium state. Accordingly, resilience becomes one of the main factors contributing to sustainability, that is a city to be sustainable, has to be resilient too.

1.1.4 Measuring resilience

The increasing interest in resilience requires methodological frameworks to assess it. Measuring disaster resilience would help understand and improve resilience of urban systems against risks and implement the most

effective strategies to bounce back from disasters. Aimed at this goal, different studies have been developed, proposing operational frameworks to quantify disaster resilience and other properties related to it.

In general, resilience is assessed according to two main approaches' typologies: qualitative and quantitative.

Paralleling this, most of the methodologies available in the scientific literature can be divided into two categories: (a) the physical resilience approach, and (b) the social-economic resilience approach. In the former, attention is focused on the physical systems performances, e.g. single structures, urban lifelines, transportation systems. In this case, resilience is measured as the capability of the physical components and systems to effectively function and to recover their functionality in case of disruption. Mainly, these methods are developed and proposed within the engineering community. In the latter, attention is focused on social systems and resilience is measured as the capability of communities to recover a good life quality level. These are methods, which are mainly proposed in social sciences community.

Furthermore, novel approaches have been recently proposed within the modern scientific debate. These are based on a new understanding of systems, as the merger between their main constituents, and by accounting for their mutual relationships. This is the case of the graph theory, which systems analyzed are modelled as complex networks.

1.1.4.1 Approaches to physical resilience assessment

One of the most cited approaches available in the literature, is that from Bruneau and the MCEER research group. Bruneau et al. (Bruneau et al. 2003) provided a conceptual framework, which defines and quantifies seismic resilience of communities. Resilience is characterized by four main properties: robustness, rapidity, redundancy, and resourcefulness (*4 R's*), to be managed and computed as proxies of it. Along with this, resilience is also conceptualize according to further four interrelated

dimensions (TOSE): technical, describing how well physical components work when subjected to earthquake; organizational, describing how well organizations respond; social, representing the capacity to reduce social impacts due to the loss of critical services; economic, representing the capacity to reduce both direct and indirect economic losses.

Bruneau et al. move from a qualitative to a quantitative and comprehensive conceptualization of resilience, by integrating these through the concept of “resilience triangle”. Robustness is related to the “*strength, or the ability of elements, systems, and other units of analysis to withstand a given level of stress or demand without suffering degradation or loss of function*”. Rapidity is “*the capacity to meet priorities and achieve goals in a timely manner in order to contain losses and avoid future disruption*”. Redundancy refers to the availability of substitutable elements or systems in the aftermath of a disruption and resourcefulness is the capacity to mobilize materials and human resources. Keeping with this, a unified framework is developed based on three complementary and quantifiable factors within systems' resilience: reduction of failure probability, reduction of cascade effects of failure and reduction of time to recover.

According to this approach, different methods have been proposed, whose final scope is to compute resilience as the ability to cope with degradation in system performance over time, $Q(t)$, being evaluated as:

$$Q(t) = Q_{\infty} - (Q_{\infty} - Q_0)e^{-bt} \quad (1)$$

where Q_{∞} represents the capacity of the studied structural system when it is fully functioning; Q_0 represents the post-event capacity; b is an empirically derived parameter (from restoration data following the event); t is the post-event time (in days). Usually, $Q(t)$ is normalized, by dividing both sides of the relationship by Q_{∞} . Limit cases are recognized by the upper and the lower bound of the interval, which $Q(t)$ is defined in. Whereas $Q(t)=1$ indicates a fully operable system and $Q(t)=0$ an

inoperable one. Values in-between these two represent varying degrees of system operability.

Furthermore, the ratio of $(Q_\infty - Q_0)$ to Q_∞ is suggested as a measure of system robustness. In addition, the parameter b is suggested as a measure of the rapidity of the recovery process. Finally, resilience can be quantified through the integration of the area under the curve $Q(t)$ (O'Rourke 2007), divided by the time to restore the pre-event performance (Figure 1.1) (Bruneau 2006; Bruneau and Reinhorn 2006):

$$R = \int_{t_0}^{t_1} [100 - Q(t)] dt \quad (2)$$

where t_0 and t_1 are the endpoints of the time interval under consideration.

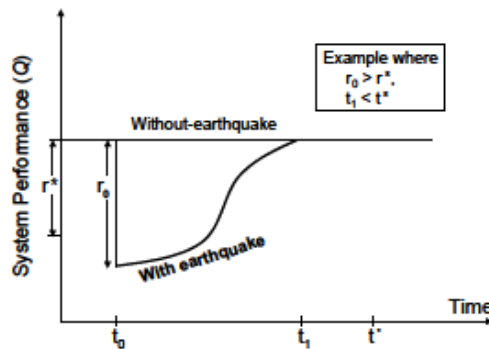


Figure 1.1 Physical resilience according to Bruneau et al. (Bruneau et al. 2003)

Being t_0 the time of the event and t_1 the time of the total recover of the pre-event performance. This approach has been applied to buildings (Bruneau and Reinhorn 2007), bridges (Decò et al. 2013), road networks (Arcidiacono et al. 2012) and urban infrastructure systems (Ouyang and Dueñas-Osorio 2012; Franchin and Cavalieri 2013), using different performance functions $Q(t)$.

Based on the TOSE framework, also Chang and Shinozuka (Chang and

Shinozuka 2004) proposed a seismic resilience metric for communities.

The framework proposes two significant refinement to the Bruneau et al.'s model: it outlines a more succinct series of resilience measures and reframes such measures in a probabilistic context.

Resilience is defined by comparing loss of system performance to pre-defined performance standards of robustness and rapidity, being compared with absolute pre-defined values of them ("maximum acceptable loss", "maximum acceptable disruption time").

It account for the quality of system performance as dependent on the system's robustness, that is in term of the level of losses, and the rapidity, that is the time to recovery. Resilience is therefore quantified as the probability of an investigated system of meeting both robustness and rapidity standards, r_0 and t_1 , summarized as A , in case of occurrence of a certain event I , of magnitude i (for instance an earthquake), according to Equation 3:

$$P_r(A|i) = P_r(r_0 < r^* \text{ and } t_1 < t^*) \quad (3)$$

whereas r^* and t^* are, respectively, the robustness and performance standards, that is the maximum acceptable loss and the maximum acceptable recovery time. These are compared with the corresponding ones, reached by the studied system, r_0 and t_1 . Particularly, r_0 represents the initial loss, and t_1 , the time need to fully recover.

Authors highlight the centrality of the definition of performance measures and standards, A , to the resilience quantification, and the consequential need for these definitions to be developed together with institutions, disaster managers and private and public stakeholders.

Hence, a broader system resilience definition is proposed, accounting for the entire range of possible events (in this case, seismic events) for a particular area, as shown in Equation 4:

$$Z_A = \sum_i P_r(A|i) \cdot P_r(i) \quad (4)$$

Also Cimellaro et al. (Cimellaro et al. 2010) quantify resilience as the area under the quality curve and consider all resilient components defined by Bruneau et al., by focusing on rapidity and robustness, which are here defined in a different way. Authors further introduce two control variable, the control time and the recovery time. As a consequence, resilience is evaluated as in the following (Equation 5):

$$R = \int_{t_{OE}}^{t_{OE}+T_{LC}} Q(t)/T_{LC} dt \quad (5)$$

where:

$Q(t) = [1 - L(I, T_{RE})][H(t - t_{OE}) - H(t - (t_{OE} - T_{RE}))] \cdot f_{Rec}(t, t_{OE}, T_{RE})$
 being $L(I, T_{RE})$, the loss function; f_{Rec} , the recovery function; $H(*)$, the Heaviside step function; T_{LC} , the control time, T_{RE} , the recovery time from event E and t_{OE} , the time of occurrence of event E .

As already explained, a particular understanding of resilience is proposed, which focuses on two of the four resilience dimensions, identified by the MCEER:

- Rapidity, that is the capability to achieve goals, while meeting economic and functional issues, and is understood as the slope of the functionality curve during the recovery time.

$$Rapidity = \frac{dQ(t)}{dt} \text{ for } t_{OE} \leq t \leq t_{OE} + T_{RE} \quad (6)$$

And that can be estimated as average recovery rate in percentage/time, if total losses and the total recovery time are known, as (Equation 7):

$$Rapidness = \frac{L}{T_{RE}} \quad (7)$$

Being L the drop of functionality in the aftermath of the event.

- Robustness, refers to engineering systems, as ability to withstand external shocks without suffering functionality loss, hence as the residual of function soon after the event occurrence.

$$Robustness = 1 - \tilde{L}(m_L, +a\sigma_L); (\%) \quad (12)$$

where \tilde{L} is a random variable, function of the mean and the standard deviation (m_L, σ_L) and a is a multiplier of the standard deviation, accounting for the specific level of losses.

Direct and indirect losses are also computed based on seismic losses assessed as a function of the event intensity, I , and on the recovery time.

Differences between the approach of Bruneau et al. (Bruneau et al. 2003) and Cimellaro et al. (Cimellaro et al. 2010), are also highlighted in the study from Bocchini and Frangopol (Bocchini and Frangopol 2011). This is evident first of all by observing the two proposed relationships. The one from Cimellaro et al., in general can be interpreted as in Equation 8:

$$R = \int_{t_0}^{t_r} Q(t)dt \quad (8)$$

being $t_r = t_{1,final}$, while it is considered as $t_r = t_1$ from Bruneau et al. (Bruneau et al. 2003). This means that the authors focus on the quantification of resilience rather than the loss of resilience, as made by Bruneau et al. (Equation 2). According to Bocchini and Frangopol this can be physically explained by observing the assessed area under the recovery curve, as shown in Figure 1.2.

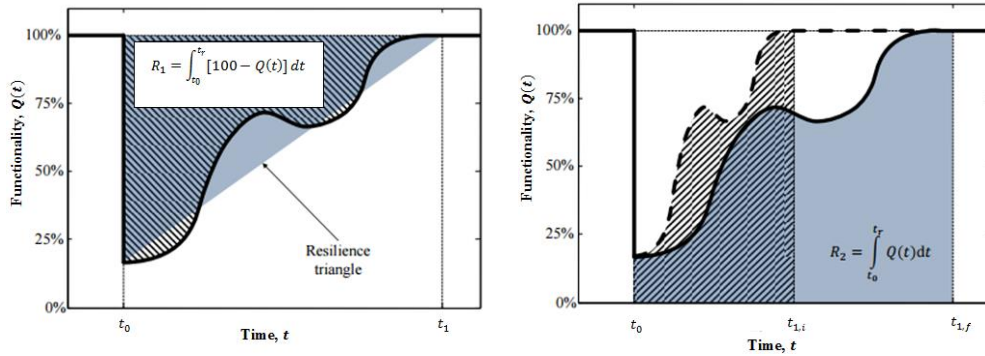


Figure 1.2 Physical meaning of the resilience metrics by Bruneau et al. (Bruneau et al. 2003) and by Cimellaro et al. (Cimellaro et al. 2010), according to Bocchini and Frangopol (Bocchini and Frangopol 2011)

It is clear evident the focus of the study by Cimellaro et al., which is most on the restoration process. Furthermore it accounts for the dynamic properties of resilience, enabling to assess the recovery also leading to a new functioning level of the system.

Nonetheless, according to Bocchini and Frangopol (Bocchini and Frangopol 2011) both of the two studies could be inappropriate for some applications, given that the integral is evaluated between t_0 and t_r hence potentially resulting in low resilience values, whether fast restoration strategies are implemented.

Hence, they propose a third relationship for the resilience quantification, which focuses on a fixed time horizon, t_h (Figure 1.3):

$$R = \int_{t_0}^{t_0+t_h} Q(t) dt \quad (9)$$

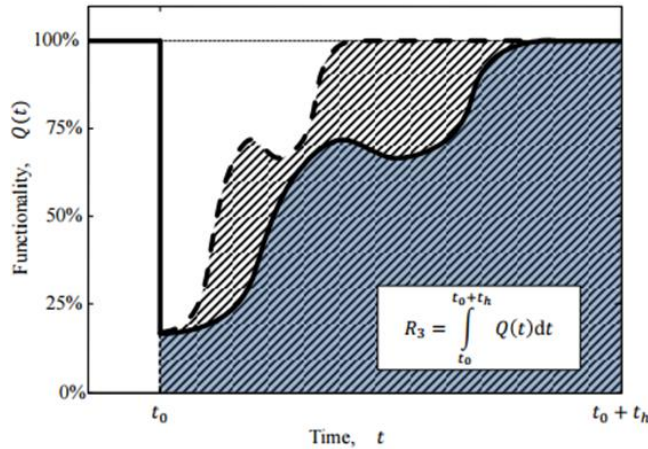


Figure 1.3 Resilience assessment with reference to the recovery curve, as proposed by Bocchini and Frangopol (Bocchini and Frangopol 2011)

According to the authors, more realistic results are thus obtained, enabling to compare various disaster management strategies. Moreover, if the recovery is not complete at $t = t_0 + t_h$, the proposed equation can be iteratively applied, yielding to a smaller resilience value, as expected.

Still according to the authors, the three equations presented for resilience quantification have a common constraint that is given by the measurement being performed in time units, being $Q(t)$ non-dimensional, hence providing values which could be difficult to interpret and share with decision makers. As a consequence, a normalization factor is introduced:

$$R = \frac{\int_{t_0}^{t_0+t_h} Q(t)dt}{t_h} \quad (10)$$

whereas the equation is composed of the numerator, representing the area under the recovery path curve, $Q(t)$, and the denominator, that represents resilience value (graphically interpreted in Figure 1.4), whenever the event did not occur or had no effects on functionality.

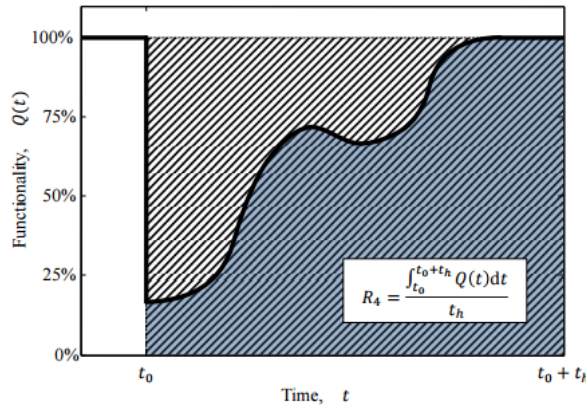


Figure 1.4 Non-dimensional resilience assessment as proposed by Bocchini and Frangopol (Bocchini and Frangopol 2011)

Authors suggests that each of proposed metrics, can be used depending on the particular aspects one wants to highlight in particular applications. Still stressing the evidence of a major versatility of the last one relationship.

Similarly to Cimellaro et al., the rapidity resilience's dimension is also defined by Decò (Decò et al. 2013), within the implementation of a resilience assessment framework, following the approach by Bruneau (Bruneau et al. 2003), Cimellaro (Cimellaro et al. 2010) and Bocchini and Frangopol (Bocchini and Frangopol 2011). The proposed formulation is the following:

$$r = \arctan\left(\frac{Q[t_f] - Q[t_0]}{t_f - t_0}\right) \quad t_0 \leq t \leq t_f = \min(t_r, t_h) \quad (11)$$

having substantially the same meaning as the one proposed by Cimellaro (Cimellaro et al. 2010).

Attention is also given to the way in which the recovery process should be represented, by accounting for all the involved variables, in this study, however a simplified model is utilized (Miles and Chang 2006). Moreover difficulties highlighted by Chang and Shinozuka (Chang and Shinozuka 2004) for the integration of different type of information are faced through

the implementation of a nonlinear model for loss assessment.

Further works are increasingly conducted on this topic and made available in literature, focusing on different urban systems and different performance functions $Q(t)$; however, the most of the works in recent literature share the theoretical scheme in Equation 1 or in Equation 2 to compute resilience. This is also the case of O'Rourke (O'Rourke 2007), and Reed et al. (Reed et al. 2009) and Vugrin et al. (Vugrin et al. 2011) the last two assessing resilience of networked systems, hence widely presented in Section 1.1.4.3.

Further attempts have been made to integrate probability-based procedure within the resilience assessment, given the aleatory nature of natural hazards. This is the case of Ouyang and Dueñas-Osorio (Ouyang and Dueñas-Osorio 2014), who propose a methodology for quantifying the hurricane resilience of contemporary electric power systems and estimating economic losses. This is a probabilistic modeling approach coupling four different model's typologies accounting: hurricane hazard, components' fragility, power system performance, and the system restoration. Ouyang and Dueñas-Osorio (Ouyang and Dueñas-Osorio 2012) also synthesize the existing definition of resilience in a unique one, they refer to distributed networks focusing on system and user evolution, hence highlight the meaning of resilience as *"the joint ability of 17-infrastructure systems to resist (prevent and withstand) different possible hazards, absorb the initial damage, and recover to normal operation one or multiple times during a period T "*.

Depending on the T value and its relative position with respect to current time, authors recognize three different type of resilience: the previous, the current potential, and the future potential resilience. Particular attention is paid to the third form, to account for potential system's evolving processes and to evaluate the effectiveness of diverse recovery strategies.

The resilience assessment model is calibrated and verified through the development of a case study analysis for the power system in Harris

County (Texas, USA), with real outage and restoration data after Hurricane Ike in 2008. Different dimensions of resilience are analyzed as well as the effectiveness of different strategies for resilience improvement. This leads to results, showing that among technical, organizational and social dimensions of resilience, the one, which affects the final resilience value the most is the organizational one, while the social one affects it the least.

Authors outline the chance to recognize three different stages within a typical response cycle of a networked system, which respectively reflects resistant, absorptive and restorative capacities of the system: the disaster prevention ($0 \leq t \leq t_0$), the damage propagation stage ($t_0 \leq t \leq t_1$), and the assessment and recovery stage ($t_1 \leq t \leq t_E$). Several diverse response cycle may take place during an interval period $0:T$. With this, infrastructure resilience over the considered time horizon is defined as the convolution of the three capacities within the time period T .

Looking at the system behaviour in a two-dimensional space P - T , where P is the performance level and T the time, two time-dependent curves are recognized. $P_T(t)$, that is the target performance curve (typically constant), and $P_R(t)$, that is the real performance curve, describing changes under disruptive events and efforts towards system recovery.

The proposed metric to quantify resilience is shown in Equation 12, as the ratio of the areas between $P_T(t)$ and the time axis and $P_R(t)$ and the time axis within the time interval $0:T$.

$$R(T) = \frac{\int_0^T P_R(t) dt}{\int_0^T P_T(t) dt} \quad (12)$$

Being defined in the range $[0,1]$. This metric is different from that proposed by Bruneau et al. (Bruneau et al. 2003; Bruneau et al. 2007), Cimellaro et al. (Cimellaro et al. 2010), Reed et al. (Reed et al. 2009),

Vugrin et al. (Vugrin et al. 2011) and O'Rourke (O'Rourke 2007), although they seem to have the same functional form. The difference, in fact, lies in the time interval such relationships refer to. Ouyang et al. propose an integration of the performance level on the interval $[0, T]$ (see Figure 1.5), while the abovementioned authors integrate in $[t_0, t_E]$.

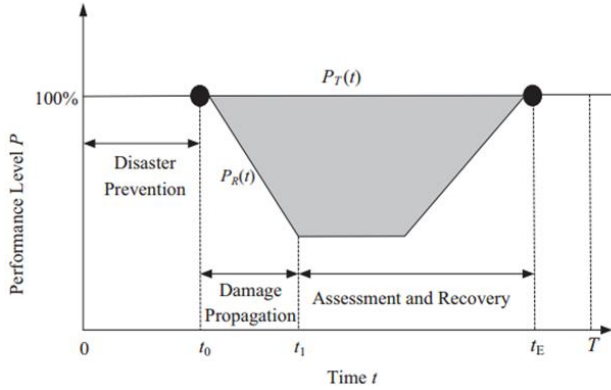


Figure 1.5 Typical performance curve of an infrastructure system after the occurrence of a disruptive event (Ouyang and Dueñas-Osorio 2014)

According to Ouyang (Ouyang et al. 2012), the equation they propose enable to account for multiple types of event and to realistically evaluate the ability of a system to withstand catastrophes, that is its resilience.

A time-dependent expected annual resilience (AR) metric is introduced, based on the correlation between and the hazard frequency, as the mean of the ratio between the area comprised between the real performance curve and the time axis and the area comprised between the target performance curve and the time axis, with reference to a one-year time slot. The proposed equation for resilience assessment can also incorporate multiple interrelated hazards:

$$AR = E \left[\frac{\int_0^T P(t) dt}{\int_0^T TP(t) dt} \right] = E \left[\frac{\int_0^T TP(t) dt - \sum_{n=1}^{N(T)} AIA_n(t_n)}{\int_0^T TP(t) dt} \right] \quad (13)$$

where: $E[*]$ is the expected resilience value; T is a 1-year time interval ($T=365$ days); $P(t)$ represents the actual performance curve, which is a stochastic process; $TP(t)$ is the target performance curve, which can be both a stochastic process or a constant line (TP) and, in this case, leads to the simplification of the abovementioned relationship for AR assessment; n is the event occurrence number, including event co-occurrences of different hazard types; $N(T)$ is the number of the total event occurrences in T ; t_n the occurrence time of the n^{th} event, which is a random variable; and $AIA_n(t_n)$ is the impact area, that is the area between the real performance curve and the targeted performance curve, for the n^{th} event occurrence at time t_n . $AIA_n(t_n)$ can be diversely computed depending on the need to account for single or multiple joint hazard types occurrences.

Further modifications to the proposed equation are also proposed, to account for specific processes to govern the hazard occurrence, as is the case of the Poisson process, or the case in which resilience has to be assessed under the hypothesis of multiple hazards occurring.

A further resilience analysis framework is proposed by Francis and Bekera (Francis and Bekera 2014) consisting of system identification, resilience objective setting, vulnerability analysis and stakeholder engagement. Its implementation is focused on the achievement of 3 resilience capacities:

- Adaptive
- Absorptive
- Recoverability

With the main objective to develop a quantitative metrics supporting engineering resilience. The quantitative framework refers to other proposed metrics, based on system functionality, but some additions are made to them, through the incorporation of both resilience capabilities and the time to recovery. This last is the length of time post-disaster until a system is brought back to reliable and sustainable conditions.

Let be S_p , speed recovery factor; F_o , original stable system performance level; F_d , performance level immediately post-disruption; F_r^* , performance

level after an initial post-disruption equilibrium state has been achieved; F_r , performance at a new stable level after recovery efforts have been exhausted. Figure 1.6 shows the above mentioned parameters.

By assuming that these quantities are reflective of specific organization's background knowledge K and time of disruption t_d , a resilience factor is defined as:

$$\rho_i(S_p, F_r, F_d, F_0) = S_p \frac{F_r}{F_0} \frac{F_d}{F_0} \tag{10}$$

where $S_p = \begin{cases} (t_\delta/t_r^*) \exp[-a(t_r/t_r^*)] & \text{for } t_r \geq t_r^* \\ (t_\delta/t_r^*) & \text{otherwise} \end{cases}$

t_δ =slack time;

t_r =time to final recovery (i.e. new equilibrium state);

t_r^* = time to complete initial recovery actions;

a = parameter controlling decay in resilience attributable to time to new equilibrium.

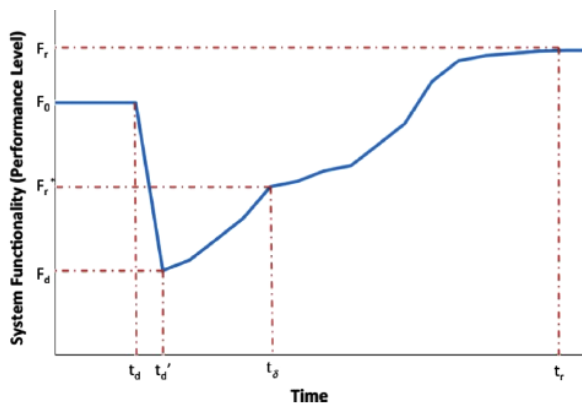


Figure 1.6 Performance curve definition by Francis and Bekera (Francis and Bekera 2014)

This is a resilience factor not accounting for system fragility, which can otherwise be integrated as a weighting factor in a subsequent decision-analytic framework or it can be directly combined to resilience factor, leading to the derivation of a system functionality degradation measure.

Two additional metrics for resilience are suggested in this study: an entropy-weighted measure of resilience for incorporating subjective probabilities for system disruption and the expected system functionality degradation. The former involves consideration of highly improbable events but also about the evaluation of the likelihood of occurrence according to different experts. So entropy is accounted in this distribution, as the total probability of an event occurring conditional to the expert-elicited distribution of vulnerability and hazard parameters. Thence an entropy-weighted resilience metric is constructed by incorporating all these parameter as multiplicative factors, according to the total probability law.

The resilience factor is then combined with fragility of the system weighted by the probability of occurrence of the event D_i , to stress the importance of the vulnerability knowledge of the studied system (Equation 14):

$$\zeta = \sum_i P_r[D_i] \cdot f(\mu|Z_i) \cdot \rho_i(S_p, F_r, F_d, F_0) \quad (14)$$

where $f(\mu|Z_i)$ is the fragility of the system conditional on event i occurring, being $f(\cdot)$ the probability density function for system failure, and μ , the probability of system failure, supposed to be a function of the Z parameter vector.

1.1.4.2 Resilience assessment according to social-economics approaches

Studies aimed at computing resilience from a social perspective focus on economic, demographic and institutional variables, in time and space. In example, economic growth and the distribution of income among people are fundamental aspects of resilience (Adger 2000) and are often used to compute resilience. Attitude to mobility and migration or amount of young people is also related to resilience (Ruitenbeek 1996; Adger 2000). Social memory of past changes and impacts (Olick and Robbins 1998) also relate to the capacity of communities to adapt and cope with disasters, that is resilience. Hence, different authors refer to this kind of variables to estimate community resilience, in terms of preparedness and coping capacity to disasters. Specific indicators have been also developed, moving from social-economic variable. This is the case of the Disaster Deficit Index (*DDI*), proposed by Cardona et al. (Cardona et al. 2008) measuring country resilience against disasters from a macro-economic perspective (Equation 15):

$$DDI = \frac{L_R}{R_E} \quad (15)$$

being L_R the maximum expected direct economic impact of possible disasters and R_E the available internal and external resources that can be made available to face disasters.

The expected loss assessment represents a major issue in this background, being intrinsically related to community resilience, to evaluate the effective availability of economic resources to be allocated to face adverse events.

Miles (Miles 2015) proposes a theoretical framework called WISC, whose based on four community constructs: well-being, identity, services, and capitals. These aspects are strictly related to the concepts of community and infrastructure, because of infrastructures being a combination of services and

capitals, supporting community activities, hence its well-being and identity, within human settlements. The four constructs are respectively defined by twenty-nine variables. Tyler and Moench (Tyler and Moench 2012) recognize three generalizable elements of urban resilience: systems (which have to guarantee flexibility and diversity, redundancy and modularity, and safe failure), agents (social agent and biochemical elements, which have to be resourcefulness, responsiveness and capable to learn), and institutions (formal or informal social rules that structure human behaviour, whose key aspects linking social actors and systems are: rights and entitlements linked to system access, decision-making processes, information flows and application of new knowledge).

Based on the three key elements of resilience, a conceptual framework is proposed, based on an organizing rubric, which focus on local planners to address the provision role of critical infrastructure and ecosystems, by linking systems and agents. The first step deals with the vulnerability assessment to focus intervention on the most vulnerable local components. Such phase is based on a structured interaction process of multistakeholder sharing knowledge to combine different perspective and provide a common understanding, namely the “Shared Learning Dialogues” (SLDs). First dialogue is established among managers, technicians and scientific experts, to define in which way climate change potentially affects systems and services. Hence, also marginal groups are asked for their opinion. The SLD is also evolving over time within the planning implementation, to keep update information about the core elements of the framework with reference to climate change and their resilience. According to the authors, such an approach enables for integrating ecological, social, infrastructure and institutional resilience factors with a focus to climate impacts.

Kimi and Shamai (Kimi and Shamai 2004) addresses social resilience as a system feature, being composed of three properties: resistance, recovery and creativity, in which (1) resistance can be understood in terms of the degree of disruption that can be accommodated without social entity undergoing long-

term change; (2) recovery relates to be understood in terms of the time taken for an entity to recover from a disruption. (3) creativity is represented by a gain in resilience achieved as part of the recovery process, and it can be attained by adapting to new circumstances and learning from the disturbance experience.

Vugrin et al. (Vugrin et al. 2011, 2010) propose a general framework, enabling to assess contextually the resilience of infrastructure and economic systems. The framework consists of three components: (1) a specific definition for infrastructure systems resilience; (2) a quantitative model for quantifying the systems' resilience to adverse events, based on the evaluation of both impacts to the cost of recovery and system performance; and (3) a qualitative method for assessing the system properties that determine resilience, which also provides insights for potential improvements in these systems.

Particularly, resilience costs are quantified through the evaluation of two key components: the systemic impact (SI), that quantify effects of system disruption in terms of productivity, and total recovery effort (TRE), that measures the system efficiency within the recovery. SI is assessed as the difference between a targeted system performance (TSP) level and the actual system performance (SP), soon after the disruption. TRE, instead, is assessed as the amount of resources spent to implement the recovery process.

Resilience indexes have been proposed in literature, being related to social-economic perspectives. For instance, Attoh-Okine et al. (Attoh-Okine et al. 2009) proposed a resilience index for urban infrastructure using a belief function framework. Li and Lence (Li and Lence 2007) proposed a resilience index, as a ratio of the probability of failure and recovery of the system.

Henry and Ramirez-Marquez (Henry and Ramirez-Marquez 2012) proposes generic metrics and formulae for quantifying system resilience, analyzed as a time-dependent function. Networks and system resilience are studied as dependent on time to assess resilience and the total cost of resilience. Three key parameters are identified, as necessary to analyze a system: disruptive events, component restoration and overall resilience strategy.

Resilience is here generally defined as the ratio $R(t)$ of recovery at time t to loss suffered by an investigated system at some previous point in time t_d , following in Equation 16:

$$R(t) = \text{Recovery}(t)/\text{Loss}(t_d) \quad (16)$$

In order to formulate a consistent quantitative approach the parameters in formula are defined. Authors consider resilience of a system with reference to three states (stable original, disrupted and recovered) and two transitions (system disruption and system recovery), both potentially activated by 2 events: a disruptive event and a resilience action.

In order to quantify resilience a time-dependent system level delivery function or figure-of-merit is defined, $F(*)$. The figure-of-merit (FOM) is the core notion, representing the level of the system's performance over time. The method requires the quantification of the system's FOMs and estimates the system's resilience for each one of them. According to the system under consideration it can be represented as network connectivity, flow or delay, with any state of the system corresponding to a value of $F(*)$.

Let E represent the set of all events $E=\{e_1, e_2, \dots, e_m\}$. Then, the set of disruptive events is defined as $D=\{e_j \in E/F(td/e_j)<F(t_0)\}$.

Henry and Ramirez-Marquez define a successful resilience action as one that restore the system to a stable recovered state, S_f , from a disrupted state, S_d , by increasing the value of $F(*)$ from $F(t_d)$ to $F(t_f)$, to be defined a priori by taking into account the component recovery mechanism and the overall resilience strategy.

Hence resilience is evaluated under a disruptive event e_j as follows (Equation 17):

$$R_F(t_f|e_j) = \frac{F(t_r|e_j) - F(t_d|e_j)}{F(t_0) - F(t_d|e_j)} \forall e_j \in D \quad (17)$$

Which indicates the proportion of delivery function that has been recovered from its disrupted state, consistently with the original meaning of the concept of resilience. Obviously resilience is quantifiable only if $F(*)$ is quantifiable.

Furthermore, the system S may be decomposed into components $\{s_1, s_2, \dots, s_n\}$, each of them exhibiting specific relationship with the figure-of-merit $F(*)$. This last one is considered to be the basis for resilience computation. According to authors, whenever a disruptive event occurs, it disrupts the performance of some of these system components, consequently reducing the figure-of-merit associated with S from $F(t_0)$ to $F(t_d|e_j)$. As a consequence, an effective resilience strategy plans and acts for disrupted components to be restored, such that the figure-of-merit value increases to $F(t_f|e_j)$.

Assumed S to be decomposed into components $\{s_1, s_2, \dots, s_n\}$, each component, s_i , has got associated the time, $t(s_i)$, and cost, $c(s_i)$, to restore it, in the case in which it is disrupted by the occurrence of an adverse event, e_j , with $e_j \in D$.

Being S_j the set of disrupted components, $T_R(e_j)$ is the time needed for $F(t_r|e_j)=F(t_0)$, that is, the time needed for the system to recover from its disrupted state S_d to its recovered state S_f , being computed as:

$$T_R(e_j) = \sum_{s_i \in S_j} t(s_i) \quad (18)$$

Similarly, let $C_R(e_j)$ is the cost incurred in implementing the resilience strategy, to guarantee the system to change from its disrupted state S_d to its stable recovered state S_f , computed as follows:

$$C_R(e_j) = \sum_{s_i \in S_j} c(s_i) \quad (19)$$

According to authors, further costs should be considered, which are the losses, L , incurred, due to the system inactivity, caused by disruption. These costs can be both direct and indirect, having different magnitude depending on the kind of service supplied by the disrupted system, causing the total costs to be:

$$C_{TOTAL} = C_{RESILIENCE ACTION} + L_{SYSTEM DISRUPTION} \quad (20)$$

Major diversification can be recognized regarding initiatives and studies across social-economical resilience, focusing only on one of the aspect or on both of them.

This is the case of the US National Institute of Standards and Technology (NIST), who developed a framework focused on community resilience planning for the built environment, where the performance goals for the physical infrastructure systems are informed by the needs of the residents and social institutions. The built environment is understood as the merger of buildings, transportation systems and infrastructure systems, such as power, communication, water and wastewater. The NIST Disaster Resilience Framework (NIST 2015) proposes methodology for communities to plan for resilience within their long-term planning processes.

Frazier et al. (Frazier et al. 2013) underline the importance of quantifying place-specific indicators of natural disaster resilience of communities, as they impact the ability to cope with and adapt to a natural disaster and climate-related events. They developed a case study of Sarasota County

(Florida), performing differential weighting of indicators, and the spatial and temporal contexts.

This research focus on the importance of local scale resilience estimates, appearing more useful than the National ones for reaching hazard mitigation and climate change adaptation goals.

Basic spatial analysis on specific resilience indicators were carried out to show variability of resilience across space. A Local Indicators of Spatial Association (LISA) analysis were performed for elevation, per capita income, percent of population under the poverty level, and persons over the age of 65, which are all factors directly influencing local resilience.

Disaster resilience is understood at the community scale in a temporal context, by placing each selected indicators along a disaster timeline and ranked according to its importance in each of the phases (Emergency, Restoration and Reconstruction).

Chang and Chamberlin (Chang and Chamberlin 2004) put particular emphasis on the importance of mitigation actions oriented to lifeline infrastructure system, in order to enhance community disaster resilience. A model focused on direct social and economic losses is developed, namely an agent-based socio-economic loss model. It is then applied to the case study of the Los Angeles Department of Water and Power (LADWP) subjected to an earthquake scenario.

A multi-source economic loss model is developed to quantify effects on community resilience. Inputs are used from MCEER engineering investigators, the status of each building is assessed according to the FEMA's loss estimation software HAZUS. A simultaneous evaluation of economic loss from disruption of water, building and electric power is performed, allowing to account also for cascading effects and more accurate estimates. Businesses disruption from lifeline damages are also computed, based on surveys on over 2000 businesses in the Los Angeles and Santa Cruz area. Finally economic and social impacts and resilience outcomes are evaluated. Functional losses are then translates into

probability values for disruptiveness to business's activities, according to a qualitative scale. Finally data on business disruption are translated into economic losses.

Cutter et al. (Cutter et al. 2008) provides a framework for the quantification of disaster resilience of place (DROP) model, that is at the local or community level, by contextually presenting the relationship between vulnerability and resilience. Vulnerability and resilience are considered as they are somehow overlapped, since there are some social characteristics influencing only one of them but also some of these characteristics influence both of them.

Gotangco et al. (Gotangco et al. 2016) adapt a generic systems dynamics (SD) model for resilience to analyse flooding impacts on household and local government assets. The loss of system performance due to adverse impacts, and the recovery of the system due to response are quantified through SD simulations. Results from the study show the decreasing levels of resilience among low-income households, and the reliance of local government on budgeting cycles to restore assets.

Rose (Rose 2015, 2009, 2004) an operational metric for quantifying economic resilience in static and dynamic contexts. Direct Static Economic Resilience (DSER) is defined as the operational level of a business or household entity. Total Static Economic Resilience (TSER) refers to the economy at a macro-level, hence including prices and quantity interactions in the economy, macro-aggregate considerations, and the ramifications of fiscal, monetary and security policies related to the disaster.

DSER is quantified according to Equation 18:

$$DSER = \frac{\% \Delta DY^m - \% \Delta DY}{\% \Delta DY^m} \quad (18)$$

being $\% \Delta DY^m$ the maximum change in direct output and $\% \Delta DY$ the actual change in direct output.

On the other hand, TSER can be quantified according to Equation 19:

$$TSER = \frac{\% \Delta TY^m - \% \Delta TY}{\% \Delta TY^m} = \frac{M \times \% \Delta DY^m - \% \Delta TY}{M \times \% \Delta DY^m} \quad (19)$$

where M is the economy-wide input-output multiplier, $\% \Delta TY^m$ the maximum change in total output and $\% \Delta TY$ the actual change in total output.

Dynamic resilience is also defined as the loss-reduction effect caused by accelerated reconstruction processes, and can be evaluated according to Equation 20:

$$TDER = \sum_{t=0}^n Y_{DR} - \sum_{t=0}^m Y_{DU} \quad (20)$$

being Y_{DR} the resilient response path and Y_{DU} the normal-course recovery path.

Rose and Krausmann (Rose and Krausmann 2013) outline also the need for a short-run economic resilience index, which is developed based on the framework proposed in Rose (Rose 2009) by focusing on business behaviour, supporting recovery potential.

1.1.4.3 Resilience assessment according to the graph theory

Recent applications in the field of civil engineering approached the resilience assessment according to the graph theory, by accounting for social and physical system city components and their mutual interrelations. Major attempts in this field have been done by Cavallaro et al. (Cavallaro et al. 2014) and Franchin and Cavalieri (Franchin and Cavalieri 2013, 2015) to assess resilience to seismic catastrophes. They

model social-physical graphs and use as the performance metric, $Q(t)$, the efficiency of the network in the “social” nodes, aiming at measuring the capability of the physical systems to serve their end-users. This highlights the understanding of civil infrastructures systems according to a human-centric perspective, which enable to evaluate contextually the performance level of physical infrastructures and its outcome on the people's life quality level. Hence, disaster resilience is evaluated by merging social and networked infrastructure resilience features. Moreover, these are approaches being addressed by the ecosystems approach, allowing to model local and global city contexts with all related components and complexities.

Franchin and Cavalieri (Franchin and Cavalieri 2013, 2015) propose a civil infrastructure simulation framework, which is extended to the evaluation of resilience through a network-based resilience metric. The recovery process is also included within the evaluation process, to focus on community resilience related to house reestablishment. The global model includes buildings, being modelled as a set of mutually connected infrastructural systems, and systems, which are modelled as network, and analyzed in terms of form and flow.

The proposed model also includes a taxonomy of a subset of systems and their component, with related fragility and functional data, selected from the SYNER-G project (SYNER-G 2012). An Object-Oriented model (OO) is used to account for interdependencies between the considered systems. Groups of objects are considered as classes and interrelation are represented graphically with class diagrams through the Unified Modeling Language (UML) implementation. Such information are projected onto a set of “*mutually exclusive and collectively exhaustive geocells using simple area ratio rules*”.

The methodology is developed for a case study analysis, referring to an artificially drawn city, modelled by authors as an Object-Oriented one, as shown in Figure 1.7:

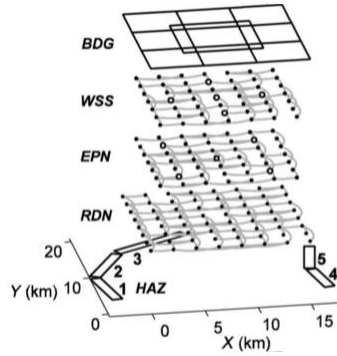


Figure 1.7 Object-Oriented civil infrastructure model, according to Franchin and Cavalieri (Franchin and Cavalieri 2015)

The area of the modelled city is discretized in cells, and residential, commercial, industrial and green areas are also identified and computed to each cell and the seismicity is accounted for, by considering a discrete number of seismic zones.

Resilience is assessed following the approach of Asprone et al. (Asprone et al. 2013), based on the notion of efficiency, according to Latora and Marchiori (Latora and Marchiori 2001), of a hybrid social-physical network.

The urban street network is assessed by also accounting for population density, being understood as the “*efficiency of the communication between citizens*”. A certain percentage of the total population, P , is computed to each cell, hence if one considers the generic cells i and l , the corresponding population share, P_i and P_l , and the relative Euclidean distance, d_{il}^e , and shortest path distance, d_{il} , efficiency can be computed as in Equation 21:

$$E = \frac{1}{P(P-1)} \sum_i P_i \left[(P_i - 1) + \sum_{l \neq i} P_l \frac{d_{il}^e}{d_{il}} \right] \quad (21)$$

Finally resilience is computed, according to Equation 22, by using the fraction of displaced population, P_d , that has been reallocated, P_r , as a measure of the progress of the recovery process instead of considering time, in order to avoid economic and time-dependent considerations:

$$R = \frac{1}{P_d E_0} \int_0^{P_d} E(P_r) dP_r \quad (22)$$

A similar approach is also used by Cavallaro et al. (Cavallaro et al. 2014), who apply the resilience within the real case study of the city of Acerra (Naples, Italy). Furthermore resilience is here evaluated with reference to diverse recovery strategies, focusing on multiple social aspects, such as: the connectivity between pair of citizens, between citizens and schools and between citizens and shops. Also the bouncing back capacity of the city is evaluated with reference to the “point of return” of the simulated strategy, hence leading the city back to the previous equilibrium or to a new one. Further details on the methodology will be given in Chapter 4 and 5, being the same adopted within the current thesis.

Mensah and Dueñas-Osorio (Mensah and Dueñas-Osorio 2015) propose a framework for quantifying resilience of electric grids and distributed wind generation to hurricane hazards, highlighting the high dependence of modern societies’ economy on high quality electricity. The proposed framework based on five models: (1) a hurricane demand model generating wind intensities, which are specific to each considered site, (2) component performance models, providing winds fragility, (3) a new Bayesian Network (BN)-based approach, enabling to evaluate the outage probability in the transmission system, (4) a system response model, to evaluate outages in 1 km² blocks, recognized as distribution nodes, and (5) a restoration model, to simulate recovery processes based on resources mobilization and time allocations from historical data.

Methods such as influence network pre-processing strategy via DC power flow analyses, Minimum Spanning Trees (MSTs), and the Recursive Decomposition Algorithm (RDA) are integrated within the framework to reduce computational complexity and time. Distribution networks are modelled as minimum spanning trees (MSTs). Substantially, a tree is a connected subgraph connecting all the nodes (vertices) with branches (edges) but without cycles, that is a tree connecting all the nodes in a graph together with the least weight. According to the author, the framework could be used for exploring a wide range of what-if scenarios, also in large real systems.

Authors evaluate resilience of networked system with a particular focus to social issues. With this, resilience is substantially assessed with the same functional form proposed by Ouyang and Dueñas-Osorio (Ouyang and Dueñas-Osorio 2014), being simply particularized with reference to the fraction of customers served or not served by the electrical power systems, after hurricane event occurrence. Hence, the electric system resilience R over time period $[0, T]$ is computed as shown in Equation 23:

$$R = \frac{\int_0^T Q_D(t) dt}{\int_0^T Q_N(t) dt} \quad (23)$$

where $Q_D(t)$ and $Q_N(t)$ are, respectively, the fraction of customers with power in the hurricane-disturbed and fully functional electric power systems at time t .

A recent attempt to integrate physical and social economic perspectives of resilience has been done with the PEOPLES Resilience Framework (Renschler et al., 2010), linking different resilience dimensions and resilience properties as proposed by Bruneau (2003). It is a holistic framework defining and measuring community disaster resilience at various scales. Seven dimensions characterizing community functionality

have been identified: Population and Demographics, Environmental/Ecosystem, Organized Governmental Services, Physical Infrastructure, Lifestyle and Community Competence, Economic Development, and Social-Cultural Capital. The Framework has been developed to provide the basis for the development of quantitative and qualitative models, enabling to measure continuously the functionality and resilience of communities against extreme events or disasters in any or a combination of the above-mentioned dimensions. Each dimension and service and its indicators are represented with a GIS layer of the area of interest, being all terms a function of location r and of time t .

As a result of all components and dimensions a global community resilience index is proposed, calculated according to Equation 24, and depending on the total functionality $Q_{TOT}(r,t)$, which combines all the considered community dimensions:

$$R = \int_{r_{LC}(t)} R(r) dr = \int_{r_{LC}(t)} \int_{T_{LC}(t)} Q_{TOT}(r,t)/T_{LC} dt dr \quad (24)$$

where $Q_{TOT}(r,t)$ is the global functionality, r_{LC} is the selected region, T_{LC} is the control time.

In analogy with the probability axiom of arbitrary events different functionalities are combined through Equation 25:

$$Q_{TOT} = \sum_{j=1}^n Q_j - \sum_{i=1}^n \sum_{j=2}^n Q_i Q_j + \sum_{i=1}^n \sum_{j=2}^n \sum_{k=3}^n (Q_i Q_j Q_k) - \dots + (-1)^{n-1} \sum_{i=1}^n \sum_{j=2}^n \sum_{k=3}^n \dots \sum_{j=1}^n (Q_i Q_j Q_k \dots Q_l Q_n) \quad (25)$$

Furthermore to account for diverse weights of the considered functionalities the mathematical expectation can be used as shown in Equation 26:

$$Q_{TOT} = E\{Q(r, t)\} = \sum_{i=1}^n p_i(r, t) Q_i(r, t) \quad (26)$$

Todini (Todini 2000) considers urban water distribution systems and design them as a series of interconnected closed and undirected loops, through which water flows are analyzed. The problem is formulated as a vector optimization problem with cost and resilience as two objective functions. This produces a Pareto set of optimal solutions, as trade-offs between cost and resilience. Surplus water supply is used to characterize resilience of the looped network, representing the capability of overcoming sudden failures. The proposed heuristic design approach begins with a target value of resilience index, and then identifies the pipe diameters for each node–node connection.

Leu et al. (Leu et al. 2010), propose an approach for quantifying resilience in transportation networks, being modelled as graphs. Based on GPS data, they model a network composed of three interacting layers, representing the physical structure, the service functioning, and the cognitive properties, that is the human dimension. Consequences and effects of network disruption are assessed through the graph theory, accounting for spatial distribution and network functionality, that is by performing degree, betweenness and clustering coefficient measures, which are typical of the complex network approach. Here the difficulty lays in the integration of metrics evaluated for the diverse layers and for their integration in a unique resilience indicator.

The use of graph theory for quantifying resilience has been proposed also by other researchers as well.

Murray-Tuite (Murray-Tuite 2006) focused on resilience of transportation networks. She proposes multiple metrics, by measuring adaptability, mobility, safety, and recovery, by using a large set of different metrics for each dimension.

Berche et al. (Berche et al. 2009) analyze the resilience of public transportations networks (PTN) under different attack scenarios. The authors mapped the PTN as graphs, hence they used network connectivity metrics to define random attack scenarios. By using the percolation theory basics and metrics, they provide graph indicators as proxies of PTN resilience. In this study, resilience quantification is performed in an indirect fashion by implementing robust mathematical models. Furthermore, here there is no need to integrate diverse metrics and resilience dimensions.

Dorbritz (Dorbritz 2011) combined the approach of Bruneau et al. (Bruneau et al. 2003), with network analysis proposed by Berche et al. (Berche et al. 2009) for quantifying resilience. Consequences of node removals in transportation networks are modelled from a topological and operational perspective. A software is used to quantify such consequences and to measure resilience, as the normalized area, according to Cimellaro et al. (Cimellaro et al. 2010), or by measuring values of the initial impact of disruption, the system performance and the time for recovery. Hence, these are associated to the four dimensions of resilience according to Bruneau et al. (Bruneau et al. 2003). According to the author's conclusion, due to the dynamic nature of the network, topological measures are not sufficient to characterize the disruption in networks. Moreover the transition to the four resilience dimensions is rather vague, due to the incompatibility between the two methods.

Omer et al. (Omer et al. 2009) propose a quantitative approach to define and measure resilience by using a network topology model. They define base resiliency as the ratio of the value delivery of the network after a disruption, to the value delivery of the network before a disruption. Whereas the value delivery is defined as the amount of information, to be carried through the network.

Miller-Hooks et al. (Miller-Hooks et al. 2012), quantified resilience as the maximum expected system throughput, in order to enhance preparedness

and recovery activities against potential system disturbances. Two stages are considered within the problem: the pre-disaster for preparedness and the post-disaster for recovery. A decomposition, L-shaped method is used to remove nonlinearity. Miller-Hooks et al. (Miller-Hooks et al. 2012) recognize the method to be computationally unaffordable for real systems and being applicable only for small benchmark problems.

Ouyang et al. (Ouyang et al. 2012) analyze two typical complex network based models for power grid networks, including a purely topological model (PTM) and a betweenness based model (BBM), as well as a direct current power flow model (DCPFM). The main goal of the study is to simulate the vulnerability of power grids according to their topology and flow under degree, betweenness, maximum traffic and importance based intentional attacks.

They proposed an expected, time-dependent, annual resilience metric that measures the system's preparedness and capacity to confront and recover from the occurrence of hazards of different types (whose functional form is shown in Section 1.1.4.1). The metric provides a performance curve that plotted in a two-axis graph defines with time an area that expresses the system's resilience. The metric is conceptually similar to other proposals, since it is based on stochastic modeling of a hazard occurrence-restoration actions-recovery iterative process; however, it differs in that it introduces the quantification of a system's resilience under multiple hazards. The method's weaknesses are that it focuses only on the technical dimension of resilience and introduces the multiple hazards effects in a non-correlated manner.

Paredes and Dueñas-Osorio (Paredes and Dueñas-Osorio 2015) developed an integrated resilience-based modeling approach for assessing the seismic resilience of coupled networked lifeline systems. Here capacity, fragility, and response actions, including those informed by engineering and community-based policy, are considered as inputs.

The concept of resilience is understood being time-dependent and lies on a flow-based core, enabling to assess performance, while contextually accounting for interdependencies among the considered systems.

Time-dependent seismic resilience is used to perform connectivity assessments for the lifelines being modelled as complex networks, but also sensitivity assessments to redundancy, robustness, and resourcefulness in the context of interdependent lifelines is performed.

Redundancy and robustness are analysed, as the core technical dimensions of resilience, according to Bruneau et al. (Bruneau et al. 2003), respectively as the availability of alternating paths to transport and deliver services; and as the reliability of local components. Also resources are considered in the form of number of components (v_k) that can be repaired in a period of time Δt_j .

Considering a time horizon T , short and long term management effects are analyzed via the ratio $\Delta t_j/T$, which enable to capture the relative time scale between time for restoration logistics and decision making.

Lifeline systems (e.g. power and potable water networks) are modelled as graphs $G(N, A)$, with N being the set of all infrastructures nodes and A the set of arcs linking all infrastructures. The commodities that can flow across infrastructures and interfaces between them is accounted for, together with the demand and supply for each of them, associated with the infrastructure of reference. Technical resilience is quantified according to Equation 2, even if, according to the authors, this is a metric, which does not supply evidence about the ability of a system to recover. Based on this observation, a time-dependent resilience is introduced and evaluated, according to Ouyang et al. (Ouyang et al. 2012), shown in Equation 12.

Heaslip et al. (Heaslip et al. 2010), developed a method to assess and quantify resilience using Fuzzy Inference Systems (FIS). They developed a framework which introduced two main concepts: a) the resilience cycle, which represents a system condition flow under a disruptive event in four phases, namely normalcy, breakdown, self-annealing and recovery, and b)

the system performance hierarchy, a structure that defines and ranks performance levels according to the hierarchy schema introduced by Maslow in his theory for the hierarchy of human needs. The combination of these concepts in a Cartesian plane results in a time-dependent curve, representing the system's performance levels during the resilience cycle. The resilience metric is defined by developing a diagram of variables hierarchy. Hence, FIS is introduced to quantify variables' described both in linguistic and numerical terms. In this way, interdependent problem variables can be modelled and assessed without the need of much data. Problems could arise when trying to refine the assessment, by introducing more fuzzy rules, hence a greater number of variables, having, as a consequence, higher computational burden.

Freckleton et al. (Freckleton et al. 2012) developed a framework, which is similar to the one from Heaslip et al. (Heaslip et al. 2010), but building the dependency diagram directly between indicators describing a system's critical attributes. These metrics were classified according to their area of interest: the individual, the community, the economic, and the recovery metric groups.

Reed et al. (Reed et al. 2009) outline a method to characterize the behaviour of networked infrastructure. Natural hazard, such as hurricanes and earthquakes, are considered, assessing resilience and interdependencies. Particularly, authors focus on the contribution of power delivery systems to post-event infrastructure recovery. A numerical example of the methodology is presented using power delivery and telecommunications data collected post-landfall for Hurricane Katrina. Resilience measures are understood as the lifelines' fragility and the quality of the studied system, as defined by the MCEER group in the paper by Bruneau et al. (Bruneau et al. 2003).

The study considers 11-system interdependent infrastructure (electric power delivery, telecommunication, transportation, building support, utilities, business, emergency services, financial systems, food supply,

government, health care), that is a networked lifeline for which resilience is assessed referring to the performance data obtained from the system.

Resilience measures are evaluated R_1 for subsystem 1 from Q_1 ; R_2 for system 2, etc.; from post-event data. In general, the system resilience R_s for a set a n total subsystems is evaluated as a function of the individual R_i , as highlighted in Equation 27:

$$R_s = g(R_1, \dots, R_i, \dots, R_n) \quad (27)$$

where $g()$ is a function, to be determined, that combines the individual resilience values, reflecting for interdependencies between them.

The study by González et al. (González et al. 2015) the Interdependent Network Design Problem (INDP) is introduced. It focuses on resilience of a partially destroyed infrastructure networks' system, which is assessed based on the reconstruction strategy providing for the minimum cost to be bear. Budget, resources, operational constraints, and interdependencies between them, are also accounted in the evaluation process. A Mixed Integer Programming (MIP) model is developed by the authors to solve the INDP. It deals with the diverse interdependencies while exploiting efficiencies from joint restoration due to colocation.

Davis (Davis 2014) understand resilience of a water systems, as its ability to provide post-earthquake services to other lifelines and emergency operations—such as hospitals, emergency operation centres, evacuation centres—in a manner which does not significantly disrupt their critical operations help increase the community resilience. He outlines that a water system resilience cannot be measured only by the service-time lost, but also by how it helps to improve overall community resilience.

1.2 FROM SOCIAL ACTORS TO CITIES: THE SCALE OF RESILIENCE

According to the 2015 Global Assessment on Disaster Risk Reduction, in last decades, losses due to extensive risks in 85 countries and territories were equivalent to a total of US\$94 billion (UNISDR 2015). With this, countries around the world, communities and human assets are ever more exposed and vulnerable to a wide range of risks. Particularly, natural hazards threaten infrastructure conservation, land use, economic and social development and human safety. To date, these represent the cornerstone of the worldwide communities' wellbeing, and the core for their conservation and progress is conserved in cities. The majority of people, in fact, resides in cities (Crane and Kinzig 2005), as a consequence of the unprecedented demographic scale of the urbanization process (UN 2004). Nonetheless, both opportunities and challenges arise from the modern urbanisation phenomena towards future scenarios of sustainable development. On the one hand, cities subsidize economies of scale, enhancing community progress and innovation across different sectors. Other junctures, however, arise because of local contexts being the main source of disease, pollution, crime and, in general, because of several critical issues related to human adaptation to urban living (Bettencourt et al. 2007; Angel et al. 2005).

Keeping with this, and also according to Bettencourt et al., a quantitative understanding of human needs and social organization and dynamics in cities is urgently needed, given that it is a *“major piece of the puzzle toward navigating successfully a transition to sustainability”* (Bettencourt et al. 2007). Paralleling this understanding of the relevance of life in cities, when dealing with natural disasters, Asprone et al. (Asprone and Manfredi 2013), Cavallaro et al. (Cavallaro et al. 2014) and Bozza et al. (Bozza et al. 2015) highlight the great dependence of sustainability on urban resilience. Basically, as already emphasized in Section 1.1.3, *“a city to be sustainable, has to be resilient too”* (Asprone and Manfredi 2013). Resilience can potentially be the long-awaited answer to the

challenge of understand and predict in which way and to what extent urbanization dynamics will affect the interrelations between the society, the built environment and the nature.

At this aim, and according to the general definition of resilience, the capability of urban systems to cope with and bounce back from external shocks, has to be guaranteed on all scales. Moreover, each urban system is characterized by a great range of diverse features, which are highly variable place-by-place resulting in an immense diversification of geographic and organizational factors, and human activities.

Hence, it is clearly evident that studying resilience and sustainability at a global scale would not enable to catch local features, which mostly rule urban behaviours. Conversely, approaching this contents on the urban scale consequently enables to obtain results, which can be expanded also at the national and international scales. This is because of cities being typical examples of fractals, that is they show the same patterns at all scales, reflecting statistical self-similarity (Batty 2008, Bettencourt et al. 2007).

Despite the acknowledged effectiveness of studying urban dynamics at the urban scale, however, a wide range of heterogeneous components and complex interrelations have to be accounted for. Hence, a lower scale has to be analyzed, by studying and modelling single urban components and then by characterizing their mutual interactions. Interrelations between urban components, in fact directly influence a city's behaviour. As a consequence, the study of cities can be regarded according to ecological models. They can be understood as ecosystems (Botkin 1997), being characterized by energy consumption, growth rates, and behavioural times, which are dynamics having counterpart on both physical, social components and their behaviour as a whole (Kates and Parris 2003). Particularly, according to the complex network theory, being a city's behaviour neither regular nor random, it can be asserted that it is ruled by a small-world principle (Latora and Marchiori 2001; Milgram 1998;

1970), hence easily to be modelled by considering few basic linkages between social and physical components.

Consequently, also when approaching to the study of resilience against natural hazards, a multi-scale approach as to be pursued: starting from single buildings and social actors, to model their isolated and then collective behaviour, to finally define the city as a whole, as a complex system.

From a civil engineering perspective, at the level of the single structure, resilience can be defined as its ability to effectively prevent from collapse and life safety of occupants and, in addition, to absorb external stresses and restore its basic functionality and structural capacity in a timely manner.

A key component of a resilient building is a robust structural system. Structural robustness is in fact defined as the ability of structure to withstand local failures without disproportionate collapse, being in turn influenced by ductility, integrity and redundancy.

When considering the matter from a hazard perspective, several potential disasters should be taken into account, including terrorist attacks, hurricanes, nuclear power plant accidents, earthquakes, tsunamis. As a result, multihazard approaches need to be used to compute diverse risks along with structural performances. Hence, advanced structural engineering and strategic disaster management methodologies, such as performance-based design and risk-based assessment, can be developed through the integration and implementation of resilience basics concepts in traditional practice. Besides, abnormal loads from extreme events have to be considered within the design process and also within the buildings' maintenance and retrofit actions. Exceptional loads are in fact often not considered in current engineering practice, whereas they need to be integrated to ensure restraining damages spreading and incipient collapse. Novel performance-based methodologies can then be implemented to assess resilience within a multiscale approach, also considering

interrelations between infrastructure and citizens. Infrastructures, in fact, fed citizens delivering urban services, and also play a critical role in achieving community resilience, since they are fundamental for the provision of emergency response, essential services and shelter. On one other hand, resilient buildings are also critical to urban resilience due to their high economic costs and potential loss of life associated with their damage or collapse.

The knowledge of structural resilience is fundamental as a support to disaster managers for the choice of the best recovery strategy to be implemented soon after a catastrophe occurrence. Diverse strategies can be hypothesized and resilience can be assessed for each of them to recognise the most efficient one to be implemented.

Resilience basics concepts and assessment methodologies have to be integrated within international building codes and guidelines to provide stakeholders with recommendations about performance-based design, structural retrofit techniques and resilience measurement assessment methods.

Criticalities have to be highlighted within the structural design basics and to provide fundamentals to address the design, the maintenance and the retrofit principles towards resilience structures. Structural design principles have to be rethought from the point of view of the practicality, reparability, robustness and serviceability in the aftermath of a catastrophe. Particularly performance goals should be recognised to define new resilience-based limit states, in light of what shown up to this point to enhance disaster preparedness and response of urban structures. Further should be also paid at the higher scale, to recognise the most critical infrastructures determining the resilience level of the overall urban environment.

In other words, resilience has to be approached in a systemic manner, broadening the defined performance-based standards from the level of the

single building, to the interconnected infrastructures and social actors and, finally, to the urban system.

Thus, given the configuration of the urban fabric, resilience can be evaluated at different levels:

- the single structure scale, where the measure depends on the strength, the resisting capacity of the single structure, and other critical parameters, such as ductility, durability, robustness, etc.;
- the single infrastructure system (e.g. urban lifelines) scale, that is given by the efficiency of the services provided to citizens, through robustness and redundancy properties;
- the single social system, as the citizens' share using specific sets of structures and infrastructures, depending on this their life quality level and well-being;
- the urban scale, as the overall complex system, depending on both efficiency and preparedness of citizens, that is social and physical bouncing back and copying capacity of all the components;
- the super-urban scale, that is the global scale, here understood as the level, at which resilience is evaluated according to national and/or international mitigation and adaptation policies aiming at enhancing resilience and sustainability from an economic, political and environmental perspective.

Hence, the wide range of urban patterns allow to define a city as a complex system, where single physical and social components are strictly interrelated.

1.3 OPPORTUNITIES AND CHALLENGES AROUND RESILIENCE

So far, wide discussions are clustered around the benefits, challenges and future directions for resilience, covering both theoretic and practical approaches. Particularly, key challenges for resilience-related practice and thinking are related to opportunities and challenges, which can arise from resilience-oriented approaches and actions. These result in the need for

integration, that is the development of a common language to discuss multi-challenges and multidisciplinary issues in a more joined way. Theories and practice around resilience should be, in fact, integrated and uniquely interpreted to guarantee understanding and sharing knowledge among both scientific researchers and institutional officers and international coordination actors. Keeping with this, following Sections make a focus on opportunities and challenges around resilience, and the consequential need for integration.

1.3.1 Opportunities

The great attention on the resilience concept from the worldwide communities has reinvented the discussion around how to support development. With this, the potential of this topic to rally different stakeholders around the common interest in enhancing development is highlighted, thanks to the ability of this topic to pull together different disciplines, sectors, people and goals.

As a consequence, many more actors are nowadays engaged in promoting the resilience development, both on a local and a global scale.

Novel approaches have been encouraged to track progress towards moving targets, above all when dealing with vulnerability-based approaches, which are often approached as static. With this, value has been added to the traditional risk assessment methodologies, accounting for high variability of hazards, exposure and vulnerability to natural disasters.

Resilience is mainly studied with a multi-scale approach from the single building or infrastructure, through the local scale to the global, national and international ones. With this, contemporary communities are understood as the merger of physical and social components, as complex systems, also considering interdependencies potentially causing cascade effects. Systems approach found great benefit in blending diverse components' type, spatial and timescales of support, to help communities sustainably escaping the burden of actual exposure and vulnerability.

The resilience is currently being integrated in many disparate contexts, such as economics, politics and land management, addressing mitigation actions towards sustainability.

1.3.2 Challenges

Current efforts around resilience highlight the need for considering specific features of each investigated system, promoting subjectivity and local identity. Nonetheless, the matter with this is that also the diverse typology of disastrous event potentially occurring, and related cascade effects, should be accounted for.

The importance of tackling multiple hazards has got nowadays a widely recognized appeal, but this is a very difficult issue to deal with. In this sense, some national agencies and institutions reneged on resilience framing, due to constraints given by existing institutions and practises. This is due to the lack of a common language to share between diverse stakeholders, representing potential opportunity but also a great practical challenge at the same time. People are often confused about resilience, and sometime have conflicting opinion about it. As an example, when dealing with post-disaster recovery some people may argue that the resilience concept is used remove the governments' responsibilities and emphasize locally mobilized response. On the other hand, a further interpretation can be given, since resilience could be used, as often already done, as an instrument for local government to subsidize support from donor systems and development agencies.

Furthermore, some institutions believe that the resilience approach could be a little too theoretical and that, due to the limited evidence based, basing long term planning policies on resilience could be ineffective and difficult to manage. On the other hand, such beliefs are tackled by the effective actions being undertaken by other institutions. This is the case of local intervention for disaster resilience fostered by the Rockefeller Foundation (Asian Cities Climate Change Resilience Network), also

together with Arup (100 Resilient Cities Framework), Iclei (Resilient Cities), United Nations (The City Resilience Profiling Programme), World Bank (Increasing Resilience to Climate Change and Natural Hazards), and many others, which are described in detail in Section 1.3.

1.3.3 Integration

The common convergence of resilience understanding and approaches is a long-acknowledged need among stakeholders from to disparate fields of interest. They all have the common goal to endorse and address resilience development at a broad level.

Worldwide communities are constantly working to find convergence in building capacity for both disaster risk reduction, social protection and climate adaptation. Governmental and research institutions are committing to reduce risks from natural disasters, while enhancing withstanding capacities.

Evidence based on knowledge and experiences have to be shared for linking the wide range of responses to the wide range of shocks.

1.4 CURRENT FRAMEWORKS AND ACTIONS ON RESILIENCE

The concept of resilience has been widely investigated and refined within last decades, being applied to multi-dimensional and multi-disciplinary topics. Particular attention has been gained by urban resilience against natural hazards, being approached by several national and international institutions and associations, constantly stressing its central role in guaranteeing sustainable development and population wellbeing (UN 2015a, 2015b, 2015c, 2015d; IPCC 2014; UNEP-DTIE 2013; UNEP 2013). Several organizations, as affected and donor members have been taking part to this discussion, such as the World Bank, IMF, OECD, UNDP and UN ISDR.

In this context, several research projects are currently ongoing within the Horizon 2020 funding programme (URBnet, TURAS, ANDROID,

SHARE, AGIR, and many others) and also within other several networks, constituted by institutional, academic and private stakeholders. Following major projects dealing with disaster resilience are briefly presented, to highlight the effective interest and actions undertaken by the world wide community.

For instance, in the United States, the Federal Government worked to improve the resilience of the nation to disruptive events such as natural and human-caused hazards (PPD-21 2013). This effort resulted in a number of guidance documents and tools for use to assess threats, hazards, and vulnerabilities in buildings and infrastructure systems and to develop approaches to reduce or eliminate those vulnerabilities. In particular, the Federal Emergency Management Agency (FEMA 2011) was tasked through Presidential Policy Directive 8 on National Preparedness (PPD-8 2011) to produce a series of frameworks to address the spectrum of prevention, protection, mitigation, response, and recovery.

The National Preparedness Goal developed by FEMA established 31 core capabilities necessary to achieve resilience. These capabilities are organized into five areas: Prevention, Protection, Mitigation, Response, and Recovery. Each mission area has a framework document that describes the roles and responsibilities of the whole community.

Further guidance documents, which are often cited for use by community are:

- the SPUR Framework (SPUR 2009), developed a Resilience plan for the city of San Francisco, that lead to the creation of the Earthquake Safety Improvement Program and a 30-year program for achieving resilience within the city's privately owned buildings.
- BRIC, Baseline Resilience Indicators for Communities (Cutter et al. 2014), which provide indicators for tracking changes in resilience over time. It is a set of 49 indicators based on theoretical, and/or empirical justification from research to represent each of the six types of resilience:

social, economic, community, institutional, housing/infrastructure, and environmental.

- The Community and Regional Resilience Institute's Community Resilience System (CARRI 2013), which recognize four key sets of metrics needed to build a profile or baseline of community resilience (social vulnerability, built environment and infrastructure, natural systems and exposure and hazards mitigation and planning).

As well as, the Oregon Resilience Plan (OSSPAC 2013); the NOAA's Coastal Resilience Index (NOAA 2015) and the Community Advancing Resilience Toolkit (CART) (Pfefferbaum et al. 2013).

Each of the initiatives cited above provides a set of dimensions or categories of community disaster resilience and, in many cases, includes a list of indicators or variables for each dimension. Some of the existing methodologies involve engaging community stakeholders, process-oriented guidelines for implementation, while others, that are heavily quantitative, typically involve readily available data. Most of these resilience initiatives only minimally address interdependencies between and among social actors and infrastructure systems.

On the international level major initiatives involve the United Nations International Strategy for Disaster Reduction Resilience Scorecard (UNISDR 2014) and the Rockefeller Foundation's 100 Resilient Cities initiative (Arup 2014), that are supporting resilience planning in cities around the world. Particularly, scientific research, real case studies and field work are contextually studied. The City Resilience Framework proposes an evidence-based definition of resilience and twelve indicators to assess resilience, based on four main aspects (health and wellbeing, economy and society, leadership and strategy, economy and society). The research merge evidence and knowledge from literature, 14 city case studies and fieldwork in six cities (Semarang (Indonesia), New Orleans (USA), Concepción (Chile), Surat (India), Cali (Colombia) and Cape Town (South Africa)).

The Sendai Framework and the Asian Cities Climate Change Resilience Network (ACCCRN) were powered by some of the above-mentioned institutions. The former promoting local intervention for disaster resilience, and being fostered by the Rockefeller Foundation (Asian Cities Climate Change Resilience Network), together with Arup (100 Resilient Cities Framework), Iclei (Resilient Cities), United Nations (The City Resilience Profiling Programme), World Bank (Increasing Resilience to Climate Change and Natural Hazards), and many others. The latter funded by the Rockefeller Foundation and supported by a large number of regional, national and local partner organizations (such as the World Bank), that is a network of ten core cities in India, Indonesia, Thailand and Vietnam, experimenting a range of activities that will collectively improve their ability to withstand, to prepare for, and to recover from the projected impacts of climate change. The approaches taken are determined by the local needs and priorities of each city, working at the nexus of climate change, vulnerable and poor communities and urbanization.

Still at the international level, UN-Habitat recently launched a new international Urban Resilience Institute (URI). It is supported by UN-Habitat, the City of Barcelona, and other partners, and will serve as the operational centre for the delivery of the UN-Habitat's City Resilience Profiling Programme (CRPP), but also as a hub for innovation, learning, policy guidance, and dissemination of best practice and information on resilience to cities around the world.

Particularly UN-Habitat's CRPP in 2012 developed the City Resilience Profiling Tool (CRPT) to enable any city to assess their urban resilience. A lite version tool for a rapid assessment of urban resilience has been developed, with an interface easily manageable and self-guiding.

As it can be observed, a great number of comprehensive frameworks incorporating elements of sustainable development, disaster risk reduction (DRR) and community engagement, are currently being developed within the international background to describing process by which resilience can

be improved. Nonetheless there are some of these, which are mostly implemented worldwide, and that comprehensively meet these requirements. They are the Climate Resilient Cities of the World Bank (CRC), Hyogo Framework for Action of UN/ISDR (HFA), Coastal Community Resilience of US/IOTWS (CCR), Community and Safety Resilience of IFRC (CSR) and Characteristics of Disaster Resilient Community of Twigg/DFID (CDRC), whose main features are described following:

- Climate Resilient Cities of the World Bank (CRC)

The CRC framework of the World Bank focuses on building resilience by sustaining and dealing with events. It has been implemented in selected cities across East Asia, the Middle East and North Africa, to bridge the lack of data and the lack of capacity of city authorities in enhancing resilience.

- IFRC Framework for Community Resilience (CSR)

The International Federation of Red Cross and Red Crescent Societies (IFRC) is the world's largest volunteer-based humanitarian network. A critical distinction is done in measuring community resilience with regards to the interrelated assessment of community's resilience, the IFRC's impact on community resilience and the IFRC's contribution to the community's resilience. IFRC activities contribute to achieving strengthened community resilience and suggests indicators to measure these activities (IFRC 2008, 2004).

- Hyogo Framework for Action of UN/ISDR (HFA) (PreventionWeb 2010; UN ISDR 2005)

Here the mid-term review (MTR) of the HFA undertaken in 2009 enabled countries to show their progress towards communities' disaster resilience and also to share knowledge and experiences with other countries, to compare their achievements. Since 2010, UN/ISDR has been holding workshops, in-depth studies and debates on how the HFA has been implemented by countries.

- Coastal Community Resilience of US/IOTWS (CCR) (US/IOTWS 2008)

The CCR framework of United Nations (UN), the Unesco Intergovernmental Coordination Group for the Indian Ocean Tsunami Warning and Mitigation System (IOTWS), and the Asian Disaster Preparedness Center (ADPC) takes a wider approach to resilience against natural disasters, to more generally include change, enabling to cope with diverse risk typologies.

- Characteristics of Disaster Resilient Community of Twigg/DFID (Twigg 2009).

The Climate Resilient Cities (CRC) framework of the World Bank, the Hyogo Framework for Action (HFA), and the Coastal Community Resilience (CCR) framework all suggest similar activities to build resilience. They provide specific steps for measuring and achieving resilience. While the other two frameworks, the CSR of the IFRC and DRC of Infrastructure Canada prescribed attributes or characteristics of a resilient community.

All of these frameworks, however suggest indicators to be used from local and global communities and institutions to monitor progress and outcome towards resilience, also referring to similar resilience components, being most of them derived from the HFA.

Further frameworks, such as the Climate and Disaster Resilience Index of Asian Cities (CDRI) from Kyoto University and the 4R Methodology (Bruneau et al. 2003) from the University of Buffalo were developed as scientific researches and consultancies for resilience building. Particularly, the University of Buffalo, together with the MCEER research group and the National Institute of Standards and Technology (NIST) further developed the definition of resilience to enhance its assessment within the PEOPLES resilience framework. It is a framework linking the four resilience properties (robustness, redundancy, resourcefulness, and rapidity) and resilience dimensions (technical, organizational, societal and

economic). The project is developing quantitative and qualitative models to measure the disaster resilience of communities in terms of capital assets such as hospitals and asset classes such as health care facilities.

CHAPTER 2

ECONOMIC RESILIENCE OF URBAN SYSTEMS: PROPOSAL OF A SEISMIC INSURANCE MODEL FOR THE ITALIAN BUILDING STOCK

The modern focus on resilience to natural hazards is currently approached with a multi-scale perspective, from the single city's component scale to the urban environment as whole, being such approach become nearly the rule. Despite this approach, resilience needs also to be addressed according to a global, "superurban" perspective.

Several national and international institutions and agencies propose to adopt this outlook when dealing with issues, which are related to politics and economics. This is the case of defining effective risk management methodologies, which are usually planned and developed at the national scale. Furthermore, to date there is a major need to recognise best practises for resilience improvement, hence to share knowledge and experiences among countries. This has got the potential for enhancing international cooperation and best managing financial resources allocation (donors, national funds, etc.) among diverse urban areas being related to the same global context.

A major issue in this background is related to the financial resilience, as the capability of a system to cope with an external stress, in terms of economic resources. In order for resilience to be improved across countries, these have to guarantee financial responsiveness and to promote mitigation actions, aiming at containing and holding the burden of reconstruction.

Financial resilience to natural hazards is a paramount concern, so that several initiatives have been undertaken internationally on this topic.

This is the case of the World Bank, which in 2006 handled part of the Mexican natural hazards' risk by issuing catastrophe bonds (World Bank 2006, 2000) or the 2015 United Nations Programme for finance and resilience to climate change (UNEP FI 2007, 2009, 2015). Moreover, the Organisation for Economic Cooperation and Development (OECD) highlighted the importance of undertaking actions towards economic sustainability to face natural disasters over and over again in last decades (Atkinson and Messy 2013).

Particularly, United Nations focus on financial resilience within the Global Resilience Project (GRP), which is oriented to “shift the focus of governments, NGOs, communities and businesses to investing in measures aiming at reducing disaster risk, rather than post-disaster relief and recovery efforts”. This approach has been further particularised within the UNEP FI “Appeal on Climate Change” Programme, that is an initiative for sustainable insurance, fostering and supporting insurers and reinsurers actions for climate change resilience improvement.

Philanthropic initiatives have also recently been developed from the Bloomberg New Energy Finance (BNEF), funded by Bloomberg Philanthropies and supported by the Climate Policy Initiative (CPI). The “FiRe, Finance for Resilience” Project focus on the development of a platform “that collects, develops and helps implement powerful and relevant ideas to raise finance for clean energy, climate, sustainability, and green growth” (BNEF 2015).

2.1 MERGING ECOSYSTEMS ENGINEERING AND ECONOMICS FOR RESILIENCE

Nowadays it is a common practice to refer to disaster resilience with a complex theory approach. This novel understanding of the resilience concepts found its basis in the need of merging ecosystem function with human dynamics, since they both rule directions towards sustainability.

These are the basis for ecological engineering, which is defined as the “design of human society with its natural environment for the benefit of both” (Mitsch and Jorgensen 2004; Mitsch 1999; Mitsch and Jorgensen 1989).

Ecological engineering is a subject, which deals with several different topics and involves different applications, such as urban modeling, national planning, solving environmental problems, managing worldwide-recognised risks, and so forth. Particularly, when dealing with economic systems in the field of disaster resilience, we are dealing with ecological economics. Ecological economics understands, in fact, human economy as a part of a complex and wider whole, whose behaviour is governed by a thick network of interrelations and dynamics, which in turn are ruled by human behaviours. Hence, it is clear evident its direct linkage with the disaster resilience according to the complex network theory, as described in Chapter 1.

Peoples are, in fact, the core component of global systems. According to a holistic view, peoples are responsible of the global system management towards resilience and sustainability (Costanza 1992). In this context, human behaviour is then seen as a key process, potentially guaranteeing sustainability, through the implementation of primary long-term policy goals, which do not necessarily need resources’ allocation and consumption. In this view, problems affecting the human safety and well-being are faced according to a cross-scale and transdisciplinary perspective, highlighting the need for novel anthropocentric approaches and social institutions integrating world communities within policy and management processes (Folke et al. 1996, 1994).

As a mitigation instrument potentially enhancing disaster resilience at the global scale and supporting economic sustainability, insurance models can be this and even more!

Insurance against natural disasters can be in fact a great instrument under a multiplicity of aspects: it enables mitigation actions enhancement in view

of even more severe natural catastrophes; it guarantees risk sharing among diverse stakeholders, such as homeowners, private companies and public institutions. Furthermore, natural disasters' insurance promotes a major risk awareness among global communities and incentivizes major responsibilities in the management, maintenance and conservation of private and public assets.

2.2 A SEISMIC INSURANCE MODEL AS AN INSTRUMENT FOR RESILIENCE AT THE SUPERURBAN SCALE

As highlighted in the previous Section, the attention of scientific community investigating natural hazards and the effects of natural disasters is ever more shifting towards the resilience of urban environment. Resilience is coined as the ability of the society to cope with a strong unexpected event and the pace of its recovery. Insurance systems for the natural hazards can be considered as effective tools aimed at increasing the socio-economic resilience of the contemporary society. In this regard, the financial conditions of the central government represents a critical point for post-disaster resilience. The Disaster Deficit Index introduced by Cardona (Cardona 2006) measures the internal and external financial resources potentially available to the government in the aftermath of a disaster. The insurance systems enter this picture as providers of external resources which can potentially reduce the burden of reconstruction. However, proper implementation of insurance systems for natural disasters can be subjected to the following challenges:

1. Insurance premium for private property owners can represent a prohibitive cost;
2. In the case of severe and rare events with widespread damages to the insured property, the insurance company system may encounter cash flow problems.

The above-mentioned challenges are particularly relevant in the case of seismic risk where the consequences in terms of loss per event can be extremely high.

In order to face the losses induced by seismic events and to facilitate the financial recovery of homeowners with damaged property, a variable range of seismic insurance systems are implemented in countries with high seismicity; such as, Japan, New Zealand, California and Turkey. In Japan and New Zealand, earthquake insurance is part of the fire insurance. Moreover, the national government provides a re-insurance program (Yucemen 2005; Brillinger 1993; Steven 1992). In Japan, the earthquake insurance also covers damages due to volcano and tsunami. In California, although the seismic insurance is provided by private companies, a state-run earthquake insurance company (CEA, formed after the Northridge earthquake in 1994) has been founded in order to overcome the potential financial difficulties encountered by the private companies (Scawthorn et al. 2003). In Turkey, the government has strived to introduce a compulsory insurance for homeowners, providing a public re-insurance support (Yucemen 2005). Although an earthquake insurance system for Italy has been often discussed, especially after significant seismic events, there are few documented efforts on the implementation of a national seismic insurance system (Amendola et al. 2000). A proposal of law was elaborated in 1998, aiming at extending the (mandatory) fire insurance so that it covers also the seismic damage. However, this proposal has been never adopted and was eventually withdrawn. After the huge economic losses due to the occurrence of L'Aquila 2009 and Emilia 2012 earthquakes, the Italian Government, together with the Civil Protection, began to discuss again about the need to ratify the compulsoriness of seismic insurance for householders.

Since this could be a potential measure having a very strong impact on the population, they developed a Legislative Decree (D.L. n°59/2012), which suggested householders to buy seismic insurance voluntarily (article 2).

Unfortunately, also due to the small number of ad hoc insurance products on the Italian market, the Decree has been approved but article 2 was abolished.

Indeed, efforts for the roll-out of the insurance systems for residential buildings against natural disasters and, particularly, against seismic risk, are related to several different issues.

On the householder side, there is a widespread low risk perception, which results in the limitation of people to voluntarily adopt cost-effective protective measures and to purchase insurance.

At the same time, Governments lacks of adequate instruments to mitigate disasters and the deriving losses and insurance and reinsurance industry are not willing to promote and to sell coverage against such events, due to the high risk of exceeding their financial capacity.

According to Kunreuther (Kunreuther 1996), the challenges associated with reducing losses from natural hazards is attributed to “the natural disaster syndrome”, which consists of two strictly interrelated components: the limited interest in adopting pre-event protections and the high costs to the Governments and insurers following a catastrophe.

Nonetheless, the need for an effective instrument aiming at mitigating risks and enhancing disaster resilience is still evident. Keeping with this, the expected life-cycle cost can be regarded as a benchmark variable in decision making problems involving insurance policy making for existing structures in seismic risk prone areas.

In the following Sections a study is presented, which has been developed Asprone et al. (Asprone et al. 2013), and which characterizes a potential seismic insurance system in Italy, that covers the whole private residential building stock. In particular, under a set of simplifying assumptions and governing equations discussed and presented hereafter, the insurance premium per year for the owners of residential property units and the expected losses per year, to be covered by insurance companies, are calculated.

The proposed risk-based insurance model, is built up upon a probabilistic loss assessments for a portfolio of buildings. The methodology is described, as it is a preliminary study aiming to calculate the expected insurance premium for Italian building stock subjected to seismic action in its service lifetime based on probabilistic seismic loss assessment. It leads to probabilistic assessment of the structural performance, expressed in terms of the discrete structural limit state exceedance probabilities, and the life cycle cost taking into account the Italian seismic zonation and the seismic vulnerability of the existing life stock. The expected insurance premium can then be evaluated based on the probabilities that the structure exceeds a set of discrete limit state thresholds and the average costs associated to them. The methodology is implemented in an illustrative numerical example which considers the Italian residential building stock discretized in 5 structural typologies and in 8088 areas, corresponding to the Italian municipalities. A monopoly market-based insurance model is built, assuming risk aversion of the property owners and risk neutrality of the insurance companies. The expected insurance premium is evaluated for each structural typology in each Italian municipality, taking into account also the maximum coverage and the insurance excess systems. Results are aggregated to compute the total annual expected loss for the entire Italian building stock, and the total income and profit margin for the insurance company assuming an insurance contract for all the property owners.

Furthermore, a back analysis of the losses to residential building stock incurred by 2009 L'Aquila and the 2002 Molise earthquakes is performed. This analysis consists in estimating the total loss caused by a seismic event to the building stock employing probabilistic loss assessment and comparing it to the actual losses.

2.3 SEISMIC LOSS ESTIMATION

Data from 2001 Italian census has been used to characterize the entire Italian building stock population (Istat 2001). To do this, Italy has been divided into 8088 areas, in correspondence Italian municipalities, assumed to belong to the same seismic zonation. For each municipality, the residential buildings have been divided based on structural typology and construction time, compatible with the building database classification, into following categories:

Structural typology

- masonry;
- RC (reinforced concrete);
- other.

Construction time

- Before 1919;
- From 1919 to 1945;
- From 1946 to 1961;
- From 1962 to 1971;
- From 1972 to 1981;
- From 1982 to 1991;
- From 1992 to 2001.

Table 2.1 reports the number of buildings belonging the each class for the whole Italian stock. It can be observed that the most of the buildings belong to the “before 1919” class. Furthermore, it can be also observed that masonry buildings are more numerous than RC buildings up to 1981; whereas, buildings belonging to “other” category are much less numerous.

Table 2.1 Number of residential buildings in Italy per construction time and structural typology (ISTAT 2001)

Construction Time	Structural typology			Total
	Masonry	RC	Other	
Before 1919	2.026.538	-	123.721	2.150.259
From 1919 to 1945	1.183.869	83.413	116.533	1.383.815
From 1946 to 1961	1.166.107	288.784	204.938	1.659.829
From 1962 to 1971	1.056.383	591.702	319.872	1.967.957
From 1972 to 1981	823.523	789.163	370.52	1.983.206
From 1982 to 1991	418.914	620.698	250.89	1.290.502
From 1992 to 2001	228.648	394.445	167.934	791.027
Total	6.903.982	2.768.205	1.554.408	11.226.595

Instead of referring to the number of buildings per category, the total surface area in square meters is used in order to be compatible with available information on the repair cost (reported per square meters of area). However, the building category break-down reported in Table 2.1 and normalized by unit area is available per only province and not per municipality. In particular, when the census was conducted, in 2001, the 8088 municipalities were divided into 103 provinces.

Hence, in order to obtain the disaggregated data per square meters per municipality, it has been assumed that the average square meters per building, for each of the category identified by the disaggregation, is constant for all the municipalities within each province. Hence, multiplying the number of buildings belonging to each subcategory in each municipality by the assumed average square meters per building, the building disaggregation reported in terms of total the square meters per

category per municipality was obtained. In Table 2.2, this disaggregation is reported for the whole Italian building stock.

Table 2.2 Total square meters in residential buildings in Italy classified per construction time and structural typology

Construction Time	Structural typology			Total
	Masonry	RC	Other	
Before 1919	452.461.897	-	27.622.990	480.084.887
From 1919 to 1945	264.320.537	18.623.487	26.018.136	308.962.161
From 1946 to 1961	260.354.844	64.476.342	45.756.179	370.587.365
From 1962 to 1971	235.856.942	132.108.359	71.417.310	439.382.611
From 1972 to 1981	183.866.663	176.195.160	82.725.408	442.787.230
From 1982 to 1991	93.530.259	138.582.249	56.015.809	288.128.317
From 1992 to 2001	51.049.873	88.067.104	37.494.355	176.611.333
Total	1.541.441.015	618.052.701	347.050.187	2.506.543.903

Regarding the building category marked as “Other”, no information is provided on the structural typologies included in this class. It can be argued that it refers to other typical structural typologies, i.e. wood structures, steel structures and combined RC-masonry structures. However, in the opinion of the authors, combined RC-masonry structures could constitute a large majority in this category. Therefore, the “other” category has been approximated to be composed totally of combined RC-masonry structures. Arguably, given the relatively small amount of square meters associated with the “other” category in comparison with “RC” and “masonry” categories, the inaccuracy caused by the above approximation most likely is not going to be significant.

2.4 SEISMIC RISK ASSESSMENT

2.4.1 Seismic hazard

The seismic hazard has been characterized in terms of Peak Ground Acceleration (PGA) and its annual probability of exceedance, in order to ensure independence on fundamental period of vibration of the buildings. The seismic hazard curve expressed in terms of the annual probability of exceeding various PGA values recorded at bedrock, has been extracted from the Italian Zonation by the National Institute of Geophysics and Volcanology (INGV) (OPCM-3519, 2006) for the centroid of each municipality, and has been assumed constant within the municipality. In order to obtain PGA hazard curves reflecting the soil category at the building foundation, the PGA values at the bedrock have been multiplied by the stratigraphic amplification factor S_S and the topographic amplification factor S_T , as defined by Eurocode 8 (EN 1998–1, 2003), that have been assumed constant within each municipality. The values for the above-mentioned amplification factors have been derived by Colombi and co-workers (Colombi et al. 2010) who estimated the average values for S_S and S_T , for each Italian municipality.

2.4.2 Seismic fragility

As the fragility curves to be used in the seismic risk model, it has been chosen to use the fragility curves available in literature and classified per structural category. An exhaustive literature survey has been conducted in order to individuate the fragility curves that could be potentially suitable for implementation in the seismic risk model. More than 70 works are identified, yielding fragility curves derived both empirically (based on in-situ observations) and analytically (based on simplified mechanical models), for the 3 considered structural typologies, namely, RC structures, masonry structures and combined RC-masonry structures. According to the adopted representation of the seismic hazard, only the fragility curves depicted as a function of PGA (and not the spectral acceleration) as

earthquake intensity measure (IM) have been selected. This has represented a major constraint for the choice of the fragility curves and has significantly restricted the number of fragility curves that were effectively suitable for this study.

Furthermore, it is observed that in many cases, for each structural typology, the fragility curves are

classified according to sub-categories that are not used in this study. For instance, in many cases, the fragility curve parameters are distinguished per different height values of the buildings (or the number of storeys) and per seismic-designed structures and gravity load-designed structures.

This is while the database available on the building stock cannot be disaggregated based on the height of the buildings. Hence, when possible, only fragility curves not classified according to specific building height values were selected. In other cases, the fragility curves referring to buildings with different height values have been collapsed in one fragility curve.

As far as it regards the distinction between the seismic-designed structures and the gravity load- designed structures, the building stock database does not provide any direct information to be used for disaggregation purposes. However, a critical review of the evolution of the seismic provisions in the Italian codes reveals some relevant information. In particular, two consecutive versions of the Italian code, released in 1974 (Legge 64, 1974) and in 1984 (DM 1984), adjourned the Italian seismic classification, established seismic design prescriptions for the new construction, and included new municipalities in the seismic zonation. Hence, for each municipality, all the structures built before the milestone date in which the municipality was classified as a risk-prone area (in 1974 or 1984), were considered to be gravity load-designed; whereas, the structures built after that date were considered to be seismic load-designed. In few cases, the municipalities have been included in the risk prone areas after 2001 (i.e., the date of the building census). In that case, the buildings in those

municipalities were considered entirely gravity load-designed. Moreover, since the census data is classified per decade (i.e. in 1971, 1981 and 2001), a linear variation with time was assumed in order to bridge the gap between the milestone years marking the code evolution and the census ten-year classification.

It is noteworthy that the above-mentioned distinction (i.e., seismic- and gravity loading- design) was done only for RC structures and combined RC-masonry. In fact, it can be argued that the masonry building stock may reveal the presence of earthquake-resistant elements (e.g. RC ring beams, metallic chains) even if built before the seismic prescriptions became mandatory. Therefore, based on the above-mentioned analysis, the original three structural categories were further split into five categories, namely:

- masonry structures;
- gravity load-designed RC structures;
- seismic load-designed RC structures;
- gravity load-designed combined RC-masonry structures;
- seismic load-designed combined RC-masonry structures.

Due to all the constraints in the choice of the fragility curves to be implemented, the final choice has been narrowed down to those works listed in Appendix 2.A and 2.B. Appendix 2.A and Appendix 2.B reports respectively 5 works for masonry structures, 11 works for seismic load- and gravity load-designed RC structures (one of them only refers to gravity load-designed structures), and only 1 work for both seismic load- and gravity load-designed combined RC-masonry structures were considered. For each of the selected works, Appendixes report the number of limit states for which the fragility curves are available, the logarithmic mean μ and standard deviation σ values, characterizing analytic lognormal fragility curves, together with a brief explanation of the methodologies, which have been used to derive them.

2.4.3 Exposed value

Each of the featured works reports the fragility curves corresponding to a number of limit states, varying between 2 and 5. The repair/reconstruction cost for each of the considered limit states, has been assumed to be deterministic and has been evaluated per square meter of the damaged property unit. A set of assumptions have been employed in order to define the unitary repair/reconstruction costs for different sets of limit states identified by each work featured. These set of assumptions have been explained in the following.

Let n be the number of limit states in a set of limit states, the reconstruction cost $RC(LS)$ corresponding to the ultimate limit state (i.e., the collapse limit state) has been assumed to be equal to $RC_{final}=1500€/m^2$. This stems from the fact that average construction costs for new structures in Italy is estimated to be to nearly $1300€/m^2$ (CRESME 2011), nearly uniform for all the Italian territory. This value has been rounded up to $1500€/m^2$ in order to account also for damages to the building content. Moreover, it has been assumed that the repair cost corresponding to the i -th intermediate limit states can be calculated from Equation 1, following, in terms of the reconstruction cost RC_{final} :

$$RC(LS) = \left(\frac{i}{n}\right)^\alpha RC_{final} \quad (1)$$

where α is a parameter that needs to be calibrated. It is evident that $\alpha=1$ renders a linear dependence of the repair costs on the final reconstruction cost; whereas, $\alpha>1$ leads to a reduction of the costs for the intermediate limit states. In this study, α has been preliminarily set equal to unity. In order to check the validity of this assumption, a back-analysis on the losses caused by L'Aquila 2009 and Molise 2002 earthquakes has been conducted (described in the following section). The definition of the

unitary loss for intermediate limits states based on Equation 1 has the advantage of rendering the definition of the intermediate limit states invariant with respect to the assumptions and definitions made in each single work with regard to these limit states.

2.5 LOSS ESTIMATION ACCORDING TO A PBEE APPROACH

Point estimates of the expected annual loss per square meter has been derived by integrating hazard, fragility and the exposed value, as described in the following. Within each municipality, seismic hazard has been computed in terms of the annual rate of exceeding a given PGA and denoted by $\lambda(PGA)$, with PGA varying between 0 and 2g. For each of the 5 structural typologies and for each of the works listed in Appendixes 2.1 and 2.2, a set of fragility curves has been computed in terms of probability of exceeding a given limit state LS given the PGA value and denoted by $P(LS/PGA)$. For each set of fragility curves composed by n limit states the reconstruction cost vector $RC(LS)$ has been computed according to Equation 1. Finally, the expected annual loss l per square meter can be calculated according to the following equation:

$$l = \sum_{LS=1}^n RC(LS) \int [P(LS | PGA) - P(LS + 1 | PGA)] d\lambda(PGA) \quad (2)$$

where for the last limit state, $P(n+1/PGA)=0$. The expected annual loss per square meter l is computed for each municipality (characterized by uniform seismicity), each structural typology and each set of fragility curves (logarithmic mean and standard deviation values for each limit state). In each municipality, this leads to distinct values of expected annual loss per structural typology; namely, 11 values for both the seismic and gravity load designed RC structures, 5 values for the masonry structures and only 1 value for both the seismic and gravity load designed combined

RC-masonry structures. Hence, for each structural typology and for each municipality, the mean value l_m has been calculated in order to take into account the uncertainty in the evaluation of the fragility curves per structural typology. Table 2.3 reports the maximum, minimum and mean value for l_m over the 8088 Italian municipalities. Looking at the range of expected annual loss per square meter in Table 2.3, significant variability in the expected annual loss can be observed within each structural typology, except for the combined RC-masonry structures where only one value has been computed. Moreover, it can be observed, by comparing the mean values, that masonry structures are expected to suffer much more significant losses than the other structural typologies. On the other hand, the seismic load-designed RC structures can be identified as the less vulnerable structural category. By comparing the seismic load-designed RC structures with the gravity load-designed RC structures, about 40% of reduction in the l_m values can be observed. This allows to appreciate the effect of retrofit operations aimed at changing the structural behaviour from that of the gravity load-designed structures towards that of the seismic load- designed structure. For each municipality, multiplying l_m by total square meters per each structural typology, the expected annual loss denoted by L_m is obtained for each structural category. The results for L_m are reported in Table 2.4. Since l_m values depend solely on the seismic hazard in each municipality, the maximum values for l_m may occur also in small municipalities located in highly seismic prone areas. On the contrary, the maximum values for L_m occur in large cities, since these values also depend on total square meters in each municipality; that is, the exposed value to seismic risk. Finally, the annual expected loss for the residential building stock in the entire Italian territory is derived and is reported in Table 2.4, by summing all the L_m values over all the municipalities.

Table 2.3 Expected annual loss per square meter

	Maximum value of l_m [€/year/m ²]	Municipality with the maximum l_m	Minimum value of l_m [€/year/m ²]	Municipality with the minimum l_m	Mean value of l_m [€/year/m ²]
Masonry structures	29.99	Giarre (Catania)	0.026	Solonghello (Alessandria)	5.21
gravity load designed RC structures	17.04	Giarre (Catania)	0.027	Cazzago Brabbia (Varese)	2.83
seismic load designed RC structures	11.34	Navelli (L'Aquila)	0.001	Solonghello (Alessandria)	1.75
gravity load designed combined RC-masonry structures	14.51	Giarre (Catania)	0.002	Solonghello (Alessandria)	2.39
seismic load designed combined RC-masonry structures	11.71	Navelli (L'Aquila)	0.001	Solonghello (Alessandria)	1.88

Table 2.4 Expected annual loss per municipality

	Maximum value of L_m [M€/year]	Municipality with the maximum L_m	Total expected loss per year [M€/year]
Masonry structures	196.4	Roma	8661.8
gravity load designed RC structures	51.5	Roma	1186.8
seismic load designed RC structures	8.0	Reggio Calabria	489.9
gravity load designed combined RC- masonry structures	25.1	Roma	667.2
seismic load designed combined RC- masonry structures	2.4	Napoli	174.0
		Total	11179.6

2.6 A BACK-ANALYSIS ON L'AQUILA 2009 AND MOLISE 2012 EARTHQUAKES

In order to validate the loss estimation model, a back analysis of the L'Aquila 2009 earthquake and the Molise 2002 earthquake has been conducted. The 6.3 moment-magnitude L'Aquila earthquake occurred on 6th of April, in 2009 and caused significant damage to the built environment. The 5.8 moment magnitude Molise earthquake occurred on 31st of October, in 2002. It was less intense than the L'Aquila earthquake, especially in terms of damages to the built environment.

A discrete version of Equation 2 reported below is used in order to calculate the specific loss values l for each municipality:

$$l = \sum_{LS=1}^n RC(LS) \left[P(LS | \overline{PGA}) - P(LS + 1 | \overline{PGA}) \right] \quad (3)$$

where \overline{PGA} denotes the PGA value at in the centroid of the municipality in question during the earthquake. Hence, the l values per square meter are treated as indicated in previous section. For each municipality, they are multiplied by total square meters per each structural category, to compute the total expected annual loss L in each municipality. It should be noted that in this case, the calculated loss values represent an average loss estimator over the entire municipality.

To derive the \overline{PGA} values, The ground motion prediction equation proposed by Sabetta and Pugliese (Sabetta and Pugliese 1996) have been used, computing the PGA at the centroid of the municipalities, given the epicentral distance and magnitude. The PGA values at the bedrock, have been amplified by the soil amplification factors, as previously described. For each municipality and each structural typology (except for the combined RC-masonry structures), different values of loss per square meters have been obtained, one for each of the considered fragility curve sets. The mean value l_m has been computed and integrated over the amount of square meters of each structural typology, deriving the loss L_m . Table 2.5 reports the values for the total loss, obtained by summing L_m over all the municipalities hit by the earthquake, for both the L'Aquila and the Molise event.

In particular, the reconstruction/rehabilitation costs for each limit state $RC(LS)$, in equation 3, have been computed, as previously illustrated, according to equation 1, assuming α equal to unity. This corresponds to a linear increase of the costs associated with each limit state, up to the reconstruction cost (i.e., 1500€ per square meter).

Table 2.5 Estimated loss caused by L’Aquila and Molise earthquakes

	Loss caused by the L’Aquila earthquake [M€]	Loss caused by the Molise earthquake [M€]
Masonry structures	4550.2	1247.3
gravity load designed RC structures	600.5	126.8
seismic load designed RC structures	301.7	17.1
gravity load designed combined RC-masonry structures	155.7	42.5
seismic load designed combined RC-masonry structures	81.4	13.1
Total	5689.5	1446.8

According to this model the total loss incurred to the residential building stock, caused by the L’Aquila earthquake, is equal to 5.7 billion Euros, whereas, the total loss caused by the Molise earthquake is equal to 1.4. In both cases, the values appear to be plausible, if compared with available data on the damages; albeit, so far, it is not easy to make a precise estimation of the damages. For the Molise earthquake, according to the Molise region administration (Regione Molise – Struttura Commissariale 2010), the damage to the private building stock is about 1.8 billion Euros, but this value includes also the non-residential structures. Gaining total loss estimates becomes more complicated in the case of L’Aquila Earthquake. As it regards the L’Aquila earthquake, the estimation is even more complicated. According to the reconstruction committee (Commissariato per la ricostruzione 2012), the amount so far allocated for the private reconstruction is about 5.9 billion Euros. However, this sum does not refer to residential buildings exclusively. Moreover, it should be also underlined that the reconstruction funds for private construction in

L'Aquila may not strictly correspond to the suffered damages; that is, a part of such funds for sure have been allocated to strengthening the buildings beyond their original conditions.

2.7 THE INSURANCE MODEL

The model here presented is based on a monopoly market insurance system. It is built for the generic home-owner of a 1 square meter property unit. The probability that an earthquake hits the structure is calculated as $\Pi = P(PGA > 0)$ or the annual probability that the peak ground acceleration is greater zero. This value can be seen as a measure of the seismicity of the zone. For each level of ground-shaking expressed as PGA_i , (e.g., $0 \leq PGA_i \leq 2g$), the home owner is going to suffer an expected annual loss value equal to $L(PGA_i) = E[l|PGA_i]$ (hereafter referred to as L_i in the text) which is going to lead to a reduction in his house wealth denoted by W_o . $L(PGA_i)$ is evaluated, for each structural typology, over all the different fragility models considered and the structural limit states, according to equation 4:

$$E[L_i | PGA_i] = \frac{1}{N_f} \sum_{j=1}^{N_f} \left[\sum_{LS=1}^n RC(LS) [P_j(LS | PGA_i) - P_j(LS+1 | PGA_i)] \right] \quad (4)$$

where N_f denotes the total number of fragility models considered per building type and $P_j(LS/PGA_i)$ denotes the fragility model j for limit state LS and ground-shaking intensity PGA_i . Denoting the annual probability that the ground shaking is equal to PGA_i as π_i , the probability that an earthquake hits the structure can be calculated as shown in equation 5:

$$P(PGA > 0) \cong \sum_{i=1}^N \pi_i = \Pi \quad (5)$$

Note that the right-hand summation is a discrete approximation of the integral over all possible PGA values and N is the number of discretized values (e.g., $N=200$ in the case-study).

However, the home-owner may decide to make an insurance contract providing him with a transfer x_i in case the loss occurs. The contract is made at a price equal p , which is the premium paid by the consumer to the insurance company. The house wealth W_0 can be assumed equal to the reconstruction cost (e.g., 1500€ for the case under study, as explained beforehand), since this is the maximum cost incurred in case of a seismic event to order in order to replace the property unit.

The insurance model can be expressed in terms of a utility function U which reflects the net profit gained by the property owner. Assuming risk aversion of the home-owner, the utility U of the property owner can be expressed with a weaker than linear function of the wealth W . Therefore, the natural logarithm of $W+I$ is used, to have only positive values for U . Hence, in case the property owner does not make an insurance contract, the expected utility U can be calculated as the sum of two terms: one is related to the case in which no earthquake occurs (with probability $P(PGA=0)=1-I$) and the value W_0 remains invariant; the second term is related to the case in which an earthquake with intensity PGA_i takes place (with probability π_i) and the value W_0 is reduced by the loss L_i . Thus, the expected utility U_n can be calculated as (equation 6):

$$U_n = (1 - \Pi) \ln(W_0 + 1) + \sum_i \pi_i \ln(W_0 - L(PGA_i) + 1) \quad (6)$$

Alternatively, in case the property owner does make an insurance contract, the expected utility U can be still calculated as the sum of two terms: the first term is related to the case in which no earthquake occurs (with probability $P(PGA=0)=1-I$) and the value W_0 is reduced by the premium p ; the second term is related to the case in which an earthquake with

intensity PGA_i takes place (with probability π_i) and the initial capital W_0 is reduced by both the premium p and the loss L_i and increased by the transfer $x(L_i)$ (which for the sake of simplicity is hereafter referred to as x_i in the text), paid by the insurance company. Therefore, the expected utility can be calculated as:

$$U = (1 - \Pi) \ln(W_0 - p + 1) + \sum_i \pi_i \ln(W_0 - p - L_i + x(L_i) + 1) \quad (7)$$

In which the insurance company is assumed to be risk neutral and makes a take-it-or-leave-it offer in a monopoly market to the home-owner for the payment x_i if the loss L_i occurs. It is assumed that the consumer accepts the contract if the expected utility U is greater than or equal to the expected utility U_n . This condition can be written as:

$$\ln\left(\frac{W_0 + 1}{W_0 - p + 1}\right)^{(1-\Pi)} + \ln\left(\frac{\prod_i (W_0 - L_i + 1)^{\pi_i}}{\prod_i (W_0 - p - L_i + x_i + 1)^{\pi_i}}\right) \leq 0 \quad (8)$$

where the loss L_i cannot be greater than the house wealth W_0 .

Generally, the transfer x_i , paid by the insurance company in case an event takes place, is fixed by the insurance contract and depends on L_i . It can be fixed as equal to L_i , that is the insurance company commits to cover all the occurred loss (i.e. full insurance), or a portion of it. In the latter case, a maximum coverage can be established, that is the transfer x_i cannot go beyond a fixed value M :

$$\begin{aligned} x_i &= L_i; \forall L_i \leq M \\ x_i &= M; \forall L_i > M \end{aligned} \quad (9)$$

Furthermore, also an insurance excess can be introduced, that is the transfer x_i is equal to L_i minus a certain amount E :

$$\begin{aligned} x_i &= 0; \forall L_i \leq E \\ x_i &= L_i - E; \forall L_i > E \end{aligned} \quad (10)$$

Conditions 9 and 10 can be also applied together, with a maximum coverage and an insurance excess. Obviously, as the maximum coverage decreases and the excess increases the company insurance is going to pay less in case of an earthquake, but the premium p , to be paid yearly by the home owner, decreases.

Thus, the expected contribution to the profit of the company insurance provided by a specific home owner can be calculated by summing up the expenses incurred to the company in case an earthquake with ground-shaking intensity equal to PGA_i takes place:

$$P = p - \sum_i x_i \pi_i \quad (11)$$

where the expenses are represented by the transfer x_i , multiplied by the probability π_i that an earthquake with intensity PGA_i takes place, in a risk neutral formulation.

In a monopoly market, the insurance company fixes the premium in order to maximize its profit. The upper bound limit to the premium is represented by the inequality 8; that is, the home owner will consider it advantageous to enter into the insurance contract and pay the premium only if it is satisfied.

Hence, the premium p can be derived by solving the following optimization problem: maximize the profit P (defined in equation 11), given that home owner utility in case of insurance contract, U , is greater than utility without insurance contract, U_n (defined in inequality 8). In this

optimization problem, loss values L_i are known (equation 4) as well as transfer values x_i (equations 9 and/or 10).

2.8 A REAL APPLICATION: THE ITALIAN RESIDENTIAL BUILDING STOCK

The loss estimation model and the insurance model have been applied to the Italian residential building stock. In particular, the insurance optimization problem (described in previous section) has been posed for a 1 square meter property owner, for each structural typology in each municipality, to derive the specific premium to be paid to buy an insurance contract. To do this, for each municipality, the vector of ground-shaking intensity probabilities π_i has been derived by discretizing the differential $d\lambda(PGA)$. For each structural typology, the loss values L_i , conditioned on the earthquake intensity i , have been derived by from Equation 4 by as an average over all the loss values calculated for the various fragility models considered (except for the combined RC-masonry structures where only one set is available). The transfer values x_i have been calculated by considering a maximum coverage M and an insurance excess E , according to equation 9 and 10, respectively. In particular, M has been assumed equal to [700; 800; 900; 1000; 1100; 1200; 1300; 1400; 1500]€/m² and E has been assumed equal to [0; 100; 200; 300; 400; 500] €/m². Table 2.6 refers to the full insurance case (i.e. $M=1500€/m^2$; $E=0€/m^2$) and reports the maximum and minimum value of the premium per year, together with the municipalities where these values occur, for all the considered structural typologies. The average value within all the municipalities is also reported. It can be observed that the maximum and minimum premium values occur in the same municipalities of the corresponding loss values. Furthermore, the premium values are about the 60% greater than the corresponding loss values. This increase is due to the risk aversion of the property owner, who prefers to pay more than the

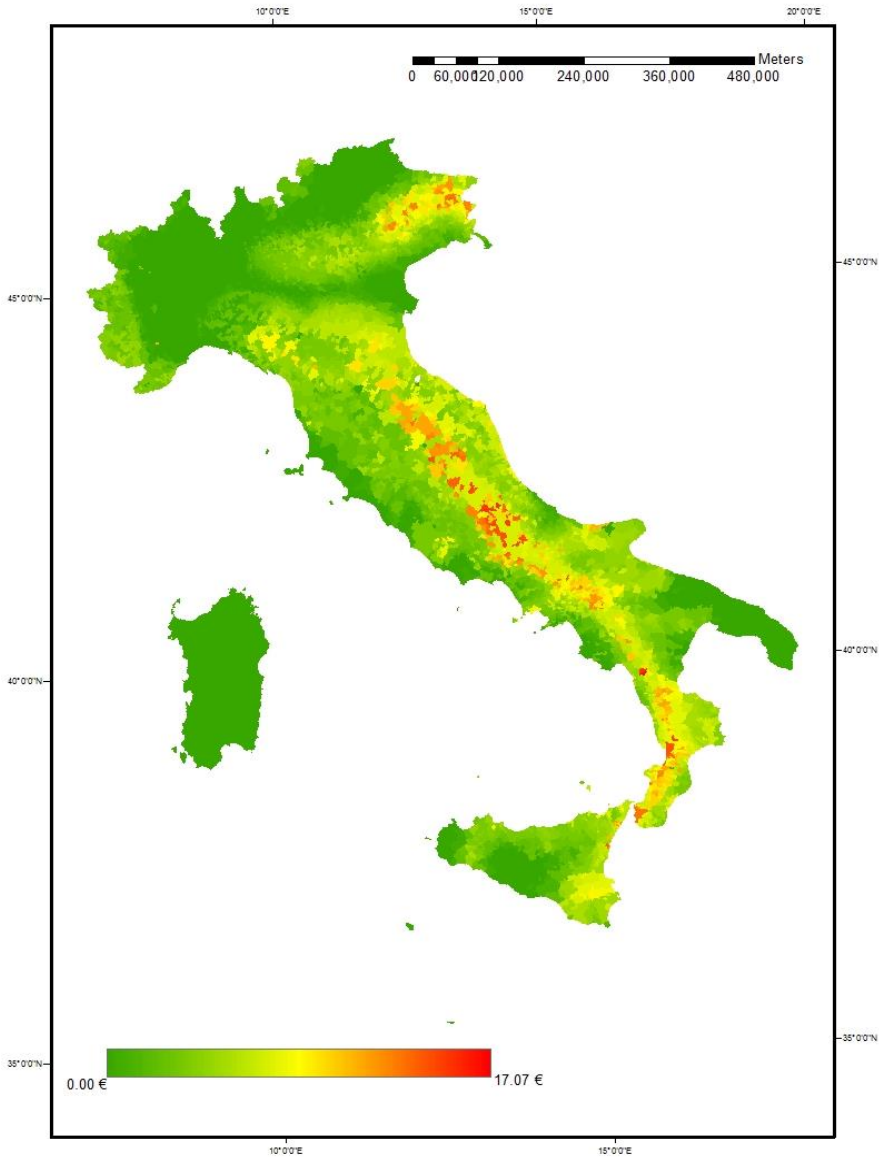
expected loss in order to avoid to directly face the actual loss, once an earthquake event would occur.

Table 2.6 Yearly insurance premium per square meter in case of full insurance model

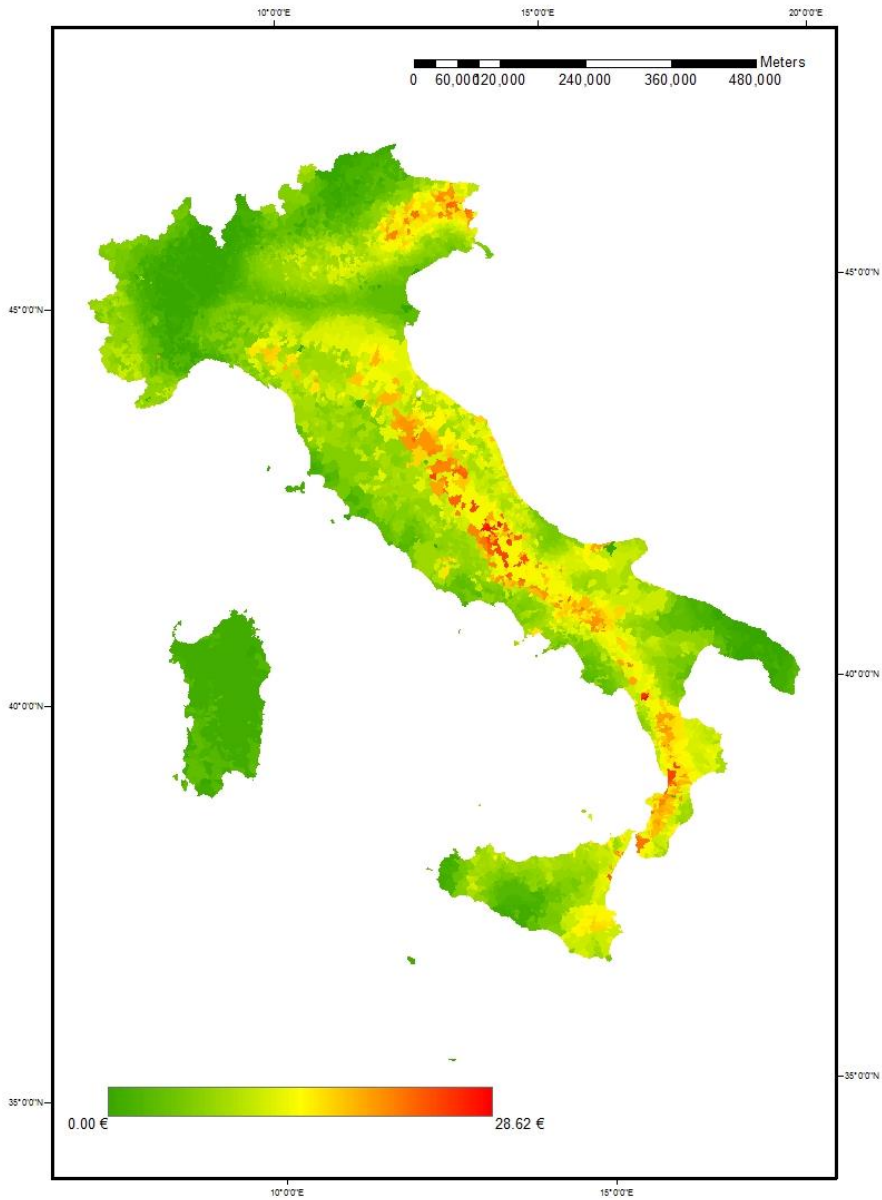
	Maximum value of p [€/year/m ²]	Municipality where the maximum p takes place	Minimum value of p [€/year/m ²]	Municipality where the minimum p takes place	Mean value of p [€/year/m ²]
Masonry structures	50.50	Giarre (Catania)	0.026	Solonghello (Alessandria)	8.62
gravity load designed RC structures	28.62	Giarre (Catania)	0.027	Cazzago Brabbia (Varese)	4.17
seismic load designed RC structures	17.07	Navelli (L'Aquila)	0.001	Solonghello (Alessandria)	2.30
gravity load designed combined RC- masonry structures	21.67	Giarre (Catania)	0.002	Solonghello (Alessandria)	3.23
seismic load designed combined RC- masonry structures	17.37	Navelli (L'Aquila)	0.001	Solonghello (Alessandria)	2.44

Figure 2.1 reports the distribution of the yearly insurance premium per square meter in case of full insurance model for the seismic and gravity load designed RC structures. It can be observed that the premium per square meter has a distribution very similar to the seismic hazard. Figure 2.2 reports the distribution of the total premium paid within each municipality, by all the property owners, in case of full insurance model. It

represents the total income for the insurance company. It can be observed that the highest values are paid by the large municipalities, even if the hazard is moderate, as Rome and Naples.



(a)



(b)

Figure 2.1 Yearly insurance premium per square meter for seismic (a) and gravity (b) load designed RC structures in case of full insurance model

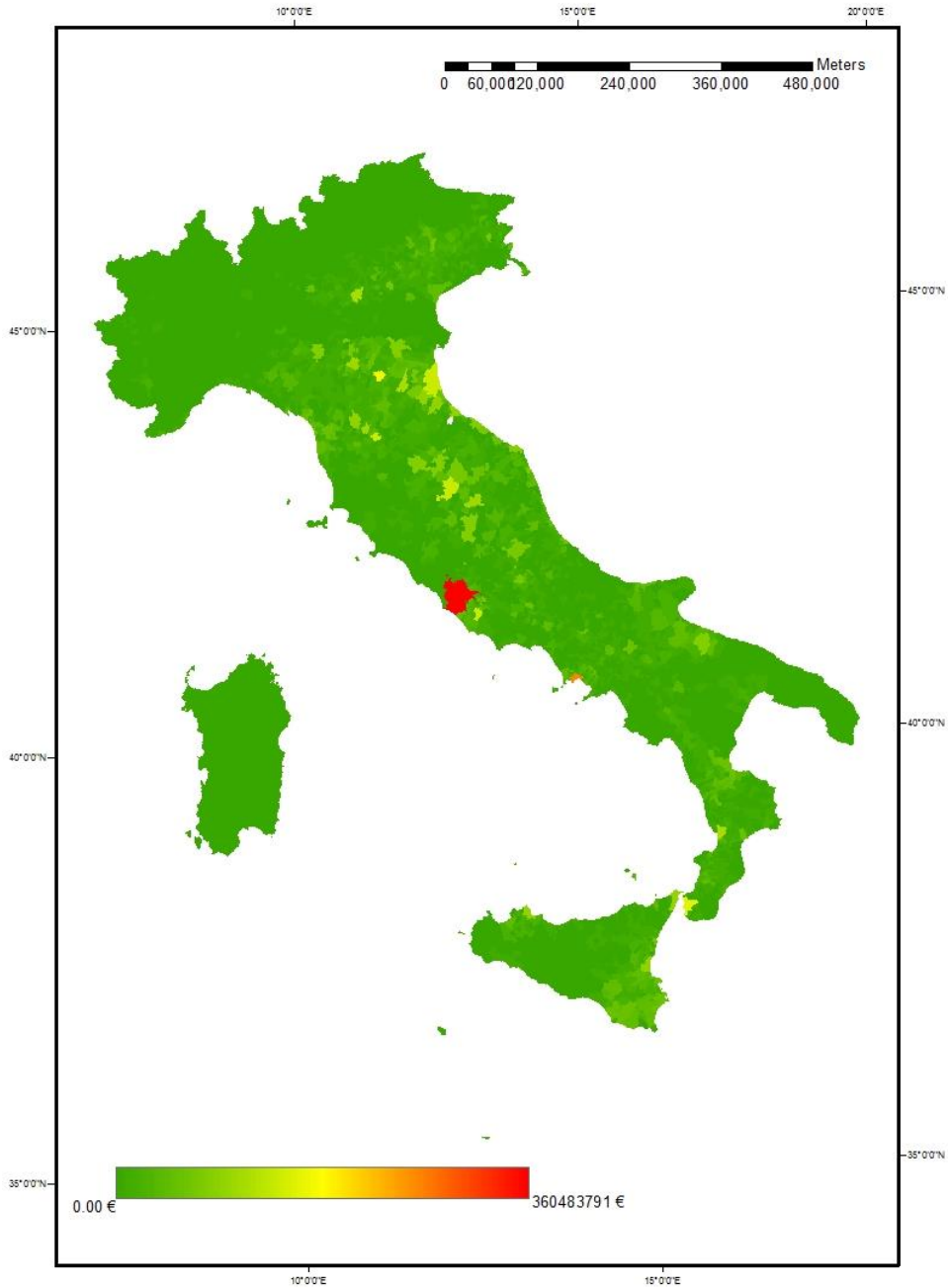


Figure 2.2 Yearly total insurance premium per municipality in case of full insurance model

The introduction of the maximum coverage and the insurance excess significantly reduces the premium values. The average p is reported in Table 2.7 for the masonry structural typology, for the considered values of M and E . It can be observed that the premium value, in case of full insurance contract, is equal to 8.62€/ m² and it significantly reduces as the maximum coverage reduces and the excess increases.

Table 2.7 Average premium for masonry structures at different maximum coverage and insurance excess values

Average premium for masonry structures [€/m ²]		Insurance excess				
		E=0€/m ²	E=100€/m ²	E=200€/m ²	E=300€/m ²	E=400€/m ²
Maximum coverage	M=700€/m ²	7.41	5.93	4.85	3.91	3.04
	M=800€/m ²	7.72	6.27	5.23	4.34	3.55
	M=900€/m ²	7.96	6.54	5.54	4.68	3.94
	M=1000€/m ²	8.17	6.76	5.78	4.95	4.25
	M=1100€/m ²	8.33	6.94	5.97	5.17	4.49
	M=1200€/m ²	8.46	7.07	6.12	5.33	4.67
	M=1300€/m ²	8.55	7.17	6.23	5.45	4.80
	M=1400€/m ²	8.60	7.23	6.30	5.52	4.88
	M=1500€/m ²	8.62	7.25	6.31	5.54	4.90

Multiplying the premium p in each municipality, the profit P and the expected expenses $\sum_i x_i \pi_i$, by the total amount of square meters per each structural typology, estimates of the total income p_{tot} , the total profit P_{tot} and the total expected expenses x_{tot} , per year, are obtained for the insurance company. Tables 2.8, 2.9 and 2.10 report these values for all the considered maximum coverage and insurance excess values. Also in this case, it can be observed that the insurance excess and the maximum coverage reduce the income, profit and expense values of the insurance company, as the risk is progressively moved from the insurance company to the home owner.

Table 2.8 Total annual income at different maximum coverage and insurance excess values

Total annual income p_{tot} [M€]		Insurance excess				
		E=0€/m ²	E=100€/m ²	E=200€/m ²	E=300€/m ²	E=400€/m ²
Maximum coverage	M=700€/m ²	15344	12029	9732	7744	5946
	M=800€/m ²	15959	12708	10490	8605	6947
	M=900€/m ²	16450	13247	11088	9276	7713
	M=1000€/m ²	16842	13674	11558	9800	8304
	M=1100€/m ²	17147	14005	11920	10199	8750
	M=1200€/m ²	17372	14249	12186	10491	9074
	M=1300€/m ²	17530	14419	12370	10693	9296
	M=1400€/m ²	17618	14513	12472	10803	9417
	M=1500€/m ²	17636	14533	12493	10827	9442

Table 2.9 Total annual profit at different maximum coverage and insurance excess values

Total annual profit P_{tot} [M€]		Insurance excess				
		E=0€/m ²	E=100€/m ²	E=200€/m ²	E=300€/m ²	E=400€/m ²
Maximum coverage	M=700€/m ²	60068	57063	52493	46548	39224
	M=800€/m ²	61727	59360	55588	50674	44735
	M=900€/m ²	62877	60987	57800	53617	48634
	M=1000€/m ²	63643	62110	59353	55703	51390
	M=1100€/m ²	64123	62850	60405	57132	53292
	M=1200€/m ²	64396	63305	61078	58069	54546
	M=1300€/m ²	64523	63555	61472	58631	55313
	M=1400€/m ²	64564	63661	61653	58903	55690
	M=1500€/m ²	64566	63676	61684	58952	55759

Table 2.10 Total expenses per year at different maximum coverage and insurance excess values

Total expenses per year x_{tot} [M€]		Insurance excess				
		E=0€/m ²	E=100€/m ²	E=200€/m ²	E=300€/m ²	E=400€/m ²
Maximum coverage	M=700€/m ²	9337	6323	4482	3089	2024
	M=800€/m ²	9786	6772	4931	3538	2473
	M=900€/m ²	10163	7148	5308	3914	2850
	M=1000€/m ²	10478	7463	5623	4229	3165
	M=1100€/m ²	10734	7720	5879	4486	3421

M=1200€/m ²	10933	7918	6078	4684	3620
M=1300€/m ²	11078	8063	6223	4829	3764
M=1400€/m ²	11161	8147	6306	4913	3848
M=1500€/m ²	11180*	8165	6325	4931	3866

*this value coincides with the total expected loss per year for the whole Italian building stock

2.8.1 Discussion on the case study

A seismic insurance model has been built for the Italian building stock, accounting for the site specific hazard in 8088 Italian municipalities and discretizing the building portfolio in 5 structural typologies. The insurance model builds itself upon a probabilistic loss estimation model resulting in the annual expected loss and in the annual insurance premium for the property owners in each Italian municipality. The obtained results showed high variations in the insurance premium among different Italian municipalities as a result of the variations in the seismic risk across the Italian territory. In each municipality, as a result of the variations in the seismic vulnerability per structural typology, a significant difference between the insurance premium calculated for various structural typologies was observed. It can be observed that the maximum insurance premium values occur in areas that are highly prone to seismic risk (Appennine area and East Sicily), whereas the minimum values are obtained in areas with relatively low seismic risk; such as, in Piemonte and Lombardia regions.

It is also interesting to compare the losses for the two companion categories, i.e. seismic- and gravity-load designed structures. It can be observed that the expected loss and insurance premium per square meter for the gravity load designed structures is almost 1.4 times that of the seismic load designed structures. This difference can be interpreted as the potential reduction, induced by seismic retrofit operations, of the expected loss and, as a consequence, of the insurance premium to be paid.

Finally, it is emphasized that this study represents an effort in analyzing the feasibility of a seismic insurance system, extended to all the Italian

residential building stock. Further investigations need to be conducted in order to introduce more detailed hypothesis and in order to obtain a more sophisticated simulation. In particular:

- The Italian residential building stock was discretized in just 5 typologies. It is desirable to perform a more refined discretization accounting for building height, regularity/ irregularity, age, retrofitting/ maintenance operations, etc.
- The costs per square meter to be incurred in case of damage, per each limit state need to be modelled as dependent on both the location of the building and also on the structural typologies;
- A full insurance-monopoly market was assumed; more complex cases such as private/public re-insurance mechanisms can be considered.
- The entire Italian residential building stock was assumed to be covered by an insurance policy. Moreover, the insurance model can also take into account the public incentive to contract the insurance policy.

CHAPTER 3

INSURANCE SCENARIOS AGAINST SEISMIC CATASTROPHES: REMARKS BASED ON HISTORICAL CATALOGUE.

Damage from natural events such as windstorms, earthquakes, storm surges and lightning causes economic losses amounting to billions of dollars throughout the world every year. Hurricane Sandy in 2012, for instance, caused losses of 19 billion dollars, while the earthquakes that occurred in New Zealand and Japan led to 2011 being a record year for catastrophic losses, with 380 billion dollars paid out, as estimated by Munich Re (2011).

It is clear from the world map of natural hazards below (Figure 3.1) that natural risks threaten global and local communities more than ever, and are thus a source of great concern for national governments today.

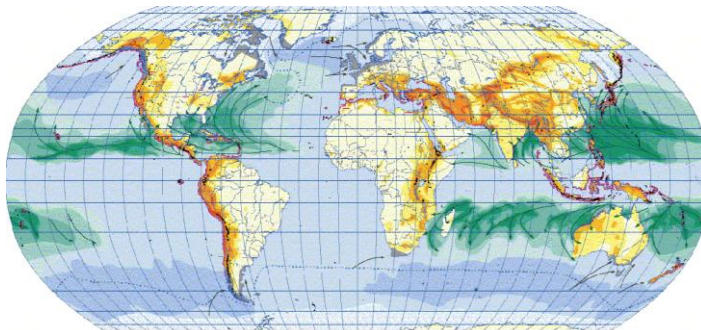


Figure 3.1 World map of natural hazards, developed and updated by Munich Re (2011)**Errore. L'origine riferimento non è stata trovata.**

Private insurance is now one of the most effective ways to mitigate losses from natural disasters. Insurance also allows for the spread of such losses, and encourages property owners to adopt risk reduction measures

and support the management of catastrophe risks within urban environments. Unfortunately, attempts to roll-out such insurance systems face a number of different problems, particularly when dealing with the private householder's market. Indeed, householders have a very low perception of risk and are risk adverse, i.e. they are unwilling to either spend their money on buying a product that will not necessarily provide value (insurance) or voluntarily adopt cost-effective protective measures (which can reduce insurance premiums). Consequently, they are often uninsured and do not invest in retrofits to prevent and mitigate the losses caused by natural disasters (Kesete et al. 2014).

Yet the risk is even higher for the insurance industry. Indeed, in the aftermath of a disaster, insurers are prone to insolvencies and significant destabilization. There are also problems due to the high risk of the industry exceeding its financial capacity and facing cash flow issues, all of which leads to very high insurance premiums.

Looking at the 10 costliest events that occurred from 1980 to 2014, it is notable that six of them were earth-quakes (Figure 3.2).

Date	Event	Affected area	Overall losses in US\$ m original values	Insured losses in US\$ m original values	Fatalities
11.3.2011	Earthquake, tsunami	Japan: Aomori, Chiba, Fukushima, Ibaraki, Iwate, Miyagi, Tochigi, Tokyo, Yamagata	210,000	40,000	15,880
25-30.8.2005	Hurricane Katrina, storm surge	USA: LA, MS, AL, FL	125,000	62,200	1,322
17.1.1995	Earthquake	Japan: Hyogo, Kobe, Osaka, Kyoto	100,000	3,000	6,430
12.5.2008	Earthquake	China: Sichuan, Miayang, Beichuan, Wenchuan, Shifang, Chengdu, Guangyuan, Ngawa, Ya'an	85,000	300	84,000
23-31.10.2012	Hurricane Sandy, storm surge	Bahamas, Cuba, Dominican Republic, Haiti, Jamaica, Puerto Rico, USA, Canada	68,500	29,500	210
17.1.1994	Earthquake	USA: CA, Northridge, Los Angeles, San Fernando Valley, Ventura, Orange	44,000	15,300	61
1.8-15.11.2011	Floods	Thailand: Phichit, Nakhon Sawan, Phra Nakhon Si Ayutthaya, Pathumthani, Nonthaburi, Bangkok	43,000	16,000	813
6-14.9.2008	Hurricane Ike	USA, Cuba, Haiti, Dominican Republic, Turks and Caicos Islands, Bahamas	38,000	18,500	170
27.2.2010	Earthquake, tsunami	Chile: Concepción, Metropolitana, Rancagua, Talca, Temuco, Valparaíso	30,000	8,000	520
23.10.2004	Earthquake	Japan: Honshu, Niigata, Ojya, Tokyo, Nagaoka, Yamakoshi	28,000	760	46

Source: Munich Re, NatCatSERVICE, 2015

Figure 3.2 List of the 10 costliest events worldwide from 1980 to 2014 (Munich Re 2015)

Italy is a particularly seismic-prone area, and has been affected by over 30,000 medium- and high-magnitude earthquakes in the last 2500 years. With this in mind, the study described in this Chapter proposes predictive relationships for the actual expected losses given the magnitude of the occurred seismic event. This methodology has been developed to help communities to improve their capacity to withstand natural catastrophes like earthquakes. As most Italian earthquakes are due to the activity of faults, their locations and mechanisms can be, at least approximately, be predicted. As a consequence, it can be assumed that expected seismic events may be similar to those in the past and collected in the Italian historical catalogue produced by the National Institute of Geophysics and Volcanology (INGV 2004).

In this study, a scenario analysis is performed of historical earthquakes with a magnitude greater than 4 within a full-scale study. Actual exposure is assumed by accounting for residential buildings located in each Italian municipality that is prone to experiencing seismic events. Total losses for the entire national building portfolio are then computed for each event, depending on the site-specific seismic hazard.

The results are processed through a regression analysis to reveal the relationships between expected losses and magnitude. Furthermore, bin processing of the empirical results was also performed to highlight the most effective predictive curve for seismic loss assessments that can potentially be used by the insurance industry in Italy.

3.1 SUPPORTING THE INSURANCE INDUSTRY WITH A PBEE-BASED METHODOLOGY

As a tool for the insurance industry, the methodology proposed in this study uses an engineering-based instrument for the efficient and prompt forecasting of seismic losses on the basis of the magnitude of an expected seismic event.

Traditional, and often too conservative, practices concerning catastrophic losses can lead to the overestimation of premiums, and can thus be improved, with the result being more affordable insurance. The scenario analysis set out in this study will ensure that more detailed knowledge of potential losses is available. As a result, insurers will be able to mitigate their insolvency risks, while reinsurers and governments can be involved in the interactions between insurers and property owners.

A realistic correlation between seismic effects at different locations and on multiple structures is considered when performing the scenario analysis. Indeed, a more accurate description of aggregate seismic losses is possible through the modelling of Italy's building stock as a spatially distributed system, with reference to each municipality (ISTAT 2011). Accordingly, the accumulation of seismic losses is also recognizable based on the seismic hazards faced by each site, as defined by the Italian seismic code.

Such a methodology also allows insurers to assess a type of region-specific loss ratio (Jaiswal and Wald 2013) that is based on historical earthquake characteristics and represents the seismic risk in a disaggregated manner. Expected direct losses are evaluated for actual assets, and a realistic correlation of seismic effects is modelled by taking into account two limit cases for the ground motion variability representation. Consequently, a case in which there is partial correlation between, and variability among, the peak ground acceleration (PGA) values in each municipality was modelled, as is a case in which there is no correlation. Losses were then evaluated for each case and the results in terms of the predictive relationship of losses against magnitude are compared.

The procedure used to draw loss curves vis-a-vis magnitude is also described.

3.1.1 What is needed to implement the methodology

The primary requirement for effectively implementing the methodology proposed in this study is a database containing the details of all previous seismic events in the studied area.

To develop the proposed macro-economic-based approach, data on losses at diverse seismic intensities (in the present study the magnitude) are needed to examine the experimental relationship between loss and the intensity measure (IM). Such information is obtained by performing a scenario analysis based on historical earth-quake data, although this information is rarely available for most historical seismic events worldwide (Jaiswal and Wald 2013).

Nonetheless, in Italy, the National Institute of Geophysics and Volcanology (INGV) and the Department of Civil Protection have developed a very precise database/catalogue that accounts for all previous seismic events in the country. In particular, this resource covers more than 1,100 events from 217 b.C. to 2002 with a magnitude greater than 4.

The INGV catalogue (Figure 3.3) provides a number of parameters that are fundamental for the implementation of the scenario analysis, such as the geographical coordinates of the epicentre and magnitude of each event.

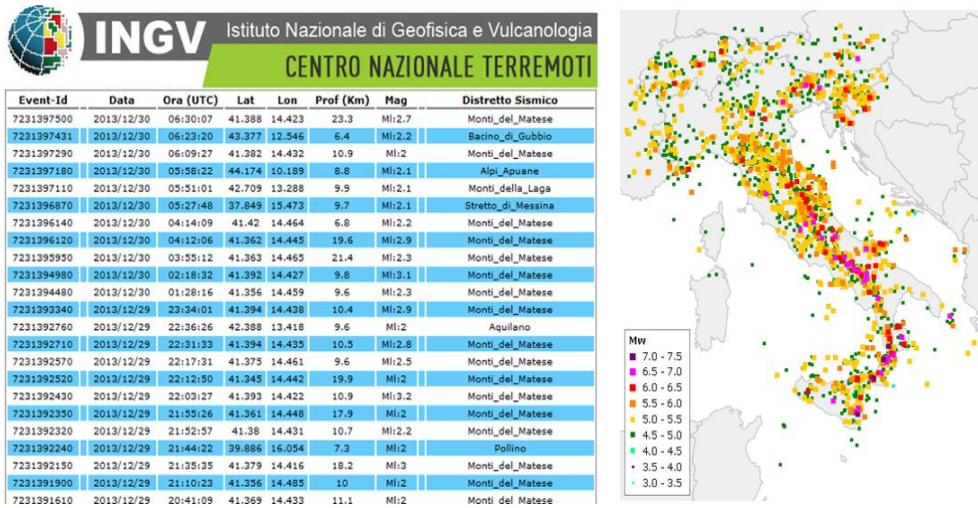


Figure 3.3 The Italian historical catalogue of earthquakes from INGV (INGV 2004)

It can be seen from the map that earthquakes with different intensities have been experienced throughout the Italian peninsula. As is well known, the seismic hazard levels in Italy, as well as the dominant earthquakes in terms of expected magnitude and damage, are different according to the area being examined. This is due to diverse local exposure and, above all, seismic hazard distribution, as shown in Figure 3.4.

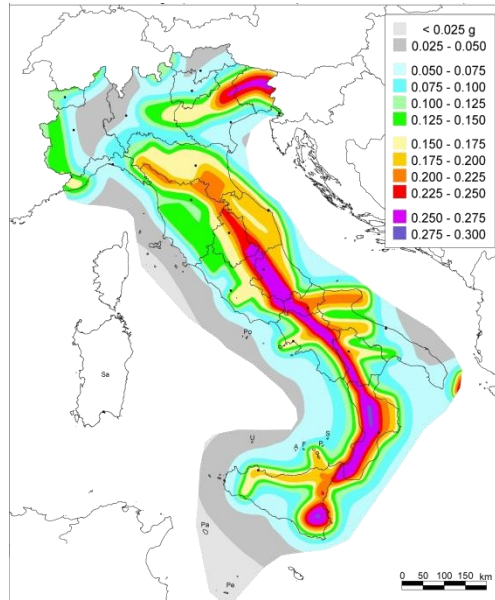


Figure 3.4 Map of seismic hazards for the Italian peninsula (OPCM 3519 - 2006); 10 percent probability of exceedance in 50 years

For instance, the most vulnerable areas are the Alps, the Apennines and the Calabrian arch. An example is the annual rate of seismic events experienced in diverse Italian municipalities over the return period of 475 years, which is a common probability level examined for seismic risk management. The annual rate in terms of the expected PGA is equal to 0.25g for the city of Messina (Calabrian arch), 0.26g for L’Aquila (Apennines) and 0.49g, which is the maximum value, for the municipality of Laino Castello (Cosenza), as it is located right on the Calabrian arch. In contrast, municipalities and cities located outside such areas have lower expected PGA values. This is, for example, the case for Milan, with a PGA equal to only 0.06g, Gallarate (Varese) with a PGA of 0.04g and Cagliari with PGA of 0.05g.

Studies of historical earthquakes show that seismic events often occur in areas that have already been hit in the past. Furthermore, expected event typologies in Italy are similar, due to the trigger sources, which are focal mechanisms that are particularly related to dip-slip (normal and reverse)

faults. As a consequence, it makes sense to develop a predictive relationship based on this type of information.

An analysis to establish the ground motion-damage relationship, which accounts for diverse structure types, can only be performed in places where building census and vulnerability data are available or can be easily inferred for each structural scheme (Jaiswal and Wald 2013).

Consequently, as a second source, data about the population and construction materials of existing residential buildings is required. Indeed, it is fundamental to know the exposure of a studied area, the age of its buildings, and the materials used to construct them.

Such information is essential when it comes to evaluating the exposure, and then also the vulnerability, of the built environment according to the performance-based earthquake engineering (PBEE) approach (Goulet et al. 2007).

The main assumption is made by assessing expected seismic losses as against actual national exposure. The Italian building stock is modelled in this study by also accounting for its spatial distribution with respect to each municipality according to the 14th census database of the National Institute of Statistics (ISTAT 2001). The database accounts for the number of residential buildings in each municipality, their diverse construction materials (reinforced concrete, masonry or mixed buildings), and the age of construction, i.e. seismically or non-seismically designed.

The vulnerability of the Italian building stock is also evaluated through the implementation of seismic fragility curves. These define the fragility of buildings in terms of the structural limit state probability of exceedance as a function of an intensity measure (IM) of an earthquake. In the present study, a set of fragility curves from the literature is used with respect to the PGA. Several studies from the literature were also investigated, with those that refer to typical European structural typologies selected for this study (Ahmad et al. 2011; Borzi et al. 2007, 2008; Crowley et al. 2008; Erberik 2008; Kappos et al. 2003, 2006; Kostov et al. 2004; Kwon and

Elnashai 2006; Lagomarsino and Giovinazzi 2006; Ozmen et al. 2010; Rota et al. 2010; Spence 2007; Tsionis et al. 2011).

The curves are selected by also referring to the structural typologies, which are identified from the ISTAT dataset (ISTAT 2011). As a result, vulnerability is evaluated for seismically and non-seismically reinforced concrete buildings, non-seismically designed masonry buildings, and seismically and non-seismically constructed mixed buildings.

Fragility curves, which classify residential buildings according to the examined diverse structural typologies, are used, while, on the basis of the PGA, the probability of exceedance of the limit state l_s is provided by Equation 1 as follows:

$$P[LS = l_s / PGA] = F_{LS,i}(PGA) - F_{LS+1,i}(PGA) \quad \text{with} \quad 1 \leq l_s \leq j \quad (1)$$

with each set of curves averaged for each building typology, i .

3.1.2 Earthquake scenario analysis: accounting for seismic ground shaking correlations

Earthquake scenarios are generated through statistical simulations of historical events. In particular, a normal distribution is used to describe the probability distribution for the intensity measure given the various ground motion source and path parameters, which is obtained in each municipality for each earthquake. The PGA is used as the intensity parameter, the values of which are calculated according to the attenuation law of Bindi et al. (Bindi et al. 2009). It is in fact possible to consider a single ground-motion parameter, as is the case in many ground-motion prediction equations (GMPE). Such a univariate approach is advocated as it regards ground-motion parameters as almost multivariate log-normal variables (Goda and Atkinson 2009).

The GMPE of Bindi et al. (Bindi et al. 2009) adopts the same functional form as the formula from Sabetta and Pugliese (Sabetta and Pugliese 1996), but updates its coefficients, as shown in Equation 2:

$$\log_{10}(PGA) = -1.344 + 0.328 \cdot M - \log_{10} \sqrt{(R^2 + h^2)} + 0.262S_i \pm \sigma \quad (2)$$

Some assumptions are made in the context of the present study: M is assumed to be equal to M_{sp} , which is the corrected magnitude according to Sabetta and Pugliese (Sabetta and Pugliese 1996), and is also provided by the INGV catalogue; and R is taken to be the epicentral distance from the centre of each municipality [km]. For municipalities less than 5 km from an epicentre, the PGA is assumed to be equal to the epicentre. Meanwhile, for municipalities greater than 100 km from an epicentre, the PGA is assumed to be zero.

In this first step, S_i is assumed to be zero, which means that the PGA is evaluated by making assumptions about rock soil conditions. Meanwhile, σ is the standard deviation of the log of the PGA and is provided by Equation 3 as follows:

$$\sigma^2 = \sigma_{inter}^2 + \sigma_{intra}^2 = (0.174)^2 + (0.222)^2 \quad (3)$$

where σ_{inter} is the inter-event standard deviation and σ_{intra} the intra-event standard deviation.

When dealing with the simulation of earthquake scenarios, the inter- and intra-event variability must be taken into account, especially when considering spatially distributed systems such as a residential portfolio. Spatially distributed systems are in fact exposed to simultaneous excitations when an earthquake occurs. Accordingly, the correlation between seismic effects is very important when assessing seismic losses, because it can potentially affect the probability distribution of seismic damage (Hong et al. 2009).

In particular, inter-event variability is also known as earthquake-to-earthquake variability and emphasizes the correlation between registrations of different earthquakes at the same site. Meanwhile, intra-event variability, i.e. the alleged site-to-site variability, indicates the variation of seismic excitations for a particular earthquake from site to site (Goda and Hong 2008b).

Inter- and intra-event variability is dependent on ground-motion parameters, although the latter is also a function of the distance between two sites. The interrelation between the ground motion parameters from site to site could have a major impact on the results obtained by the GMPE at short separation distances, due to saturation effects (Goda and Atkinson 2010). This is certainly true for distances up to 1 km, since the degree of correlation decreases with the increasing distance between two sites (Goda and Hong 2008a). In view of this, it must be taken into account that the current study uses a full-scale approach to the Italian peninsula, where the separation distance is evaluated between municipalities with a mean distance of over 10 km from each other. As a consequence, in order to properly take into account the correlation, only the inter-event element was considered, as seismic losses could otherwise be overestimated, leading to excessively cautious evaluations (Hong 2000).

On the basis of such considerations, two limit cases are investigated to evaluate the differences obtained in the evaluation of expected losses when performing scenario simulations. The cases modelled are: a completely uncorrelated PGA, in which $\sigma = \sigma$, i.e. the total correlation in the residuals of the ground motion prediction equation is computed; and a partially correlated PGA, in which only the interevent correlation is considered.

This could be achieved because inter- and intra-event correlations are usually considered to be independent, and could therefore be studied separately (Goda and Hong 2008b).

In both the fully uncorrelated and partially correlated PGA cases, error simulation according to a multivariate normal distribution is performed, with a median equal to the PGA calculated according to the attenuation law of Bindi et al. (Bindi et al. 2009). Consequently, on the basis of this law, 100 values of the residuals are randomly extracted for each simulated earthquake for each Italian municipality.

Error simulation is performed by defining the covariance matrix (assuming that it is normally distributed) with a zero mean and a covariance matrix Σ , which varied depending on the case being examined. So, in the case of the completely uncorrelated PGA, it accounted for the total standard deviation provided by Bindi et al. (Bindi et al. 2009). This is while it only accounted for the inter-event allocated share in the case of the partially correlated PGA.

Figures 3.5 and 3.6 set out the adopted covariance matrixes in the two studied limit cases, together with the related trends of the residuals.

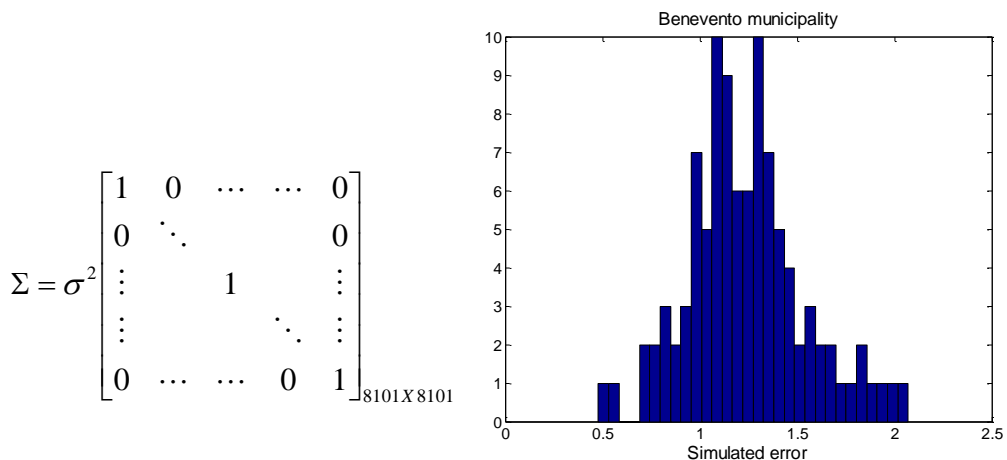


Figure 3. 5 Error simulated (Nsim=100) for Molise 2002 (Msp=5.59) for the Benevento municipality in the case of the fully uncorrelated PGA

In the case of fully uncorrelated PGA, an $N \times N$ matrix with unit diagonal term and zero off-diagonals is obtained, where N was the number of Italian municipalities.

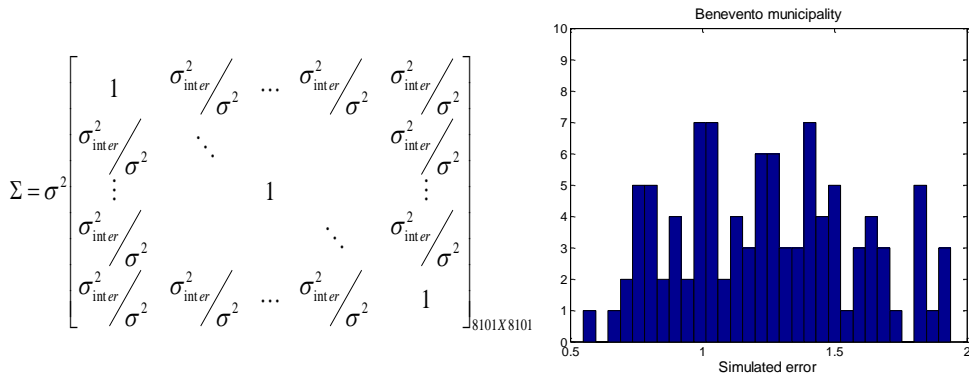


Figure 3. 6 Error simulated (Nsim=100) for Molise 2002 (Msp=5.59) for the Benevento municipality in the case of the partially correlated PGA

In the inter-event correlation case, the resulting correlation between the residuals is accounted for through the incorporation of the spatial correlation model in the covariance matrix that is associated with inter-event variability.

The results in terms of the frequency of the residuals show a clear log-normal trend, which is more scattered in the case of the uncorrelated than the inter-event correlated assumption. Such an observation can be justified by the major interrelation accounted for in the second case, which makes the residuals obtained more similar.

Once the PGA field is derived from each earthquake, it is evaluated for the entire Italian territory (assuming rock soil type). The PGA values are then amplified according to the topographical and stratigraphic coefficient of each municipality, as defined by the INGV (2004) report.

3.1.3 Expected losses against spatial correlation

Direct economic losses are computed by implementing a discrete version of the PBEE equation set out in Asprone et al. (Asprone et al. 2013) and shown in Equation 4 as follows:

$$l_i = \sum_{LS=1}^n RC(LS) \cdot [P(LS | \overline{PGA}) - P(LS + 1 | \overline{PGA})] \quad [€ / sqm] \quad (4)$$

where l_i represents the specific expected loss, i.e. per square meter of residential units i , $RC(LS)$ is the resto-ration/reconstruction cost function, and IM is the earthquake IM evaluated for each municipality through the attenuation law and then amplified for the stratigraphic and topographical coefficients S_S and S_T . The PGA value also takes into account the respective error in the two cases of the completely uncorrelated and partially correlated PGAs.

The term $[P(LS | \overline{PGA}) - P(LS + 1 | \overline{PGA})]$ represents the probability of exceedance of the limit state given the particular PGA within each discrete set considered.

Fragility curves are selected from the literature, to evaluate such a probability for masonry and reinforced concrete buildings, as done in Asprone et al. (Asprone et al. 2013).

The results in terms of the expected economic loss per square meter are averaged for each fragility curve considered and each structural scheme, according to the age of construction. Mean values are then integrated on the entire square meters amount and summed up for all the municipalities in order to compute the total national loss for each simulated earthquake, L_m .

The seismic retrofitting or reconstruction unit costs are also included in the loss curve derivation in this step for the diverse structural typologies. The reconstruction cost per square meter when the collapse limit state is attained is assumed to be equal to 1'500 €/sqm according to information from the Italian Centre for Sociological, Economics and Market Research (CRESME 2011).

Consequently, according to the study by Asprone et al. (Asprone et al. 2013), the repair costs are expressed as a function of the reconstruction cost $RC_{collapse}$. Moreover, they are assumed to have a linear trend against the limit states i for each vulnerability curve, as shown by Equation 5.

$$RC(LS) = \left(\frac{i}{n} \right) \cdot RC_{collapse} \quad (5)$$

The presented relationship allowed to also evaluate the unit loss for intermediate limit states and to retain this invariant for the assumptions made. It also ensured adequate flexibility with respect to the set of discrete limit states, which had a different number of damage state levels n for each investigated fragility curve study.

Expected national losses are evaluated for each earthquake simulation performed and then plotted against the magnitude of Sabetta and Pugliese, as provided by the INGV catalogue (INGV 2004) in the cases of the fully uncorrelated PGA (Figure 3.7) and the inter-event PGA correlation (Figure 3.8).

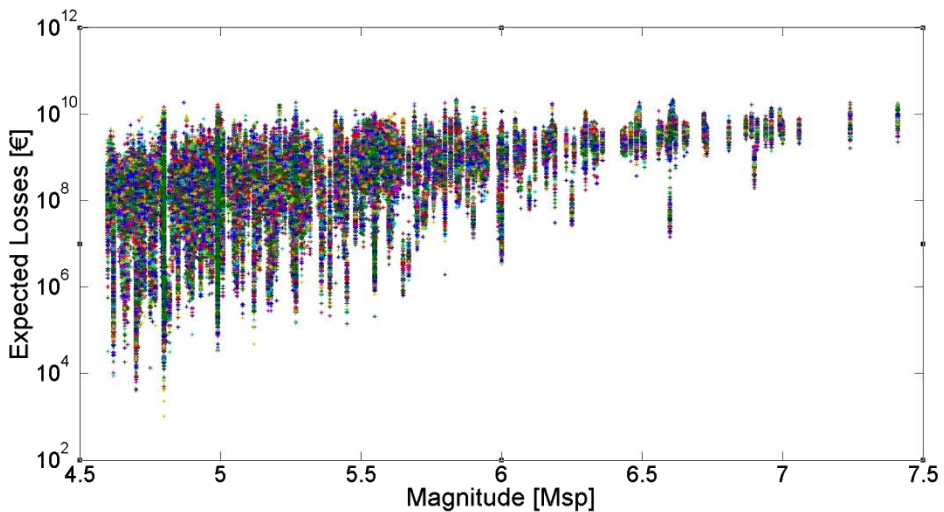


Figure 3.7 Total expected losses for each simulated earthquake in the case of the fully completely uncorrelated PGA

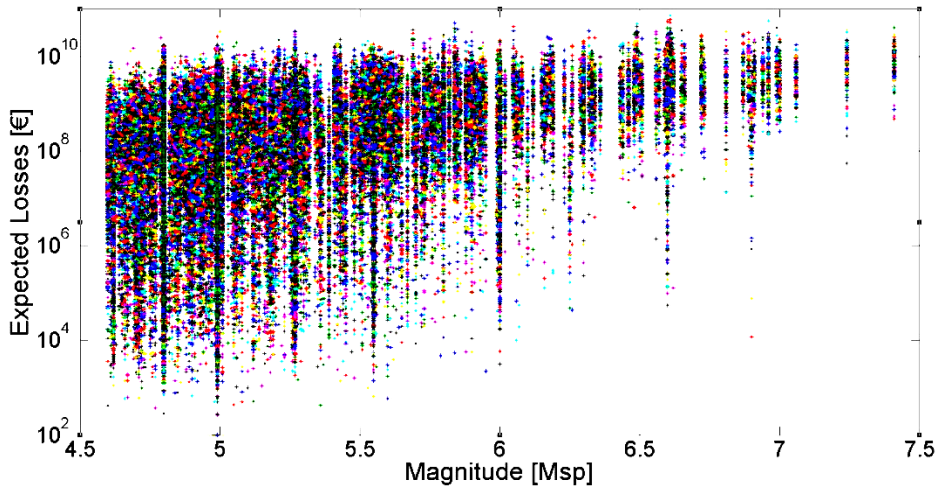
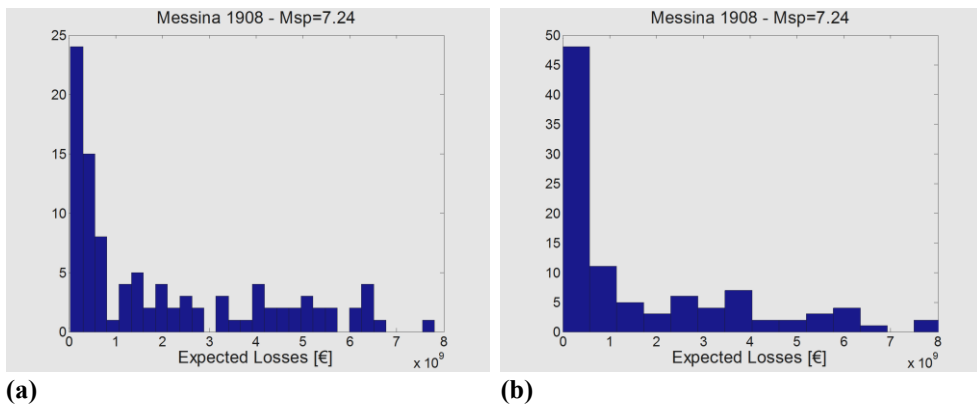


Figure 3.8 Total expected losses for each simulated earthquake in the case of the partially correlated PGA

Experimental evidence revealed a more concentrated distribution of total losses in the case of the fully correlated PGA, as expected. As a further assumption, the PGA is computed for the centroid of each municipality, and is considered to be uniform across the entire municipality. Figure 3.9 below demonstrates the distribution of loss values for the events of Messina 1908 and Irpinia 1980 based on the assumption of fully uncorrelated and partially correlated PGA values.



(a)

(b)

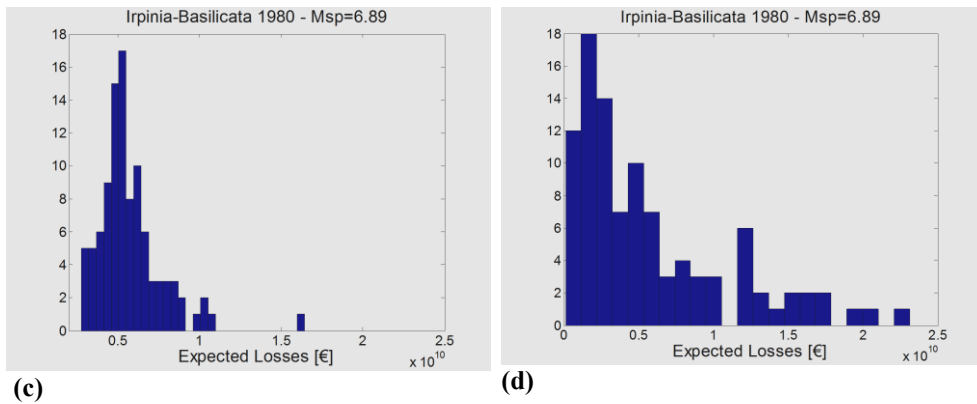


Figure 3.9 Expected losses for the Italian peninsula evaluated in the cases of the fully uncorrelated (left side) and the partially correlated assumptions (right side). The results refer to the historical seismic events in Messina in 1908 (9.a-9.b) and Irpinia in 1980 (9.c-9.d)

The results show the sensitivity of the annual expected loss (AEL) to different correlation cases, although it is often not recommended, as it could fail to capture the extent of the loss distribution, especially when dealing with rare events (Yoshikawa and Goda 2013).

As the proposed methodology would help the insurance market to mitigate the risk of insolvencies, with the objective being to estimate expected losses as realistically as possible, adopting AEL as a scalar risk metric seems to be appropriate. Insurers in fact mostly assess possible solutions and actions based on financial and monetary indicators. Moreover, the proposed approach allows us to adopt a risk-neutral approach, which is fundamental as it is very difficult to evaluate the actual behaviour of the stakeholders involved.

3.2 PROCESSING ANALYSIS' RESULTS

Spatial modelling of the ground motion for each municipality allows to take into account the spatial distribution of the residential building system

in Italy. Doing this enables to perform the scenario simulation according to the joint distribution of ground motion parameters at different sites.

The right spatial tail of the loss distribution can also be assessed according to the local exposure and the annual ground motion rate.

The results demonstrate more scatter in terms of expected losses based on magnitude for the partially correlated than the uncorrelated PGA case. An example is the 1873 earthquake in Venafro, which had an $M_{sp}=4.99$, with statistics on the event's assessed loss values confirming the observed trend.

As expected, it can be seen (Table 3.1) that the mean loss values are almost equal in the two PGA cases, but the partially correlated case shows significantly greater dispersion.

Table 3.1 Statistics on the expected losses for the Venafro seismic event

Venafro 1873	PGA fully uncorrelated	PGA partially correlated
Mean	1.06e+009	9.37e+008
Standard deviation	5.71e+008	1.22e+009

3.2.1 Derivation of expected loss relationships through regression analysis

Once the scenario simulations are run, a linear regression analysis is conducted. The approach adopted is the least square method, which assumes that all the assessed loss values are equally important. Accordingly, this technique can be effective in processing expected seismic losses vis-a-vis magnitude.

The values of the magnitudes are fixed within the study, because of the deterministic nature of the event being simulated. Starting with magnitude, losses are generated from randomly-generated variables, i.e. the residuals. A logarithmic regression of the 50th percentile of the estimated losses L^{50th} for both limit cases is performed, and the regression curve is fitted in the

semi-logarithmic plane. Consequently, the equation of the regression curve is as follows:

$$\log_{10} L^{50th} = \log_{10} a + b \cdot \log_{10} M_{sp} \quad (6)$$

with $\log_{10}a$ and b being the intercept and slope of the regression curve, respectively. A logarithmic linear regression is then performed, also on the basis of the 16th and 84th percentile values for both the complete and partial PGA correlation cases.

The predictive model for expected loss against the magnitude is shown in Figure 3.10 for the fully uncorrelated PGA case and in Figure 3.11 for the inter-event correlated PGA case.

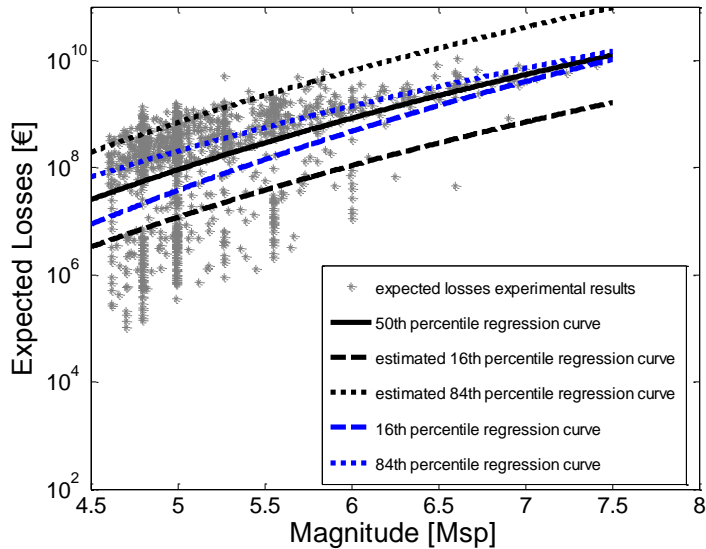


Figure 3.10 Expected losses data points and regression curves for the case of the fully uncorrelated PGA

Regression can also be understood as a probabilistic model for the distribution of residuals in order to define the probability distribution of L/M , where the homoscedasticity assumption subsists.

Consequently, by assuming constant dispersion, the regression curves for the 16th and 84th percentiles of the loss are estimated in the case of full uncorrelation between PGAs. Starting from the regression curve drawn from the median loss values, these curves can be obtained by simply summing up and subtracting the logarithmic standard deviation (obtained from Equation 7) to the regression curve.

$$\sigma \approx s = \sqrt{\frac{\sum_{i=1}^n e_i^2}{n-2}} \quad (7)$$

Figure 3.10 shows the trend for the 50th, 16th and 84th percentile regression curves, which are depicted with black dots. It is clearly evident that for higher magnitudes the 16th and 84th percentile curves tend towards the median (the central one). This is due to the smaller number of historical high magnitude events, as also shown by the data points.

Meanwhile, in the case in which 16th and 18th percentile curves are estimated from the median (the black lines) curve, the confidence interval remains constant, because of the underlying homoscedasticity.

The same procedure is also performed for empirical data obtained when the scenario analysis is conducted assuming inter-event correlation (Figure 3.11).

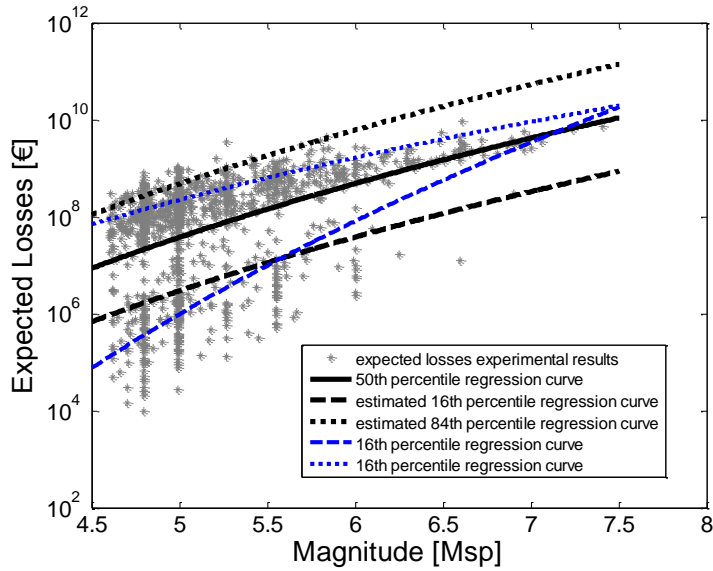
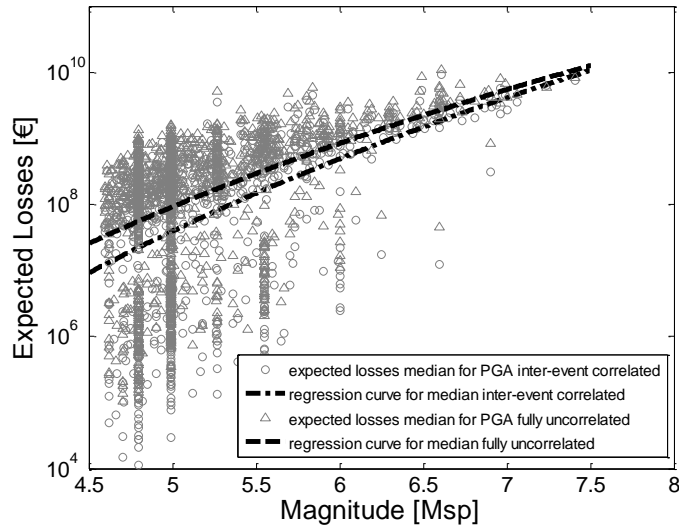


Figure 3.11 Expected losses data points and regression curves for the case of the inter-event correlated PGA

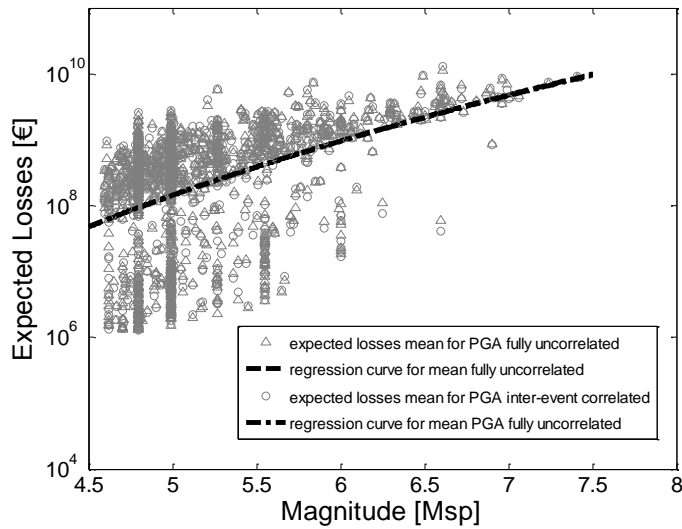
Results similar to those of the uncorrelated PGA case are also observed in the inter-event correlation case. In the case of the homoscedasticity assumption, a similar confidence interval is observed between the median curve and the 16th and 84th percentile curves. On the other hand, in the uncorrelated case assumption, there is greater consistency between the curves. Meanwhile, in Figure 3.11, there is less correspondence between the median curve and the 16th percentile regression curve due to the larger dispersion.

The percentile curves are derived from both homoscedastic regression and by also directly calculating the 16th and 84th percentiles from experimental data.

The Figures below show the regression curves fitted to the median (Figure 3.12a) and the mean values (Figure 3.12b) of the calculated expected losses for the two cases of uncorrelated (dashed dot) and partially correlated (dashed) PGA values.



(a)



(b)

Figure 3.12 Regression curves fitted to the median (a) and the mean (b) in the two cases

The correspondence between the predictive relationships for the two cases when they are fitted to the mean value is perfect. Diversely, the median values for the partially correlated case are lower than for the fully uncorrelated case. This is reasonable, as the partially correlated case is associated with higher standard deviations, meaning that the median must be smaller so that the expected values are equal. Accordingly, as already expected, the analysis of the results in terms of the median values shows that, based on the uncorrelated case assumption, the predictive relationship would be very conservative due to an overestimation of seismic losses.

3.2.2 Bin processing of the empirical results

The number of historical earthquakes is not uniformly distributed within the INGV catalogue (INGV 2004). This is because of the intrinsically random nature of earthquake occurrences. The logarithmic regression based on the homoscedasticity assumption cannot capture the smaller number of historical earthquakes, for very large magnitude events. There are, in fact, a larger number of lower magnitude seismic events, as depicted in Figure 3.13 (as also expressed in the Gutenberg-Richter relation).

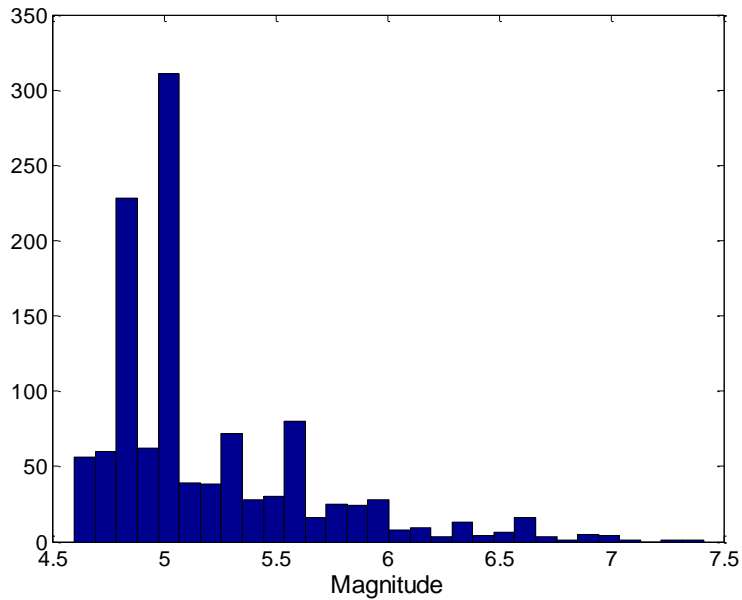


Figure 3.13 Frequency of historical earthquakes in terms of magnitude

It can be seen that the rate of occurrence of earthquakes falls as the magnitude rises. This is also reflected in the fact that there are fewer faults that are physically capable of causing very high-magnitude events.

A total of 1'172 events are listed in the INGV catalogue, but some of these have their epicentre's location close to the borders of the country or deep in the Tyrrhenian Sea. Obviously, the expected seismic damage from such events is slight, and accounting for them may thus produce an unjustified shift of the prediction curve. To avoid such a phenomenon, events with the epicentre in these areas are removed from the catalogue. Accordingly, 960 instead of 1'172 earthquakes are simulated.

Furthermore, to account for the diverse distribution of the number of earthquakes against the magnitude, historical events are grouped in bins, and expected losses are computed for each of them (Table 3.2).

Table 3.2 Historical earthquakes for which the scenario analysis is performed, gathered in bins with a 0.10 M amplitude

Bin	N° events	Event interval	
4.6:4.7	56	1	56
4.71:4.81	189	57	245
4.82:4.92	54	246	299
4.93:5.03	243	300	542
5.04:5.14	47	543	589
5.15:5.25	41	590	630
5.26:5.36	67	631	697
5.37:5.47	26	698	723
5.48:5.58	62	724	785
5.59:5.69	29	786	814
5.70:5.80	29	815	843
5.81:5.91	24	844	867
5.92:6.02	21	868	888
6.03:6.13	9	889	897
6.14:6.24	8	898	905
6.25:6.35	14	906	919
6.36:6.46	5	920	924
6.47:6.57	6	925	930
6.58:6.68	14	931	944
6.69:7.05	13	945	957
7.06:7.42	3	958	960
960			

A bin width of 0.10 M is used to group the expected loss data in order to perform the regression analysis. A greater width - equal to 0.36 M - is assumed for the last two bins, being empty the magnitude intervals 7.07:7.23 and 7.25:7.40.

A logarithmic regression analysis is again performed for the 16th, median and 84th percentiles of loss according to the least squares method. The results are shown in Figure 3.14 and Figure 3.15, as follows:

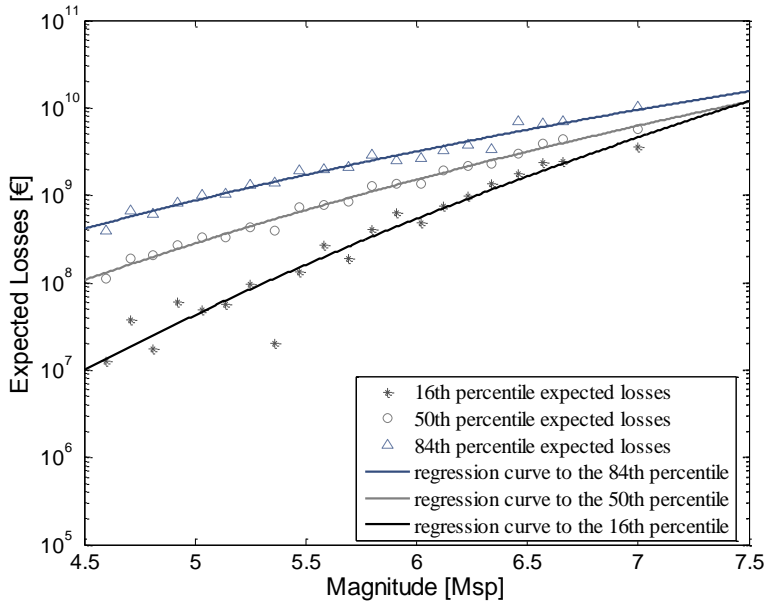


Figure 3.14 Bin regression in the case of the fully uncorrelated assumption

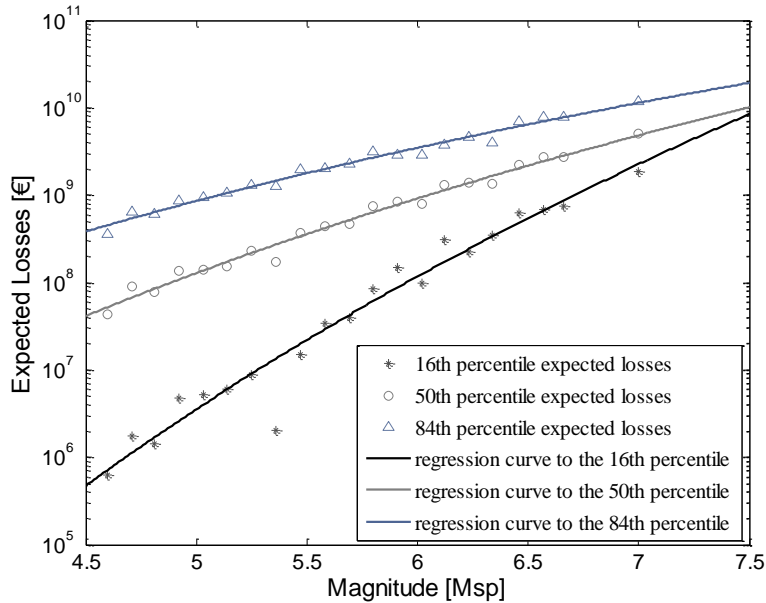


Figure 3.15 Bin regression in the case of the partial correlation assumption

As expected, lesser data points can be observed, and reflect the expected loss assessment based on the bin division according to the magnitude intervals.

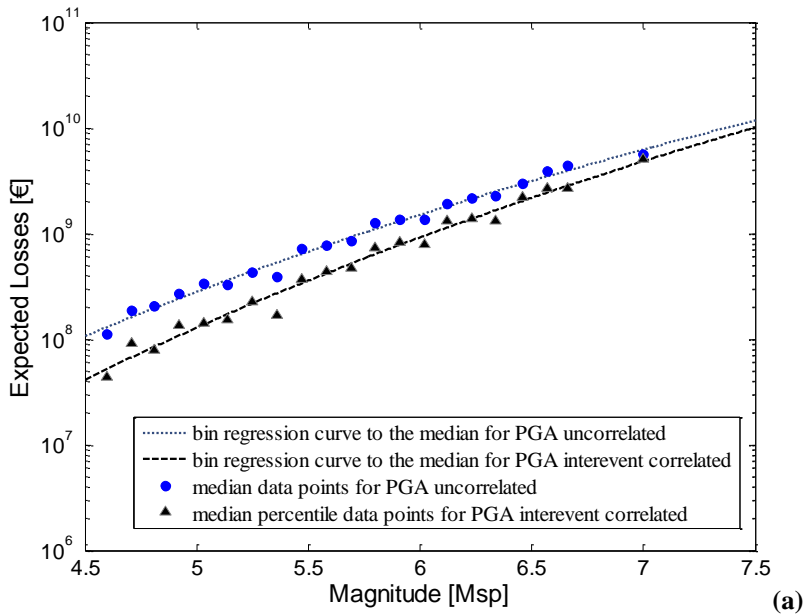
The regression curves show similar trends for the fully uncorrelated and partially correlated PGAs. Nonetheless, due to the wider distribution of the data points in the case of the inter-event correlation assumption, major scatter is detected.

3.3 COMPARISONS AND RESULTS

The assumption of the fully uncorrelated PGA clearly leads to a steeper regression curve and a smaller confidence interval. On the other hand, the partially correlated PGA values are more scattered and, as a consequence, the confidence intervals around the regression curve are wider.

The most of the difference in the distribution provided by the two simulation cases is due to the standard deviation values.

In the case of fully uncorrelated simulations, where no spatial correlation is taken into account, the loss values demonstrate less scatter, as expected (Figures 3.16a and 3.16b).



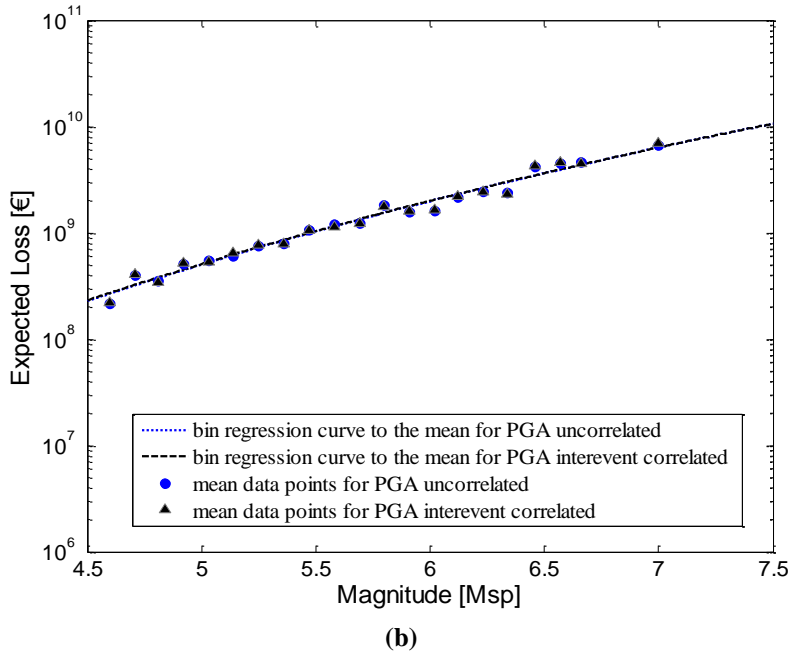


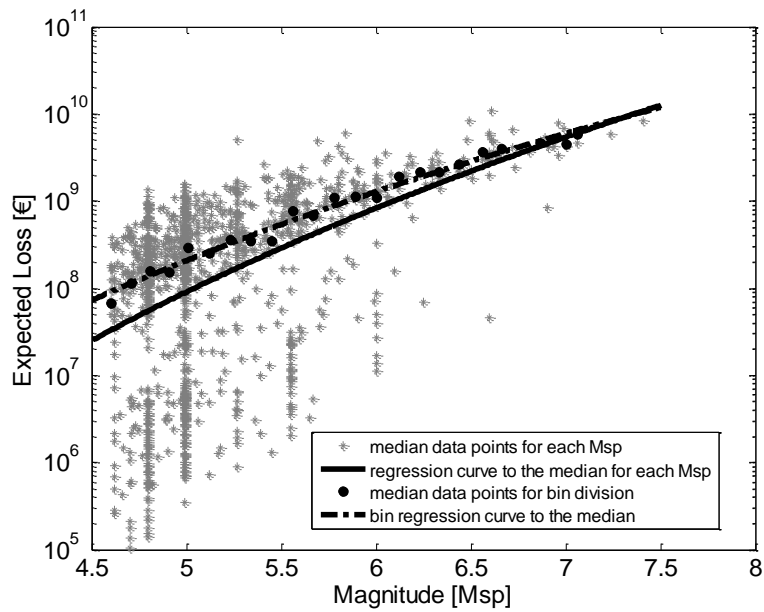
Figure 3.16 Regression curves for the median (a) and the mean (b) values for the two limit cases

Logarithmic regression curves fitted to the mean values coincide in the two cases, as they also do in the case of bin regression. The regression curve to the median instead has higher values in the case of the fully uncorrelation assumption, as is also in the case of simple linear regression previously implemented without performing bin division.

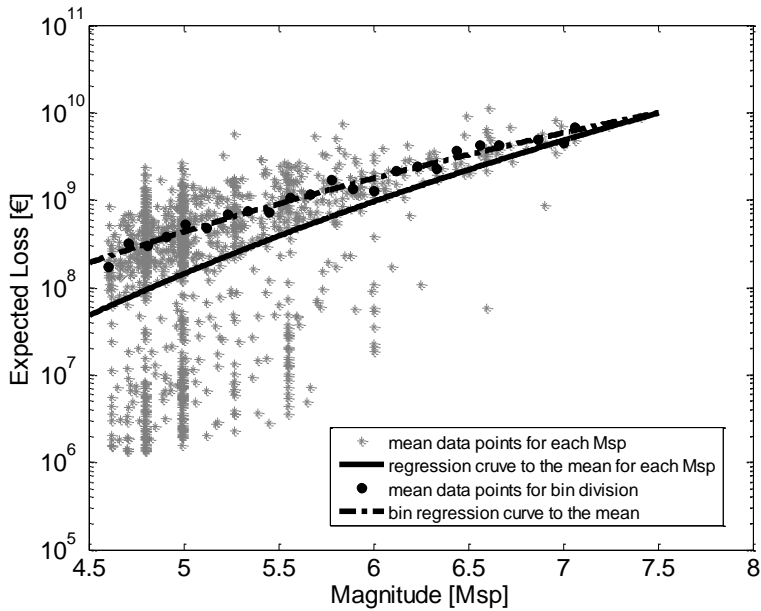
As a result, more conservative predictions are produced according to the regression analysis used in the fully uncorrelated PGA hypothesis. Otherwise, lower expected losses are estimated in the case of inter-event correlation, thereby one can expect that a lower margin of safety is attained, allowing for a more realistic evaluation. The experimental observations are also confirmed by studying the size order of the intercept of the plotted curves. According to the median values, at a 4.5 magnitude, about $8.2e+08$ € seismic losses are expected in the case of the fully

uncorrelated PGA and $5e+07$ € in the case of the correlated PGA inter-event.

Further remarks are related to the differences between the case in which a regression analysis is performed according to the bin division and one according to each magnitude (M_{sp}) value. The regression curves are set out in Figure 3.17 for the fully uncorrelated assumption.



(a)



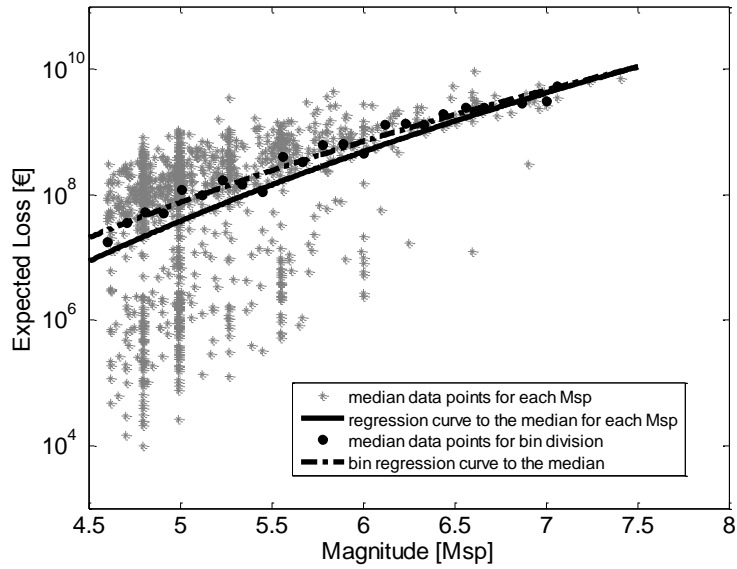
(b)

Figure 3.17 Case of the fully uncorrelated PGA: comparison between the regression curves of the median (a) and the mean values (b) in the case of bin regression and the case of regression for each magnitude (M_{sp}) value.

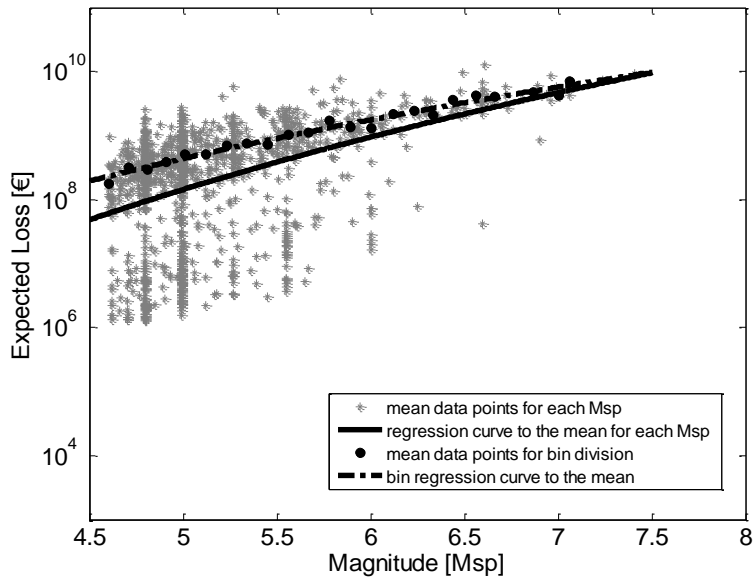
The expected loss in the case in which the regression analysis is performed according to the bin division provides higher loss values than the regression case implemented for each M_{sp} value. Performing the regression to the median or the mean values by considering the real loss distribution for each magnitude value allows to fore-cast more realistic seismic losses.

The precision observed in the case of the regression for each M_{sp} value can also be understood in the sense of a better evaluation of the actual loss distribution given the magnitude. Greater scatter between the regression curves obtained respectively in the case of the bin division and in the case of the simple regression performed for each magnitude value, in fact, can be observed when referring to the mean loss values.

There are similar results when the inter-event correlated PGA is observed for the two kinds of regression (Figure 3.18).



(a)



(b)

Figure 3.18 Case of inter-event correlated PGA: comparison between the regression curves for the median (a) and the mean values (b) in the bin regression case and the case of regression for each magnitude (M_{sp}) value

It can be seen that the dotted curves – referring to the bin regression case – are also higher in the case of the inter-event correlation assumption. Furthermore, the scatter between the curve related to the bin regression and the curve according to the single M_{sp} values is less in the case of the regression curve fitted to the median.

Some common features can be observed with reference to the scatter trend between the curves in the bin and M_{sp} value regression cases. The scatter is greater for lower magnitudes and tends to zero for higher ones. This is obviously due to the lesser number of rare events.

The major effectiveness of using the M_{sp} regression curves with respect to the median values is also confirmed by the difference between the mean and median values, as calculated in the two limit cases (Table 3.3).

Table 3.3 Comparison between the mean and median values calculated in the case of the scenario analysis performed according to the fully uncorrelated and inter-event correlation assumptions

Case analysis	Bin		M _{sp} values	
	Mean, μ	Median, η	Mean, μ	Median, η
PGA fully uncorrelated	2.01 e+09	1.09 e+09	8.44 e+08	3.29 e+08
PGA inter-event correlated	1.99 e+09	4.48 e+08	8.51 e+08	1.88 e+08

The results show diverse scattering between the curves fitted to the two limit cases when the bin or M_{sp} regression is performed. A slight drop is observed in both cases with reference to the mean values. In particular, in the case of the M_{sp} regression analysis, only about a 1% drop from the inter-event PGA case with respect to the uncorrelated PGA is evaluated. In the case of the bin regression, a 4.5% drop is observed from the inter-event to the uncorrelated case.

On the other hand, substantial differences are assessed in the case in which the median values are considered; 9.54% and 42.42% increases are evaluated for the bin regression and M_{sp} regression cases, respectively.

3.4 DISCUSSION ON RESULTS

Seismic insurance is a potential tool for risk mitigation, although the modelling currently used is a matter of great concern. On the insurers' side, a deep knowledge of exposed goods and site-specific hazards is a major requirement. The main issue that insurers have to face when dealing with private seismic insurance concerns the knowledge needed of effective economic resources. Indeed, this is fundamental when it comes to the insurers' capacity to both pay the insured without becoming insolvent and cover expenses without having cash flow problems. By collecting information about previous earthquakes (960 events) and the population living in residential buildings today, this study establishes predictive relationships for expected economic losses based on magnitude.

The approach employed for deriving predictive relationships takes into account the spatial correlation in the residuals of the ground motion prediction equation. Such correlations are accounted for within the process by using two limit cases: one where there is a full uncorrelation between the attained PGA values, and another in which there is partial correlation. According to the former hypothesis, the PGA affecting each municipality does not depend on the PGA in an adjacent municipality. Meanwhile, in the case where inter-event standard deviation is considered, a partial correlation is assumed between PGA values. The proposed methodology allows to optimize insurers' pricing. It also allows interactions among the diverse stakeholders involved in disaster management and recovery processes to be optimized.

For instance, experimental evidence shows that a better knowledge of expected losses allows insurers to increase market penetration; a firm can sell insurance at a lower profit margin, as it does not need to prevent insolvency and does not pay as much for reinsurance by relying more on its own reserves (Kesete et al. 2014).

The results are presented in terms of the 16th, median and 84th percentiles for expected loss curves given magnitude based on the two distinct assumptions.

The difference in the distribution produced by the two simulation cases is obvious regarding the standard deviation values. More scatter is actually observed when a scenario analysis is performed in the partial correlation assumption case. Accordingly, when no spatial correlation is taken into account, more aggregated loss values are obtained.

As a consequence, in the case of the partially correlated PGA values with respect to the uncorrelated case, the confidence intervals of the 16th/84th percentiles around the median are higher, in agreement with similar results in the literature (Goulet et al. 2007).

For low probability values, there is a higher scattering of values from the median.

More confidence is given to the regression curves referring to lower magnitude values, due to the high number of historical events.

In general, the predictive relationships derived for expected losses given the magnitude clearly have a significant dependence on how the PGA correlation is modelled. A substantial exception is represented by the curves fitted to the mean, which demonstrates insensitivity to the spatial correlation model. This also confirms (e.g. see Yoshikawa and Goda 2014) that the choice of a suitable risk metric for insurers is extremely important for decision-making.

Further processing of the obtained results in terms of the expected losses is performed. The expected loss values, which are obtained from simulation of the events in the INGV catalogue, are also divided into bins before conducting the regression analysis. The bins were modelled by considering the same amplitude of the interval according to the magnitude of the simulated events. Each bin accounted for a diverse number of historical seismic events, but the same weight is assigned to each of them within the regression analysis.

The results of the logarithmic regression according to the median and mean values are similar to those obtained in the case in which the results are processed according to each single magnitude value (M_{sp}).

In fact, the predictive relationships drawn in the case of regression according to the M_{sp} result are less conservative than in the case of the bin regression analysis. As a result, more realistic forecasting can be expected when referring to the M_{sp} regression, above all with respect to the median curve.

Consequently, major caution is needed both in the case in which full uncorrelation is assumed and also when the predictive relationship is derived from the bin processing of expected losses.

The main strength of the proposed methodology is that it allows for the prompt and easy forecasting of seismic losses given the magnitude of an event. This can be easily integrated into insurers' decision-making processes within an integrated regional catastrophic loss estimation model that accounts for the spatial distribution of buildings at the municipality level. This approach provides an accurate and disaggregated representation of the risk to be managed, including the spatial correlation and variability of the fragility model. Moreover, retrofit actions can actually be easily integrated within the evaluation process by changing the fragility curves used within the scenario analysis to characterize vulnerability.

3.5 ALTERNATIVE INSURANCE PRODUCTS ENHANCING RESILIENCE OF LOCAL AUTHORITIES: THE CAT BOND MODEL

Once a country's financial capacity to face risks has been assessed, institutions and officials have to choose what kind of risk-financing instrument best fits the national needs. Potential benefits of mitigation efforts and cost trade-offs between different types of intervention have to

be analysed, to ensure for adequate and pro-active financing of disaster risks.

Despite the well-known efficiency of insurance systems to guarantee financial resilience of nations and countries to natural hazards, they have also the potential to reveal as inadequate to fully cover losses from catastrophes. Like Governments, insurance companies have often to face severe post-event deficits for financing relief and reconstruction. Such deficit is turns out naturally because of the cash flow availability of insurance companies not being unlimited. This is the reason why insurers usually turn to third bodies, which sell them insurance products, to face the insolvency risk they continually incur in, that are the reinsurance companies.

On the other hand, reinsurance is usually a one-year contract, which continuously expose both the insurance and the reinsurance company to insolvency and cash flow problems. Also, companies subscribing reinsurance contracts are also subjected to the price fluctuations in the reinsurance market, that are not always sustainable (Cummins 2007).

Recently some central governments worldwide, like the Japanese and the Mexican one, have experienced the great advantages deriving from handing over the risk to the capital market by issuing Catastrophe Bonds. They are insurance-linked securities representing an effective instrument, which allow stakeholders (governments, insurance and re-insurance companies and householders) to take advantage of the cash availability and the capability of capital market to cope with great risks, while preventing huge expected losses from natural catastrophes occurrence. Hence, Cat Bonds are an innovative asset class whose high yield shows a double decorrelation, being independent both from events occurrence and financial market trends. Because CAT bonds are fully collateralized, they eliminate concerns about credit risk, and because catastrophic events have low correlations with investment returns. As a counterpart, CAT bonds are more expensive than reinsurance, above all due to their high transaction

costs, being assumed until 2% of the covered risk (Cardenas et al. 2007). CAT bonds may provide lower spreads than high-layer reinsurance because they are attractive to investors for diversification. Moreover CAT bonds also can lock in multi-year protection, unlike traditional one-year reinsurance (Cummins 2007).

A typical CAT bond structure is diagrammed in Figure 3.19. First of all a single purpose vehicle reinsurer (SPVR) is established. The SPVR issues bonds to investors and invests the proceeds in safe, short-term securities such as government bonds or AAA corporates, held in a trust account and ensuring continually current assets availability. The bonds embed a call option, that is triggered by a defined catastrophic event according to specific condition (for instance its intensity level or simply its occurrence). On the occurrence of the event, the SPVR release the proceeds to help the insurer pay claims arising from the event. A particular focus has to be done in this case on the stakeholder, which buy reinsurance for risk protection. This can be, in fact, both an insurance company, but also a public institution, as is a Government.

In most CAT bonds, the principal is fully at risk, i.e., if the contingent event is sufficiently large, the investors could lose the entire principal in the SPVR. In return for the option, the insurer pays a premium to the investors. The fixed returns on the securities held in the trust are usually swapped for floating returns based on LIBOR or some other official market index. The reason for the swap is to immunize the insurer and the investors from interest rate (mark-to-market) risk and also default risk. The investors receive LIBOR plus the risk premium in return for providing capital to the trust. If no contingent event occurs during the term of the bonds, the principal is returned to the investors upon the expiration of the bonds (Cardenas et al. 2007).

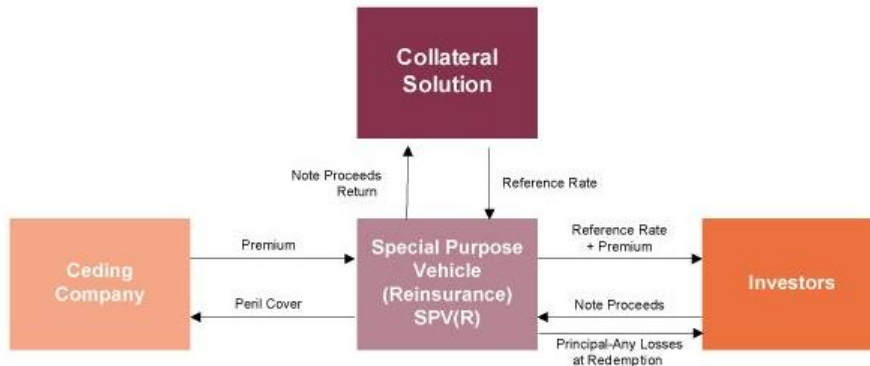


Figure 3.19 Typical Cat Bond model functioning

As well as insurance, also Cat Bonds can be modelled according to a risk-based framework, as an instrument for contingent financing of municipalities. Cat Bonds are high-potential means of seismic risk mitigation, which can help local communities to face the post-event reconstruction and to avoid the related cash flow problems.

CHAPTER 4

DEVELOPING AN INTEGRATED FRAMEWORK TO QUANTIFY RESILIENCE OF URBAN SYSTEMS AGAINST DISASTERS

The current Chapter illustrates the development of a framework from Bozza et al. (Bozza et al. 2015) aimed at quantifying disaster resilience of urban systems while ensuring an adequate level of sustainability, all according to a social and human-centric perspective.

The basic idea is to model urban networks are modelled as hybrid social-physical networks (HSPNs) by accounting for their physical and social components. These are city models, whose behaviour can be assessed through the implementation of engineering metrics, as a measure of city efficiency and functionality. Thence, social indicators can be identified in order to characterize the quality of life level in the aftermath of a catastrophic event. Both efficiency and quality of life indicators are evaluated using a time-discrete approach before and after an extreme event occurs and during the recovery phase in order to measure inhabitant happiness and environmental sustainability. This approach allows handling different kinds of information simultaneously, being potentially implemented both in peacetime and during the recovery process. The former can be effective for urban coping capacity assessment in order to reduce risks as a mitigation instrument. The latter can be used in the after-event to identify the best recovery paths needing to be followed for adaptation.

4.1 RESILIENCE AS A CATALYST TO SUSTAINABLE DEVELOPMENT

Future cities have to be as sustainable as possible and the fundamental prerequisite to realise this condition is strictly related to their resilience characteristics. In other words, the link between sustainability and resilience relies on the quality of life levels of cities: if a city is resilient, it can recover from a disaster in an effective manner, reaching the previous level of quality of life, both in terms of happiness of inhabitants and environmental sustainability.

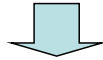
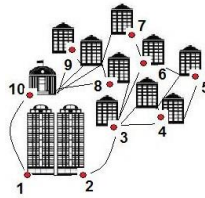
With this, by measuring the capability of urban systems to recover these properties, a rigorous framework, merging the engineering and ecosystems resilience approaches, can be developed in order to quantify the actual resilience of cities, and in particular, whenever they are subjected to extreme events.

The framework proposed by Bozza et al. (Bozza et al. 2015) is composed of 3 fundamental steps, as summarised in Figure 4.1:

1. global urban networks are defined by merging the social and physical networks in the un-damaged and damaged configurations. Efficiency, through robustness and redundancy measures, of these hybrid social-physical networks can be measured through well-established and rigorous complexity network theories. Such quantities represent a proxy of the capability of the city system to provide its citizens the services and the facilities they expect to receive.
2. quality of life and city performance indicators have to be identified to measure inhabitants' happiness and environmental sustainability.
3. specific functions need to be calibrated to make such indicators dependent on the social-physical network metrics, identified in the previous step, also including social and economic background conditions. This step can be developed by means of well-established techniques in

decision-making and ecosystem theories (e.g. fuzzy logic, genetic algorithms, etc.).

1. Given a configuration of the city, damaged or undamaged, we can compute the efficiency of the HSPN networks, by means of different rigorous indicators.



2. Citizens are “fed” by the physical systems. Their happiness somehow “depends” on the rigorous indicators (efficiency, robustness, etc.) previously calculated. We can establish a metrics for “happiness” and quality of life, that is city sustainability indicators.



3. We can find a system functions linking the “happiness” indicators to the network efficiency indicators. These functions will depend also on social-economic background conditions. By reiterating this process in different city configurations, during the recovery path and for different recovery paths, we can quantitatively manage resilience.

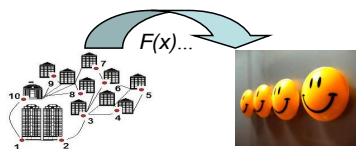


Figure 4. 1 The proposed framework’s conceptual scheme (Bozza et al. 2015)

Particularly, hybrid social-physical networks (HSPNs) can be modelled as both topological and typological ones, being different through the methodology adopted for the quantification of resilience in the two cases.

In order to better evaluate the effectiveness of the recovery process and to recognise the best strategies, scenario analysis can be performed and the framework can be reiterated for each scenario. Measurements, given by both engineering metrics and sustainability and quality of life indicators, have to be chosen in order to better describe social sustainability in the post-event phase.

As a result, the output of the proposed methodology is a set of indicators that can be evaluated for each considered strategy. As they are very synthetic measures of the efficiency of a recovery strategy, institutional authorities and local governments could use them to perform rapid choices soon after the occurrence of a catastrophe.

Present policies might be enhanced and best practices could be recognised, since when local authorities decide a recovery strategy will be implemented, they do not always know what the response of the urban environment will be. While the implementation of the suggested procedure allows for recognition of the strategies which best enhance resilience, sustainability and quality of life of a city are also applied by the performance of scenario analysis and a pre-event assessment of the city.

According to Sperling et al. (Sperling F. and Szekely F. 2005), disaster managers have to overcome several barriers for an effective reconstruction. The main limitations are in the form of institutional barriers, efforts to access relevant information, lack of financial frameworks and limited financial resources, structural limit and the diversity of institutional structures all changing from one urban context to another. Moreover, disaster managers are also subjected to restrictions via regulatory compliance.

One of the major problems that a disaster manager has to face, given his human nature, is short-term thinking. This can easily lead to mistakes in

the case of a catastrophic event, when prompt decisions need to be made and when panic and chaos rule.

Obviously, it is not possible to solve all the problems that disaster managers usually have to face, but certain aspects may be enhanced, of course. Time and resources can be saved and scenario analysis might help to recognise the most efficient actions to adopt. For instance, whenever an earthquake occurs, it affects different adjacent urban contexts, or municipalities. Each municipality can be modelled in the post-event as a HSPN, both typological and topological, for known local damages. Hence, nodes and edges that are out-of-order are assumed to be unusable.

Once the actual damaged configuration is defined, a disaster manager can hypothesise different recovery strategies. They can be chosen as a set of the most resilient and sustainable strategies, already assessed with the scenario analysis previously performed for such municipalities. Simulations can be performed to evaluate resilience, efficiency, sustainability and quality of life indicators with a step-by-step procedure. Such measures are performed in the context of the typological approach as well the topological. As an output, the manager can acquire a set of indicators, where the values are varied according to the higher or lower resilience of the urban context. Therefore, the best strategy to be implemented can be chosen in a timely manner. The expected efficiency of such a methodology is stringently related to the time needed to use it. This is because of its straightforwardness, allowing managers to implement it as an automatic procedure given the simplicity of the instruments needed.

The disaster manager can also compare expected efficiency and resilience from each of the best strategies recognised for each municipality within the same urban context. This can be a further added value for the methodology, like in an example where two different best strategies are recognised for two adjacent municipalities and few differences are expected in the resulting resilience level. The manager can then choose to

implement the same strategy for both because of the opportunity to use the same means and resources. This would also result in saving economic resources, an important issue when dealing with post-catastrophe recovery.

4.2 DEFINING AND MEASURING HYBRID SOCIAL-PHYSICAL NETWORKS

The main idea behind the framework put forth herein is related to the complexity of cities, comprised of interconnected physical and social systems. Hence, first of all, the definition of hybrid social-physical networks (HSPN) is needed (Cavallaro et al. 2014). As already mentioned, they can be modelled both topologically and typologically.

When dealing with the topological, each network can easily be considered a layer and modelled through the theory of graphs, where components/actors are modelled by nodes, and the relationships between them are modelled by edges (Newman 2003). That is, each physical network, which interacts with citizens, can be modelled as a HSPN, according to Asprone (Cavallaro et al. 2014). As an example, one can model the residential network (Figure 4.2) as a set of layers mutually overlaid and interacting. Given that this network is a hybrid one, two different parts can be recognised: the physical one and the social.

Regarding the physical part, one can consider:

- the intersection nodes, which represent the street intersections;
- the building nodes, which represent single residential buildings.

Moreover, two kinds of link can be modelled:

- the street link, connecting street intersections;
- the door link, connecting single buildings and the single intersection nodes.

Regarding the social portion of the network, further nodes and links can be modelled:

- the citizen nodes, representing the inhabitants of each building;
- the inhabitants links, representing the interactions between citizens and buildings.

For instance, a citizen lives in building A, works in building B and goes to building C for training. The links between the buildings are modelled as inhabitants' links, because they represent the typical daily urban patterns established by citizens.



Figure 4.2 Modeling of a hybrid social-physical network, a case study for the city of Acerra (NA) (Cavallaro et al. 2014)

A further example can be designed as the “hospital network”. Here, for the physical network, there are:

- the hospital nodes, representing single hospitals;
- the street nodes, representing street intersections;
- the residential nodes, representing residential buildings located near each hospital.

The layer of arches has to instead account for two different types of links:

- the street links, representing all possible urban paths, connecting each street intersection to each hospital;
- the door links, linking each building to each intersection node, as in the previous example.

Furthermore, the social network has to be also accounted for, with further nodes and links:

- the citizens nodes, representing citizens served by each hospital;
- the inhabitants links;
- the hospitalisation links, representing the interactions between citizens and hospitals. These portray the services that each citizen asks for of each hospital, closest to their residential building.

Given these examples, one can discretely evaluate efficiency by means of an engineering measure of resilience, as the “point-by-point” efficiency of the network.

Moving past this concept, resilience can only be assessed focusing on the social components, the citizens and their level of satisfaction, as “sensors” of the level of functionality of urban systems.

Unfortunately, such a model assumes a fixed network size and underlying topology that does not allow for the provision of the city dynamics in the aftermath of a shocking event. Hence, it does not allow reaching the case in which the equilibrium condition achieved in the post-event is different from the previous one, and also where city topology and size can change. In order to account for this additional possibility, a further approach has to be investigated. Keeping with this, HSPNs can be modelled as “typological evolving dynamical networks”. Here, each class of actors can be identified depending on their primary function and the relationships

between them given by non-linear mathematical laws. Depending on the phenomena they describe, these numerical relationships exhibit different trends, governed by particular variables, calibrated through scenario analysis and simulations.

As an example, one can consider the residential network, as illustrated in Figure 4.3, characterised by the presence of different actors, such as homeowners and inhabitants. Conversely, inhabitants can be both homeowners and leaseholders, so the relationship between them can be calibrated by purchase and rent agreements. In this way, one can describe the undamaged configuration of the urban network by grouping components and actors based on their “typology”. However, when dealing with an extreme event occurrence, such as an earthquake, it is expected that some buildings will become unusable, while others not. In the case this happens, different circumstances can arise:

- residents are displaced because of their dwelling inhabitability, so they can decide to buy or rent another house;
- residents are not displaced, they can choose to stay in their home, which is still feasible, but they can also decide to move away to new buildings, because they no longer feel safe.



Figure 4. 3 Typological evolving dynamical network scheme (Bozza et al. 2015)

Moreover, during the recovery phase, some buildings are retrofitted, getting back to feasibility and new buildings are built. Citizens can then go back to their dwellings or buy new ones.

According to Bettencourt (Bettencourt 2013), by performing such simple modelling, the multifaceted structure of a city, with its underlying mechanisms and dynamics, can be clearly evident. Consequently, in the literature, it is often equated to biological systems. This analogy also intends to emphasise the importance of forces acting on the existing links and the dynamics with which they become denser on an increasing scale.

Further, a city structure in terms of existing links and dynamics can be considered common to the majority of cities, as is the case with biological systems (biological organisms, insect colonies, food chain, etc.). This can be done disregarding its topology, when considering cities, where the socio-economic contexts may be compared. As an example, links and dynamics can be determined to be very similar when studying European capital cities similar in size. So, one can consider that each city is approximately a scale version of another. With this in mind, the average properties for infrastructural, socio-economic and spatial performances can be evaluated as scaling relations and then be applied to other urban systems (Bettencourt 2013). Accordingly, the single municipality model

can be first singularly modelled as a typological network, and then identically repeated in a sort of “compartmental network”. Finally, the mutual links between municipalities, and then cities, can be also modelled with simple linear mathematical laws.

The methodology for the modelling of a compartmental network have been already studied by D’Alessandro (D’Alessandro 2007), who applied it to the characterisation of the relationships between human and natural renewable resources. This kind of study takes as a basis the Lotka-Volterra model for “predator-prey” characterisation (Brander and Taylor 1998, D’Alessandro 2007), where the relationships between humans and natural resources are described in the food chain. Therefore, one can define the population as the predator and the local structures and services as the prey. The final outcome can be defined as a “typological-compartmental network”, an approach that accounts for both city dynamics and potential urban evolution in space and time. For each of the physical components of the modelled HSPNs (e.g. residential buildings, hospital, etc.), a fragility model can be assigned in order to also take into account their vulnerability. Then, several earthquake example scenarios can be generated and Monte Carlo simulations performed. Given the damaged configuration, different recovery strategies can then be simulated. The proposed framework aims to assess:

- the efficiency level of the performances of HSPNs in terms of robustness and redundancy measures, according to different configurations of the components (e.g. the nodes);
- the efficiency level of the performances of compartmental networks through the definition and evaluation of control parameters, obtained through the comparison between engineering indicators evaluated before and after an extreme event occurs and for each step of the recovery process.

All these engineering measures are a proxy for urban resilience and can be evaluated for each step of time within the context of the various considered recovery strategies. The analyses have to be run in the case where no event has occurred and also after an extreme event, causing damages to the physical and social components of the urban system that can be simulated within a scenario analysis. Resilience can be therefore assessed with a systemic perspective, evaluating the damages to the physical components and their seriousness within the city-system through the level of satisfaction of citizens, actually focusing on the social components of the city itself.

4.3 QUALITY OF LIFE INDICATORS ACCORDING TO A SUSTAINABLE APPROACH

The concept of quality of life was born in the 1930s as a new, multidimensional and challenging objective for modern societies. In the last decades, the interest in empirical evaluation of quality of life and social indicators has steadily risen, as a result of the inception of novel objectives for the development of societies. Moreover, it represents the answer to the challenge of quantifying the level of well-being of communities and to the increasing information demand based on the implementation of active social policies. This concept becomes even more perplexing in the context of complex urban networks, as the human part constitutes a social network itself.

Social indicators are represented by statistics and other information (Bauer 1966), reflecting the actual conditions of local and global societies. According to De Vaus (De Vaus 2007), they are specific measures of a more abstract concept, which allow social change to be measured (Felson 1993). Therefore, they are measurements of social health that allow investigation of the evolution of social conditions. The international scientific community recognises a huge need to identify a scientifically effective tool for quality of life assessment through the use of indicators.

Indicators have been used since the 1960s to quantify social characteristics that might influence public policy (Newman 1997). However this has never been simple by any means. Working with indicators is very difficult and requires significant attention and valid consideration. More specifically, defining indicators necessitates the implementation of a specific procedure, as outlined by De Vaus (De Vaus 2007), whose first step is implied with the definition of the concept itself which the indicator attempts to describe. Also, according to the methodology that one may want to adopt, it could be important to find a sample of persons for contingent questionnaires to be administered, constructing questionnaires, and managing data.

The indicators also have to be consistent with the dimension of the concept, which one wants to describe, since the number of indicators used depends on it. Moreover reliability and validity are fundamental for the selected set of indicators. National and international authorities have, in fact, underlined a lack of adequate data, concepts and methodologies to quantify the social perception of quality of life (Noll 2002). They have also emphasised the need for collecting homogeneous data, reusable and clearly understandable, in order to both monitor social changes and assess social health and sustainability, so that one can use them within more complex, analytical models, too (Sen 1993, 2008).

Furthermore, the evaluation of quality of life for a specific community can be evaluated in both an objective and a subjective way. In the first case, indicators refer to the efficiency of services and relationships from an exclusively technical perspective, regardless of a person's perception (Erikson 1993). Otherwise, social indexes are calibrated just setting up the citizens' judgment, their satisfaction and happiness (Thomas et al. 1928; Ortiz et al. 2009).

Basically, social indicators are empirical measurements of the happiness of people and their level of satisfaction with reference to specific conditions. In particular, within urban contexts, the level of satisfaction of

citizens can be interpreted as a measure of the efficiency and functionality of the city itself. This therefore means that social indicators are able to gauge the social resilience of a community. Moreover, when dealing with extreme events having taken place, resilience depends on several different factors and on the community behaviour itself, and so indicators must refer to all involved mechanisms.

For this reason, the primary objective of this section is related to the definition of a strategy, aimed at identifying a set of adequate indicators that can be also assembled in different categories. Each of these categories can be referred to as a particular social dimension, influencing the level of satisfaction of citizens. This allows for the quantification of the “happiness” of citizens as an integral part of city resilience, and hence, of social sustainability. As an example, one can assemble the category “health and well-being”, which can take into account indicators referring to families with or without smokers, safety perception, police services efficiency, citizens with long term illness, death rate, child health, public medical services efficiency, etc. (McMahon 2002). To take this point further, indicators can also be processed as indexes, aggregations of indicators, and can provide a multidimensional and coherent view of a complex system (Cobb 2000; Mayer 2008), like the city.

In order to more consistently pursue this idea, some fundamental requirements are needed: the number of indicators have to be controlled in order to better manage the collected data (Tanguay et al. 2009), and the indicators possessing the most important linkages with engineering resilience measures have to be chosen to produce a more integrated overview.

Given that the primary intention of the present study is to quantify disaster resilience of urban communities, a further issue to account for is related to the need to perform all the specific measurements in the aftermath of the event. Indicators which describe the post-event phase as best possible have to be selected and evaluated for each step of time within each of the

considered recovery phases. In such a way, the social impact of a recovery strategy within the local environment can be effectively examined, together with its feasibility and effects on urban resilience. Another important feature is related to the capability to identify a threshold for each of the recognised indicators - a scientific measure of the limit value that it can reach. When dealing with resilience in the field of constructions, one can take into account further, more specific indicators: “number of displaced citizens”, “time of displacement”, “percentage of unfeasible buildings”, but also “number of workers”, “quantity of produced ruins”, “building process energy consumption”, and so on. Doing so permits evaluation of the social and environmental impacts, namely the measure of social and environmental sustainability. Also, when dealing with social indicators, it is actually fundamental to consider all sustainability dimensions (Figure 4.4) according to a life-cycle approach (Hodge 1991) within a human perspective. This is because an urban strategy targeting increasing the quality of life is not always the more sustainable one.

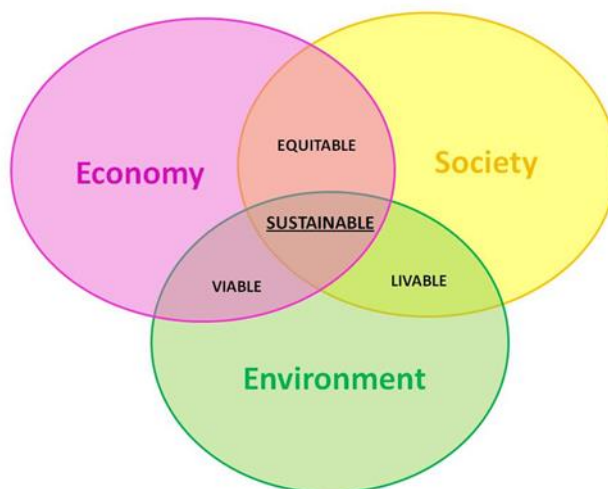


Figure 4.4 Sustainability dimensions Venn diagram (Bozza et al. 2015)

As an example, the lighting network of a city can be improved by simply providing a major number of streetlights. In this way, a category of indicators referring to the dimension “society” will increase, of course, as it takes into consideration indicators such as “security”, “community services” and “well-being”. On the other hand, the economic indicator “community expenses” will increase and the environmental indicators “energy consumption” and “environmental impacts” will increase, too.

When looking to integrate all approaches and studies investigated, a set of both qualitative and quantitative indicators may be developed:

- economic indicators, accounting for local enterprise presence, accounting for the effects on the local economy of the regional and national economies, employment rate, household income and expenses. Also, a variety of indicators involving national financial capacity can be considered, such as the Gross Domestic Product, gasoline prices, economic welfare, insurance market trends, etc. (Cardona 2013; Sharp 1999);
- social indicators, like urban well-being as perceived by citizens, security, education, health, demographic incidence on national levels, etc.;
- environmental indicators within the life cycle of an urban context, ex. ecological footprint, soil use, air quality, noise, waste, etc.

One important issue in dealing with social indicators, in particular, is related to the choice of what are deemed the most significant indicators. Current debate in the social sciences is deeply focused in determining what the indicators should be and which indicators best describe all the variables related to human well-being and quality of life. As a preliminary step, social resilience can be assessed by referring to the most common indicators used by universally recognised institutions, such as the United Nations (UN) and the World Bank (United Nations Conference on Environment and Development 1992; World Bank 1992). Such

institutions make national indicators available to everyone so that they can be used on a mass scale while also serving as reference points for the identification of local indicators, like, for instance, the “human poverty index”, “social disparity”, “unemployment” and so on. These are usually available with national census data, even if not all countries have such data readily available. In the case of the latter, indicators can be acquired through processing locally available data and by designing simple and brief questionnaires and having local administrators fill them out. In addition, well-being can be appraised through interviews with local actors, asking them about their level of satisfaction regarding urban services. Moreover, general information about the constructed environment can be employed. As has already been completed by the Inter-American Development Bank (IDB) for the Caribbean, the “Disaster Deficit Index” (DDI) and the “Local Disaster Index” (LDI) are used to classify mortality risk. However, when dealing with social resilience assessment, there are many problems widely recognised by the scientific community (e.g. gaps in data, knowledge and understanding, conceptual, methodological and application gaps). According to Tapsell et al. (2010), it is important to know the links between risk governance and local activities and processes in order to recognise the way which social vulnerability analysis fit within (and with which) societal aspects.

However, because the procedure to define and quantify indicators is rather complex, as a first step, all indicators that are determined easier to evaluate can be used when performing a hybrid approach, taking into account observed data, expert judgments and scenario analysis. Further, these easier-to-evaluate are employed in such a manner that the less precise and crude results produced can be controlled for by considering the relevant uncertainties during this phase of the study.

4.4 LINKING ENGINEERING METRICS ON NETWORKS AND SUSTAINABILITY INDICATORS

The final phase of the proposed study is related to the definition of the comprehensive methodology utilised to quantify disaster resilience in urban contexts, all within a social perspective. In particular, providing that resilience suggests a fundamental issue when dealing with social sustainability, depending on several engineering and social factors, the framework also aims to link them depending on socio-economic background.

Transfer functions, fuzzy logic processes or neural network models (Munda et al. 1995), typically used in ecosystem studies or in decision support engineering, can all be favourably implemented in the present discussion. These are all methodologies that may be used to define a system of functions to make quality of life and city performance indicators dependent on network metrics. In this context, city performance indicators measure inhabitants' happiness and environmental sustainability, and they have to be chosen in order to better describe the post-event recovery phase by a step-by-step time-discrete methodology. In contrast, network metrics can be conceived as a proxy of efficiency for the city system and urban resilience, performed on both HSPNs and typological-compartmental networks, also measured with each step of time. Such functions can be calibrated by means of real data from, expert judgments on and scenario analysis of natural and human-induced disasters.

Owing to the fact that the used indicators have different nature and unit measures, initial transformation functions could be used. They would allow for the standardisation of the gross values of the descriptors, transforming them into comparable factors. Through the employment of such a simple mathematical procedure, it is possible to integrate different kind of measurements within the current framework. In particular, measures previously identified for social and infrastructural resilience can be integrated and compared with sustainability indicators using transfer

functions. As a case in point, in order to link efficiency and happiness indicators, a fuzzy logic process can be implemented, assuming this kind of procedure better for all variables involved within the current study.

Essentially, a fuzzy logic is a mathematical method that adopts scientifically sounded laws in order to translate different kind of data, such as engineering measures, observed data and expert judgments into a homogeneous and comparable set of indicators. According to Borri (Borri et al. 1998) and Balas (Balas et al. 2004), in addition, data and indicators expressed in linguistic terms can be interpreted and finally shown as discrete numbers within a holistic perspective. Such a methodology can be a very useful tool in when putting the proposed framework into place. Indeed, it might allow comparison of the engineering measurements on complex networks, and qualitative and quantitative indicators on urban efficiency, sustainability and quality of life within an urban resilience assessment.

A suitable example, would be to define a HSPN composed by the physical hospital network, constituting a public urban service, the physical networks of all possible street paths leading to each hospital and the social network of citizens served by each hospital close to their homes. It is possible to model this kind of hybrid network through the application of the theory of graphs, as already shown previously, and model the urban topology by overlaying single networks. The considered networks are:

- the physical network of residential buildings;
- the physical network of hospitals;
- the physical network of streets;
- the social network of local citizens.

Such a network can be also modelled considering the typology of the relevant actors, goods and services and performing a “by group” modelling, according to the more general theory of networks, as a

“typologically evolving dynamical network”. Then, other groups can be considered:

- the group of physical structures representing hospitals, which can be more or less important;
- the group of residential buildings, closer or further from each hospital;
- the group of physical structures representing streets, mutually linked and connecting residential buildings to hospitals;
- the group of citizens, that can be very young, young or old and are therefore differentially served by hospitals.

Within this scenario, making provisions for an extreme and unexpected event occurrence, such as an earthquake, engineering measurements can be performed on disaster scenarios within a time-discrete analysis:

- in the case of the topological network, the global efficiency level is computed using a punctual measurement with a synthetic efficiency indicator, which is then averaged throughout the overall system. Each measurement can be performed on a single node according to the importance of the street and/or hospital considered and on the number of citizens it serves, while also depending on the number of residential buildings that are closer to it. This allows characterisation and assessment of the hospital-citizen network;
- in the case of the typological network, the global efficiency level is supplied by engineering measurements performed on the overall system. Specific relationships, producing quantitative measures between the interacting components and actors can be calibrated via the aid scenario analysis.

Finally, a resilience measure can be deduced in both cases simply through the evaluation of the difference between the values that the global efficiency indicators assume when measured before an extreme event occurs (peacetime) and after it has occurred (recovery phase). Moreover, the measure of the rapidity and effectiveness of the adopted urban strategies can be appraised by the implementation of methodology for each step of time during the recovery phase.

The same technique (application scheme is shown in Figure 4.5) can also be applied to the police-citizen network to explore the level of urban safety; the school-citizen network, in order to evaluate the level of education for citizens; the citizens-citizens network, in order to understand the quality of interactions between local inhabitants, and so on.

However, it should be noted that efficiency measures do not allow assessment of the social, economic and environmental sustainability of the recovery process. So, in order to also comprehend the social dimension of resilience, the use of social indicators is warranted and linkages existing between engineering metrics and social and sustainability indicators have to be characterised.

Given the illustrated example, a major efficiency of health services and a higher safety level for buildings representing hospitals, within the urban area, can positively affect the quality of life perceived by a city's citizens and this can be demonstrated through the examination of a set of suitable indicators. Obviously, based on the case that one is analysing, a number of variables have to be considered when dealing with social networks. As an example, the social network where "strong and weak ties" exist has been reviewed by Granovetter (Granovetter 1973) and refers to the efficiency in communication between people. Here, strong ties are relationships governed by a highly shared knowledge base. An example can be found in the relationship between two friends that possess a long relationship. They share hobbies, activities and may have even studied at the same Institute

or work for the same company. Hence, links between such social actors are expected to be much denser.

On the other hand, weak ties are fortuitous for short-term relationships. For instance, this is the case of the link between a former smoker and a tobacconist from whom he once bought cigarettes.

Granovetter has remarked as well that weak ties play an important role, allowing an understanding of the mechanism of holes within a communication network. This is apparently the result of the wide range of variables influencing human choices and mutual relationships. Following Granovetter, further studies have been performed that have established all humans belonging to networks where both strong and weak ties exist, as in the case of “small-world” network, as described by Watts and Strogatz (Watts and Strogatz 1998). With this, it is very important to choose indicators according to adequate criteria. For instance, one can evaluate indicators related to: life quality perception, health services efficiency, mortality rate, street maintenance, job creation, number of sick citizens, etc. All factors that impact the urban economic and social conditions, yielding a measure of the “happiness” of citizens, should also be easily related to efficiency indicators.

Several advantages can be seen when dealing with this form of methodology (Figure 5) : according to Munda (Munda et al. 1995), it permits the collection of more interpretable and comparable results, assimilating transdisciplinary information and taking into account system complexity; moreover fuzzy logic can deal with uncertainty and can be supported by probability techniques, as done by Chavas and Marchini (Chavas 2000; Marchini et al. 2011).

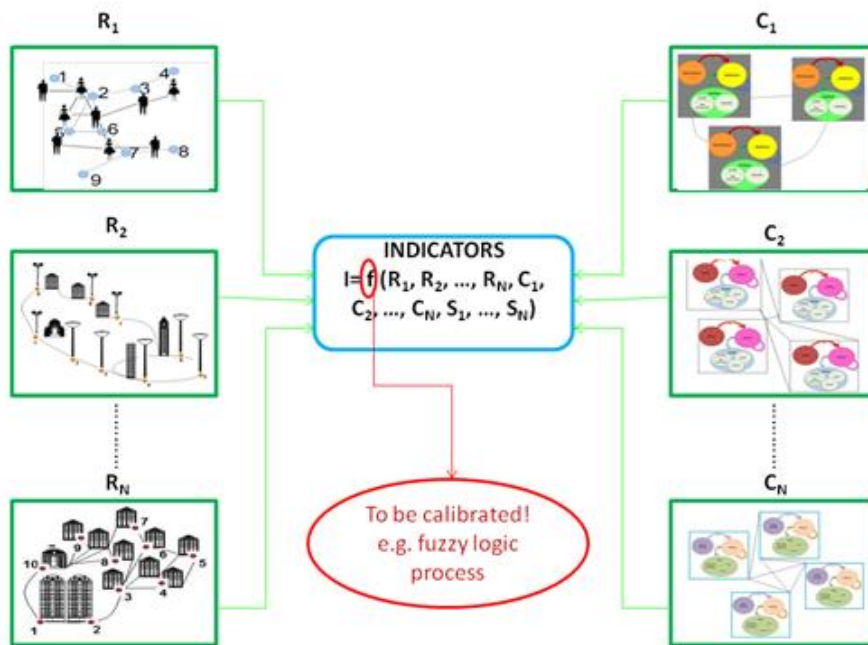


Figure 4.5 The proposed framework, where: R_i are the efficiency measures performed first on the punctual nodes and then on the global HSPNs; C_j are the resilience and efficiency measures performed on the typological groups and S_k are indicators referring to the social-economic background (Bozza et al. 2015).

The present work aims to propose a rigorous framework to allow the evaluation of urban resilience within a multidisciplinary and integrated approach, according to a human perspective.

A dual application field is recognised within this framework:

- peacetime, that is the phase in which no extraordinary, shock event has occurred and the urban context is in a stationary equilibrium state.

The framework can represent an effective mitigation instrument for authorities and risk managers, targeting assessment of the local coping capacity in the case of disaster and to reduce risk. This is a reasonable approach to gauge the effectiveness of the available local instruments and resources and to identify all aspects of the situation needing improvement.

Within this context, the proposed framework also represents an instrument for monitoring local resilience properties;

- recovery phase, that is the case in which a catastrophe has occurred.

The framework, integrating resilience and sustainability concepts, can be a suitable instrument to recognise the best practices and strategies to put into effect after the event in order to guarantee the selection of the best recovery path. In this circumstance, one deals with an adaptation instrument, provided that the strategies are oriented towards recovering functionality and equilibrium while also trying to adapt the local context to the new urban configuration. The best recovery strategy can be identified as the one able to maximise the “happiness” and the quality of life during recovery using the described methodology as a tool for decision support.

A measure of the resilience level of the investigated urban context and its sustainability can be arrived at to identify the best recovery solution in the aftermath of a catastrophe. An overview of the proposed framework is depicted in Figure 4.6:

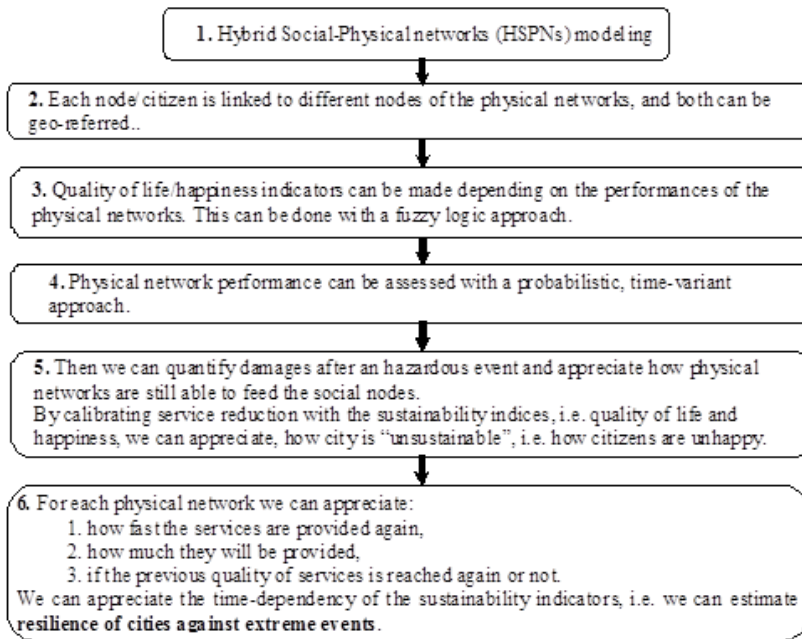


Figure 4.6 Methodology exploiting scheme (Bozza et al. 2015)

The reason why the proposed framework focuses mainly on the local level stems from the ease in identification of the responsibilities of all parties involved, the clearer contrast between those parties and the easier control of their actions (Campbell 1996). Furthermore the comparison between municipality and cities may also lead to a more comprehensive national overview, further enhancing the identification process of the most optimal recovery strategies in the aftermath of an extreme event. This instrument can also facilitate superior coordinated actions between cities within the same region or of the same size to eventually share effective strategies and tools and to ensure compatibility. Finally, it is also possible to perform a global assessment of different urban configurations within this comprehensive approach. One can recognise the strategies that afford the most superior level of resilience, and therefore sustainability, too. Hence, it can also be said that this allows identification of the best recovery solution in the aftermath of an extreme event for each unique urban

configuration. The primary aim is, in fact, to give authorities and risk managers an effective tool to improve both mitigation and adaptation strategies and render them usable for all municipalities, while also being employed as a decision-making instrument. In order to estimate where the best path to recovery lies, one can build diagrams, for example, where all possible recovery paths are listed, so-called “influence diagrams” (McDaniels 2008). For each considered strategy, all positive and negative aspects and each class of indicators associated with it, as provided as the output from the fuzzy logic process, are listed. This is a well-known approach, developed in the decision sciences (Howard and Matheson 1963), attempting to compare all possible solutions when exploring decision alternatives (Clemen and Reilly 2004), in order to identify the choice exhibiting the maximum sustainability rate.

Such an approach also allows technicians and scientists to perform a visual characterisation of the relationships present among all the variables involved. It can be a powerful device to collect data resultant from the implementation of the current proposed framework for different urban configurations and seemingly disparate recovery strategies. Additionally, influence diagrams can be developed to take into account the dynamic nature of the recovery process after an event has taken place and to foster communication and understanding between authorities, designers and policy makers.

CHAPTER 5

SEISMIC CATASTROPHE RESILIENCE AGAINST URBAN SHAPE AND SIZE

The increasing complexity of urban dynamics rules modern societies worldwide, marking an important landmark in human history, as it characterizes the urbanization era. This inexorable trend leads contemporary cities to be the cornerstone of social and technological development at the same time, being even more exposed and vulnerable. Opportunities and challenges arise from such phenomena, causing novel approaches to urban management to be needed. Particularly, a major issue is related to natural hazards, to be accounted for according to a pioneering, engineering and also human-centric vision, to build sustainable and resilient cities. In the present study, urban resilience against disasters is understood as the engineering one according to the ecosystems theory.

An engineering-based methodology for resilience quantification is proposed. It allows to model any urban context as a complex network and to assess resilience as the regained efficiency after a catastrophe occurred, and for each stage of the recovery process.

Due to the high rate of occurrence and to the huge economic losses caused by seismic events in last decades, earthquake scenarios are simulated to endorse the methodology. A real case study is developed for the historical centre of the city of Naples (Italy). Furthermore, according to the more widespread city configurations, urban contexts are modelled, with diverse shapes and sizes, to study the trend of urban resilience against the geographical configuration and scaling relation with the city size. The social and physical city sub-systems are individually modelled as complex networks and then overlaid to account for their interrelations as

a hybrid social-physical network (HSPN) (Cavallaro et al. 2014; Bozza et al. 2015).

The vulnerability of infrastructures - buildings and streets - is accounted for through the integration of probability-based models. Efficiency measures are performed, allowing for the local and global loss of functionality to be assessed, hence to evaluate also the urban damage in a systemic manner. Finally, diverse recovery strategies are simulated and resilience is calculated for each studied city context.

5.1 AN ENGINEERING FRAMEWORK TO QUANTIFY URBAN RESILIENCE

Contemporary patterns of urbanization lead cities to be the cornerstone of human activities and technological development. Indeed, according to the 2014 revision of the world urbanization prospects from United Nations, 54% of the world's population lives in cities, expecting for such a proportion to increase to 66% by 2050 (UN 2015). As a consequence, also infrastructures and community assets are increasing in number, causing urban areas to be exposed and vulnerable now more than ever.

With this, urban management is nowadays one of the most important challenges to guarantee local and global communities development and to build sustainable and resilient cities.

A major issue, in this background, is constituted by disaster risk management, in step with the raising awareness on problems related to climate change, global warming and the alarming increase of the rate of occurrence of natural hazards worldwide.

One of the most threatening of these is the seismic risk. Since 2004 to present, six of the ten costliest catastrophic event are earthquakes, having caused huge human and economic losses (Munich Re, NATHAN 2011).

To date, seismic hazards are, in fact, an ordinary issue with which local authorities have to deal with. With this, scientific community and urban stakeholders pay particular attention on the search for innovative

solutions. New paths of prevention and emergency management, mitigation and adaptation actions, such as response and recovery strategies are continually developed. Nonetheless many doubts still remain about the way to choose the best of these interventions. So, which are the relevant criteria for selecting the most feasible strategy after a catastrophe? How can local administrator choose to undertake an action rather than another one?

The buzzword is to build resilient cities.

Resilience is the capability of a system to withstand external stresses and recover from them, to reach an equilibrium state. Hence, each potential action is as much effective as higher is the contribution it can give at increasing resilience. Such feature is strictly related to the capability of the studied system to be sustainable too. Indeed, the more the system is efficient in using its own resources to recover from a shock, the more it can strive for future sustainable development. This is even more evident when dealing with natural disasters affecting urban areas, where a more efficient recovery is guaranteed from a higher sustainability of the reconstruction phase, within the life cycle of a city. A city is, in fact, as much resilient as it is more sustainable during the hazardous event occurrence, that is when it suffers an external stress and makes an effort to reconfigure its equilibrium (Asprone and Manfredi 2013; Bozza et al. 2015).

On the other hand, the concept of resilience is a very multidisciplinary one, being used in psychology and social science (Garmezy 1991; Werner and Smith 1982), medicine (Lotka 1924) and engineering too (Bruneau et al. 2003). In this study, it is understood as the engineering resilience definition (Bruneau et al. 2003; Pimm 1984; Holling 1973), according to the ecosystems theory. Hence, resilience is defined as the capability of the city system to withstand external stresses, bouncing back to an equilibrium condition that can be the same as the pre-event one, but also a new, different one (Asprone and Manfredi 2013; Bozza et al. 2015).

In this study, the considered external stress is the earthquake and the city system is modelled as a complex network, being assimilated to an ecosystem (Holling 1973, 1986, 2001), hence merging within the geographical space, which it is embedded in, all interacting urban components: the social and the physical one. However, serious attention has to be paid when modelling urban contexts, because city complex systems may be far cry one from each other. On the one hand, urban environments typically differ in size and geographical shape, hence when attempt to model a city, it is fundamental to account for its territorial extent and for the spatial distribution of its component. Nonetheless, on the other hand, they share similar socio-economic dynamics and topological features (Cardillo et al. 2006), which enable to compare them. Hence, despite the huge diversification among urban tissues worldwide, some general rules can be observed, whose magnitude typically scales with the city size (Bettencourt 2013; Bettencourt and West 2011; Bettencourt and West 2010; Bettencourt et al. 2007). The way such scaling arises strongly depends on the type of the observed phenomena. According to Lobo (Lobo et al. 2013) and Bettencourt (Bettencourt and West 2011; Bettencourt et al. 2007), the thick network of interrelations, which develops within urban contexts is based on very diverse underlying mechanisms. They observed changes in a huge quantity of indicators with the city size and recognize two predominant trends, which can be associated to social or economic dynamics. In particular, indicators being related to economy of scale mechanisms exhibit a superscaling with the city size, while subscaling is observed for indicators being related to social processes (Bettencourt et al. 2007).

To characterise the trend of urban efficiency, damage indicators and resilience against the city size and shape, the present study proposes an integrated framework, which simulate the seismic event and enables to assess expected damages and to quantify resilience.

According to Batty (Batty 2008), since contemporary cities are typically fractals, the most effective use to model and simulate their behaviour is to deconstruct the rules that have been used in the past and design idealized cities. On the other hand, most of these realizations rarely provide the quality of life of their inhabitants as they are too simple with respect to the real workings of the development process. Hence, keeping this in mind, synthetic city models are developed within the current framework, while also accounting for typical features of actual urban contexts. Also a real case study is performed to validate the proposed metrics, for the inner city Naples (Italy), the Quartieri Spagnoli area.

Cities are modelled according to the graph theory, as complex networks. The infrastructure and the social networks are separately modelled and then overlaid and included in the related geographical space, to finally obtain a hybrid social-physical network (HSPN) (Bozza et al. 2015; Cavallaro et al. 2014). Georeferencing is performed through a geographic information system (GIS), which enables to integrate specific information on the built environment and a large range of data.

Particularly, synthetic HSPNs are modelled based on the geometric shapes, which are the most common worldwide and of which historically contemporary cities took the form. Hence, diverse cities are modelled with rectangular, circular, hexagonal and star shape. Each of these shapes is then increasingly scaled and seismic scenario is simulated for each of them.

Scenario analysis are performed, accounting for the vulnerability of the built environment through a probability-based methodology. Two diverse recovery strategies are modelled and simulated, being the former focused on social dynamics and the latter on economies of scale, being related to a city service. Efficiency, as it is a robustness metric of the network, representing the urban connectivity, is evaluated before the event, soon after its occurrence and for each stage of the recovery process. Hence, urban damage is assessed in a systemic fashion, as the city efficiency decays in the aftermath of the earthquake. Finally, urban resilience is

quantified, as the city capability to bounce back to the equilibrium. Furthermore, an alternative resilience metric is used to evaluate the city performances according to its damage level.

Results are analysed and compared to recognise the most efficient city shape and the trend of resilience against the city size.

5.1.1 Contemporary city ecosystems modelling

So far, cities have always been studied as entities with a well-defined functional structure. Hence, when dealing with disaster management, each urban context was usually understood as a unique system, being then placed and considered in a wider national framework. Nowadays, this is a perspective, which can sound too restrictive, since it does not account for complex dynamics and interdependencies arising from typical self-organising processes in each city.

With this, one should consider that each city is characterised by underlying mechanisms, which are governed by people living in it. City inhabitants live, indeed, following rules and making choices, which can diversely influence the urban structure both from a human and a topological point of view. These are social dynamics, having different outcomes depending on the city geographical configuration and its sociological, cultural and economic background.

On the other hand, citizens are fed by urban services, hence always acting through a dense infrastructure network, which they are strictly interrelated with.

It is clearly evident that each urban context should be modelled starting from its life at the small scale, that is by considering the linkage between each citizen and each physical structure.

The major reason for this lies in the chance to assess urban performances, according to the peculiarity of each studied city. Hence, in this study, the focus is put at the local scale. This is the basis for a multi-scale approach,

which can finally lead to an upper scale, the global one, according to the modern bottom-up thinking.

Cities are modelled as spatial networks, which are a particular kind of complex networks, being embedded in a two-dimensional space, whose typical metric is the Euclidean distance. A system of typical street patterns is created to model each urban geometry, into a GIS environment, whose topology is inspired to the major European and US cities and ancient city centres.

Particularly robustness of the proposed approach is studied on a real case study, that is the historical centre of the city of Naples. Furthermore, to study differences with the size and shape of the studied urban centre four different city geometries are modelled, as shown following:

- Circular (ex. Rome, Figure 5.1; l’Enfants’ plan for Washington DC; Regent’s park in London; Karlsruhe);



Figure 5.1 Picture of Rome and the city map, showing analogy with the circular shape

- Rectangular (ex. Savannah, Regensburg on the southern bank of river Danube, from Roman times (Milgram 1967)), better known as the typical structure of US modern cities, ex. Orlando, New York, Philadelphia (Figure 5.2), etc., they typically exhibit T-shaped crossing as self-organised urban networks. Also Venice and Cairo shows similar geometric shapes, actually they are not just rectangular but self-organised cities as well;

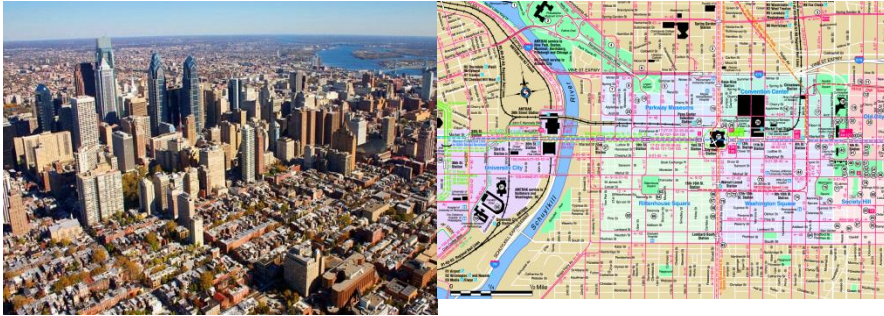


Figure 5.2 Picture of Philadelphia and the city map, showing its typically rectangular shape

- Star, ideal city model of renaissance, an example is the Italian city of Palma Nuova (Figure 5.3), outside Venice, originally accredited to the architect Scamozzi.



Figure 5.3 Picture of the city of Palmanova and its typically star shaped planimetry

Each investigated urban centre is modelled as a hybrid social-physical network (HSPN) (Bozza et al. 2015; Cavallaro et al. 2014). HSPNs' is a novel approach based on the complex network theory, which enables us to account for all the city components. Moreover, interrelations between urban physical – buildings and infrastructures – and social components – citizens – can be characterised, to understand the city's physiological behaviour with a human-centric perspective.

Essentially, first the infrastructure and the social network are individually modelled as graphs and then they are overlaid in the global network, the HSPN (Bozza et al. 2015; Cavallaro et al. 2014).

Particularly, in this study, the infrastructure network is represented through the modelling of the street network. This is because of most of urban services being typically arranged along urban street patterns. As a consequence, this simplification enables to study the interactions between the city inhabitants and services, by simply modelling only two planar graphs. A complex network is, in fact, always represented by a graph $\Gamma = (N, L)$, being constituted by a discrete set of nodes, $N = \{1, 2, \dots, n\}$ and a discrete set of links $L \subseteq N \times N$.

In the case of HSPN modelling two set of links and two set of nodes are modelled to create the social and the physical network.

The former is given by the set of nodes representing residential buildings, N_b , and the set of door links, L_b , connecting each building to the street junction's nodes. Whereas the latter is constituted by the set of nodes, N_s , which represents the street junctions, and the set of links, L_s , which represents urban street patterns, where also the number and the length of links representing streets are taken into account.

Finally the city's HSPN is obtained and denoted as $G(N_b \cup N_s \cup L_b \cup L_s)$. A further simplification is done regarding the vehicular and inhabitant's flow, that is assumed to be bidirectional in each street in order to bypass the traffic modelling issues. As a consequence, the HSPN is defined as an undirected graph, implying for each arch linking the generic nodes i and j , the converse arch to exists too.

The proposed approach clearly enables us to model any kind of city, provided the availability of information about the location, the number and the typology of buildings and streets. These data can be acquired from national databases and surveys.

This is the case of the Italian National Institute of Statistics (ISTAT) (ISTAT 2001), which hypothesis in the present study refer to. ISTAT

enables us to know the incidence of buildings out of the entire urban building portfolio, according to their structural typology, number of storeys and age of construction. Further data can be obtained by processing urban statistics, such as the number of people living in each residential building or the number of students attending a school.

This last information is fundamental to model a city's social network. In this work 1 citizen each 30 square meters of each considered building is assumed, based on ISTAT data, to finally account for the total number of citizens living in each city.

Finally the physical and the social network are merged. Each building, in fact, has got a double significance within the HSPN: on one hand it represents an essential component of the physical network, together with the streets' system; on the other hand it represents a group of citizens, i.e. the city's social component. Starting from the city's buildings, the linkage between the physical and the social network is also characterized and then modelled. The buildings' network is in fact connected to the streets' network through the outgoing door links. Furthermore it is also connected to the other buildings, being social networks' nodes, through the outgoing street links, representing interactions subsisting between group of citizens.

5.1.2 Scenario simulation: the citizen-citizen and citizen-school case study

Two different case analysis are presented and seismic scenarios are run for both of them. Once the HSPN is modelled, efficiency is evaluated in case no event has occurred. Consequently, an earthquake is simulated, causing disruption to the entire city model and, in particular, buildings damages and/or collapse and street interruptions, due to safety purposes or to the debris fallen from buildings, which obstruct adjacent streets.

The proposed study is not focused on the buildings' vulnerability only from a strictly engineering perspective, otherwise it is also focused on how the buildings' vulnerability impact the whole city operation conditions

whenever a catastrophic event occurs. Hence, city damages are simulated by assuming structural vulnerability to be uniformly distributed on the territory and imposing diverse extreme seismic scenarios.

With this, the damage state suffered by the city physical network is computed in a deterministic fashion. Two diverse earthquake severity levels are simulated for the HSPN, by assuming, respectively, the 15% and the 30% of buildings to collapse.

Furthermore, in each scenario a particular assumption is made depending on the type of efficiency that has to be assessed. In the case citizen-citizen efficiency has to be evaluated, a certain percentage (15% or 30%) of the residential buildings is imposed to collapse based on their identification number (ID). On the other hand, when dealing with the case, which citizen-school efficiency has to be evaluated in, the imposed percentage of buildings to be considered severely damaged or collapsed is both evaluated for the set of the residential buildings and for the set of school buildings. However, in this case, the same percentage is used to impose the buildings' collapse, according to the same approach adopted for the case of citizen-citizen efficiency evaluation. Hence, the connectivity features of the network are evaluated with reference to both the links between couples of residential buildings and the links between each residential building and each school.

To do this, in both the case analysis, a fully random methodology is implemented, that generate a random permutation of integers in $1:N$. Hence numbers extracted from the permutation will decide which building will not survive, by recognizing their ID.

Furthermore, streets being adjacent to such buildings are considered to be impracticable according to a probability-based approach. Based on the ratio between each damaged building's height, h , and the streets' width, l , that it is located on, the probability of street interruption is accounted for as shown by Equation 1 (Cavallaro et al. 2014), following:

$$P_r(h,l) = \begin{cases} 1 & \text{if } h \geq l \\ \frac{h}{l} & \text{otherwise} \end{cases} \quad (1)$$

Stream of uniform pseudorandom numbers is generated and values from the standard uniform distribution are selected on the open interval (0,1), and compared to the assessed values of the streets' interruption probability, P_r . Being such values larger or smaller than those obtained from the stream simulation, decide respectively whether the street will be not obstructed by the adjacent buildings or will be made inaccessible by them.

Notice that a higher ratio between the building's height and the street's width has got a cascade effect on the city functionality level, being higher the probability of street's interruption. In fact, the higher is the adjacent building, the higher is the chance that debris fall on the street or that civil protection closes the street for safety purposes.

This has got a further effect on the behaviour of the HSPN itself: due to the street being eventually become inaccessible, the link which represents it, will not be useful for network connectivity purposes. Keeping with this, to evaluate efficiency in the aftermath of a catastrophic event, it has to be considered that whether an shocking event occurs (particularly a seismic one), buildings' damage and/or collapse is expected, as well as streets' interruption due to the buildings' debris fallen or to civil protection issues. As a consequence, nodes representing damaged buildings and links representing streets subjected to usage restrictions, are considered to be inactive. Hence, they are removed from the network topology model and efficiency in the aftermath of the earthquake is evaluated by only accounting for the survived city's components.

Moreover damages on buildings result, for each simulated earthquake and damaged city configuration, in a certain number of citizens to be

reallocated. Accordingly, the same approach is also used to compute the number of users being fed by the school service.

As a consequence, in both the case analysis, a zero stage is recognized where a certain percentage of buildings (only residential or residential and scholastics) and streets are unusable, hence to be removed from the HSPN model and causing some parts of this to be disconnected.

As a case in point, at this stage a suitable recovery strategy has to be selected and simulated to monitor progress in the HSPN restoration. In this study, a “status quo down-up” strategy is implemented (Cavallaro et al. 2014). It is directed to recover the urban HSPN to its initial configuration with buildings being progressively put back in place, citizens being relocated in their residential and damaged streets being restored.

The recovery process is simulated through n discrete stages, both for the citizen-citizen and the citizen-school case analysis. Each stage provides for a fraction $1/n$ of the displaced citizens to be relocated, starting from the smallest buildings, which are also the cheapest ones, and progressing step by step to the largest ones. Paralleling also street links, that were interrupted, are reactivated within the HSPN, once the buildings that caused their interruption are reconstructed. Hence, street nodes and links and building nodes and door links are gradually reactivated, causing in each stage of the selected recovery process a certain quantity of buildings and streets to be restored and a certain number of inhabitants to be relocated. As a consequence, in each of the recovery stage a different efficiency value, both for citizen-school and for citizen-citizen case studies, is assessed.

For each HSPN and for each scenario and case study three sets of measures are evaluated: the number of damaged buildings and streets; the values of citizen-citizen efficiency, E_{cc} , and citizen-school efficiency, E_{cs} , respectively for the residential HSPN and the school one, both being evaluated before the earthquake occurrence, soon after it and for each recovery stage; the systemic damage, D , the damage-dependent, R^D , and

the damage-independent resilience, R^E , to finally quantify the recover capacity.

5.1.3 A novel understanding of complex networks metrics: assessing the urban systemic damage

In this study, urban efficiency is understood as the city network capability to fed citizens, depending on their geographical location and the buildings' spatial configuration. Efficiency is evaluated in the pre-event network's configuration by accounting for all existing nodes and links, as the global connectivity level of the studied urban environment. Hence, efficiency is a measure of the services' usability to citizens, consequently enabling us to assess the damage to the urban services' quality and to the entire city system, as perceived by its inhabitants.

Once the damaged configuration of the city HSPN is known and efficiency has been evaluated, a recovery strategy has to be hypothesized and planned. According to the chosen strategy, recovery actions are then simulated within a discrete steps procedure, which streets and buildings are gradually restored through. Hence, efficiency can be reassessed in each recovery stage by considering streets and buildings having been repaired.

Basically, to assess city efficiency according to the graph theory, the quality of the connections between pair of nodes i and j has to be evaluated. To do this a cost is associated to each walk or path, by summing up on all the involved edges. Whereas a walk from i to j is defined as an alternating sequence of nodes and edges. A walk is called path, whenever each node is crossed only once. Hence, a relationship on the distances between nodes is recognised in Equation 2:

$$d = \frac{d_{ij}^{eucl}}{d_{ij}} \quad (2)$$

where d_{ij}^{eucl} is the Euclidean distance between node i and node j and d_{ij} is the length of the shortest path, that is the one between i and j having the minimal length.

Typically a one-dimensional graph, G , can be defined through two measures the characteristic path length, L , and the clustering coefficient, C_c (Cardillo et al. 2006). The former is a global feature of the network, representing the mean graph distance over all couple of vertices and is evaluated as shown by Equation 3:

$$L = \frac{1}{N \cdot (N - 1)} \cdot \sum_{i,j \in N, i \neq j} d_{ij} \quad (3)$$

where N is the number of network's nodes and d_{ij} the shortest path between each couple of nodes, hence the graph distance. L can be defined if and only if the graph is connected, otherwise it cannot be a finite quantity, with d_{ij} tending towards infinite. On the other hand, the clustering coefficient, C_c , is a local feature. Let us consider the generic node i , C_c represents “the subgraph of the neighbours of i , divided by the maximum possible number $k_i \cdot (k_i - 1)/2$ ”, according to Latora and Marchiori **Errore. L'origine riferimento non è stata trovata.** Latora and Marchiori (2001), and can be evaluated as shown in Equation 4:

$$C_c = \frac{1}{N} \cdot \sum_i C_i \quad (4)$$

with C_i being the number of edges in the graph, G_i , that is the subgraph of the given graph, G , induced by the first neighbours of i . Basically, the clustering coefficient enable us to evaluate the number of triangles in a real system.

According to Watts and Strogatz, it is possible to rewire independently and continuously each edge of G at random with probability p and observe that it can be suited from a regular lattice, whether $p=0$, into a random graph, whether $p=1$ (Watts and Strogatz 1998). In this transition, it is observed an intermediate state, where at small p the system shows high clustering, like regular lattices, while still presenting small characteristic path length like random graphs. This is a typical feature exhibited by real networks, that are usually scale-free networks like social, informatics and biological networks, called the small world behaviour (Cardillo et al. 2006; Watts and Strogatz 1998; Milgram 1998). It means that such networks have got a connection topology, that is neither typically regular nor typically random. Still according to Latora and Marchiori (Latora and Marchiori 2001), man-made urban networks and neural networks show a small-world behaviour, hence they are efficient systems both at a local and at a global extent. With this, a single-variable definition is given based on the general concept of efficiency, E , that enables us to withdraw all the constraints, being related to the system's unweightedness, connectedness and sparseness.

Efficiency has got a physical meaning, that embrace the system's features both at the local and at the global scale and enable us to measure its functionalities in any condition. Of course, if we consider all the possible paths in the graph, G , from i to j , d_{ij} is the smallest sum of the physical distances throughout them. Hence, by supposing that the system is parallel, i.e. material, information and/or people flows progress concurrently along the network, through its arches, from each node, it can be assumed that the global efficiency of a real network is inversely proportional to its shortest paths. As a consequence it can be calculated as shown in Equation 5 (Cavallaro et al. 2014; Latora and Marchiori 2001; Watts and Strogatz 1998):

$$E = \frac{1}{N \cdot (N - 1)} \cdot \sum_{i,j \in N, i \neq j} \frac{1}{d_{ij}} \quad (5)$$

where, whether there is no path between the generic nodes i and j , d_{ij} tends to infinite and efficiency turns out to be zero. Furthermore, the efficiency can be normalized in $[0,1]$ by dividing the shortest path length between i and j by the Euclidean distance, d_{ij}^{eucl} , that is the geographical distance between from i to j as the crows flies. Subsequently, the normalized pairwise efficiency can be calculated and averaged on each couple of nodes, hence representing the global network efficiency, according to Equation 6 (Cavallaro et al. 2014; Latora and Marchiori 2001):

$$E = \frac{1}{N \cdot (N - 1)} \cdot \sum_{i,j \in N, i \neq j} \frac{d_{ij}^{eucl}}{d_{ij}} \quad (6)$$

In the present study, the global efficiency has to be evaluated by accounting for the distance between the network's nodes feeding city inhabitants but also for the number of citizens living in each building. As a consequence, a modified version of the proposed relationship is herein used, in consistency with the HSPN approach. It enable us to evaluate the connectivity level between groups of inhabitant, that is the case of the citizen-citizen efficiency, or also between groups of inhabitants and urban services, for instance in the case of the citizen-school efficiency. Equation 7 and Equation 8 show the relationships (Cavallaro et al. 2015), whereas E_{cc} represents the citizen-citizen efficiency and E_{cs} the citizen-service efficiency (in the example, citizen-school efficiency):

$$E_{cc} = \frac{1}{H_{tot} \cdot (H_{tot} - 1)} \cdot \sum_{i \in B} H_i \cdot \left((h_i - 1) + \sum_{j \in (B \setminus I)} H_j \cdot \frac{d_{ij}^{eucl}}{d_{ij}} \right) \quad (7)$$

here i, j are the building nodes' ID, H_{tot} is the total number of the city's inhabitants, H_i and H_j are respectively the number of citizens living in building i and the number of citizens living in building j . B is the set of the building nodes, d_{ij} is the shortest path's length and d_{ij}^{eucl} is the Euclidean distance, between node i and j , and h_i is the number of inhabitants living in buildings having zero distance from building i , which belong to the set I .

Hence, the efficiency for services' HSPNs can be also assessed, if the outer summation in Equation 7 is substituted with a summation over the set S of the buildings representing facilities, such as schools. Furthermore also the term H_{tot} is substituted with the term S_{tot} , that is the summation of the total number of citizens using the buildings, that supply the considered urban service, and that represents their importance in the HSPN. Instead, S_i is the number of citizens, that benefit from the service supplied by the facility building $i \in S$.

$$E_{cs} = \frac{1}{S_{tot} \cdot H_{tot}} \cdot \sum_{i \in S} S_i \cdot \left(h_i + \sum_{j \in (B \setminus I)} H_j \cdot \frac{d_{ij}^{eucl}}{d_{ij}} \right) \quad (8)$$

Basically the difference in terms of the efficiency typology that can be evaluated, depends on the distances used to compute it. As an example, in the case of citizen-citizen efficiency to be computed, the shortest path distances and the Euclidean distances are both evaluated between couple of buildings, representing residencies. Conversely, if citizen-school efficiency has to be computed, both distances have to be evaluated between each city's physical component, representing a school, and each city's physical component, representing a residential building.

The global efficiency can be therefore evaluated for each city's HSPN and this approach is employed to assess the city damage in a systemic fashion. Despite the traditional approaches in civil engineering, that focus on the single structure, in this way it is possible to obtain a global overview of

the urban system by focusing on the way urban damages affect the city functionalities. With this, once efficiency is evaluated before, E_{pre} , and soon after the event occurrence, $E(t=0)=E(0)$, or in any recovery stage, $E(t>0)$, it is possible to define a function, called the recovery function, $Y(t)$, that returns the residual city system's capacity to feed citizens. Equation 9 shows the formula:

$$Y(t) = \frac{E(t)}{E_{pre}} \quad (9)$$

where $t=0$ is the time at which the seismic event is just occurred and the city's HSPN presents its "worst", i.e. damaged, configuration.

The proposed relationship can be then evaluated in each time stage of the recovery process, $Y(t)$, once efficiency at that time has been also assessed. Keeping with this, it is possible to quantify the systemic damage on the whole urban network, by simply observing the drop in the HSPN efficiency, $E(t)$, in terms of the recovery function, $Y(t)$.

This is the novelty of the study herein presented, due to the chance to assess the state of service of the urban environment after the occurrence of a catastrophic event by merging civil engineering and complex networks methodologies. Such an approach, allow to perform a measurement of the after-event level of performance of the city, which is a systemic and integral one. The systemic damage measure, being normalized with respect to the pre-event city's efficiency, E_{pre} , can be simply evaluated as shows Equation 10:

$$D(t) = \frac{E_{pre} - E(t)}{E_{pre}} = 1 - Y(t) \quad (10)$$

and is defined in the close interval $[0,1]$. The observation of such indicator, becomes critical when observing the city's HSPN soon after the event occurrence (at the zero stage), $D(0)$.

Obviously the most the value of D tends to unity, the most the observed systemic damage is severe. As a consequence, the two limit cases can be defined as, $D(0)=1$ “total damage”, while $D(0)=0$ “no damage”.

5.1.4 The quantification of urban resilience

Urban resilience is understood as a fundamental component of sustainability, in particular as the capability of a city ecosystem to be sustainable during the hazardous event occurrence phase. Basically, a city has to show readiness and promptness in disaster response and it has to effectively bounce back to an equilibrium condition, that can be new or the same as before the event occurrence. For the resilience quantification purpose, this study proposes a novel approach, that enable us to contextually evaluate urban life quality, according to a humanitarian approach, disaster resilience and city robustness to structural damages. Damages suffered by a urban context are, in fact, here evaluated as the decay of the city's state of service after the occurrence of an adverse event in an integral fashion. This is an approach that does not look at the city as a global system, but that analyze it by accounting for each single city's component, both physical and human, and for their mutual interrelations. As a consequence, the city model is built through the gradual annexation of such components, according to the modern multi-scale approaches, from the lowest to the highest degree of network complexity.

Resilience can be assessed by integrating in time the recovery function, $Y(t)$, at all recovery stages. Physically, this can be interpreted by observing the trend of the recovery function in the $t - Y(t)$ plane, describing the recovery curve (Figure 5.4).

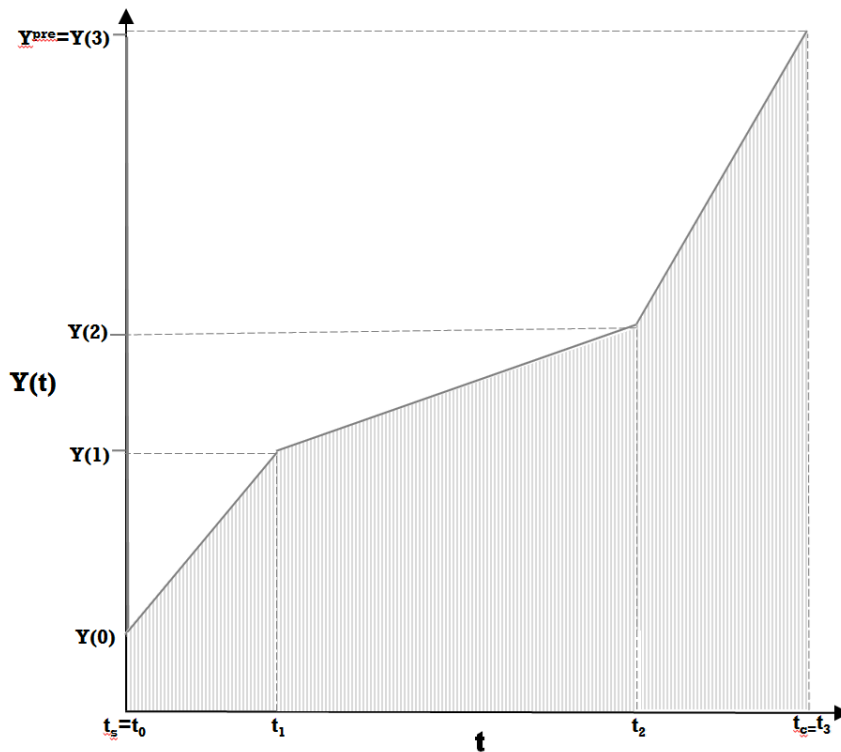


Figure 5.4 Trend of the recovery function, $Y(t)$, across the recovery strategy against the time, t

Whereas resilience is the area under the curve, being divided by the time needed to implement the selected strategy, that is the time passed by from t_s , when the recovery process has started, to t_c , when it is completed. With this, the resilience quantification can be performed through the calculation of Equation 11 (Cavallaro et al. 2014; Bruneau et al. 2013; Reed et al. 2009):

$$R = \frac{\int_{t_s}^{t_c} Y(t) dt}{t_c - t_s} \quad (11)$$

Actually, the city's liking to efficiently recover from a disaster is strictly related to a huge quantity of complex and often uncontrollable variables. As it is worth notice, decision making in such context is ascribable to

disaster managers, that, depending on the time, money and human and material resources' availability, choose which strategy has to be undertaken for recovery. Issues related to this process affect the city recovery in different ways, being almost all related to time, t , so that they cannot be considered in detail. As a consequence, a good approach should totally remove the dependence of resilience on time, in order to avoid embedding further uncertainties in the evaluation process. To do this, both HSPN efficiency and the recovery function are defined as dependent on the number of inhabitants being relocated in each recovery stage, as highlighted in Equation 12 (Cavallaro et al. 2014):

$$Y(C) = \frac{E(C)}{E_{pre}} \quad (12)$$

That is the ratio between the city's efficiency level when C inhabitants have been relocated and the city's efficiency level when no inhabitants need to be relocated, that is when the seismic event has not occurred yet. Furthermore, also the dependence on the total state of damage is removed, enabling us to evaluate a normalized recovery function (Equation 13):

$$y(C) = \frac{Y(C) - Y(0)}{1 - Y(0)} \quad (13)$$

where $Y(0)$ indicates the residual HSPN's efficiency soon after the event occurrence (relocated citizens $C=0$) and $Y(C)$ indicates the residual HSPN's efficiency in each generic recovery stage (C citizens relocated). According to Cavallaro et al., with this, resilience can be finally quantified, according to Equation 13, being defined in $[0, 1]$:

$$R = \frac{\int_0^{C_{max}} y(C) dC}{C_{max}} \cong \frac{\sum_{c=0}^{C_{max}} y(C) \cdot \Delta C}{C_{max}} \quad (14)$$

Where C_{max} is the total number of citizens, whose homes have been damaged, hence to relocate after the seismic event occurrence, and the integral is simplified with a summation, being the strategy implemented in a discrete number of steps (Cavallaro et al. 2014).

In this context, a further issue is related to the dependence of resilience on the city's state of damage, given that it directly affects the quantification of the city's capability to recover, according to the damage suffered soon after a certain event occurrence.

Keeping with this, two alternative approaches are proposed to evaluate resilience, being directly related to the physical meaning of resilience based on the observation of the recovery curve. In the former resilience is evaluated as independent on the initial state of damage, as shown in Equation 13, and in the latter resilience is evaluated as dependent on it. This last metric is based on the definition of the systemic damage, D , as given in Equation 10, being this time dependent on the number of relocated citizens, as shown in Equation 14:

$$D(C) = \frac{E_{pre} - E(C)}{E_{pre}} = 1 - Y(C) \quad (15)$$

5.1.4.1 Quantification of damage-independent resilience

To show the meaning of the proposed damage-independent resilience metric, the recovery curve has to be observed.

For instance, whether considering that a city has been stroke by an earthquake, whose intensity is I . Let now suppose that local authorities undertake actions for recovery, that is completed in three stages. That is, the city's global efficiency bounced back to the pre-event value.

One can then graphically describe the above-mentioned recovery path in the $E-C$ plane, being E the normalized global efficiency and C the number of relocated citizens (Figure 5.5).

Basically the normalized efficiency is evaluated by accounting for the drop of the efficiency of the city’s HSPN in each recovery stage and also for the efficiency drop between the HSPN condition in the pre-event and soon after the event occurrence.

Hence, by considering that at the i^{th} reconstruction step, C citizens are reallocated, normalized to the maximum number of citizens to be relocated, C_{max} , and by normalizing efficiency with respect to the efficiency drop soon after the earthquake occurrence ($E^{pre} - E^{post}$), the normalized global efficiency, E , can be evaluated as shown in Equation 16:

$$E(C) = \frac{E(C) - E^{post}}{E^{pre} - E^{post}} \tag{16}$$

Which is the same result that can be analogously obtained, if we consider Equation 13 and substitute the formula of the recovery function, as it is given in Equation 12, in terms of the efficiency.

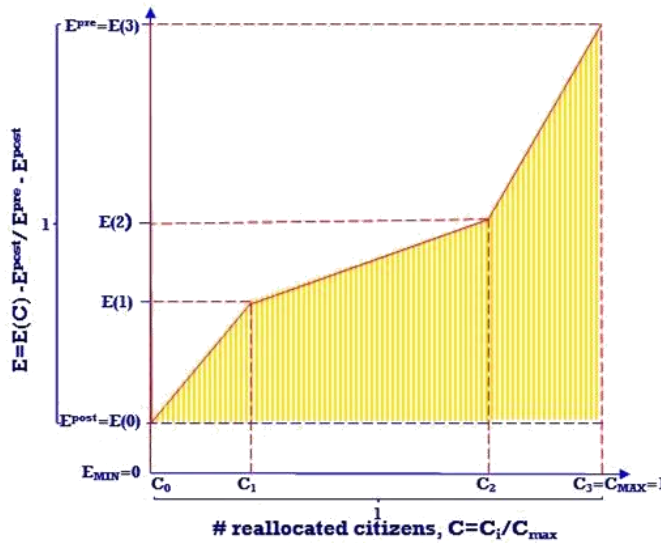


Figure 5.5 Recovery curve in terms of the global efficiency, normalized to the pre-event efficiency value, as a function of relocated citizens in each stage of the recovery process, in turn normalized with respect to the maximum number of evacuated citizens

Hence the proposed relationship for the normalized efficiency is substantially the same of the recovery function defined in the previous Section, resulting $y(C) = E(C)$. Paralleling it, now the recovery function is explicitly defined as the ratio between the efficiency drop when C citizens have been relocated, with respect to the efficiency soon after the event occurrence, and the efficiency drop between the pre- and the post-event stage. Equation 17 shows the formula:

$$y(C) = \frac{E(C) - E^{post}}{E^{pre} - E^{post}} \quad (17)$$

Hence resilience can be evaluated as the area underneath the recovery curve, that is as the integral of the recovery function across all the recovery stages. The proposed relationship is the following (Equation 18):

$$R^E = \frac{\int_0^{C_{max}} y(C) \cdot dC}{C_{max}} \cong \sum_i \frac{[y_i(C_i) + y_{i+1}(C_{i+1})]}{2} \cdot \Delta C_{i,i+1} \quad (18)$$

where $\Delta C_{i,i+1} = \frac{C_{i+1} - C_i}{C_{max}}$, that is the reallocated citizen share normalized to C_{max} . As a consequence resilience is defined in the $[0,1]$ interval, where a particular condition is recognized to the 0.5 value. This is a crossing point between the city functionalities recovery according to an sub- or super-linear trend respectively.

Such limit conditions are shown in the following, Figure 5.6 and Figure 5.7.

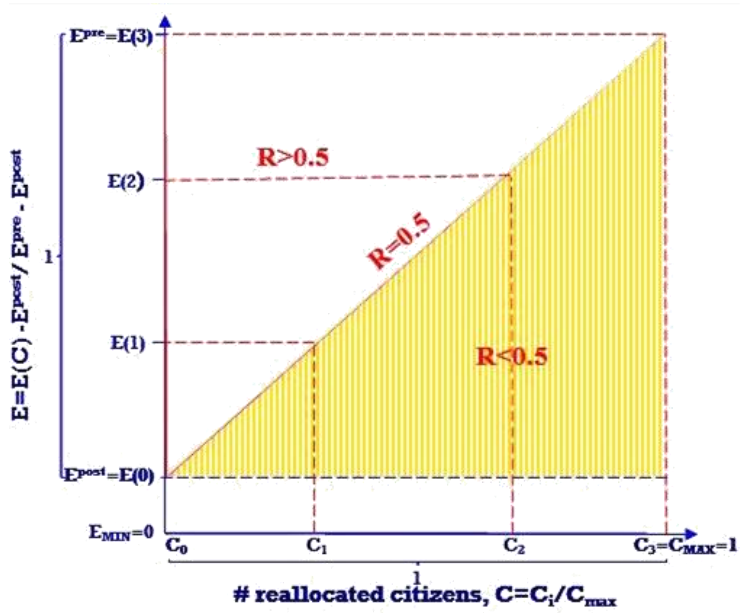


Figure 5.6 Perfectly linear recovery curve

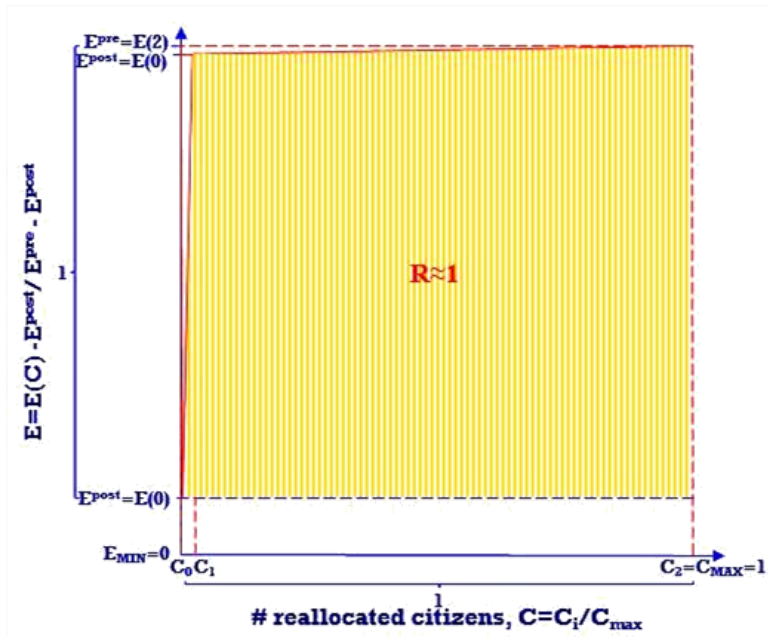


Figure 5.7 Limit case in which recovery is almost instantaneous and resilience attains its maximum value

It is clearly that whether the curve is linear, resilience would attain the value $R=0.5$.

Conversely, whether the curve trend is super-linear $R>0.5$ with values always greater, until recovery is attained almost instantaneously.

This last is the case in which the area under the curve would tend to a unit-side polygon, being normalized both efficiency and the number of reallocated citizens.

5.1.4.2 Quantification of damage-dependent resilience

According to the kind of issues one has to deal with, it could be necessary to evaluate resilience without removing its dependence on the total state of damage soon after the event has occurred, instead specifically accounting for it. This is the case, that a damage-dependent resilience metric is needed.

The proposed approach is basically the same as the previous one shown for the quantification of the damage-independent resilience. The only difference lays in that resilience is evaluated as dependent on the systemic damage, that is the global damage to the city's HSPN functionalities, D , as evaluated in Equation 15, Section 5.1.3.

Hence, resilience is evaluated by accounting for global city's efficiency, which is this time not normalized with respect to the pre-event performance level (Equation 19).

Paralleling this, by representing the recovery curve in the C - D plane (Figure 5.8), being C the number of reallocated citizens and D the systemic damage level in each recovery stage, resilience is clearly represented by the area under the curve, also this time.

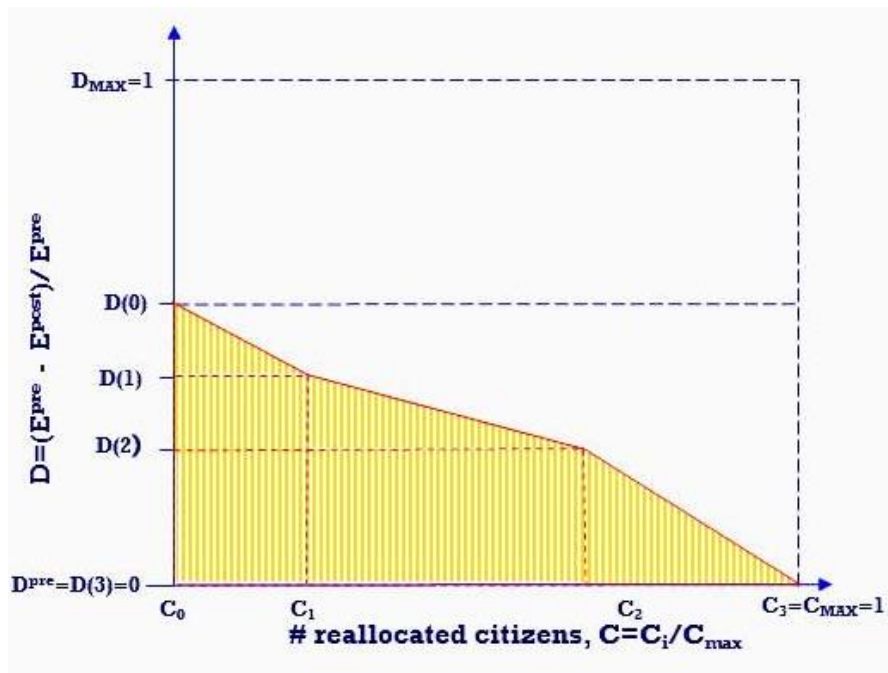


Figure 5.8 Graphical representation of the recovery path in the C - D plane

$$R^D = \frac{\int_0^{C_{max}} D(C) \cdot dC}{C_{max}} = \sum_i \frac{[D_i(C_i) + D_{i+1}(C_{i+1})]}{2} \cdot \Delta C_{i,i+1} \quad (19)$$

This is because using a synthetic indicator to quantify resilience, may be misleading if one does not consider efforts done to bounce back to an equilibrium condition after an event. With this, one has to consider the damage condition, which the city starts from, with respect to its initial performance level, E_{pre} .

5.2 THE HISTORICAL CENTRE OF THE CITY OF NAPLES: THE QUARTIERI SPAGNOLI EARTHQUAKE CASE ANALYSIS

5.2.1 Modeling Quartieri Spagnoli as a complex network

To validate the proposed approach and to verify the robustness of the proposed metrics, a real case study is developed. The historical centre of

Naples, i.e. the Quartieri Spagnoli area, is modelled as a HSPN and earthquake scenarios are simulated to assess its resilience level, according to the recovery strategy highlighted in Section 5.1.2 (status quo down-up strategy).

The Quartieri Spagnoli area is located in the inner city of Naples (Figure 5.9), being composed of the Avvocata, San Ferdinando and Montecalvario neighbourhoods. The origin of Quartieri Spagnoli dates back to the XVI century, when they were built to host the Spanish military garrisons, which were in Naples to repress insurrections from the Neapolitan population.

Despite the poor conditions and the disrepute of this area, it represents the core of the historical and cultural local tradition. It is mostly constituted by masonry buildings, accommodating small artisan shops, place of worships and typical local residences.

The selected area has got a 3.57 km perimeter and a 0.569 km² wide in-plane geometry. There are 614 residential buildings made of masonry, with reference to which the local population is estimated, being almost 30,007 inhabitants.



Figure 5.9 Map of Naples' historical centre (red markers represent school buildings).

As a start, only residential buildings have been considered. The selected area has been modelled as a HSPN (Figure 5.10) and two diverse seismic scenarios are simulated.

In the former, collapse or severe damage is assumed to be attained for the 15% of buildings, while in the latter this percentage is assumed to be 30%. As already outlined in Section 5.1.2, damaged buildings are selected according to a fully randomize procedure.

As also shown in Section 5.1.2, the street usability after the earthquake occurrence is evaluated according to probability-based approach. Hence, the probability of street links to become inaccessible is evaluated as a function of buildings being located along them and of their width.

Finally the connectivity between couples of residential buildings is quantified across the simulated recovery strategy, as the citizen-citizen efficiency.



Figure 5.10 HSPN of the historical centre of the city of Naples (the Quartieri Spagnoli Area), where only residential buildings have been modelled

A further HSPN of the Quartieri Spagnoli area is modelled (Figure 5.11), which accounts also for school buildings (17 buildings).

The 17 buildings being computed in addition to the residential HSPN account for about 3,000 users.

Accordingly to the previously shown case analysis, in this case, two earthquake scenarios are simulated (15% and 30% buildings to collapse are imposed) and the status quo down-up strategy is simulated for recovery. The only difference is in the assessed city efficiency, which this time refers to the citizen-school connectivity.

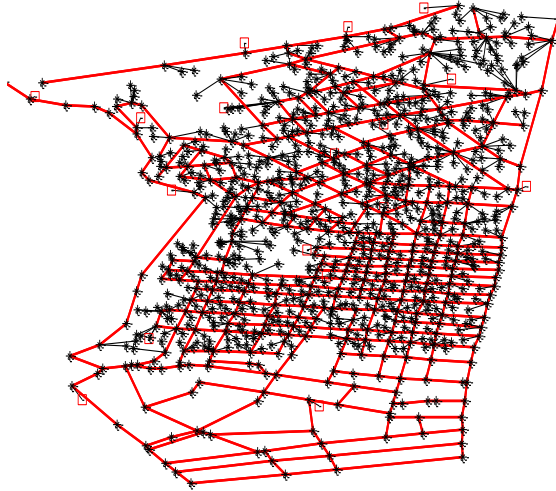


Figure 5.11 HSPN of the historical centre of the city of Naples (the Quartieri Spagnoli Area), where both school (red squared markers) and residential buildings (black starred dots) have been modelled

In both the case analysis, each simulation is iterated ten times, to observe different scenarios and to evaluate eventually substantial gaps. The following Section show analysis results and discussion on it.

5.2.2 Discussion of results

Once the city is modelled the methodology allow for the damage assessment right after a seismic event occurred, both in terms of damaged street patterns and buildings, and also in terms of citizens, which remain without their homes and need to be reallocated. Because of scenario analysis is iterated ten times, drawing values from the pseudorandom number simulation, median values are finally computed.

Damages suffered by the city are measured starting from the single building. This is conceived as a physical structure itself, but also as an “ideal reference point”, in which citizens live and from which they are served. Urban services, such as gas and water pipelines and electric grids, and also road infrastructures are linked to such buildings. Hence, once the links between buildings and all urban services are modelled, one can simply assume that when the building goes out-of-service, even all services which are linked to it are useless. Particularly, in this work the link between the couple of nodes representing buildings are modelled based on the street patterns of the studied city. This assumption is justified by the fact that in urban centres, urban services infrastructures (pipelines for instance) are usually located on the streets.

Tables 5.1 and 5.2, following, show results of the 15% and 30% case analysis in terms of the HSPN citizen-citizen efficiency, E , the recovery function and systemic damage values in the aftermath of the event, $Y(0)$ and $D(0)$, and the urban resilience, being assessed both as damage-dependent, R^D , and damage-independent, R^E . Notice that, for the sake of simplicity, both E_{cc} and E_{cs} are hereafter referred to as E in the text.

Also the HSPN configuration in the aftermath of the event can be observed in the following tables, where black starred points represent residential buildings and black and red lines represent respectively the door link and the street links.

Table 5.1 Analysis results and post-event graph in the case of 15% collapsed buildings, where citizen-citizen efficiency is computed (only residential buildings)

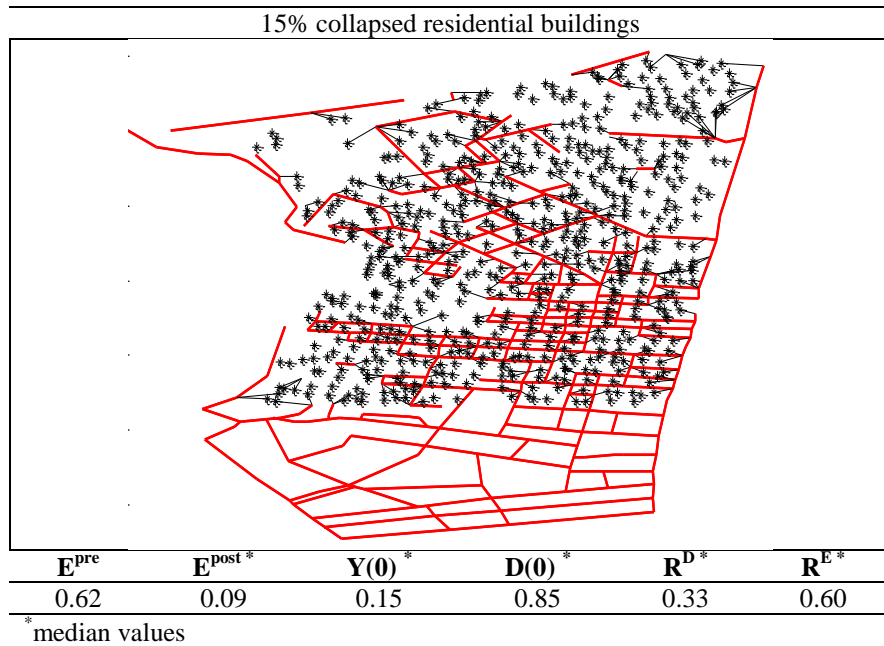
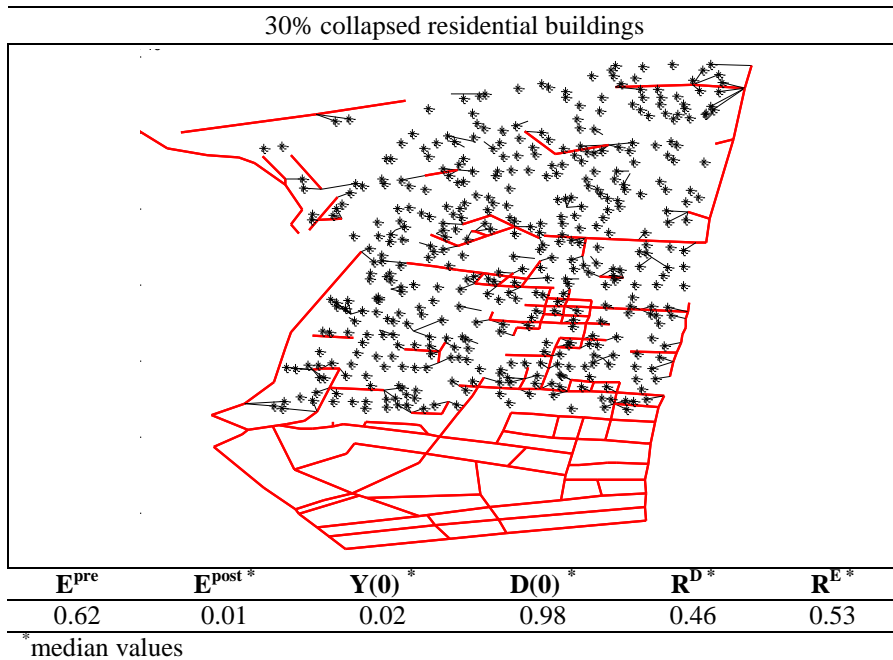


Table 5.2 Analysis results and post-event graph in the case of 30% collapsed buildings, where citizen-citizen efficiency is computed (only residential buildings)



Tables 5.3 and 5.4, following, show results of the 15% and 30% case analysis in terms of the HSPN citizen-school case analysis.

Table 5.3 Analysis results and post-event graph in the case of 15% collapsed buildings and schools, where citizen-school efficiency is computed

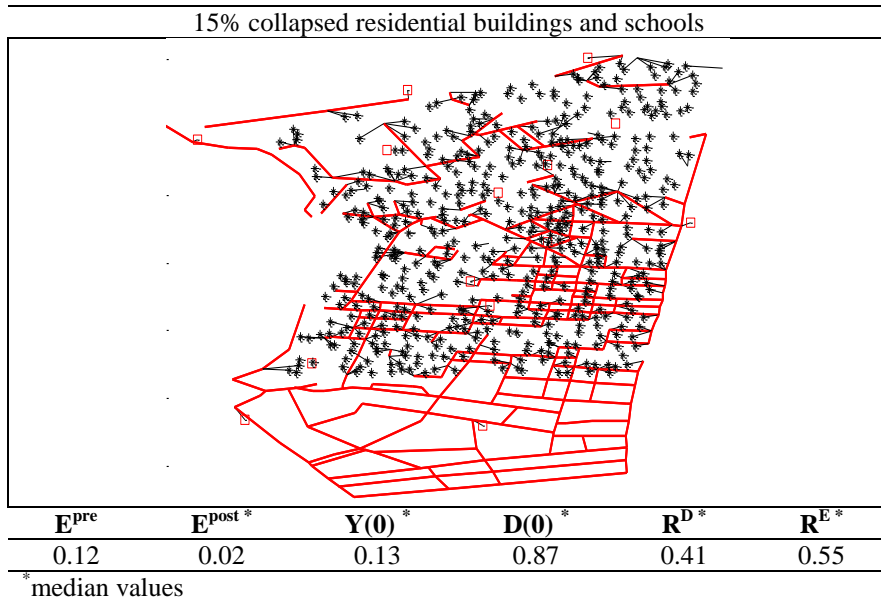
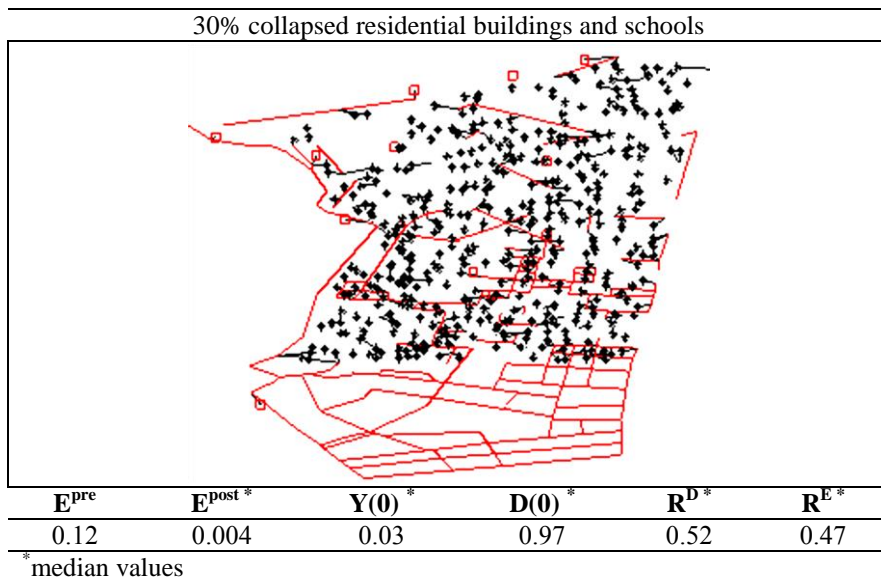


Table 5.4 Analysis results and post-event graph in the case of 30% collapsed buildings and schools, where citizen-school efficiency is computed



As one can observe, the pre-event efficiency is very different in the two case studies: it is 0.62 in the citizen-citizen case study and 0.12 in the citizen-school one. This can be easily explained if we consider that efficiency is evaluated as inversely proportional to the shortest path distances. In the citizen-school case study, such efficiency is the measure of the urban connectivity between each school buildings and each residential buildings, then averaged on the whole HSPN. Hence, being the number of schools in a minor quantity with respect to the residential buildings, obviously shortest path distances reveal to be higher. As a consequence, the resulting efficiency results to be lower in this case, with respect to the citizen-citizen case study.

Similar results for both the case analysis are underlined, regarding the post-event efficiency, $E^{post}=E(0)$, the systemic damage, $D(0)$, and the recovery function, $Y(0)$. Both for the citizen-citizen and the citizen-school case analysis, the efficiency drop, with respect to the pre-event, is about 83% in the case in which 15% of buildings to collapse are assumed, and about 97% in the 30% case. Hence assuming damages to buildings 15% to increase (from 15% to 30% collapsed buildings), this results in a difference in the efficiency drop, which is proportional to it (about 13%).

The same trend is also observed for the systemic damage, being obviously directly related to the HSPN efficiency, when comparing the difference in terms of $D(0)$ between the 15% and the 30% scenarios. On the other hand, in terms of the order of magnitude, the systemic damage is different when related to the efficiency values. For instance, in the citizen-citizen case analysis, the damage is 0.85 in the 15% scenario and 0.98 in the 30% scenario. While the post-event efficiency is 0.09 in the 15% scenario and 0.01 in the 30% scenario, being the systemic damage and the HSPN efficiency inversely correlated. Notice that, in fact, whether considering the 30% case analysis, $D(0)=0.98$ means that the HSPN is almost totally destroyed, hence its residual efficiency is minimal ($E^{post}=0.01$).

It is clearly evident, instead, that the recovery function is complementary to the systemic damage, being in this case $Y(0)=0.02$, hence equal to $(1-D(0))$.

Finally the HSPN resilience is observed. Both the damage-dependent and the damage-independent resilience indicators are defined in $[0,1]$, hence being comparable their order of magnitude. On the other hand, they have different meaning.

When observing the damage-dependent resilience it is $R^D=0.33$ in the 15% case analysis and $R^D=0.46$ in the 30% case analysis, highlighting a 39% increase. Damage-dependent resilience increase with the damage level because a major ability to recover is exhibited by the HSPN. In fact, it bounces back to the pre-event equilibrium in the same number of steps, but starting from a severer damage condition, hence needing to reallocate many more citizens and to restore many more buildings. This means, that the most damaged HSPN has been quicker and more efficient in resource use than the least one.

Conversely, when considering the damage-independent resilience values, a 12% decrease is observed from the 15% to the 30% case analysis. This is because of this metric being directly related to the attained efficiency values, and to the drop suffered from the pre- to the post-event condition and across all the recovery stages.

It can be asserted that the two proposed metrics are not mutually exclusive, otherwise they can be used complementarily, since they catch diverse aspects of the urban resilience.

R^D is useful to compare urban contexts being stroke by the same catastrophic event, to contextually evaluate the systemic damage and the bouncing back capability at the local level. Paralleling this, R^E can be used to compare urban contexts, which are very different or that have been stoke by different event typology. Hence, it can be effectively used to collect and compare best practises, according to the event typology, even though they occurred in different geographical and urban contexts,

enabling for observations and understandings related to resilience issues on the global scale.

5.3 CITY RESILIENCE AGAINST URBAN SIZE AND SHAPE: CASE STUDIES

5.3.1 Numerical simulation and graph modelling

Four different city's shapes are artificially built up as HSPNs, referring to the planimetry of real, existing urban centres, such as Barcelona, Paris and Los Angeles. In particular, rectangular, circular, hexagonal and star shaped HSPNs are modelled, with their size being increased according to their geographical extent and number of buildings, hence to the number of citizens living in it. Particularly HSPNs with 50 (about 2,000 inhabitants), 200 (about 9,000 inhabitants), 1,250 (about 55,000 inhabitants) and 5,000 buildings (about 225,000 inhabitants) are modelled.

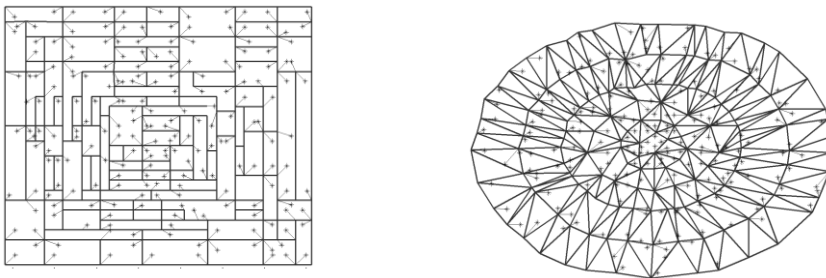
Primarily only residential buildings are considered, and the HSPN efficiency is computed as the citizen-citizen one. Then, in each modelled HSPN 2% of buildings are assumed to be school buildings, in order to evaluate the efficiency in the city's connectedness between residential buildings and school buildings, hence between pair of citizens being fed from the school urban service.

Urban system modelling is performed through the use of a geographic information system (GIS), which enables us to integrate a large range of data and to identify more specific information, through acquisition, georeferencing and documenting data. In particular, information about the population, the geographical extent, the buildings' spatial distribution and the buildings' number and structural typology are also embedded in the GIS-based software.

Some assumptions and hypothesis are made to characterize HSPNs:

- structural typology is assumed to be frame buildings made of reinforced concrete, with all buildings designed for gravity loads, regular both in plane and in height;
- buildings considered for city scenario simulations are assumed to be typical European 70s – 80s constructions, with number of storeys being comprised between 2 and 5;
- citizens living in each city are accounted depending on the total floor area of each structural typology and assuming about 1 citizen each 30 square meters, as suggested by ISTAT (ISTAT 2001);
- the percentage of buildings with reference to their number of storeys is taken fixed: residential buildings are modelled for 10% as 2-storey, 40% 3-storey, 30% 4-storey and 20% 5-storey;
- school buildings are all considered to be 5-storey buildings;
- each urban geometry is modelled with an increasing number of buildings and its territorial extent is adequately scaled according to this.

Figure 5.12 shows the four different city shapes, for the case in which 200 buildings are modelled and the citizen-citizen efficiency is evaluated:



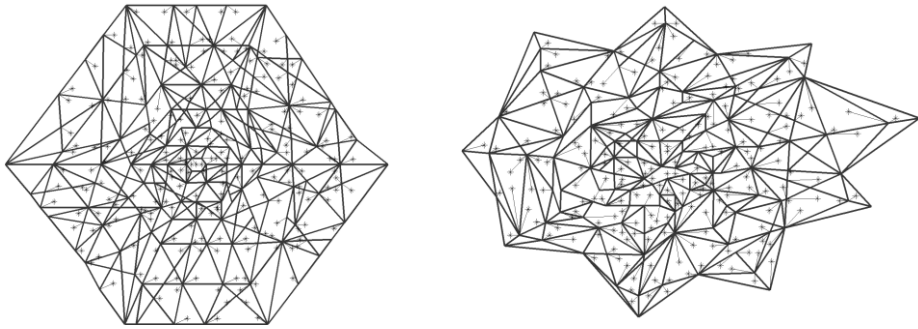
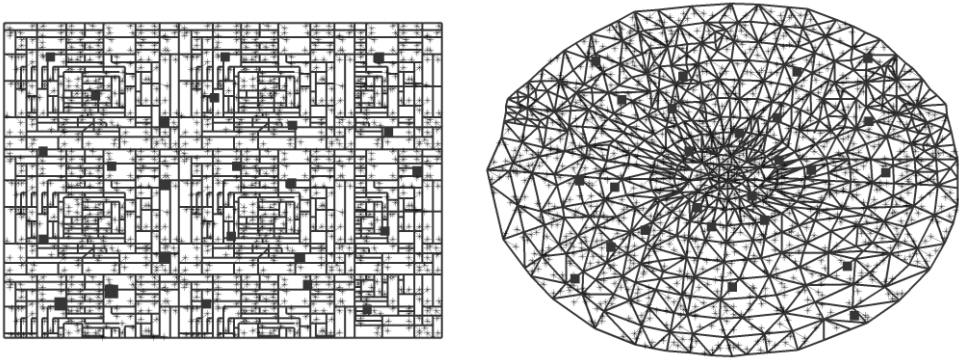


Figure 5.12 City shapes modelled for the 200 buildings case analysis

whereas grey lines represent street patterns, whose intersections are street junctions, black lines represent the door links between building's and street's nodes and black starred points represent residential building nodes. On the other hand, in order to compute citizen-school efficiency, also building nodes representing schools are modelled and spatially distributed in a uniform fashion, as it can be observed from Figure 5.13, in the case of 1,250 buildings case analysis.



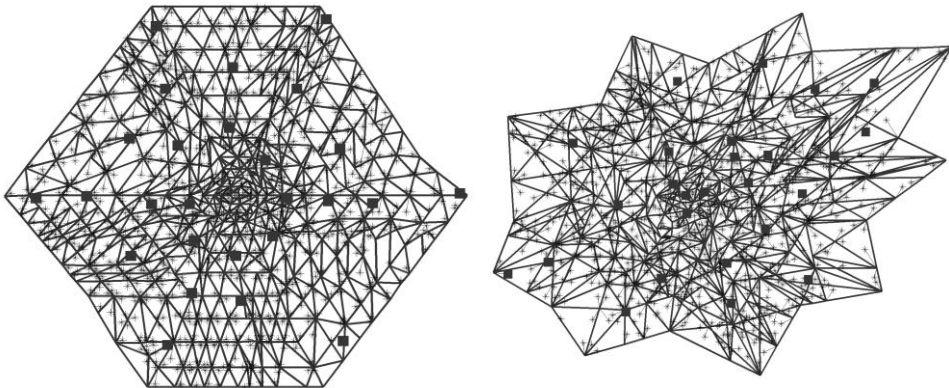


Figure 5.13 City shapes modelled for the 1250 buildings case analysis, 25 of which are considered to be schools

Here grey squared nodes represent city's schools and black starred nodes city's residential buildings, which are in number of 25. While in the case which 200 buildings are modelled, 5 of them are considered to be schools, in the case of 5000 buildings, 100 are considered to be schools. Finally the case of 50 buildings is not run for the citizen-school efficiency evaluation, since if a 50 buildings city exists, of course it has got at most one or two schools and, owing to this, it would make no sense to simulate a certain percentage of schools to collapse to the aim of the present study.

Table 5.5 and Table 5.6 show the modelled HSPN's shape on which scenario analysis are run, with their related features, in the case of citizen-citizen and citizen-schools efficiency assessment:

Table 5.5 HSPN shapes modelled and related features in the case of citizen-citizen efficiency assessment

Shape	Size [CAD units]	Number of residential buildings	Number of inhabitants
Rectangular	918	50	1,945
	4,380	200	9,354
	27,482	1250	57,547
	110,230	5000	230,246
Circular	875	50	1,945
	4,536	200	8,583
	29,230	1250	55,931
	112,167	5000	226,355
Hexagonal	972	50	1,945
	4,180	200	8,369
	24,605	1250	57,368
	129,944	5000	222,682
Star	1,122	50	2,029
	4,256	200	8,506
	30,176	1250	53,867
	107,146	5000	225,593

Table 5.6 HSPN shapes modelled and related features in the case of citizen-school efficiency assessment

Shape	Size [CAD units]	Number of residential buildings	Number of inhabitants	Number of schools
Rectangular	4,380	195	9,354	5
	27,482	1,225	57,547	25
	110,230	4,900	230,246	100
Circular	4,536	195	8,583	5
	29,230	1,225	55,931	25
	112,167	4,900	226,355	100
Hexagonal	4,180	195	8,369	5
	24,605	1,225	57,368	25
	129,944	4,900	222,682	100
Star	4,256	195	8,506	5
	30,176	1,225	53,867	25
	107,146	4,900	225,593	100

As an further example, Figure 5.14 shows the scaling for the star-shaped HSPN:

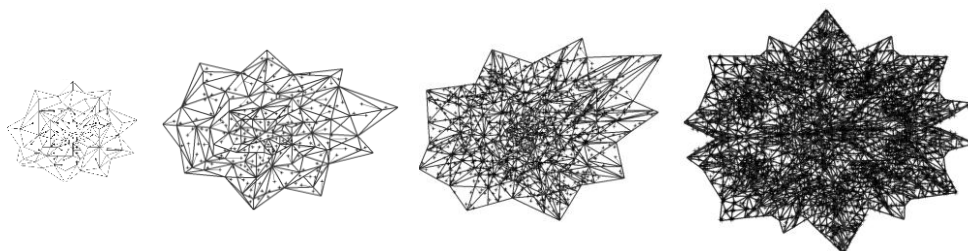


Figure 5. 14 Example of scaling in the case of star-shaped city with 50, 200, 1250 and 5000 residential buildings

When performing scenario analysis two earthquake intensity are considered and damages to each HSPN are assumed to cause 15% and 30% of first only residential buildings and then both residential and school buildings to collapse, being selected with the fully random procedure highlighted in previous Sections. A strategy is designed, which consider the HSPN structure to be restored to the pre-event configuration, hence with the global efficiency to bounce back to the pre-event value (status quo down-up).

The recovery strategy is implemented in a discrete number of steps, n , in this case too. Finally efficiency, systemic damage and the resilience values are calculated.

5.3.2 Discussion on analysis results

As for the Quartieri Spagnoli case study, results of the 15% and 30% case analysis in terms of the HSPN citizen-citizen efficiency, E , the recovery function and systemic damage values in the aftermath of the event, $Y(0)$ and $D(0)$, and the urban resilience, being assessed both as damage-dependent, R^D , and damage-independent, R^E , are presented in the following Tables.

Table 5.7 Analysis' results for each HSPN's shape and size for the 15% citizen-citizen case analysis

Strategy citizen-citizen 15%												
Shape	Rectangular								Circular			
#bldgs	$E_{cc,pre}$	$E_{cc,post}$	Y(0)	D(0)	R^D	R^E	$E_{cc,pre}$	$E_{cc,post}$	Y(0)	D(0)	R^D	R^E
50	0,60	0,25	0,426	0,574	0,24	0,57	0,94	0,51	0,540	0,460	0,22	0,55
200	0,75	0,38	0,500	0,500	0,25	0,51	0,93	0,43	0,458	0,542	0,27	0,51
1250	0,75	0,39	0,521	0,479	0,22	0,53	0,95	0,23	0,243	0,757	0,40	0,46
5000	0,78	0,40	0,510	0,490	0,23	0,53	0,94	0,18	0,193	0,807	0,37	0,55
Shape	Hexagonal								Star			
#bldgs	$E_{cc,pre}$	$E_{cc,post}$	Y(0)	D(0)	R^D	R^E	$E_{cc,pre}$	$E_{cc,post}$	Y(0)	D(0)	R^D	R^E
50	0,86	0,51	0,588	0,412	0,19	0,53	0,91	0,54	0,598	0,402	0,17	0,57
200	0,93	0,45	0,487	0,513	0,28	0,48	0,90	0,37	0,414	0,586	0,29	0,50
1250	0,93	0,20	0,216	0,784	0,36	0,54	0,93	0,20	0,212	0,788	0,39	0,50
5000	0,92	0,20	0,213	0,787	0,37	0,53	0,92	0,14	0,152	0,848	0,36	0,56

Table 5.8 Analysis' results for each HSPN's shape and size for the 30% citizen-citizen case analysis

Strategy citizen-citizen 30%												
Shape	Rectangular								Circular			
#bldgs	$E_{cc,pre}$	$E_{cc,post}$	Y(0)	D(0)	R^D	R^E	$E_{cc,pre}$	$E_{cc,post}$	Y(0)	D(0)	R^D	R^E
50	0,60	0,13	0,224	0,776	0,35	0,56	0,94	0,20	0,208	0,792	0,38	0,53
200	0,75	0,13	0,170	0,830	0,43	0,48	0,93	0,16	0,171	0,829	0,43	0,48
1250	0,75	0,07	0,095	0,905	0,41	0,52	0,94	0,01	0,013	0,987	0,58	0,41
5000	0,78	0,08	0,100	0,900	0,41	0,55	0,94	0,00	0,003	0,997	0,51	0,49
Shape	Hexagonal								Star			
#bldgs	$E_{cc,pre}$	$E_{cc,post}$	Y(0)	D(0)	R^D	R^E	$E_{cc,pre}$	$E_{cc,post}$	Y(0)	D(0)	R^D	R^E
50	0,86	0,32	0,368	0,632	0,27	0,57	0,91	0,32	0,349	0,651	0,28	0,57
200	0,93	0,22	0,237	0,763	0,41	0,47	0,90	0,07	0,072	0,928	0,49	0,46
1250	0,93	0,01	0,009	0,991	0,51	0,48	0,93	0,01	0,009	0,991	0,57	0,43
5000	0,92	0,00	0,005	0,995	0,52	0,49	0,92	0,00	0,002	0,998	0,52	0,48

The citizen-school efficiency, the systemic damage and the two proposed resilience metrics are also assessed for each HSPN size and shape, when modelling HSPN by also accounting for school buildings. Analysis results are shown in Tables 5.9 and 5.10, following.

Table 5.9 Analysis' results for each HSPN's shape and size for the 15% citizen-school case analysis

Strategy citizen-school 15%												
Shape	Rectangular						Circular					
#bldgs	$E_{cc,pre}$	$E_{cc,post}$	$Y(0)$	$D(0)$	R^D	R^E	$E_{cc,pre}$	$E_{cc,post}$	$Y(0)$	$D(0)$	R^D	R^E
200	0,16	0,05	0,343	0,657	0,41	0,30	0,185	0,08	0,435	0,565	0,36	0,34
1250	0,15	0,06	0,393	0,607	0,40	0,35	0,189	0,03	0,180	0,820	0,47	0,43
5000	0,16	0,07	0,439	0,561	0,35	0,38	0,187	0,03	0,179	0,821	0,46	0,44

Shape	Hexagonal						Star					
#bldgs	$E_{cc,pre}$	$E_{cc,post}$	$Y(0)$	$D(0)$	R^D	R^E	$E_{cc,pre}$	$E_{cc,post}$	$Y(0)$	$D(0)$	R^D	R^E
200	0,183	0,07	0,379	0,621	0,37	0,33	0,177	0,05	0,262	0,738	0,50	0,34
1250	0,186	0,03	0,182	0,819	0,46	0,43	0,187	0,03	0,150	0,850	0,48	0,45
5000	0,185	0,03	0,167	0,833	0,45	0,45	0,184	0,02	0,119	0,881	0,47	0,46

Table 5.10 Analysis' results for each HSPN's shape and size for the 30% citizen-school case analysis

Strategy citizen-school 30%												
Shape	Rectangular						Circular					
#bldgs	$E_{cc,pre}$	$E_{cc,post}$	$Y(0)$	$D(0)$	R^D	R^E	$E_{cc,pre}$	$E_{cc,post}$	$Y(0)$	$D(0)$	R^D	R^E
200	0,16	0,02	0,119	0,881	0,55	0,36	0,19	0,02	0,116	0,884	0,61	0,34
1250	0,15	0,01	0,064	0,936	0,65	0,30	0,19	0,00	0,008	0,992	0,68	0,32
5000	0,16	0,01	0,043	0,957	0,61	0,36	0,19	0,00	0,002	0,998	0,66	0,34

Shape	Hexagonal						Star					
#bldgs	$E_{cc,pre}$	$E_{cc,post}$	$Y(0)$	$D(0)$	R^D	R^E	$E_{cc,pre}$	$E_{cc,post}$	$Y(0)$	$D(0)$	R^D	R^E
200	0,18	0,04	0,218	0,783	0,55	0,35	0,18	0,01	0,071	0,929	0,71	0,28
1250	0,19	0,00	0,006	0,994	0,66	0,33	0,19	0,00	0,005	0,995	0,69	0,31
5000	0,19	0,00	0,004	0,996	0,66	0,34	0,18	0,00	0,001	0,999	0,67	0,33

Appendix 5.A shows results in terms of the HSPN configuration before and soon after the earthquake occurrence.

Mainly, it can be observed that the higher is the buildings' share being imposed to collapse, the higher is the assessed systemic damage. Subsequently, also the HSPNs' resilience has got a higher value, both in the damage-dependent and in the damage-independent assessment.

Paralleling this, a major drop is observed in the efficiency level, E , as a higher systemic damage, $D(0)$, is evaluated in the after-event.

It is clearly evident that results in terms of the HSPNs' resilience, R^D and R^E are not always in agreement. In fact, damage-independent resilience gives information about the capability of the studied HSPN to respond to a seismic event in terms of responsiveness, quickness, resourcefulness and also robustness. This last is a very important feature, since whether a city's physical system is robust enough to suffer damages to a lesser extent whenever an adverse event occurs, it is consequently more resilient too. Conversely, being damage-dependent resilience directly related to injuries suffered by the HSPN, it highlights the capability of the HSPN to respond to the event in terms of responsiveness, quickness and resourcefulness.

The seismic performance of the modelled HSPNs can also be investigated from a strictly civil engineering perspective, in terms of the systemic damage in the after-event, $D(0)$.

Regarding both the case analysis and both the seismic scenarios, the rectangular HSPN reveals to be the one suffering less damages almost in all the cases, being followed by the hexagonal HSPN. Hence a major robustness of such HSPN's shapes can be asserted. In fact, in terms, of the systemic damage both rectangular and hexagonal shapes exhibit the lowest values. Paralleling this, they result to be the most resilient geometries in terms of the damage-independent resilience, R^E .

On the other, when considering the damage extent, the star-shaped HSPNs result to be the most resilient, according to the damage-dependent resilience metric, R^D . This can be understood as the star HSPN bounces back to the pre-event efficiency within the same number of stages of the other HSPNs, starting from a severer level of damage.

Accordingly, results have also to be understood in light of the pre-event efficiency level, which each HSPN exhibits. This is because, in order to effectively quantify resilience, one should consider both the damage level,

which recovery starts from, and the initial efficiency level, as well as the post-event, that is the residual one.

As an example, if we consider the citizen-citizen case analysis, when 30% collapsed buildings is assumed, the lesser systemic damage value is attained for rectangular and hexagonal HSPNs shapes, regardless their size. On the other hand, an important difference is observed in terms of the pre-event efficiency, which is lower in the case of the rectangular-shaped HSPN than for the hexagonal-shaped HSPN. As a consequence, obviously this last geometry suffer a lesser damage, $D(0)$. While in the rectangular HSPN case the lower damage is effectively understood as a higher urban network's robustness, also having its equivalent in a lower pre-event efficiency.

These are, however, circumstances, whose consideration is embedded in both the systemic damage and the resilience assessment, since they refer to the normalized efficiency with respect to the pre-event one. As a result, $D(0)$ makes all HSPN sizes and shapes comparable, regardless their higher or lower pre-event efficiency with respect to the post-event one.

The assessed resilience is also observed with reference to the HSPN size. According to Bettencourt et al. (Bettencourt et al. 2007) processes being governed by community-based dynamics usually exhibit a sublinear trend against the city size, while processes being governed by economies of scale exhibit a superlinear trend. Nonetheless, when observing the trend of the proposed resilience metrics against the city size, the same cannot be asserted, since fluctuations are observed in their values, in both the case analysis, when compared with the HSPN scaling. Such observations can be even clearer whether studying histograms shown in Appendix 5.B.

CHAPTER 6

NOVEL RESILIENCE METRICS FOR CITY ECOSYSTEMS SUBJECTED TO NATURAL HAZARDS

Over the past 50 years, many urban ecosystems worldwide have been jeopardized faster and more extensively than ever before following the occurrence of natural disasters.

Although these are unpredictable and unavoidable events, their effects can be mitigated by human intervention in the form of adequate protection measures and rational land use that respects the environment's equilibrium.

Paying greater attention to safety is thus required, including by implementing actions, which can be even more effective when coordinated at the urban scale, where great control is ensured in public management of both the pre- and post-event phases.

On the other hand, cities are very complex systems, as they are the outcome of convoluted interrelations between physical and social components. These are cities' key elements, which define and shape the urban structure on all scales (Bozza et al. 2015b).

Hence, measuring urban resilience to disasters is a key issue for the global scientific community.

In the presented study, resilience is understood from an engineering perspective in the sense of the ecosystem approach. In this light, the present study proposes the urban environment to be modelled as a complex network, which accounts for both social and physical components, and is defined as a hybrid social-physical network (HSPN) (Cavallaro et al. 2014, Bozza et al. 2015a). This kind of approach, in the sense of graph theory, enables us to monitor the city's efficiency: as the

connectivity of the urban environment in the pre-event stage soon after the event's occurrence, and for each step of the recovery process. On the other hand, the city efficiency assessment can be understood as a systemic measure of the urban damage. Accordingly, infrastructure damage can be evaluated for the city in its entirety, rather than at the level of the single structure.

The primary goal of this study is to recognize dissimilarities in urban damage and resilience assessments when changing the type of disaster and the related, different, modality and areas of impact.

To this end, the proposed framework is implemented for the case study of the municipality of Sarno. Sarno is a small town in southern Italy about 50 kilometres from Naples, which, due to its hydrogeological and geomorphological characteristics, is a very seismic- and landslide-prone area. Sarno is also known for being hit by a severe flow-type landslide in 1998, which caused huge economic and human losses.

6.1 ASSESSING URBAN RESILIENCE TO DIVERSE HAZARD TYPOLOGIES

The municipality of Sarno is modelled as an HSPN. According to the type of hazard being considered, fragility curves are selected from the literature to account for the vulnerability of the built environment that is masonry and reinforced concrete buildings within the studied area. Different intensity measures (IM) are also considered with respect to the two kinds of hazard. The peak ground acceleration (PGA) is used in the seismic case, while the debris flow velocity (v) is used in the landslide case study. The probability of street links becoming inaccessible is also accounted for. In particular, in the seismic case analysis, that probability is considered as a function of the buildings' height. This is fully consistent with the requirements of the national building code, NTC 2008 (D.M. 14.01.2008). According to these regulations, the maximum building height must be cautiously designed depending on the overlooking street width. Designers

have to perform such evaluations according to the buildings' strength, strain and dissipation capacity, and the seismic classification of the considered area. Furthermore, urban regulations and city planning can also impose specific restrictions on the height of buildings.

Conversely, in the case of the flow-type landslide analysis, all the street links located within the urban area affected by the landslide are considered to be inaccessible due to the debris heap.

Practically, in both case analyses, the urban graph links and nodes, which are damaged and/or inaccessible according to the damage assessment, are turned off. As a result, the undermined connectivity of the city graph has to be reactivated, starting with the restoration of such nodes and links.

To this end, a reconstruction strategy is hypothesized and its implementation is simulated. Then, a network efficiency index to assess the performance of the HSPN is evaluated before and after the shock occurrence, and for each stage of the recovery strategy.

Such an approach enables us to evaluate changes in the response to the type of disaster in terms of city efficiency and systemic damage, and, finally, in the resilience assessment. Urban resilience is evaluated using alternative approaches, including: as a function of the urban state of damage soon after the event occurrence, the initial number of inhabitants, and the displaced people.

6.1.1 The methodology

The current study proposes a framework to assess the systemic damage at the local scale as a proxy for city efficiency, i.e. its connectivity (Bozza et al. 2015b). Moreover, depending on the capacity of the urban environment to return to an equilibrium condition after a disaster occurs, engineering resilience according to the ecosystem approach is also evaluated (Bozza et al. 2015a).

Diverse types of hazard are analyzed and simulated through scenario analyses to assess differences in city efficiency, systemic damage and urban resilience assessments. The framework's flow-chart is outlined in Figure 6.1, following:

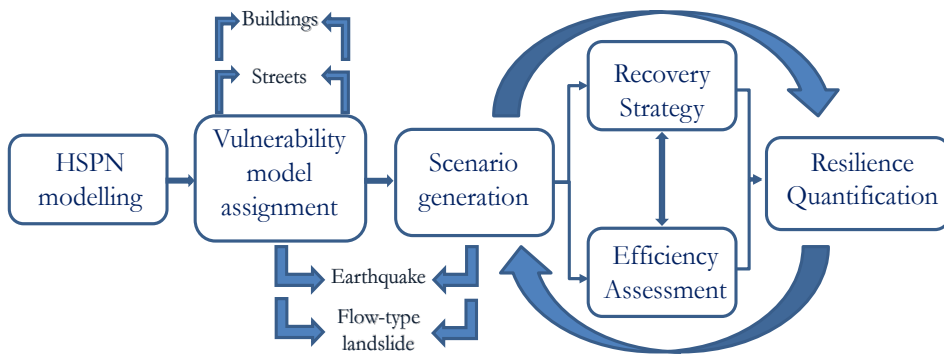


Figure 6.1 The framework's flow-chart

6.1.2 HSPNs modeling

The first phase of the proposed methodology requires the investigated urban system to be modelled. The intricate architecture of urban connections among physical components (such as the buildings, services and infrastructures) and the social agents (the citizens) residing and interacting through and within the physical frame can be easily assimilated into a complex system (González & Dueñas-Osorio 2015).

Here, the infrastructure and social network can be first individually modelled as a graph and then overlaid in a unique global network, namely the hybrid social-physical network called HSPN (Cavallaro et al. 2014, Bozza et al. 2015a), as already shown in the previous Section.

A complex network is usually represented by a graph $\Gamma = (N, L)$, consisting of a discrete set of nodes $N = \{1, 2, \dots, n\}$ and a discrete set of links $L \subseteq N \times N$. In particular, the case of the city modelling implies two set of nodes and two sets of links that are to be defined. With this, the social network is produced by the set of nodes representing residential

buildings, N_b , and the set of links, L_b , being the door links that connect each building to the street network's intersection nodes. On the other hand, the street network is modelled by hypothesizing that the urban services system is arranged on the city streets. Accordingly, the physical urban network is defined as a functional graph, whereas the set of nodes, N_s , represents the street intersections, and the set of links, L_s , urban street patterns.

Finally, the HSPN is defined for the considered city as graph $\Gamma = (N, L)$, where $N = N_b \cup N_s$ and $L = L_b \cup L_s$. Furthermore, due to the particular vehicular and citizen flow modelling issues (Dueñas-Osorio & Rojo 2011), the city graph is defined as undirected. This means that the presence of the link connecting the generic nodes i and j inevitably also implies the existence of the converse link.

Essentially, this type of network is located in a two-dimensional Euclidean space, and the Euclidean distance is used as a metric, providing the probability of finding a link between two nodes, which decreases with the distance (Bozza et al. 2015b).

It is clearly possible to model any city for which information about the number, typology and location of residential buildings is known. These are data that can be easily obtained from national databases, as is the case with the Italian National Institute of Statistics (ISTAT). The Italian databases enable us to know, for each considered city, the percentage of buildings according to the structural typology and age of construction. Moreover, the human component of the urban network is modelled by considering the mean square metres being occupied by each citizen. For instance, based on ISTAT, 1 citizen each 30 square metres of residential building is assumed. Accordingly, the total number of city inhabitants can also be computed, according to the total area of a residential building. Finally, the merger between the physical and the social network is performed exactly through this last phase. Each building node in fact represents a group of citizens, being the main component of the social network, connected to the

infrastructure network's nodes through outgoing door links and to the social network's nodes through the outgoing street links.

Once the HSPN is modelled, the next stage involves analyzing it to assess its performances. A network analysis allows its ability to provide services to citizens to be assessed. In particular, it allows us to consider the global performance of the HSPN as a measure of the accessibility of services for citizens. Performing this analysis before and after the event, and for each reconstruction stage, means that it is possible to quantify the damage to the quality of urban services and the entire city.

The urban system modelling is performed using a geographic information system (GIS). Such GIS-based modelling enables a large range of data to be integrated, and more specific information identified, through acquisition, georeferencing and documenting data.

6.1.3 Seismic and flow-type landslide fragility

Once the city is modelled as an HSPN, it is necessary to know the vulnerability of its building portfolio for different solicitation levels.

Vulnerability takes into account the knowledge of parameters that predominantly influence the capacity response of the structures. It is clearly evident that the values referring to such parameters are characterized by a degree of uncertainty that is evaluated through the use of so-called fragility curves. These are curves showing the conditional probability of exceedance of a certain damage state under the occurrence of an event with a given intensity.

Fragility curves are a powerful tool for characterizing the damage susceptibility of the city's physical sub-system and, indirectly, also its social sub-system.

Each building can be characterized by a fragility model given its construction material and structural scheme.

With this, the vulnerability is assessed within the current study for both masonry and reinforced concrete residential buildings affected by earthquakes or landslides.

As a case in point, and owing to the fact that earthquakes and flow-type landslides are natural events ruled by diverse dynamics and geomorphological mechanisms, various indicators have to be used to describe their intensity.

To this end, in the case of the seismic analysis, the peak ground acceleration (PGA) is used as the earthquake intensity measure (IM). On the other hand, the selected IM for the landslide analysis is the debris flow velocity (v).

According to a more general approach, from an analytical point of view, a fragility curve represents the probability of exceedance of a specific damage state, due to a disaster with an $IM = x$, which is lognormally distributed. Accordingly, this can be drawn by a lognormal cumulative probability density function as shown in Equation 1:

$$P_b(x; \mu, \sigma) = \Phi\left(-\frac{\ln x - \mu}{\sigma}\right) \quad (1)$$

where μ is the mean, σ is the standard deviation, and $\Phi[\cdot]$ is the standard normal distribution function.

Given the intensity of the simulated event – earthquake or landslide – it is thus known that the probability of each building located in the studied urban centre attains a certain limit state (LS). Consequently, according to the proposed methodology, the circumstance of a building losing its functionality is given by the comparison between the probability value, as obtained from the fragility curve for the given IM, and the value drawn from a numerical generation.

Streams of uniform pseudorandom numbers are generated, while values from the standard uniform distribution are selected on the open interval

(0,1) and compared to the value from the fragility function, which is related to the given IM of the simulated event. As such values are larger or smaller than those obtained from the pseudorandom numerical generation, it must be decided respectively whether the building will be damaged or not.

Furthermore, it is important to highlight that whenever a seismic disaster occurs, buildings located along each street could become damaged or even collapse when the ultimate limit state (ULS) is attained, thus making the same street inaccessible. Accordingly, to take into account such a building damage cascade event in the network, the probability of street interruption is also accounted for (Equation 2), as:

$$P_r(h,l) = \begin{cases} 1 & \text{if } h \geq l \\ \frac{h}{l} & \text{otherwise} \end{cases} \quad (2)$$

where h is the height of the building and l is the width of the road.

It is evident that a higher road interruption probability is associated with a higher ratio between the height of the building and the width of the street that is adjacent to it. Dually, this is clearly because the greater a building's height, the higher the probability of debris falling on to the street.

The proposed framework account for a street to become inaccessible is obtained through the comparison between the probability values calculated as previously illustrated and values generated from uniform pseudorandom distribution.

Meanwhile, in the case of landslide scenarios, the probability of street links becoming unusable is given as deterministic. This is because of the different dynamics related to a flow-type landslide. In this last case, the impact area is completely invaded by the debris heap. Accordingly, street links will be obstructed and, as a consequence, become inaccessible.

6.1.4 The systemic damage assessment

On the basis of the type of hazard simulated, different scenarios are generated and characterized by different IM values.

With reference to the studied area, the proposed fragility models enable us to recognize which buildings become unusable and which streets inaccessible.

The fragility assessment has a crucial outcome for the modelled urban HSPN: each street threatened by the catastrophe becomes an unfeasible link for the modelled network.

Such street segments are thus removed from the network, directly undermining the local and global city connectivity. Moreover, since the street interruption is directly linked to the collapse or damage of the overlooking residential buildings, the building nodes are also removed from the network.

As a result, the social components in the affected areas, i.e. the citizens, cannot benefit from city services or use their residence and must be relocated. To achieve this, a specific reconstruction strategy has to be designed and planned for the city.

The estimate of the number of citizens needing to be relocated after a certain event is carried out by considering the total number of citizens in the city according to ISTAT and assigning approximately 30 m² to each of them. Furthermore, statistical data provide the number of floors of each building, allowing more accurate and realistic modelling and a comparison of the simulation's result with real data.

Earthquake and landslide scenarios are generated through a Monte Carlo simulation technique performed with the mathematical computing software MATLAB[®]. For each simulated scenario, and by way of complex network theory, it is possible to evaluate the connectivity feature of the HSPN between a pair of nodes representing the city's human component through the street links network that is the efficiency citizen-citizen.

Efficiency measures describe the capacity of the city when it comes to keeping its own functionality as the connectivity between social agents and urban services. According to such an understanding, it is evaluated as a function of the ratio between the Euclidean distance, d_{ij}^{eucl} , and the length of the shortest path, d_{ij} , (minimum distance between each couple of nodes, i and j).

The city global efficiency normalized in [0.1] and averaged over all possible pairs of nodes is defined as shown in Equation 3, following:

$$E = \frac{1}{N(N-1)} \cdot \sum_{\substack{i,j \in N \\ i \neq j}} \frac{d_{ij}^{eucl}}{d_{ij}} \quad (3)$$

where N is the total number of nodes belonging to the network (Latora & Marchiori, 2001).

To also take into account the number of citizens living in each building, i , the relationship becomes (Equation 4):

$$\begin{aligned} E_{cc} &= \frac{1}{H_{tot}(H_{tot}-1)} \sum_{i \in N_b} H_i \cdot \left[(H_i - 1) + \sum_{j \in N_b, j \neq i} H_j \frac{d_{ij}^{eucl}}{d_{ij}} \right] = \\ &= \frac{1}{H_{tot}(H_{tot}-1)} \sum_{i \in N_b} H_i \cdot \left[(h_i - 1) + \sum_{j \in (N_b \setminus \{i\})} H_j \frac{d_{ij}^{eucl}}{d_{ij}} \right] \end{aligned} \quad (4)$$

where h_i is the number of citizens living in buildings a zero distance from i , H_{tot} is the total number of city inhabitants, H_i is the total number of residents in the building i , H_j is the number of citizens living in the remaining building nodes with the Euclidean distance d_{ij}^{eucl} from i , N_b is the set of all the building nodes, and d_{ij} is the length of the shortest path between node i and node j .

The citizen-citizen efficiency, which is assessed before and soon after the occurrence of a catastrophic event, can be regarded as an integral measure of systemic damage.

Given the efficiency of the residential HSPN, a recovery function is actually defined as in Equation 5:

$$Y(0) = \frac{E_{cc}^{post-event}}{E_{cc}^{pre-event}} \quad (5)$$

where $E_{cc}^{post-event}$ is the citizen-citizen efficiency evaluated soon after the event occurrence and $E_{cc}^{pre-event}$ is the citizen-citizen pre-event efficiency. The recovery function provides a measure of the residual capacity of the city after the event occurs (Bozza et al. 2015b). Accordingly, it can be understood as an indicator of the urban systemic damage. This enables a simple and prompt estimation of the widespread damage in the studied area that is quite different to the traditional damage assessment approach at the single structure level.

6.1.5 Alternative resilience metrics

In this study, the intrinsic complexity of social-physical urban systems is understood according to a systemic approach. Urban environments are interpreted in the sense of complex network theory, linking the urban physical space, its quality and the social agents that use it to the degree of satisfaction of citizens' needs (Nejat & Damnjanovic 2012).

According to such an approach, resilience can be evaluated as the capacity of the city to again reach the pre-event performance level in terms of urban functionality by respecting the complex urban structure.

The classical approach to urban resilience defines a recovery function $Y(t)$, whose value at time t provides the residual performance level of the system.

If the recovery process starts at time t_b and ends at t_c , the resilience is defined as the area under the recovery curve, being evaluated as in Equation 6, following (Cavallaro et al. 2014):

$$R = \frac{1}{t_c - t_b} \cdot \int_{t_b}^{t_c} Y(t) dt \quad (6)$$

So, for each step of the recovery process, it is possible to evaluate the performance level of the urban system as (Equation 7):

$$Y(t) = \frac{E_{cc}(t)}{E_{cc}^{pre-event}} \quad (7)$$

whose integration in the total recovery time enables us to quantify city resilience.

Nonetheless, the time dependence has to be removed, since it requires knowledge of the network structure at each phase of the recovery, thus representing a complicated and uncontrollable reality. This is a requirement that should take into account several dynamics. The operational efforts, typically carried out after a disastrous event, can actually rarely be reproduced, being influenced by several factors such as the availability of an economic budget, how quickly aid is available, the ease of reconstruction, the reconstruction costs and emergency management.

If these are key factors, which depend on specific conditions and several uncertainties, they can be hard to quantify and know in detail.

Accordingly, in this study, and to remove any explicit dependence of resilience on time, a pseudo-temporal parameter is considered, namely the recovery function, which is conceived as being dependent on relocated

citizens, C , at each stage of the recovery process. Equation 8 shows the adopted formulation.

Regardless of random variables, this enables us to monitor progress in the recovery by quantifying restored buildings, and so relocated citizens, at each stage of the recovery process.

$$Y(C) = \frac{E_{cc}(C)}{E_{cc}^{pre-event}} \quad (8)$$

The removal of total damage dependence $1 - Y(0)$ is also performed, enabling further simplification (Equation 9):

$$y(C) = \frac{Y(C) - Y(0)}{1 - Y(0)} \quad (9)$$

where $y(0)$, which is the function value when no displaced citizens have yet been relocated, is zero. This is what we obtain soon after the event occurs, when the recovery function is equal to $Y(0)$. While $y(C) = 1$, if $Y(C) = 1$, this means that all displaced people are relocated and the actual city efficiency is returned to the pre-event value.

Resilience is then calculated using the following, Equation 10:

$$R_1 = \frac{\int_0^{C_{max}} y(C) dC}{C_{max}} \cong \frac{\sum_{C=0}^{C_{max}} y(C) \cdot \Delta C}{C_{max}} \quad (10)$$

where C_{max} is the total number of citizens to relocate after a certain event and the integral is approximated as a summation, since the strategy is implemented in a discrete number of steps, as also shown in the diagram in Figure 6.2, following.

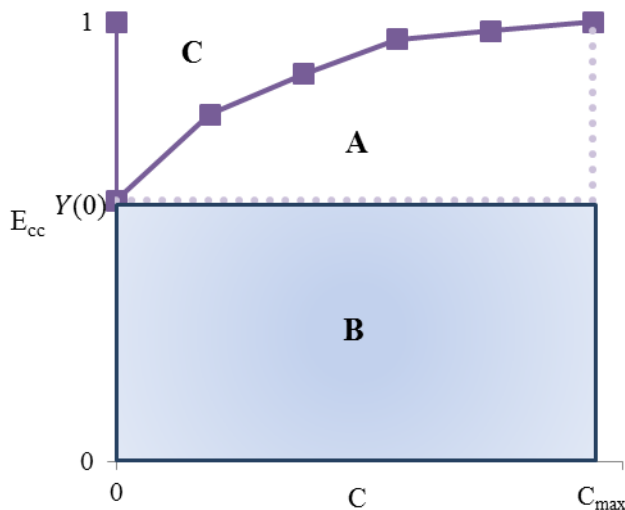


Figure 6.2 Normalized efficiency against the number of relocated citizens

In fact, when assessing the capability of a city's ecosystem to regain its functionality, one should also consider the bulk of the efforts needed to do so. For this reason, and particularly when performing a comparison between two different urban environments, one should always consider the damage extent suffered by each of them. Essentially, one city is more resilient than another if it suffers less damage. This is obviously because fewer resources are needed for it to recover and, consequently, fewer reconstruction stages are required. Accordingly, a further relationship (Equation 11) is proposed for quantifying resilience, which is oriented to compensate for the non-dependence caused by the damage, which depends on the state of the damage soon after the event occurs, $Y(0)$. In this case, a diverse physical meaning of resilience can be understood. With reference to Figure 2, resilience is now defined as the area under the recovery curve given by $A + B$, whose calculation is particularized as follows:

$$R_2 = \frac{\sum_{c=0}^{C_{max}} Y(C) \cdot \Delta C}{C_{max} \cdot Y(0)} \quad (11)$$

Furthermore, a third relationship is proposed to evaluate resilience, called hybrid resilience, which is not directly related to its physical meaning. With this, urban resilience can be quantified by accounting for the initial state of the damage, $Y(0)$, by simply summing up the recovery function, $C=0$, which is evaluated when no citizens have yet been relocated, to the resilience value, R_1 . Equation 12 shows the calculation in detail:

$$R_3 = \frac{\sum_{C=0}^{C_{max}} y(C) \cdot \Delta C}{C_{max}} = R_1 + Y(0) \quad (12)$$

Finally, a further resilience measure is defined as (Equation 13):

$$R_4 = R_3 \frac{C_{max}}{H_{tot}} \quad (13)$$

which enables us to normalize the evaluated resilience level according to a coefficient, which accounts for the number of displaced citizens with respect to the total number of city inhabitants, C_{max} .

Both of the resilience measures, R_3 and R_4 , are damage-dependent, as is R_2 , but the former represent the advantage of being defined in the limited interval $[0, 1]$. This allows for an easier comparison to be made between the resilience values obtained from the diverse event typology simulations. One should also take into account the fact that urban functionality can be restored through the implementation of different reconstruction strategies. The proposed metrics in fact enable us to compare diverse alternative actions, which can be undertaken if an event affects a city's ecosystem. In this way, local authorities could assess in advance the potential of diverse strategies to enhance their city's resilience and to promptly implement them according to available resources, ultimately choosing the one that best meets the city's needs.

A reconstruction strategy is hypothesized and implemented herein for this reason. The selected strategy first establishes the reconstruction of the cheaper buildings and the recovery of efficiency to the pre-event level. According to such a strategy, the restored buildings are progressively reintegrated into the network, which is also progressively reconnected.

6.2 A REAL CASE STUDY: THE CITY OF SARNO

Sarno is a small town of 32,000 inhabitants about 50 km from Naples (Campania Region) in Southern Italy. The name of the town means “born under the mountain”, because it is surrounded by a mountain range, whose highest peak is Mount Saro, which is over 1000 m high (Catapano et al. 2001). The building portfolio is located in the valley floor of the area, with the oldest part up the hill, and a further quarter, called Episcopio, situated just down Mount Saro (Figure 6.3).



Figure 6.3 Picture of Mount Saro, Italy

Mount Saro and its highest peak, Pizzo D'Alvano (1133 m M.S.L.), is part of a limestone relief complex, and is about 20 km wide and 70 km long. Such reliefs stretch NW–SE from Mount Maggiore (close to the town of Caserta) to the Solofrana Valley, and are composed of a very deep succession of Mesozoic carbonate rocks interrupted by tectonic valleys (Arturi et al. 2003).

Due to its geomorphological characteristics, Sarno is a high risk area, as it is landslide prone and highly exposed due to the antiquity of the built environment.

The landslide risk is mainly related to cumulative rainfall, which constitutes an increasing danger, especially due to the lack of suitable vegetation cover and an efficient surface water drainage network.

In May 1998, 14 landslides came down from Mount Sarò in a few hours, affecting the municipalities of Sarno, Quindici, Siano, Bracigliano and San Felice a Cancellò. The landslides hit the residential area of Sarno, causing severe damage to the built environment and 161 fatalities (Basile et al. 2003).

In the early stages, the soil collapsed from the steepest parts of the Pizzo d'Alvano slopes, climbing down on surfaces inclined at 40–50°. The estimated flow velocity was 5 to 15 m/s, as shown by the destructive impact on most of the urban structures, reaching up to 20 m/s near the toe of the slopes. The flow depths were 4–5 m, and the maximum thickness of the deposit was 3.5–4 m in the central part of the current (Revellino et al. 2003).

The typical flow-type landslide scheme is shown in figures 6.4 and 6.5 (Highland 2004).



Figure 6.4 Typical flow-type landslide

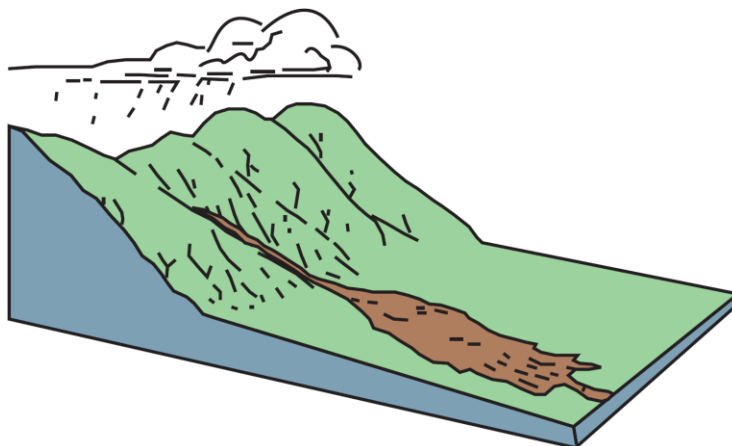


Figure 6.5 Flow-type landslide scheme (Highland 2004)

Sarno is also an earthquake prone area, as made clear by current Italian legislation.

According to the decree PCM n. 3519 of 28th April 2006, Italian municipalities are classified into four main seismic categories according to their seismic risk (OPCM 3519/2006). Sarno is in zone 2, as it is a medium-risk seismicity area, with an expected PGA between 0.15g and 0.25g, as shown in Figure 6.6:



Figure 6.6 Seismic classification of the Campania region, with the low (yellow), medium (blue) and high (red) seismicity areas outlined

6.2.1 Modelling Sarno as a complex network

As already shown in Section 6.1, the initial step of the methodology proposed in this study is aimed at creating a network topology of the Sarno territory. This is built up into a GIS environment, which enables us to manage the spatial data and identify the configuration and location of the network components in detail. In particular, starting from the LIDar data from the national databases, the Digital Surface Model (DSM) and the Digital Terrain Model (DTM) were analyzed. The difference in terms of the local height between the two models was evaluated and enabled us to recognize the number and location of the residential buildings within the municipality. The diverse street paths existing within the urban territory were also recognized.

Figure 6.7 shows the street network of Sarno, in which the buildings' locations are also embedded, as in the shape file provided by the national databases.

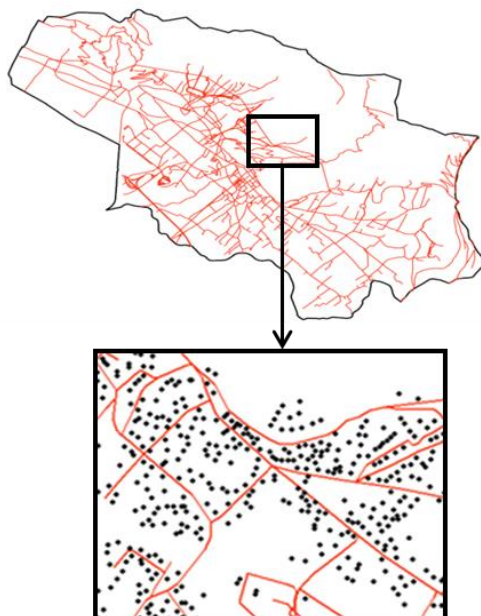


Figure 6.7 Building (black points) and street pattern (red bold lines) networks for the city of Sarno

GIS data also enables us to ascertain the length of each street link, while their width is randomly assigned according to the mean typical street width. As a result, it is possible to geographically position each component of the physical network accurately. Accordingly, street-to-street intersections are modelled as nodes, N_s , and street arches as links, L_s , to build up the Sarno physical network.

The city's residential network is further particularized by referring to the ISTAT data, which supplies information about the number of buildings in each Italian municipality and their number of storeys and structural typology. The ISTAT data were processed and the percentage of buildings was provided for each structural type: 37% of reinforced concrete buildings and 63% of masonry buildings for the city of Sarno. The number of storeys considered for each building category is between two and five, thus placing them in the low-to-mid rise building class.

Furthermore, the physical network was enriched by considering fictitious connections between the set of residential building nodes, N_b , and the set of street intersection nodes, N_s . These are the door links, L_b , representing the entry points for the buildings' inhabitants from the building residence to the street network. Consequently, they represent interrelations between the physical and the social network.

Finally, the social network was completed by estimating the number of citizens living in each residential building. According to the ISTAT data, a population density of one citizen per 30 m² of the total area covered by buildings is assumed. Consequently, the number of citizens living in each building was computed through the assessment of the total floor area of each typology and multiplying it for the storey number to finalize the HSPN modelling.

Once the city HSPN is modelled, it is important to know the vulnerability of its building portfolio for the different levels of damage. In particular, only residential buildings were considered within the proposed case study.

6.2.2 Fragility of the Sarno physical network

To recognize the buildings' failure or damage due to the occurrence of a seismic or landslide event, a fragility model was selected for each structural typology according to the event type. This enables us to estimate the probability of damage to the buildings prone to the event, depending on the attained IM, which is the PGA in the case of an earthquake and v in the case of a flow-type landslide.

Seismic analytical fragility curve parameters were selected from Ahmad (Ahmad et al. 2011), which provides logarithmic values of μ and σ for each structural limit state (Table 6.1):

Table 6.1 Parameters of the seismic fragility curves by Ahmad (Ahmad et al. 2011)

<i>Structural Type</i>	μ	σ
Masonry buildings	- 1.03	0.35
RC buildings	- 0.91	0.29

Figure 6.8 shows fitted curves from which the vulnerability of the diverse building typologies is deduced.

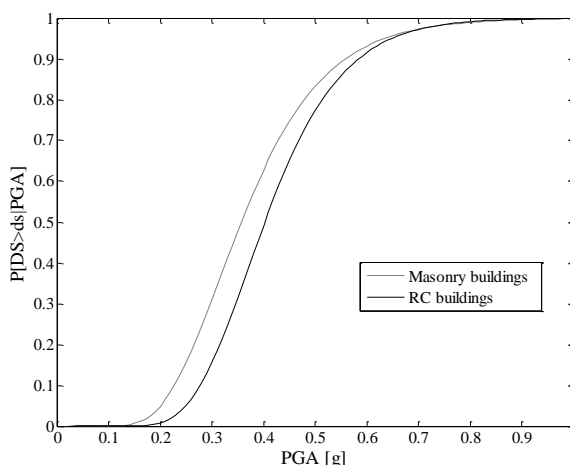


Figure 6.8 Fragility curves according to Ahmad (Ahmad et al. 2011) for reinforced concrete and masonry buildings

On the other hand, the vulnerability of Sarno's building network to landslides is accounted for according to the FP7-funded SafeLand project (2009–2012, Grant Agreement No. 226479) (Corominas et al. 2011), considering $\mu = 1.39$ and $\sigma = 0.43$ for masonry buildings. Furthermore, for reinforced concrete buildings, fragility curves from Parisi (Parisi et al. 2015) were considered, with the parameters $\mu = 1.39$ and $\sigma = 0.30$, which are shown in Table 6.2.

Table 6. 2 Parameters of the landslide fragility curves from the FP7-funded SafeLand project (Corominas et al. 2011) and Parisi (Parisi et al. 2015)

<i>Structural Type</i>	μ	σ
Masonry buildings	1.39	0.43
RC buildings	1.39	0.30

Both the fragility functions are shown in Figure 6.9. **Errore. L'origine riferimento non è stata trovata.:**

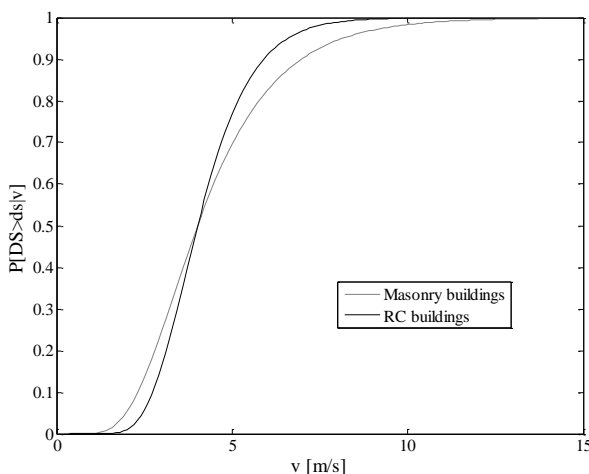


Figure 6.9 Fragility curves according to Parisi (Parisi et al. 2015) for reinforced concrete buildings and the FP7-funded SafeLand project (2009–2012, Grant Agreement No. 226479) (Corominas et al. 2011) for masonry buildings

As expected, the fragility models show that masonry buildings are more vulnerable than reinforced concrete buildings according to the higher standard deviation values. As a consequence, the area of Sarno is proved to be extremely susceptible to both earthquake and landslide risks, given the prevalence of masonry buildings (see Section 3.1).

Seismic scenarios with $PGA=0.25g$, i.e. medium intensity earthquakes, were simulated in accordance with the hazard level in Sarno. To study and check the variability of the results, each simulation was iterated five times using Monte Carlo techniques.

The developed algorithm refers to a simulation procedure which evaluates both the probability of the buildings exceeding the considered state of damage (according to Equation 2) and the joint probability of the streets becoming inaccessible as a result of the damaged buildings (according to Equation 3).

Consequently, for each simulation, damage to the built environment was randomly generated according to the fragility models used, leading to a certain quantity of building nodes and street connections becoming unusable. As a result, a number of citizens were considered to be deallocated because of such damage, and the related set of street connections and building nodes were removed from the HSPN.

According to the same methodology, a flow-type landslide scenario was also generated. Specifically, the 1998 Sarno event was reproduced through a back analysis, where the flow velocity was assumed to be equal to the estimated one, $v=10m/s$.

The difference between the seismic scenario and the landslide back analysis simulations was related to the way in which street intersections and links were considered to become unusable. While in the former case the street links damaged by the earthquake were randomly recognized depending on the buildings' height, in the latter, all the street links located within the impacted area were removed from the HSPN.

This is due to the different nature of the simulated events. In the case of an earthquake, there is no material as a by-product of the event, and so unusable streets are the only ones obstructed by the debris from the overlooking damaged buildings. If a flow-type landslide occurs, streets located along the landslide travel paths are obstructed by the muddy material sliding down from the slope, and so all have to be regarded as impassable.

Moreover, in the case of the landslide back analysis, damage to the buildings was randomly generated according to the related fragility curves, as in the seismic case analysis, although such generation was referred only to the buildings located along the landslide travel paths.

6.2.3 Approaches to the event type and systemic damage assessment

The generation of seismic and landslide scenarios was different, because of the diverse areas of impact that typically result from these two phenomena. In fact, earthquakes are low-probability-high-consequence events, which can cause widespread damage to an entire city, while flow-type landslides usually only affect restricted areas of the urban centre. Accordingly, in this study, when performing seismic scenarios, the related infrastructure damage was assessed through the use of fragility curves for the entire built environment. Meanwhile, when dealing with landslide scenarios, specific travel paths were determined based on empirical evidence of the damage from the 1998 Sarno landslide, as shown in Figure 6.10, and a back analysis was carried out.

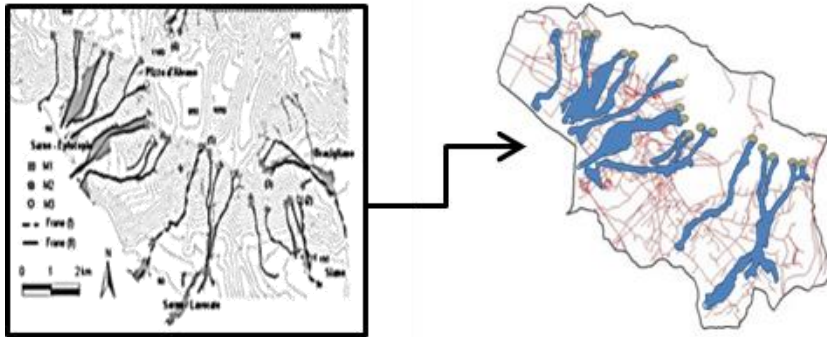


Figure 6.10 Travel paths of the landslides by Cascini (Cascini et al. 2011) drawn on the Sarno HSPN, May 1998, for the analysis of the run-out distance

This approach enables us to evaluate the city's efficiency and resilience if subjected to a flow-type landslide without resorting to two- or three-dimensional models, which are typically used to simulate this kind of event. Contextually, the availability of detailed information about the landslide travel paths and the flow velocity empower the analysis's reliability.

In particular, a comparison study was performed between the research carried out by Cascini (Cascini et al. 2011) and the Sarno urban network built into the GIS environment (Figure 6.10). As a result, the coordinates of the buildings located within the areas affected by the landslide were identified, while a mean debris velocity of $v=10$ m/s estimated for the real landslide event was assumed.

Alternatively, the seismic scenario was run assuming the earthquake intensity was $PGA=0.25g$.

Simulations for the two cases were run once the simulation model of the considered recovery strategy was also characterized. The city reconstruction process was considered to be implemented in a discrete series of steps. In each stage of the process, a certain number of buildings, starting from the cheaper ones, with the related street connections and junctions, were rebuilt. Accordingly, a certain share of citizens whose

residences were damaged were relocated, with a gradual increase in city efficiency.

Each simulated scenario provides the corresponding post-event HSPN, and the ratio between the efficiency of the network before the earthquake and immediately after the event is evaluated as the residual capacity of the city.

The results, in terms of relocated citizens and collapsed buildings, as well as urban efficiency and normalized urban efficiency, are presented for both the landslide and earthquake case scenarios (Table 6.3, Table 6.4, Table 6.5, Table 6.6).

As expected, only one simulation, namely a back analysis, was implemented in the case of the flow-type landslide. Consequently, the results are all set out in Table 6.3.

Table 6.4 is as an example of the results typically obtained when seismic scenarios were simulated. In view of this, five simulations were run, and tables 6.5 and 6.6 show the standard deviation and the median referring to all the simulations.

Table 6.3 Efficiency, relocated citizens and collapsed buildings in the case of the landslide back analysis

		<i>Landslide</i>						
<i>step</i>		<i>0</i>	<i>1</i>	<i>2</i>	<i>3</i>	<i>4</i>	<i>5</i>	<i>6</i>
Relocated citizens		0	0	849	1699	2548	3398	4247
Efficiency	$E_{cc(C)}/E_{cc, pre-event}$	0.630	0.166	0.220	0.368	0.484	0.561	0.630
Residential buildings		2756	2362	2486	2575	2648	2707	2756
$E_{cc(C)}/E_{cc, pre-event}$		1.000	0.264	0.349	0.584	0.769	0.890	1.000

Table 6.4 Efficiency, relocated citizens and collapsed buildings in the case of earthquake simulation #1

<i>step</i>	<i>Earthquake</i>						
	<i>0</i>	<i>1</i>	<i>2</i>	<i>3</i>	<i>4</i>	<i>5</i>	<i>6</i>
Relocated citizens	0	0	721	1442	2164	2885	3606
Efficiency _{citizen-citizen}	0.630	0.014	0.052	0.187	0.356	0.531	0.630
Residential buildings	2756	2440	2540	2609	2665	2714	2756
$E_{cc}(C)/E_{cc, \text{pre-event}}$	1.000	0.023	0.082	0.296	0.565	0.844	1.000

Table 6.5 Efficiency, relocated citizens and collapsed buildings in terms of the standard deviation of the five seismic simulations

<i>step</i>	<i>Standard deviation, σ</i>						
	<i>0</i>	<i>1</i>	<i>2</i>	<i>3</i>	<i>4</i>	<i>5</i>	<i>6</i>
Relocated citizens	0	0	51	102	153	204	255
Efficiency _{citizen-citizen}	0.000	0.018	0.027	0.032	0.064	0.017	0.000
Residential buildings	0	17	12	9	6	2	0
$E_{cc}(C)/E_{cc, \text{pre-event}}$	0.000	0.028	0.043	0.050	0.101	0.027	0.000

Table 6.6 Efficiency, relocated citizens and collapsed buildings in terms of the median of the five seismic simulations

<i>step</i>	<i>Median, η</i>						
	<i>0</i>	<i>1</i>	<i>2</i>	<i>3</i>	<i>4</i>	<i>5</i>	<i>6</i>
Relocated citizens	0	0	666	1332	1998	2665	3331
Efficiency _{citizen-citizen}	0.630	0.024	0.091	0.222	0.356	0.531	0.630
Residential buildings	2756	2461	2554	2618	2671	2717	2756
$E_{cc}(C)/E_{cc, \text{pre-event}}$	1.000	0.037	0.145	0.352	0.565	0.844	1,000

The statistics shown in Table 6.5 for the seismic case analysis highlight the diverse scatter between the results through the five seismic simulations.

In particular, when dealing with relocated citizens, increasing scatter is observed through the reconstruction steps. This trend diverts in the case of the restored residential buildings, which is obviously down to the fact that the number of city inhabitants is assessed as a function of the residential buildings' square meters. Accordingly, when more citizens are relocated, there are fewer residential buildings left to reallocate.

On the other hand, referring to the normalized efficiency values, no specific trend is recognizable, as the standard deviation values differ at each stage.

6.2.4 Discussion of results

A systemic damage measure can be understood from the recovery function, $Y(0)$, which is defined by Equation 3 as the ratio between the efficiency before the event and soon after its occurrence. This enables us to quantify the functionality that the investigated urban system can still capitalize on.

The recovery function is also evaluated for each stage of the recovery to quantify the residual city efficiency, $Y(C)$. Obviously, the lower the ratio, the greater the damage to the city.

A first important result that can be drawn from this study is the relationship that exists between the recovery function, $Y(C)$, and the total number of people needing to be relocated after a certain event, C . In particular, the trend of the normalized efficiency is observed over the recovery process in order to monitor progress in citizen–citizen connectivity. The obtained curve is the recovery curve, which is shown in Figure 6.11 for the case of the landslide back analysis and Figure 6.12 for the earthquake analysis for each simulation. The diagram in Figure 6.12 clearly shows the trend of each recovery curve for each simulation. The

curves corresponding to the median (black line), the 16th percentile (dark grey dashed line) and the 84th percentile (light grey dashed line) are also shown.

It is important to highlight that, according to the simulated recovery strategy and the considered city infrastructure, different measures of city connectivity can be evaluated by referring to different urban dynamics.

In the proposed case study, the citizen–citizen efficiency is evaluated and observed for each stage of the city recovery process. Following the occurrence of the typology of both simulated disasters, a certain number of citizens will actually be deallocated, remaining homeless and needing to be relocated. The recovery curve trend shows an immediate and rapid drop soon after the event occurrence, due to the violent impact of the disaster and the consequential reduction in efficiency. Progressively, the curve tends to rise again during the reconstruction stages, with a gradual slope fall the pre-event efficiency level is achieved.

The slope change is due to the diverse number of buildings needing to be restored, and thus to the number of citizens needing to be relocated.

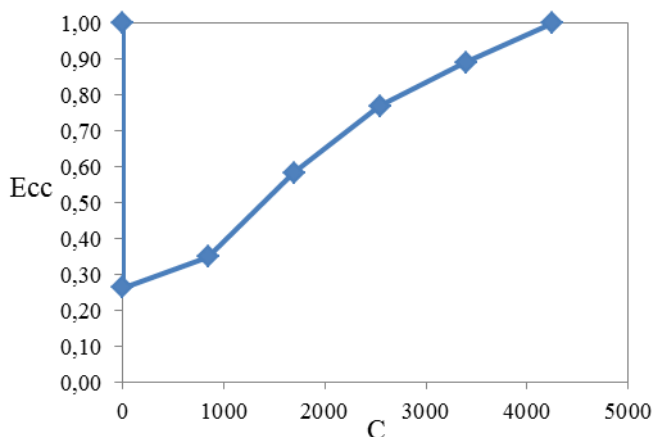


Figure 6.11 Normalized efficiency of the residential HSPN, $Ecc(C) / Ecc_{pre-event}$, as a function of the number of reallocated citizens, C , for the landslide scenario with $v=10$ m/s

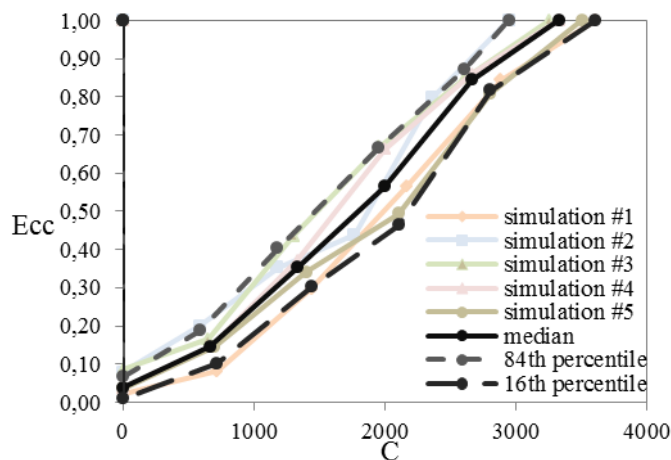


Figure 6.12 Normalized efficiency of the residential HSPN, $E_{cc}(C)/E_{cc,pre-event}$, as a function of the number of relocated citizens, C , in the earthquake scenarios with $PGA=0.25g$

The analysis of the results shows that:

- in both the cases, a major slope is observed for the second and third recovery stages. This is because of the adopted recovery strategy, which hypothesizes that the cheaper buildings are rebuilt first, and these are also the smaller ones;
- according to the preliminary assumptions made, one citizen is computed for each $30m^2$ of residential buildings. Consequently, many more citizens are computed for larger buildings. As a result, once cheaper buildings are rebuilt, the recovery process begins to involve the reconstruction of increasingly expensive residential buildings and tends to level off at the final stage, where a minor number of buildings are left to restore. Accordingly, many more citizens are relocated and a higher number of street links restored, resulting in a major rise in efficiency and a substantial increase in both the slope of the recovery curve and the final resilience value;
- the citizen–citizen efficiency in the aftermath of the event, calculated in the case of the seismic simulation, is lower compared to that of the

landslide simulation. This can be understood on the basis that an earthquake is an event causing widespread damage, while a landslide causes localized damage. So, soon after the event occurrence, a significant disruption of the urban HSPN is observed in the seismic case, resulting in a major fragmentation of the network. As a consequence, provided that $E_{cc,pre-event}$ is the same in the two cases, lower connectivity and more serious damage are observed;

- the decrease in efficiency, like in the $Y(0)$ value, which is the normalized efficiency soon after the event occurrence, is different with reference to the type of catastrophic event, as shown in Table 6.7. In fact, a 71% drop in normalized efficiency, $Y(0)$, is observed in the case of a landslide, while a 94% drop is obtained in the case of an earthquake.

Table 6.7 $Y(0)$ value in the case of an earthquake and landslide

$Y(0) = E_{cc,post-event}/E_{cc,pre-event}$	
<i>Earthquake</i>	<i>Landslide</i>
0.038	0.264

This is because of the number of interrupted street links, which is higher in the case of an earthquake (1,949) than in the case of a landslide (1,301). As a consequence, more severe decay at the urban connectivity level, and so in global efficiency, are observed with respect to the major area of impact affected by the earthquake. On the other hand, the landslide affects a higher number of buildings, with this figure being 19.8% higher than in the seismic case;

- the severity of the simulated events is also different. In the case of the landslide, a back analysis was implemented, where the damaged areas are identified according to an empirical approach. The flow-type landslide in Sarno in 1998 caused severe damage to the residential area of the city, but cannot be regarded as a major catastrophe. In contrast, in the case of a seismic event, the simulations are related to a design earthquake characterized by a return period of $Tr=2,475$ years, which is potentially more destructive than a landslide. This is also the reason why a major drop in efficiency is observed in the seismic case analysis;
- the extent of the damage caused by the events affecting the Sarno area can also be observed by comparing the undamaged (Figure 6.13) and damaged network configurations graphically following the occurrence of a landslide (Figure 6.14) and an earthquake (Figure 6.15).



Figure 6.13 Pre-event graph

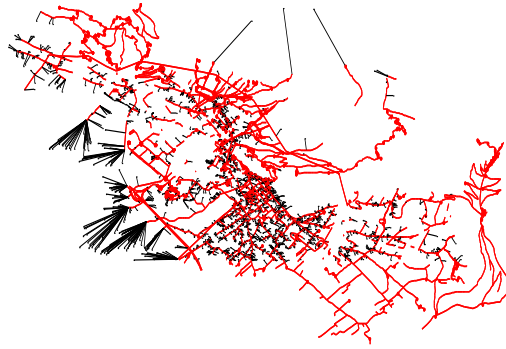


Figure 6.14 Post-landslide graph

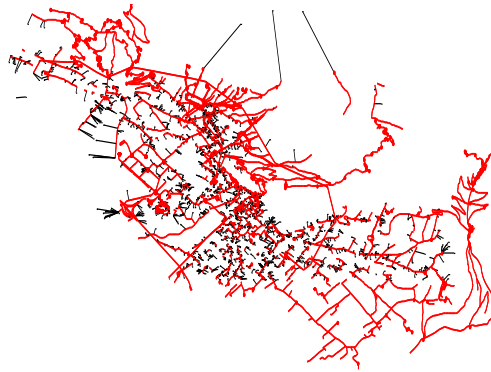


Figure 6.15 Post-earthquake graph

The graphs are representative of the post-event network configuration, and show the destructive effect of the simulated events. In the case of the earthquake, where a major drop in urban efficiency is recognized, it should be noted that the degree of connectivity of the network is still rather high, because of the high network redundancy. Such evidence is peculiar to big cities, where the occurrence of external stresses causes a reduction in city efficiency, although basic functionalities can still be guaranteed until a certain level of event intensity occurs.

Following the scenario analysis, urban resilience is calculated with reference to four different formulations, according to equations (10)10, 5, 6 and 13.

Tables 6.8 and 6.9 show the results in terms of urban resilience being respectively evaluated for the earthquake scenario simulations and the flow-type landslide back analysis. Furthermore, the resilience of the Sarno city ecosystem is quantified for each simulated event typology according to the four proposed alternative metrics.

Table 6.8 Resilience results with reference to an earthquake event

<i>RESILIENCE</i>	<i>Earthquake</i>						
	η	σ	<i>Simulations</i>				
			<i>1</i>	<i>2</i>	<i>3</i>	<i>4</i>	<i>5</i>
R ₁	0.447	0.033	0.447	0.420	0.488	0.500	0.441
R ₂	12.8335	9.9002	0.0595	9.9106	2.2171	3.8231	2.833
R ₃	0.485	0.208	0.470	0.499	0.573	0.492	0.477
R ₄	0.053	0.022	0.055	0.047	0.060	0.053	0.054

Table 6.9 Resilience results with reference to a landslide event

<i>RESILIENCE</i>	<i>Landslide</i>
R ₁	0.518
R ₂	2.447
R ₃	0.781
R ₄	0.107

The main goal of this work is to assess urban resilience in the face of disasters. In particular, this methodology aims to compare different resilience measures with reference to the same urban environment, but different types of disaster with different severity levels. Accordingly, the proposed study enables us to identify the resilience measure which best captures the wide range of urban resilience aspects according to a systemic

damage approach. Alternatively, the goal is to recognize the best resilience metric for the urban element that one wants to observe.

The results show differences in the proposed resilience measure according to the typology of the event simulated. In fact, with reference to the case study of Sarno, it can be argued that the landslide event is the one affecting the city's efficiency to a limited extent, while the seismic one is the most serious. This is true when observing the resilience values R_1 , R_3 and R_4 , while the measure R_2 shows greater city resilience in the seismic case. This is because of the high dependence of this last measure on the recovery function at the zero stage, $Y(0)$. This outlines the major effort needed to recover from a seismic event compared to a landslide in terms of the same number of recovery strategy stages.

On the other hand, such observations emphasize the opportunity to use the proposed resilience measures as complementary according to the following remarks:

- R_1 indicates damage-independent resilience, as it is fully normalized with respect to the observed damage. Accordingly, it obtains a resilience perspective that is strictly related to the urban normalized efficiency in the pre- and post-event stages, regardless of the initial damage level;
- R_2 is highly influenced by the damage level soon after the event occurrence, $Y(0)$. This enables a resilience assessment to be made from an engineering point of view, which is related to the structural systemic damage suffered by the studied urban system in the aftermath of a catastrophe;
- R_3 and R_4 are both damage-dependent measures. R_3 obtains urban resilience depending on the post-event damage, with the same approach used for R_2 . Conversely, while R_2 is defined in the open interval $[1, +\infty[$, R_3 and R_4 are defined in a restricted interval, $R_3, R_4 \in [0, 1]$, as is R_1 ;

- R_4 has a physical meaning, which emphasizes the social dimension of resilience normalized according to the total number of the city's inhabitants. The measures R_3 and R_4 both exhibit similar trends, with R_4 tending to R_3 if the ratio between C_{max} and H_{tot} tends to a unit value, as shown by the results in tables 6.8 and 6.9;
- $R_1, R_3,$ and $R_4 \in [0, 1]$ show the advantage of having an upper boundary, which makes the comparative analysis between diverse cities and diverse event typologies easier;
- In particular, R_3 and R_4 have the potential to enable a sort of ranking between different types of event, where the difference between the two is just an order of magnitude. As an example, the R_4 value is, in the cases of a landslide and an earthquake, respectively, 0.107 and 0.053, meaning that local authorities could use this measure to choose a potential mitigation strategy. For instance, with reference to the obtained results, the most appropriate choice could be the seismic retrofit of residential buildings, with the seismic resilience lower than the landslide resilience.

In parallel with this consideration, R_1 appears to be a more objective resilience measure, which enables us to compare different urban networks and different types of event scenario.

R_2 shows how an urban system can recover to an equilibrium state following the drop in efficiency resulting from an event. In the present work, R_2 is actually the only resilience measure that is higher in the case of an earthquake (12.83) than a landslide (2.45). This highlights the almost linear dependence of this measure on the residual efficiency, $Y(0)$, which is equal to 0.26 in the case of a landslide and 0.04 (median value) in the seismic case. This is because the latter causes a significant loss of urban connectivity.

6.3 CONCLUSIONS

This study uses a systemic damage approach to propose an integrated framework for the quantification of urban resilience in the face of diverse natural disasters, specifically earthquakes and landslides. Different event scenarios were simulated and alternative resilience measures assessed, with the aim being to prove and validate the robustness of the proposed metrics.

The novelty of the proposed approach is the damage assessment at a widespread level rather than at the single structure level according to traditional engineering approaches. At the bottom of the methodology, a simple multi-scale approach is considered. This moves from the level of each citizen and their residence, to the upper level of the infrastructure system, until the global city system with respect to which the systemic damage is assessed is modelled.

According to the methodology, the city can be assimilated in a complex network, the hybrid social-physical network (HSPN). A probabilistic approach is then used to assess the buildings' vulnerability and the probability of street interruptions. In order to implement the framework, the simulation of different seismic and landslide scenarios is performed. Seismic analyses are carried out with $PGA = 0.25g$, while in the case of the landslide, a back-analysis is performed with reference to the Sarno event in 1998, assuming a mean flow velocity of $v = 10m/s$.

A recovery strategy is hypothesized to simulate the reconstruction process of the city in the two scenarios. Analytical efficiency measurements are evaluated with reference to the HSPN, according to the complex network theory. They are in the pre-event stage soon after the event occurs and for each stage of the recovery process.

They are then integrated with the number of relocated citizens in order to finally compute the observed systemic damage and resilience, i.e. the city's capacity to recover its functionality after the disaster.

The obtained results clearly show that the HSPN modelled for the case study of Sarno exhibits a seismic resilience that is lower than its landslide resilience. These dissimilarities are due to the nature of the simulated disasters and the metrics. The damage is, in fact, more severe when dealing with an event that strikes the entire urban network, such as an earthquake, compared to an event affecting discrete urban areas, such as a flow-type landslide. Moreover, the resilience measures outline comparable, but also complementary, results. In order to compare different urban systems that are prone to the same hazards, the proposed alternative metric, R_1 , can be effectively used to compute resilience in the case in which no dependence in terms of the state of damage is considered.

On the other hand, such metrics can be used with the damage-dependent metrics R_2 and R_3 - which are equivalent to R_4 - with reference to the same urban environment, which can potentially be affected by different disaster typologies, with different intensities. R_4 puts a particular focus on the urban damage from a human perspective, while R_2 is strictly related to the magnitude of the damage observed in the aftermath of the event. With this, mitigation actions can be more easily assessed and implemented by considering the capacity to withstand each event typology shown by the city model. According to such an approach, urban management choices are driven by engineering-based evaluations, which can improve urban resilience and preparedness.

Further considerations concern the potential effectiveness of the simulated recovery strategy, which hypothesizes that cheaper and, so, the smaller buildings are rebuilt first, depending on the actual allocation of economic resources. If a city, in fact, has a high budget available, as hypothesized here, then the proposed recovery strategy could work. Alternatively, larger buildings hosting a higher number of citizens, being the more strategic structures, should be rebuilt first. Further possible recovery strategies can, however, be easily implemented in the proposed framework. The framework has the potential to be used as an effective support for risk

mitigation and planning policies, and as a practical precautionary instrument to be used by disaster managers. The local disaster manager can evaluate the applicability of diverse hypothesized strategies and choose the best one in a prompt and economic manner. This will maximize efficiency and urban resilience, according to the results provided by the simulations that are run.

CHAPTER 7

CONCLUSIONS

The present PhD Thesis work has been developed to address issues related to resilience of urban systems to natural catastrophe risks. Resilience has been studied from multiple perspectives, trying to catch its high interdisciplinary nature.

The most critical issues related to the quantification of resilience at the urban scale and to the development of mitigation instruments devoted at enhancing disaster resilience at the global scale are discussed and investigated.

A particular focus is done in *Chapter 1* to highlight the great attention that the concept of resilience has gained from the worldwide scientific community, according to different understandings and applications.

The origin of the concept of resilience are herein investigated, as well as the variability of its definition within various subject area, which resilience is applied in.

A novel understanding of resilience is proposed in this Chapter, being the theoretical basis, which the thesis is based on. Resilience is defined as the engineering one in the sense of the ecosystems theory. In this view, it is the capability of a system to face an external stress and bounce back from it to an equilibrium condition, that can be the same but also different from the pre-event one.

The deep link between resilience and sustainability is also highlight, according to a human-centric perspective. Resilience is, in fact, understood as one of the main factors contributing to sustainability. Accordingly, a city to be sustainable, has to be resilient too.

Hence, approaches proposed in the literature to quantify resilience are discussed, according to the field of application they are related to.

Particularly, the quantification of resilience of physical, social-economics and complex systems is analyzed. Particularly, when dealing with complex systems, one of the most recent approaches is highlighted, referring to the modelling of the studied systems according to the graph theory. This is also the methodology being adopted within the current thesis (Bozza et al. 2015; Cavallaro et al. 2014; Asprone et al. 2013) to assess urban resilience, which enable us to account for both single system's components and their mutual, underlying, interrelations (Ouyang and Dueñas-Osorio 2014; Franchin and Cavalieri 2015, 2013). According to this approach, disaster resilience can be quantified by using complex networks' theory's metrics (Latora and Marchiori 2001). With this, also the scale of resilience is accounted for, encompassing variables and dynamics, which affect resilience importantly, and derive from the most disparate scale: from the single social actor, to the whole urban infrastructural system, and to the merger of the two, until the highest, global scale, as can be the national one. Such an approach reveals to be fundamental in dealing with disaster resilience, due to the modern, always increasing urbanization and to the great need to share knowledge and best practises around resilience, both at the local and the global scale.

This last consideration, is highlighted in Chapter 1, as one of the most important opportunities, being created from modern studies on resilience. Furthermore, also important challenges arise from the deep analysis being performed within the present Chapter. They are related to the tackling of multiple hazards being very tricky and to the issue of integrating modern approaches into traditional disaster management and governmental processes.

Chapter 2 discusses the proposal of a seismic insurance model as an instrument potentially increasing resilience, according to a superurban perspective.

To date, there are several philanthropic initiatives, research projects and worldwide development programmes, addressing disaster resilience on the

global scale, through incentives to insurance and reinsurance products. Innovative financial products represent, in fact, an effective instrument supporting communities to strive for enhancing international cooperation and best managing financial resources allocation.

Keeping with this, a study proposing a seismic insurance model is presented in this Chapter. The model has been built for the Italian building stock, accounting for the site specific hazard and discretizing the Italian peninsula in its 8,088 municipalities and the building portfolio in 5 structural typologies. It is based on a probability-based methodology for loss estimation, enabling to obtain the annual expected loss and the annual insurance premium for homeowners in each municipality. High variations are observed in the insurance premiums across the Italian municipalities, that can be understood as the result of the variations in the seismic risk across the Italian territory. As a result, a significant difference between the insurance premium calculated for various structural typologies was observed for each municipality. As expected, the assessed insurance premium values are maximum in highly seismic prone areas, whereas they are minimum in areas with relatively low seismic risk.

Losses for the seismic- and gravity-load designed structures are also compared, resulting in the expected loss and insurance premium per square meter for the formers being about 1.4 times that of the latters. Discussion about this difference highlight the chance to interpret this difference in terms of the reduction of expected loss, due to seismic retrofit operations, and, as a consequence, of the insurance premium to be paid.

A probability-based methodology is proposed in *Chapter 3* to derive relationships enabling to predict expected economic losses based on the expected magnitude of seismic events. To develop such relationships, information about previous seismic events in Italy are collected from the national catalogue of historical earthquakes, from INGV. These are data, being integrated with those regarding the number of inhabitants living

today in residential buildings, from ISTAT. Hence, actual exposure is assumed, to assess actual losses potentially suffered by Italian regions, whenever an earthquake with the same intensity of a past one would occur.

Spatial correlation in the residuals of the ground motion prediction equation (Bindi et al. 2009) has been also accounted for. Particularly relationships are derived in two limit case analysis: the former considering full uncorrelation between the PGA values derived from the attenuation law, and the latter assuming for partial correlation. In this last case, inter-event correlation is considered between the attained PGA values.

The main goal of the proposed methodology is underlined, aiming at supporting insurers and reinsurers in pricing and forecasting insolvency risk. Moreover, the chance to optimize communication between stakeholders being involved in disaster management and recovery processes is also highlighted. The thesis highlight the capability of such a methodology to effectively enhance resilience, at the global scale, being usually financial instruments shared on a national extent.

Results are presented as the loss curves against the event magnitude, in terms of the 50th, 16th and 84th percentile for the two limit cases. Furthermore, results are also processed, after being discretised into bin before performing the regression analysis. The resulting relationships are however similar to those obtained when data are processed for each single magnitude level.

The main remark regards the observed standard deviation, being higher in the case where inter-event correlation is assumed in comparison with the case of full uncorrelation assumption, as expected. Consequently, higher confidence intervals are observed around the median, being even higher for high magnitude values, where a lesser number of data on seismic events were available.

Despite results highlighted for all the curves, an exception is outlined for the curve fitted to the mean, which is insensitive to the spatial correlation assumptions.

Finally, relationships derived from regression on single magnitude values and fitted to the median, in the case of the inter-event correlation assumption, are observed to be the less conservative. Hence, they can enable insurers and reinsurers to perform prompt and more realistic evaluation. Moreover, the ease for potential integration in current risk assessment processes is also outlined. It also enables for risk managers to have available a loss estimation model, that accounts for spatial distribution of buildings, in addition providing a disaggregated representation of risks to manage.

Chapter 4 presents a methodological framework for resilience quantification, which gather all multidisciplinary aspects being embedded in the concept of disaster resilience. The framework is composed of 3 steps: the modelling of urban networks as hybrid social-physical one and the evaluation of complex networks metrics; the assessment of quality of life and city performance indicators to evaluate life quality and sustainability; the definition of particular functions linking network metrics and social and economic indicators.

A particular focus is done on the local level in this Chapter. This is due to the chance to easily recognise responsibilities and control actions of diverse stakeholders, being involved in recovery processes.

Moreover, according to the modern multi-scale approaches, starting from the single city's component, to model the whole urban network and then establishing interrelations and similarities between diverse cities can be very beneficial. In this way, in fact, a wider national overview is guaranteed, allowing for the identification of best strategies in the after-event. According to diverse urban configuration and features, strategies affording the best resilience level, thence also sustainability, can be recognized and eventually replayed.

The primary goal of the presented methodology is, in fact, to put the basis to build up an effective tool for supporting institutions and officers. Mitigation and adaptation strategies can be, with this tool simulated to assess their potential resilience. Paralleling this, data on strategies, that have already been implemented, can be collected and archived according to criteria, which consider local environments' peculiarities. Hence, whenever a similar event occurs, according to past experiences, the best strategy can be easily selected, already knowing what to do and how many resources to employ.

The last two Chapters, **Chapter 5** and **Chapter 6**, present an engineering framework for resilience quantification of urban areas, which merges civil engineering and complex networks theory basis.

In this thesis, it is in fact stressed the fact that contemporary cities emerge as complex systems, being constituted by physical and social components, mutually interrelated and interacting. Whether an external stress hits a city system, and in particular herein natural hazards are considered, it mainly threatens the physical components and the service they are appointed to supply to citizens, consequently causing injuries on the social components too. This is a cascading effects, which directly affects the citizens life quality, as their satisfaction degree towards to the efficiency of urban facilities and services. Basically, **Chapter 5** and **Chapter 6** propose the same methodology, when dealing with the urban environments' modelling and with the theoretical basis of the proposed framework, also highlighted in Chapters 1 and 4, aiming at quantifying resilience with a human-centric approach. On the other hand, **Chapter 5** proposes a methodology to quantify urban resilience of cities' HSPN, according to their size and shape, by performing seismic scenarios and considering vulnerability according to a fully random procedure. A particular focus is put on earthquakes and on the effect their occurrence can have on contemporary complex city systems, according to the topology and size.

Two alternative resilience metrics are proposed, which respectively account for the dependence on the initial state of damage suffered by the HSPN and for the independence on it. A real case study is also presented, assessing resilience to seismic events for the inner city of Naples (Italy), i.e. the Quartieri Spagnoli area.

In *Chapter 6* the same HSPNs' modelling technique is presented, but conversely the vulnerability of the physical subsystem is accounted through the use of probability-based relationships. Fragility curves from the literature are used to compute the damage probability of masonry and reinforced concrete buildings. The proposed resilience metrics are in number of four, considering damage-dependence, damage-independence both normalized and not normalized with respect to the pre-event efficiency, and finally the dependence on the number of relocated citizens in each recovery stage, with respect to the maximum number of citizens to be relocated. The study focus on resilience quantification according to the event typology. Indeed, two diverse events' type are analyzed: earthquakes and flow-type landslides, to validate the robustness and the applicability of the proposed metrics.

Experimental results show a major downfall of the HSPN efficiency in the aftermath of the seismic event, which is gradually recovered towards the simulated strategy. Obviously the more intense is the earthquake the many more buildings are damaged, and many more citizens are deallocated too.

When studying results from *Chapter 5*, major damages are observed for the real case study of the Quartieri Spagnoli area, in comparison with those of the synthetic HSPNs, due to the particular street patterns configuration. Indeed, ideal streets are designed for the artificial HSPNs, whose width and spatial distribution is almost regular and homogenous on the territory. In the real case study, being the studied HSPN modelled according to the inner city Naples features, it presents narrow streets and buildings, which are very close one to each other, as typically observed in Italian historical centres.

Furthermore, comparison are performed between HSPNs' shapes and sizes, with regards to damage-dependent and damage-independent resilience metrics.

Based also on the observed systemic damage and efficiency in the pre- and post-event, for the studied HSPN's configuration, the two resilience metrics result to be collaterals. In view if this, damage-independent resilience is a useful metric, that enables us to compare urban environments with sound different features. On the other hand, damage-dependent resilience enables us to assess a city's capability to recover from a disaster, accounting for its initial state of damage, hence also on the resources needed to recover to the pre-event equilibrium condition.

Similar results are also presented in *Chapter 6*, whose real case study is referred to the city of Sarno (Campania Region, Italy). Results herein show the seismic resilience being lower than the landslide one, primarily due to the nature of the simulated events. It is worth notice that earthquakes and landslides mainly differ due to their area of impact, being wider in the former case and affecting discrete areas in the latter.

Experimental results in this Chapter, confirm and further outline the comparability and also the complementarity between the proposed resilience metrics. Particularly, similar meanings are outlined for damage-dependent resilience, as evaluated in Chapter 5, and damage-dependent resilience R_2 , R_3 and R_4 , as evaluated in Chapter 6. Also the damage-independent resilience formula proposed in Chapter 5 results to be analogous to the one proposed in Chapter 6, R_1 .

In conclusion, resilience metrics presented in Chapter 5 are recommended as the most efficient to be used, due to their higher computational simplicity and to their 360 degrees meaning. Damage-dependent and damage-independent resilience metrics are mutually exhaustive, dealing with a humanitarian view of city complex systems, and also accounting for their structural performance and robustness from a strictly engineering perspective.

Resilience is understood in this thesis as the ideal point meeting engineering and ecosystems theories' concepts. Resilience is here interpreted as the response to many of actual issues distressing contemporary worldwide communities.

The proposed studies approach to resilience from diverse perspectives and with different methodologies. Both global and local approaches are presented, being diversely addressed respectively to national social-economic issues or urban quality of life goals.

Seismic insurance model and loss predictive relationships, based on the event magnitude, are methodologies proposed for resilience improvement. These are studied for the optimization of mitigation actions, as they can be effective instruments to be easily replicated at the national scale. Furthermore they can also be integrated within current risk managers and traditional loss assessment procedures.

The presented framework for resilience quantification, indeed, has got the potential to be used as a support for mitigation and adaptation actions, and planning policies assessment at the urban scale. It allows for accounting local peculiarities and define tailored recovery strategies. As a result, urban management choices can be driven by engineering-based evaluations, which can contextually improve resilience and preparedness.

Finally, the need for further experimentations is outlined. Also real case studies data need to be collected to refine the proposed approaches and to ensure for their reliability. Insurance models and loss forecasting curves can be further improved with data from empirical evidence and expert judgements. Also a more effective means for financial resilience improvement should be developed, based on the Cat Bond model, which is currently the most widely used, together with reinsurance.

Several diverse recovery strategies need to be simulated to validate the methodology for resilience quantification and to prove its effectiveness, due to the particularly tricky field, which its application is demanded to.

Paralleling this, also the focus on the trend of resilience indicators with the urban environments' scale need to be deepen, due to the always increasing urbanization phenomena.

Appendix 2.A: seismic fragility curves for reinforced concrete buildings from the literature

Table 2.A.1 illustrates parameters of the fragility curves selected from the literature, to compute seismic vulnerability, hence risk, to each Italian municipality, with reference to reinforced concrete (RC) and RC-masonry combined structures.

Table 2.A.1 Parameters of fragility curves from the 12 literature studies, used to implement the loss assessment methodology, described in Chapter 2

Structural typology	Authors	Number of limit states	Lognormal distribution mean value μ		Lognormal distribution standard deviation value σ	
RC structures	Kappos et al. 2006	4	-1.78	-1.32	1.14	0.29
			-1.12	-0.95	0.80	0.27
			-0.70	-0.57	0.63	0.27
			-0.59	-0.24	0.57	0.28
	Spence et al. 2007	4	-1.01	-0.87	0.32	0.29
			-0.55	-0.46	0.32	0.28
			-0.28	-0.02	0.31	0.29
			-0.09	0.15	0.32	0.27
	Crowley et al. 2008	2	-0.77	-0.80	0.24	0.18
			-0.62	-0.61	0.26	0.22
	Ahmad et al. 2011	3	-1.07	-1.07	0.22	0.22
			-0.91	-0.91	0.29	0.29
			-0.59	-0.44	0.26	0.26
	Borzi et al. 2007	2	-0.74	-0.56	0.32	0.32
			-0.46	-0.37	0.34	0.33
	Borzi et al. 2008	2	-0.68	-0.41	0.45	0.35
			-0.41	-0.31	0.36	0.35
	Kostov et al. 2004	3	-0.48	-0.44	0.47	0.48
			-0.34	-0.28	0.48	0.49
			-0.29	-0.19	0.48	0.49
Kwon and Elnashai 2006	2	-1.08	n.a.	0.22	n.a.	
		-0.73	n.a.	0.22	n.a.	
Ozmen et al.	2	-0.37	-0.36	0.35	0.30	

	2010		-0.17	-0.12	0.23	0.15
			-1.57	-1.14	0.44	0.43
	Kappos et al.	4	-0.92	-0.57	0.44	0.43
	2003		-0.67	-0.18	0.44	0.43
			-0.51	0.10	0.44	0.43
	Tsionis et al.		-0.67	-0.64	0.27	0.28
	2011		-0.22	0.18	0.38	0.79
combined			-0.62	-0.52	0.50	0.49
RC-	Kostov et al.		-0.44	-0.34	0.49	0.49
masonry	2004					
structures			-0.35	-0.24	0.49	0.49

The first and the second row refer to gravity load and seismic load designed structures, respectively.

Table 2.A.2, following illustrates details about the methodologies, that have been used to derive vulnerability curves presented in each of the selected literature studies, regarding RC civil structures and mixed ones, i.e. combined RC-masonry structures.

Particularly, investigated building's typologies and structural details are highlighted. Approaches used to derive the seismic demand, which such buildings are subjected to, according to their geographical location, and their structural response, according to the structural modeling and analysis being performed, are also shown.

Table 2.A.2 Methodologies used for the development of fragility curves selected from the literature for RC buildings

CHARACTERISTICS OF THE VULNERABILITY STUDIES FROM THE LITERATURE USED FOR RC BUILDINGS' LOSS COMPUTATION								
N	Study	Structural Typology	BUILDINGS CLASSIFICATION	CAPACITY	DEMAND	N° samples	Results	Geographical Reference
1	<p>A hybrid method for the vulnerability assessment of R/C and URM buildings A.J. Kappos G.Panagopoulos C.Panagiotopoulos G.Penelis</p>	Mid-rise RC buildings (typical south-European structures)	<p>Height: Medium (<5 storeys) High (6:10 storeys) Structural System: Infilled frames Double-infilled frames Design level: Low code (pre '80 for southern Europe, pre '59 for Greece) High code (≈EC8)</p>	Hybrid methodology: combination of statistical data (damage matrixes) observed on buildings subjected to the Thessaloniki earthquake (ATC1985) and static and dynamic analysis results, nonlinear	Seismic events databases	72 buildings, 36 of which 2D analyzed	<p>Statistics of the fragility curve in terms of PGA for high-rise, low code buildings</p> <p>Statistics of the fragility curve in terms of S_d for high-rise, high code buildings</p> <p>Fragility curve in terms of PGA for mid-rise (infilled and</p>	GREECE (Thessaloniki, Aegion)

				<p>for RC or nonlinear static for masonry.</p> <p>Level 1: intensity measures (I o PGA)</p> <p>Level 2: from capacity spectrum to the fragility curve derivation in terms of the spectral displacement, S_d.</p>			<p>double-infilled frames), low and high code (for each damage state- D0:D5)</p> <p>Fragility curve in terms of S_d for mid-rise buildings (infilled only) low and high code (for each damage state- DS0:DS5)</p>	
		<p>Unreinforced masonry (2 storeys) (typical south-European structures)</p>	<p>Structural System: Brick Stone (pre anni'40=historical data)</p>		<p>Database: 5740 (Thessaloniki)+2014 (Aegion)</p>		<p>Curve in EMS'98 for brick masonry 2-storey buildings (for each damage state-</p>	

							DS1:DS4) Fragility curve in terms of S_d for 2-storey brick masonry buildings (for each damage state-DS1:DS4) Fragility curve in terms of S_d for 2-storey stone masonry buildings (for each damage state-DS1:DS4)	
2	LESS LOSS, Progetto SP10 SP10 European Project LESSLOSS Report 2007/07	RC (from RISK-UE surveys) Masonry (from RISK-UE)	Year of Construction (pre seismic code, post seismic code)	Observed data in terms of EMS intensity, discrete	Groundmotion on deterministic scenarios (INGV – Lisbon,	Istanbul: (n°562613 RC, n°173639 masonry, n°1401 RC and precasted mixed)	Fragility curve in terms of PGA for double-infilled	INSTANBUL, THESSALONIK I, LISBON

	Reviewer: Mustafa Erdik	surveys)	<p>N° storeys (low-, mid- and high-rise buildings)</p> <p>Structural Typology (infilled, double-infilled and bare frames, pilotis, mixed, brick and stone masonry, precasted)</p>	<p>data, though damage matrixes (D0:D5). Furthermore, nonlinear static analysis has been performed with the HAZUS methodology, based on the expected performance assessment through a quasi-static “performance-based” procedure. Here the damage state has been defined in terms of the</p>	<p>Istanbul and Thessaloniki) combined with probabilistic scenarios from PSHA. Here, starting from a discrete set of expected accelerograms on bedrock, through the simulation technique DSM from INGV, and through the implementation of diverse attenuation laws, the fault-site mechanics has been simulated, and, for each site, the</p>	<p>Thessaloniki: (n°5032) Lisbona: (n°103069 masonry, n°374101 RC)</p>	<p>frames (for 5 damage levels, D0:D5);</p> <p>Fragility curve in terms of S_d (Istanbul) for low-rise RC buildings, post seismic code, for 5 damage levels (D0:D5);</p> <p>Fragility curve in terms of PGA (Thessaloniki) for double-infilled RC frame buildings, mid-rise, pre- and post-seismic code.</p>	
--	----------------------------	----------	----------------------------------------------------------------------------------------------------------------------------------------------------------------------------------------------	----------------------------------------------------------------------------------------------------------------------------------------------------------------------------------------------------------------------------------------------------------------------------------------------	----------------------------------------------------------------------------------------------------------------------------------------------------------------------------------------------------------------------------------------------------------------------------------------------------------------------------------------------	----------------------------------------------------------------------------	---------------------------------------------------------------------------------------------------------------------------------------------------------------------------------------------------------------------------------------------------------------------------------------------------------------------------	--

				Interstorey Drift ratio. An elastic damped response spectrum has been then developed, which takes into account of site effects and of the structural hysteretic behaviour to combine it with the capacity curve, to finally obtain the “performance point”.	expected surface shaking has been obtained by using specific stratigraphic profiles.			
3	Comparison of Two Mechanics-Based Methods for Simplified Structural Analysis in	4-storeys RC buildings	N° storeys: 2 8	Comparison between FEM push-over, SP-BELA and D-BELA	Static and dynamic load condition, by accounting	Montecarlo methodology for buildings population generation, where material	Fragility in terms of PGA, for each damage state (slight, severe,	ITALY

	Vulnerability Assessment H. Crowley B. Borzi R. Pinho M. Colombi M. Onida			methodologies	material and geometrical non-linearity	properties are assumed as random variable, while geometrical features are not	collapse)	
4	Analytical Fragility Functions for reinforced concrete and masonry buildings and buildings aggregates of euro-mediterranean regions-UPAV methodology N. Ahmad H. Crowley R. Pinho	RC frames	Height: Low Medium High Tipology: Regular Irregular Ductility: ductile non ductile	Nonlinear SDOF dynamic analysis and capacity models development	10 real western Europe bedrock accelerograms set	400 samples for each structural class, design to simulate typical existing built environment of Mediterranean Europe	Fragility in terms of S_d Fragility in terms of PGA for low-, mid- and high-rise buildings, ductile and non-ductile, regular and irregular Tables of statistics of fragility curves (σ and μ)	MEDITERRANEAN EUROPE (GREECE, ITALY, TURKEY)
5	SP-BELA: un metodo meccanico per la definizione della	RC frames	N° storeys: 2 4 8 Tipology:	SP-BELA	Real western Europe bedrock accelerograms set	Montecarlo methodology sample generation	Fragility in terms of PGA (n°15) for 3 damage state	ITALY

	vulnerabilità basato su analisi pushover semplificate B. Borzi R. Pinho H. Crowley		seismic non-seismic Seismic action % mass: 5 7.5 10 12				(LS1:LS3) Tables of statistics of fragility curves (σ and μ)	
6	The influence of infill panels on vulnerability curves for RC buildings B. Borzi R. Pinho H. Crowley	4-storeys RC frames	Infilling: Infilled Non-infilled Regulation: seismic non-seismic Tipology: frames infilled frames pilotis	SP-BELA	Real bedrock accelerograms set from western Europe	Montecarlo-based generation of samples	Fragility in terms of PGA for 3 damage states (LS1:LS3) Tables of statistics of fragility curves (σ and μ)	ITALY
7	RISK-UE WP13, application to Sofia M. Kostov E. Vaseva A. Kaneva N. Koleva G. Varbanov D. Stefanov	RC frames (Bulgaria)	Mixed buildings 1:5 storeys: Pre '45 Post '45 Big panels buildings 5:9 storeys: 1964:1987 Post '87	Technical opinion	Real record from Bulgaria earthquake in 1858	Existing buildings' models (in diverse historical period in Sofia)	Fragility ($n^{\circ}8$) in terms of PGA for 4 damage states (slight:collapse) Tables of	BULGARIA (Sofia)

	E. Darvarova D. Solakov S. Simeonova L. Cristoskov	Masonry	Flexible floor 1:4 storeys (wood and steel): Pre 1919 Post 1919 RC floor 1:5 storeys: 1920:1945 Post '45				statistics of fragility curves (σ and μ)	
8	The effect of material and ground motion uncertainty on vulnerability curves of RC structures O.S. Kwon A. Elnashai	3-storeys mid-rise, non- seismic, RC buildings	% reinforcement: low medium high	Push-over	3 real accelerogra m sets and 6 synthetic accelerogra ms set		Fragility in terms of PGA for 4 damage states (service, damage control, prevention, collapse) Tables of statistics of fragility curves (σ and μ)	USA AND NORTH- CENTRAL EUROPE
9	Vulnerability of low and mid- rise R.C. buildings in Turkey	RC buildings	Height: 2 storeys (16 MPa concrete) 4 storeys (16 MPa and 25 MPa	Nonlinear dynamic analysis	292 Real earthquakes record with diverse intensity	48 3D buildings, modeled according to the existing ones	Fragility in PGA ($n^{\circ}4$) per i 3 stati di danno (immediate	TURKEY

	H.B. Ozmen M. Inel E. Meral M. Bucakli		concrete) 7 storeys (16 MPa concrete)		levels		occupancy-life safety-collapse prevention) Tables of statistics of fragility curves (σ and μ)	
10	RISK-UE WP4-R.C. buildings (level 1 and level 2 analysis) A.J. Kappos G.Panagopoulos C.Panagiotopoulos G.Papadopoulos	RC buildings	Height: low (1-3 storeys) medium (4-7 storeys) high (>8 storeys) Regulation: no code low code medium code high code Structural Typology: frame infilled frame -regular -irregular mixed -bare -with RC walls -regularly infilled	Hybrid approach (statistical data combined with analysis' results)	16 accelerograms set, in addition real Thessaloniki's earthquake record has been used	Greek buildings damaged from the Thessaloniki's earthquake, and a high number of building's models	Fragility in terms of PGA ($n=26$) for 6 damage states (DS0:DS5) Tables of statistics of fragility curves (σ and μ)	GREECE

1 1	<p>Analytical fragility functions for R.C. buildings and buildings aggregates of euro-mediterranean regions - UPAT methodology G. Tsionis A. Papailia M.N. Fardis</p>	Civil RC buildings	<p>Typology: Frame -infilled -bare -ductile -non ductile With walls Mixed, non ductile</p> <p>Regulation: Old code Low code Medium code High code</p> <p>Height: High Medium Low</p>	Nonlinear dynamic analysis		Regular buildings' prototypes generation (43 typologies)	<p>Fragility in terms of PGA (n°43) for 2 damage states (yielding, collapse)</p> <p>Tables of statistics of fragility curves (σ and μ)</p>	MEDITERRANEAN BASIN
<p><i>Most of the selected studies come from the SYNER-G Project.</i></p>								

Appendix 2.B: seismic fragility curves for masonry buildings from the literature

Table 2.B.1 illustrates parameters of the fragility curves selected from the literature, to compute seismic vulnerability, hence risk, to each Italian municipality, with reference to masonry structures.

Table 2.B.1 Parameters of fragility curves from the 5 literature studies, used to implement the loss assessment methodology, described in Chapter 2

Structural typology	Authors	Number of limit states	Lognormal distribution mean value	Lognormal distribution standard deviation value
			μ	σ
Masonry structures	Rota et al. 2008	3	-2.03	0.36
			-1.65	0.27
			-1.35	0.22
	Ahmad et al. 2011	4	-1.13	0.35
			-1.03	0.35
			-0.85	0.26
			-0.77	0.23
	Erberik 2008	2	-0.47	0.35
			-0.33	0.35
	Lagomarsino and Giovinazzi 2006	3	-1.00	0.41
			-0.75	0.34
			-0.61	0.37
Rota et al. 2010	3	-0.85	0.24	
		-0.70	0.18	
		-0.58	0.14	

Table 2.B.2, following illustrates details about the methodologies, that have been used to derive vulnerability curves presented in each of the selected literature studies.

Table 2.B.2 Methodologies used for the development of fragility curves selected from the literature for masonry buildings

CHARACTERISTICS OF THE VULNERABILITY STUDIES FROM THE LITERATURE USED FOR MASONRY BUILDINGS' LOSS COMPUTATION								
N	Study	Structural Typology	BUILDINGS CLASSIFICATION	CAPACITY	DEMAND	N° samples	Results	Geographical Reference
1	<p>A methodology for deriving analytical fragility curves for masonry buildings based on stochastic nonlinear analyses M. Rota A. Penna C.L. Strobbia</p>	<p>RC (classification is made based on RISK-UE).</p> <p>Masonry</p>	<p>Regulatory Framework: Seismically designed (pre '75) Seismically designed (post '75) N° storeys: 1-3 >4</p> <p>Horizontal structure: Rigid floor Flexible floor N° storeys: 1-2 >3 Layout: regular irregular Seismic detail: without tie-rod (post 1909) with tie-rod (pre</p>	<p>Post-earthquake surveys on the major seismic events in last 30 years, empirical damage probability matrixes have been developed for investigated buildings (23 classes). Hence, the probability of exceedance of each limit state has</p>	<p>Attenuation law from Sabetta and Pugliese (Sabetta and Pugliese 1996) from the Italian database of historical seismic events across last 30 years (Irpinia '80, Est-Sicilia '90, Umbria-Marche '97, Umbria '98, Pollino '98, Molise 2002). With this a PGA value has</p>	<p>91374 investigated buildings (about 7000 units each class)</p>	<p>Fragility Curves in terms of PGA for masonry buildings with 1-2 storeys, flexible floor, without tie-rods and both regular and irregular layout (weighted and non-weighted); μ and σ parameters, for each structural class and damage level (European Macroseismic Scale=DS1:DS5);</p>	ITALY

			1909)	been evaluated, for each PGA interval (10 classes), according to the experimentally observed frequencies, the damage levels have been ordered from the higher to the lower.	been determined for each municipality. Furthermore a random error has been generated to account for the PGA values' variability within the attenuation law (several error values have been applied, and no substantial variations have been observed to the log-normal curve).		Fragility Curves in terms of PGA for mixed buildings, 1-2 storeys; RC buildings, 1-3 storeys, Seismically and non-seismically designed; non-regular masonry, 1-2 storeys with flexible floor, with and without tie-rods; regular masonry, 1-2 storeys, rigid floor, with and without tie-rods.	
		Steel						
		Mixed	N° storeys: 1-2 >3					
2	Analytical fragility functions for	Masonry	Height: Mid-rise (2 storeys)	SDOF push over defined through	10 natural accelerograms from US	Building prototypes, designed to	Fragility Curves in terms of PGA and	MEDITERRANEAN REGIONS

	<p>R.C. and masonry buildings and buildings aggregates of euro-mediterranean regions - UPAV methodology N. Ahmad H. Crowley R. Pinho</p>		<p>Low-rise storeys) Material Typology: High voids % Low voids % Blocks of stone</p>	(4 nonlinear dynamic analysis	<p>seismic databases and IBC-2006 bedrock spectrum</p>	<p>simulate typical built environment in Mediterranean areas (mostly Italy and Slovene)</p>	<p>spectral displacement ($n^{\circ}10$), for 5 damage states (none:complete) Parameters (μ and σ)</p>	
3	<p>Generation of fragility curves for Turkish masonry buildings considering in-plane failure modes M.A. Erberik</p>	Masonry	<p>Tipologia: Rural Urban N° storeys: 1:5 Building Technique: Engineering Non- Engineering</p>	<p>Nonlinear Static and Dynamic Analysis</p>	<p>50 bedrock accelerometric records with PGA varying between 0.01 and 0.8 g</p>	<p>Existing buildings gathered in 120 sub-categories from Dinar databases, Turkey (post-earthquake '95), Zeytinburnu, Turkey (examined during the seismic project in</p>	<p>Fragility Curves in terms of PGA ($n^{\circ}13$), for 2 limit states (moderate-collapse), each of which account for all 5 storeys, based on the in-plane response Parameters (μ and σ)</p>	TURKEY

						Instanbul)		
4	<p>Macroseismic and mechanical models for the vulnerability and damage assessment of current buildings</p> <p>S. Lagomarsino S. Giovinazzi</p>	Non-reinforced Masonry	<p>Structural Typology: Brick Stone RC floor</p>	Empirical Methodology		Existing buildings	<p>Fragility Curves in terms of PGA ($n^{\circ}3$), for 5 limit states (slight:total)</p> <p>Parameters (μ and σ)</p>	ITALY
5	<p>A methodology for deriving analytical fragility curves for masonry buildings based on stochastic nonlinear analyses</p> <p>M. Rota A. Penna</p>	Stone Masonry	<p>Unique typology: 3 storeys</p>	Nonlinear Dynamic Analysis	Real accelerograms obtained from online databases	Unique building's prototype, being representative of 50s structural typologies in Benevento	<p>Fragility Curves in terms of PGA ($n^{\circ}3$), for 5 limit states (none:DS4)</p> <p>Parameters (μ and σ)</p>	ITALY

	G. Magenes							
--	------------	--	--	--	--	--	--	--

Appendix 5.A: graphs of the city models configuration before and soon after the earthquake occurrence

Some examples of the modelled urban HSPNs are presented in the present Appendix. Different city shapes can be observed, with different geographical extension, depending on the number of buildings and on the topology. HSPN configuration before the event and in the aftermath of it are illustrated, in case 15% or 30% collapsed buildings is assumed.

Table 5.A.1 Rectangular HSPN's configuration before and after the earthquake

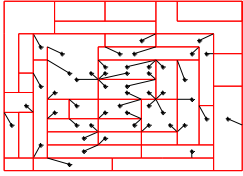
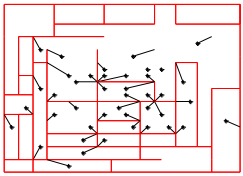
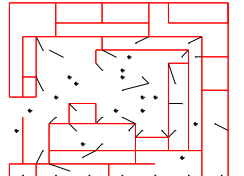
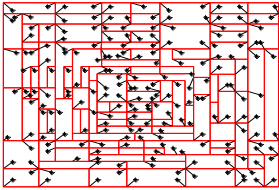
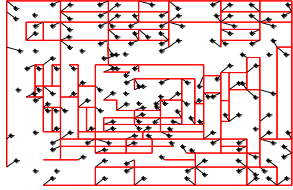
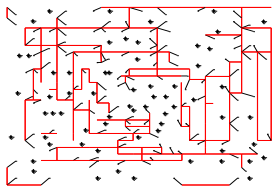
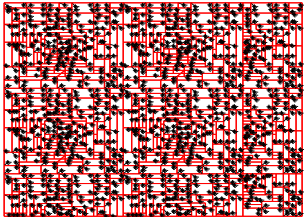
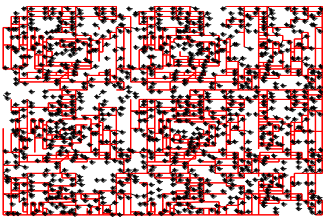
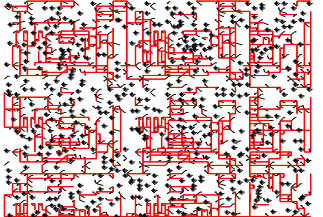
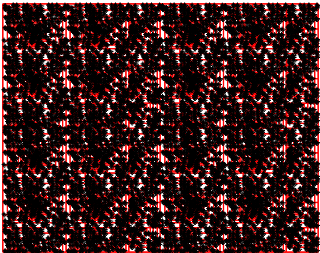
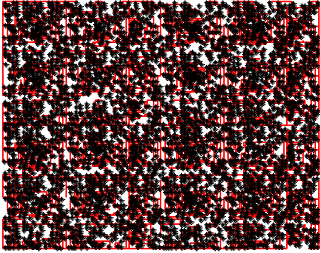
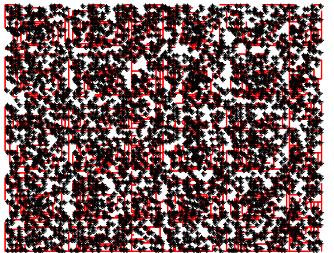
Citizen-Citizen efficiency case study		
Rectangular HSPN	15% collapsed buildings	30% collapsed buildings
50 residential buildings		
		
200 residential buildings		
		
1,250 residential buildings		
		
5,000 residential buildings		
		

Table 5.A.2 Examples of different HSPNs' shapes subjected to 30% buildings' damage

Examples of different HSPN shapes (50 e 1250 buildings)	30% collapsed buildings

Appendix 5.B: Analysis results in terms of the resilience histograms

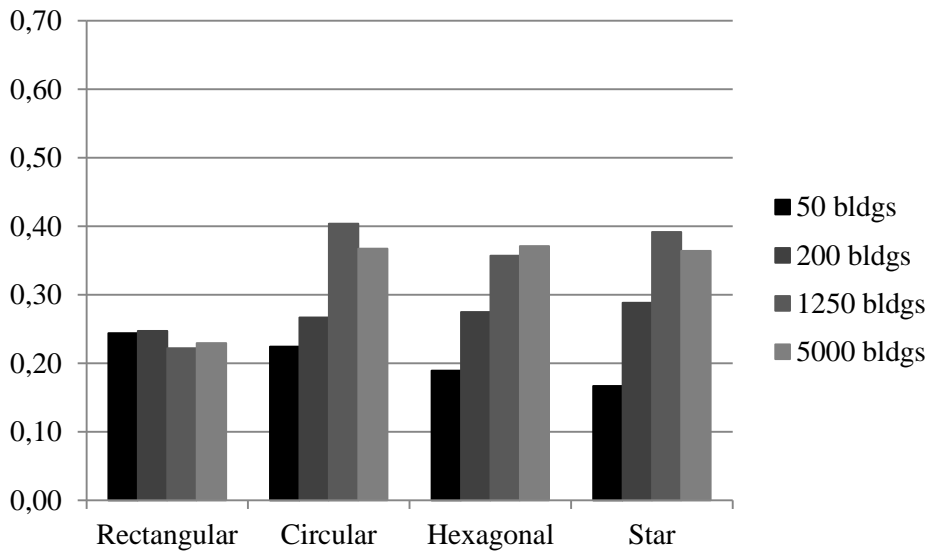


Figure 5.B.1 Damage-dependent resilience, R^D , in the citizen-citizen case analysis, when 15% collapsed buildings are assumed, as a function of the HSPN's shape and size

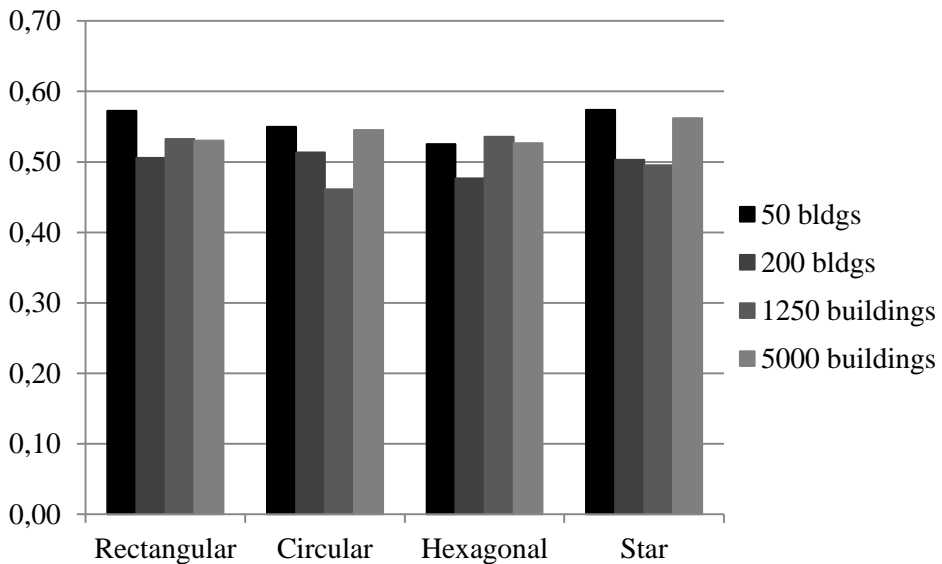


Figure 5.B.2 Damage-independent resilience, R^E , in the citizen-citizen case analysis, when 15% collapsed buildings are assumed, as a function of the HSPN's shape and size

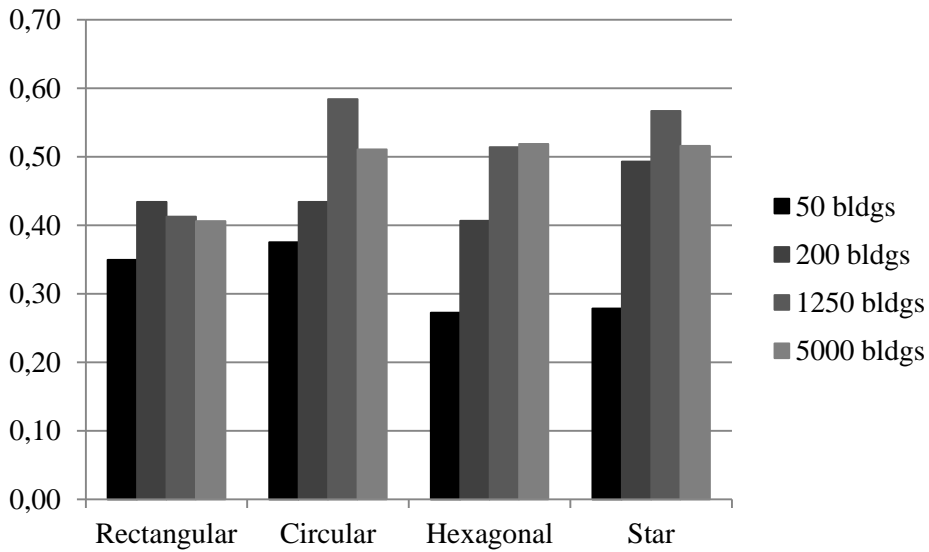


Figure 5.B.3 Damage-dependent resilience, R^D , in the citizen-citizen case analysis, when 30% collapsed buildings are assumed, as a function of the HSPN's shape and size

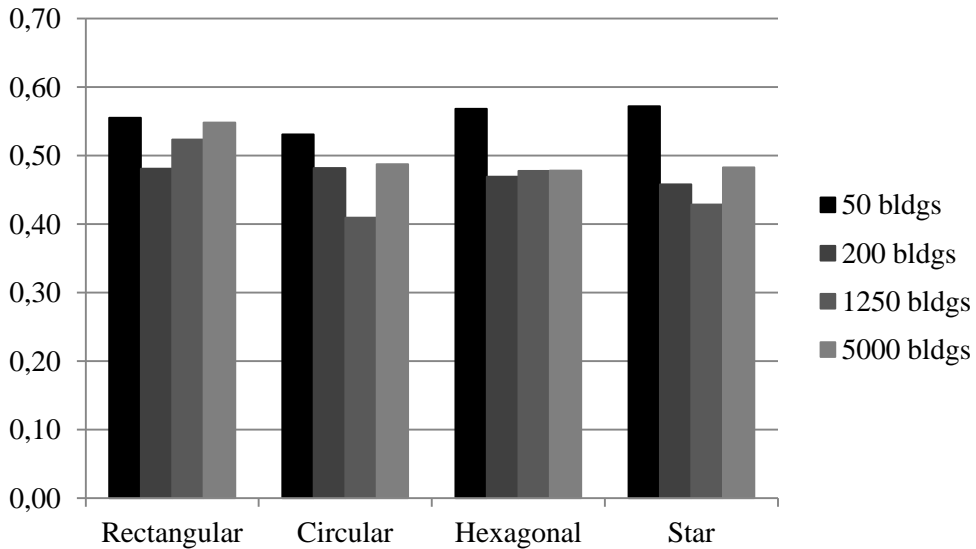


Figure 5.B.4 Damage-independent resilience, R^E , in the citizen-citizen case analysis, when 30% collapsed buildings are assumed, as a function of the HSPN's shape and size

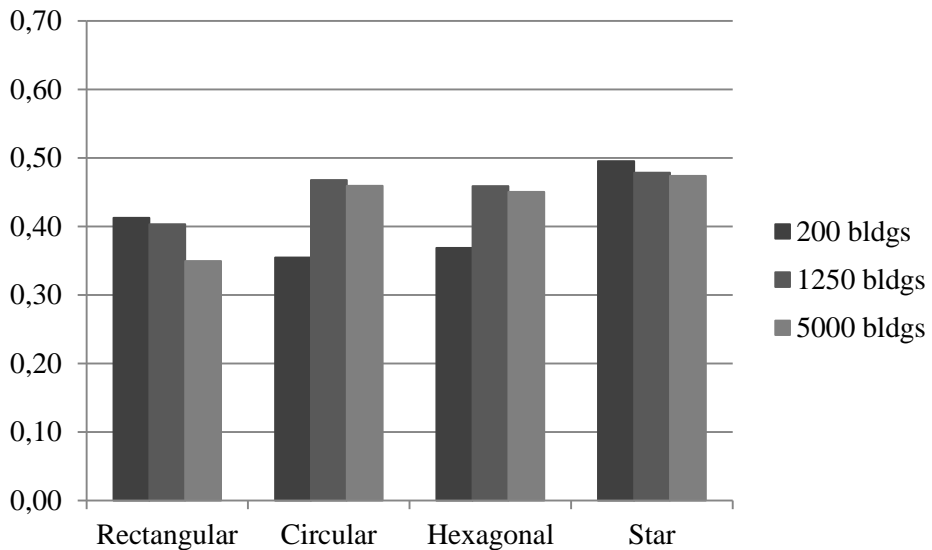


Figure 5.B.5 Damage-dependent resilience, R^D , in the citizen-school case analysis, when 15% collapsed buildings are assumed, as a function of the HSPN's shape and size

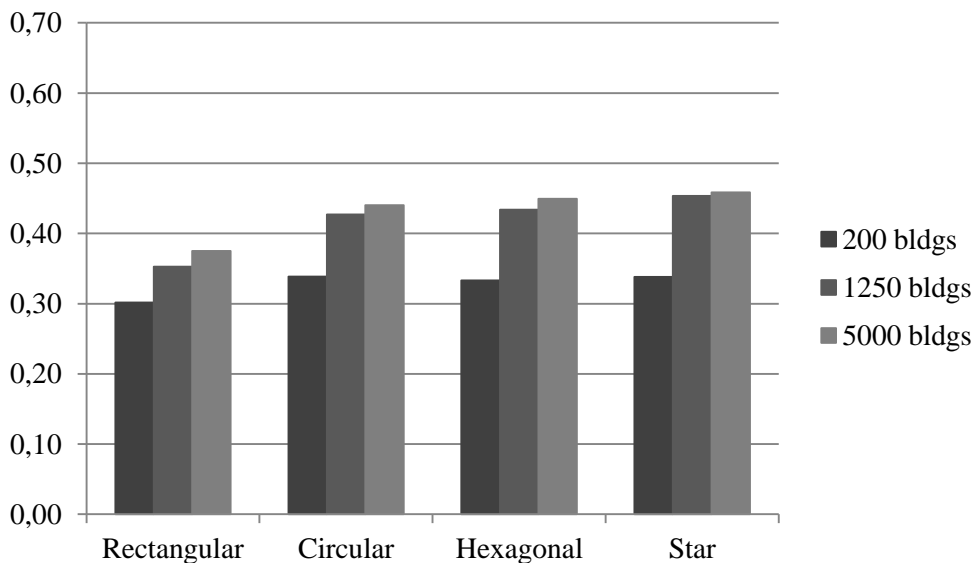


Figure 5.B.6 Damage-independent resilience, R^E , in the citizen-school case analysis, when 15% collapsed buildings are assumed, as a function of the HSPN's shape and size

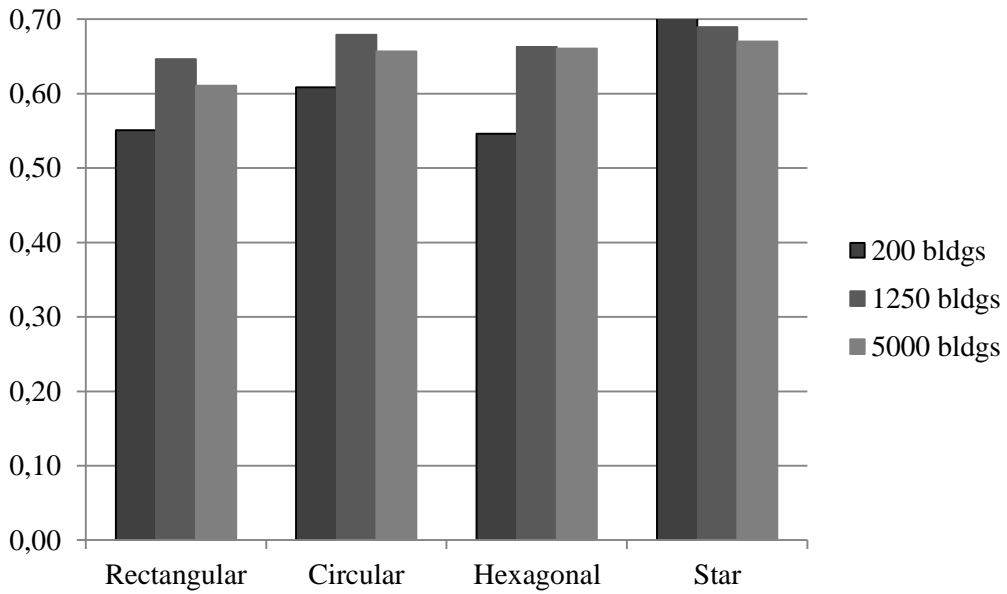


Figure 5.B.7 Damage-dependent resilience, R^D , in the citizen-school case analysis, when 30% collapsed buildings are assumed, as a function of the HSPN's shape and size

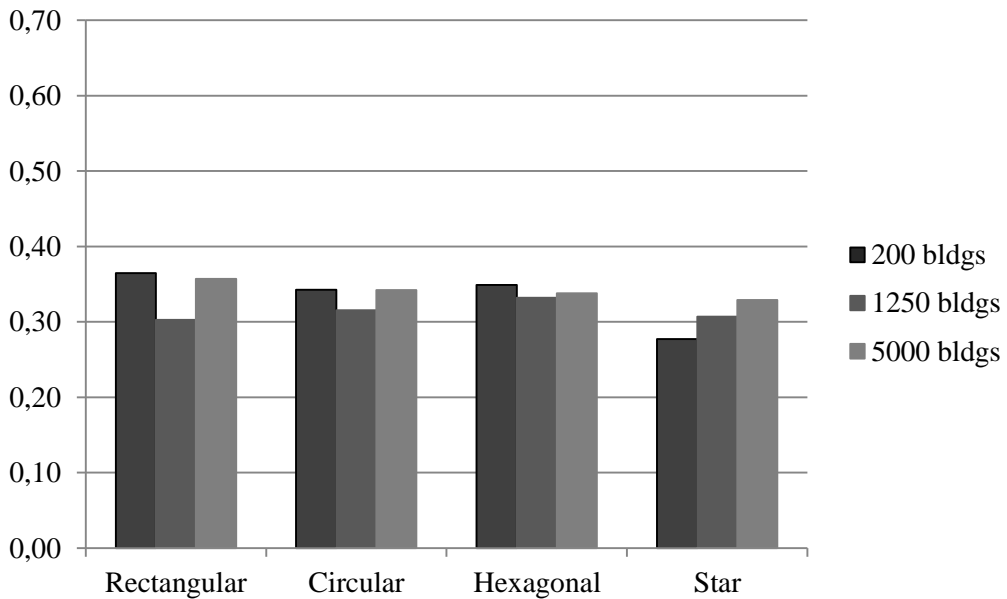


Figure 5.B.8 Damage-independent resilience, R^E , in the citizen-school case analysis, when 30% collapsed buildings are assumed, as a function of the HSPN's shape and size

REFERENCES

- 100 Resilient Cities (2015), <http://100resilientcities.rockefellerfoundation.org>.
- Adger WN. (2000) Social and ecological resilience: are they related? *Prog Hum Geogr* 24(3):347–364.
- Adger WN. (1997). Sustainability and social resilience in coastal resource use. CSERGE working paper series, Centre for Social and Economic Research on the Global Environment, University of East Anglia, Norwich and University College London, UK.
- Aguirre B. (2006). On the concept of resilience. Disaster Research Center, University of Delaware, Delaware.
- Ahmad N., H. Crowley, R. Pinho (2011). Analytical fragility functions for reinforced concrete and masonry buildings aggregates of euro-mediterranean regions – UPAV methodology. Internal report, Syner-G Project, 2009/2012.
- Alberti M. (1996). Measuring Urban Sustainability Environ Impact Assessment Rev, 16 (4–6), pp. 381–423.
- Allenby B, Fink J. (2005). Toward inherently secure and resilient societies. *Science* 2005;309(5737):1034–6.
- Amador, J.A., Olivar, G., Angulo F. (2013). Smooth and Filippov Models of Sustainable Development: Bifurcations and Numerical Computations, *Differ Equ Dyn Syst (Jan&Apr 2013)* 21(1&2):173–184.
- Amendola, A., Ermoliev, Y., Ermolieva, T. (2000). Earthquake Risk Management: A Case Study for an Italian Region, Proceedings of the Second EuroConference on Global Change and Catastrophe Risk Management: Earthquake Risks in Europe IIASA, Laxenburg, Austria, 6–9 July.
- Angel, S., Sheppard, S., Civco, D. L., Buckley, R., Chabaeva, A., Gitlin, L., ... & Perlin, M. (2005). The dynamics of global urban expansion (p. 205). Washington, DC: World Bank, Transport and Urban Development Department.
- Arcidiacono, V., Cimellaro, G. P., Reinhorn, A. M., & Bruneau, M. (2012). Community resilience evaluation including interdependencies. In 15th World Conference on Earthquake Engineering (15WCEE) (pp. 24-28).
- Arturi, A., Del Frate, F., Lategano, E., Schiavon, G., & Stramondo, S. (2003). The 1998 Sarno (Italy) landslide from SAR interferometry. In Proc. of FRINGE.
- Arup (2014) City Resilience Framework, The Rockefeller Foundation and Ove Arup & Partners International Limited, April, http://www.arup.com/~media/Publications/Files/Publications/C/City_Resilience_Framework_pdf.ashx
- Asprone, D., De Risi, R., & Manfredi, G. (2016). Defining structural robustness under seismic and simultaneous actions: an application to precast RC buildings. *Bulletin of Earthquake Engineering*, 14(2), 485-499.
- Asprone, D. & Manfredi G. (2015), Linking disaster resilience and urban sustainability: a global approach for future cities, *Disasters*, 39(s1), s96-s111.

- Asprone D, Jalayer F, Simonelli S, Acconcia A, Protà A, Manfredi G (2013). Seismic insurance model for the Italian residential building stock. *Structural Safety*, 44, pp 70-79.
- Asprone, D., Cavallaro, M., Latora, V., Manfredi, G. & Nicosia, V. (2013). Urban network resilience analysis in case of earthquakes, in *Proceedings of the 11th International Conference on Structural Safety and Reliability*, New York, USA.
- Atkinson, A. and F. Messy (2013). Promoting Financial Inclusion through Financial Education: OECD/INFE Evidence, Policies and Practice, OECD Working Papers on Finance, Insurance and Private Pensions, No. 34, OECD Publishing, Paris. DOI: <http://dx.doi.org/10.1787/5k3xz6m88smp-en>
- Attoh-Okine, N. O., Cooper, A. T., & Mensah, S. A. (2009). Formulation of resilience index of urban infrastructure using belief functions. *Systems Journal*, IEEE, 3(2), 147-153.
- Balas, C.E., Ergin, A., Williams, A.T., Koc, L. (2004). Marine litter prediction by artificial intelligence. *Mar. Poll. Bull.* 48, 449-457.
- Basile, A., Mele, G., & Terribile, F. (2003), Soil hydraulic behaviour of a selected benchmark soil involved in the landslide of Sarno 1998, *Geoderma*, 117(3), 331-346.
- Batty, M. (2009). Urban modeling. *International Encyclopedia of Human Geography*. Oxford, UK: Elsevier.
- Batty, M. (2008). The size, scale, and shape of cities. *science*, 319(5864), 769-771.
- Batty M, Longley PA (1994). *Fractal cities: a geometry of form and function*, Academic Press.
- Bauer, R.A. (1966). Ed., *Social Indicators*. Cambridge, Mass./London: The M.I.T. Press.
- Berche, B., Von Ferber, C., Holovatch, T., & Holovatch, Y. (2009). Resilience of public transport networks against attacks. *The European Physical Journal B*, 71(1), 125-137.
- Bettencourt LM (2013). The origins of scaling in cities. *science*, 340(6139), 1438-1441.
- Bettencourt LM, & West G (2010). A unified theory of urban living. *Nature*, 467(7318), 912-913.
- Bettencourt LM, & West GB (2011). Bigger cities do more with less. *Scientific American*, 305(3), 52-53.
- Bettencourt LM, Lobo J, Helbing D, Kühnert C, & West GB (2007). Growth, innovation, scaling, and the pace of life in cities. *Proceedings of the national academy of sciences*, 104(17), 7301-7306.
- Bindi, D, Luzi, L, Pacor, F, Sabetta, F, Massa M (2009). Towards a new reference ground motion prediction equation for Italy: update of the Sabetta-Pugliese (1996). *Bulletin of Earthquake Engineering* 9.6, 1899-1920.
- Bloomberg New Energy Finance (BNEF) (2015). *FiRe, Finance for Resilience, the FiRe rulebook*. <http://www.financeforresilience.com/wp-content/uploads/2015/11/The-FiRe-Rulebook.pdf>
- Bloomberg, M. R. (2013). *A Stronger, more Resilient New York*. The City of New York Special Initiative for Rebuilding and Resilience <http://www.nyc.gov/html/sirr/html/report/report.shtml>. Retrieved on 02/13/2015.
- Bocchini, P., & Frangopol, D. M. (2011). Resilience-driven disaster management of civil infrastructure. 5th Thematic Conference on Computational methods in structural dynamics and earthquake engineering, COMPDYN 2011.

- Borri, D., Concilio, G., Conte, E. (1998). A fuzzy approach for modelling knowledge in environmental systems evaluation. *Comput. Environ. Urban* 22, 299–313.
- Borzi B, Crowley H, Pinho R (2008). The influence of infill panels on vulnerability curves for RC buildings. *Proceeding 14th World Conference on Earthquake Engineering*, Beijing, China.
- Borzi, B, Crowley, H, Pinho, R (2007). SP-BELA: Un metodo meccanico per la definizione della vulnerabilità basato su analisi pushover semplificate. *Proceedings of XII Convegno L'Ingegneria Sismica in Italia ANIDIS 2007*, Pisa, paper no 160 (in Italian).
- Botkin, D. B., & Beveridge, C. E. (1997). Cities as environments. *Urban ecosystems*, 1(1), 3-19.
- Bozza, A., Asprone, D., & Manfredi, G. (2015). Developing an integrated framework to quantify resilience of urban systems against disasters. *Natural Hazards*, 78(3), 1729-1748.
- Bozza, A., Asprone, D., Fiasconaro, A., Latora V. & Manfredi G. (2015), Catastrophe resilience related to urban networks shape: preliminary analysis, in *COMPDYN 2015: 5th ECCOMAS Thematic Conference on computational methods in structural dynamics and earthquake engineering*, Crete, Greece.
- Brander, J., Taylor, M. (1998). The simple economics of Easter Island: a Ricardo-Malthus model of renewable resource use. *The Am. Econ. Rev.*, 88, 119–138.
- Brillinger, D. R. (1993). Earthquake risk and insurance. *Environmetrics*, 4 , 1–21.
- Bruneau, M., & Reinhorn, A. (2007). Exploring the concept of seismic resilience for acute care facilities. *Earthquake Spectra*, 23(1), 41-62.
- Bruneau, M. (2006). Enhancing the resilience of communities against extreme events from an earthquake engineering perspective. *Journal of Security Education*, 1(4), 159-167.
- Bruneau, M., & Reinhorn, A. (2006, April). Overview of the resilience concept. In *Proceedings of the 8th US National Conference on Earthquake Engineering* (pp. 18-22).
- Bruneau M, Chang S, Eguchi R, Lee G, O'Rourke T, Reinhorn A, Shinozuka M, Tierney K, Wallace W, von Winterfeldt D (2003). A framework to quantitatively assess and enhance seismic resilience of communities. *Earthq Spectra* 19:733–752, 2003.
- Callaghan E.G. , Colton J. (2008). Building sustainable and resilient communities: A balancing of community capital *Environ Dev Sustain*, 10, pp. 931–942.
- Campbell, A. (1972). *Aspiration, Satisfaction and Fulfillment*, In: A. Campbell, P. Converse. Eds. *The Human Meaning of Social Change*. New York: Russell Sage Foundation, pp. 441-446.
- Campbell, S. (1996). Green cities, growing cities, just cities? Urban planning and the contradictions of sustainable development. *Journal of the American Planning Association* 62.
- Cardenas, V., Hochrainer, S., Mechler, R., Pflug, G., & Linnerooth-Bayer, J. (2007). Sovereign financial disaster risk management: the case of Mexico. *Environmental Hazards*, 7(1), 40-53.
- Cardillo, A., Scellato, S., Latora, V., & Porta, S. (2006). Structural properties of planar graphs of urban street patterns. *Physical Review E*, 73(6), 066107.
- Cardona, O. D., Ordaz, M. G., Marulanda, M. C., & Barbat, A. H. (2008). Estimation of probabilistic seismic losses and the public economic resilience—an approach for a macroeconomic impact evaluation. *Journal of Earthquake Engineering*, 12(S2), 60-70.
- Cardona, O.D. (2006). A system of indicators for disaster risk management in the Americas. In J.Birkmann (ed.) *Measuring Vulnerability to Hazards of Natural Origin: Towards Disaster Resilient Societies*. United Nations University Press, Tokyo.

- Carpenter S, Walker B, Anderies JM, Abel N (2001). From metaphor to measurement: resilience of what to what? *Ecosystems* (N Y, Print) 4(8):765–781.
- Carreño, M.L., Cardona, O.D., Barbat, A.H. (2011). New methodology for urban seismic risk assessment from a holistic perspective, *Bull Earthquake Eng* DOI 10.1007/s10518-011-9302-2.
- Cascini, L., Cuomo, S. & Della Sala M. (2011), Spatial and temporal occurrence of rainfall-induced shallow landslides of flow type: A case of Sarno-Quindici, Italy, *Geomorphology*, 126(1), 148-158.
- Catapano, F., Malafrente, R., Lepre, F., Cozzolino, P., Arnone, R., Lorenzo, E., ... & Maj, M. (2001), Psychological consequences of the 1998 landslide in Sarno, Italy: a community study, *Acta Psychiatrica Scandinavica*, 104(6), 438-442.
- Cavallaro, M., Asprone, D., Latora, V., Manfredi, G., & Nicosia, V. (2014). Assessment of urban ecosystem resilience through hybrid social–physical complex networks. *Computer-Aided Civil and Infrastructure Engineering*, 29(8), 608-625.
- Chang, S. E., & Chamberlin, C. (2004). Assessing the role of lifeline systems in community disaster resilience. *Research Progress and Accomplishments 2003–2004*, Multidisciplinary Center for Earthquake Engineering Research, 87-94.
- Chang, S. E., & Shinozuka, M. (2004). Measuring improvements in the disaster resilience of communities. *Earthquake Spectra*, 20(3), 739-755.
- Chavas, J.P. (2000). Ecosystem valuation under uncertainty and irreversibility. *Ecosystems* 3, 11–15.
- Chen SC, Ferng JW, Wang YT, Wu TY, Wang JJ (2008). Assessment of disaster resilience capacity of hillslope communities with high risk for geological hazards. *Eng Geol* 98(3–4):86–101.
- Cimellaro, G. P., Reinhorn, A. M., & Bruneau, M. (2010). Framework for analytical quantification of disaster resilience. *Engineering Structures*, 32(11), 3639-3649.
- Clemen, R.T., Reilly, T. (2004). *Making Hard Decisions with Decision Tools*. Duxbury Resource Center; Book & CD edition.
- Cobb, C.W. (2000). *Measurement Tools and the Quality of Life. Redefining Progress*. San Francisco. www.rprogress.org/pubs/pdf/measure_qol.pdf
- Colombi M, Crowley H, Di Capua G, Peppoloni S, Borzi B, Pinho R, Calvi GM (2010). *Mappe di Rischio Sismico a Scala Nazionale con Dati Aggiornati sulla Pericolosità Sismica di base e locale. Progettazione Sismica 1*.
- Colten, C.E., R.W. Kates and S.B. Laska (2004). *Community Resilience: Lessons from New Orleans and Hurricane Katrina*. CARRI Research Report 3. Oak Ridge: Community and Regional Resilience Institute.
- Comfort L (1999) *Shared risk: complex systems in seismic response*. Pergamon, New York, 1999.
- Commissariato per la Ricostruzione, “Ricostruzione: Stato di attuazione e programmazione. Aggiornamento al 31 maggio 2012”, in Italian, www.commissarioperlaricostruzione.it
- Commonwealth of Australia. *Critical infrastructure resilience strategy*. Canberra: Commonwealth of Australia; 2010.
- Community and Regional Resilience Institute (CARRI 2013) *Community Resilience System*, Community and Regional Resilience Institute (CARRI 2013) *Community Resilience System*

- Corominas, J., Mavrouli O.-C. & other SafeLand partners (2011), Guidelines for landslide susceptibility, hazard and risk assessment and zoning, Deliverable D2.4 of SafeLand Project, 173 pp., available at: <http://www.safeland-fp7.eu>.
- Costanza, Robert (1992). *Ecological economics: the science and management of sustainability*. Columbia University Press.
- Crane, P., & Kinzig, A. (2005). Nature in the metropolis. *Science* (New York, NY), 308(5726), 1225-1225.
- CRESME IL MERCATO DELLE COSTRUZIONI 2011-2015 Rapporto congiunturale e previsionale Novembre 2011.
- Crowley H, Borzi B, Pinho R, Colombi M, Onida M (2008). Comparison of two mechanics-based methods for simplified structural analysis in vulnerability assessment. *Adv Civil Eng* 2008, Article ID 438379.
- Cumming GS, Barnes G, Perz S, Schmink M, Sieving KE, Southworth J, et al. (2005). An exploratory framework for the empirical measurement of resilience. *Ecosystems* 2005;8(8):975–87.
- Cummins, J. D. (2008). CAT Bonds and Other Risk-Linked Securities: State of the Market and Recent Developments. *Risk Management and Insurance Review*, 11(1), 23-47.
- Cutter, S.L.; K.D. Ash; and C.T. Emrich (2014) The geographies of community disaster resilience, *Global Environmental Change*, 29, pp. 65-77.
- Cutter, S. L., Barnes, L., Berry, M., Burton, C., Evans, E., Tate, E., & Webb, J. (2008). A place-based model for understanding community resilience to natural disasters. *Global environmental change*, 18(4), 598-606.
- D.M. 14.01.2008 DEL MINISTERO DELLE INFRASTRUTTURE (2008) – Norme Tecniche per le Costruzioni. S.O. n. 30 alla G.U. del 04.02.2008, No. 29.
- D'Alessandro, S. (2007). Non-linear dynamics of population and natural resources: The emergence of different patterns of development. *Ecol. Econ.* 62, 473–481.
- Dalziell E.P., McManus S.T. (2004). Resilience, vulnerability, and adaptive capacity: implications for system performance *International Forum for Engineering Decision Making*.
- Davis, C. A. (2014). Water system service categories, post-earthquake interaction, and restoration strategies. *Earthquake Spectra*, 30(4), 1487-1509.
- De Vaus, D. (2007). *Social surveys II: History, ethics and criticisms*. Vol. 1. Sage.
- Decò, A., Bocchini, P., & Frangopol, D. M. (2013). A probabilistic approach for the prediction of seismic resilience of bridges. *Earthquake Engineering & Structural Dynamics*, 42(10), 1469-1487.
- DHS Risk Steering Committee, U.S. Department of Homeland Security Risk Lexicon, United States Department of Homeland Security. Washington DC; 2008
- Dovers, S.R., and J.W. Handmer. (1992). Uncertainty, sustainability and change. *Global Environmental Change* 2.4, 262-276.
- Dueñas-Osorio, L., & Rojo, J. (2011). Reliability assessment of lifeline systems with radial topology. *Computer-Aided Civil and Infrastructure Engineering*, 26(2), 111-128.
- EN 1998–1(2003): Eurocode 8: Design of Structures for Earthquake Resistance. Part 1: General rules, seismic actions and rules for buildings. Commission of the European Communities, European Committee for Standardization, October 2003.

- Environment and Development Division, UNESCAP (2008). Sustainability, resilience and resource efficiency, UNESCAP. Bangkok, Thailand.
- Erberik MA (2008). Generation of fragility curves for Turkish masonry buildings considering in-plane failure modes. *Earthquake Eng and Str Dyn*, 37.
- Erikson, R. (1993). Descriptions of Inequality: The Swedish Approach to Welfare Research, In: M. Nussbaum, A. Sen. Eds. *The Quality of Life*. Oxford: Clarendon Press, pp. 67 – 87.
- Feld, C.F., Sousa, J.P., da Silva, P.D., Dawson, T.P. (2010). Indicators for biodiversity and ecosystem services: towards an improved framework for ecosystems assessment, *Biodivers Conserv* 19:2895–2919.
- Felson, M. (1993). Social indicators for criminology, *Journal of research in in crime and delinquency* 30.4.
- FEMA (2011) Presidential Disaster Declarations, January 10, 2000 to January 1, 2011, 387 <https://www.hssl.org/?view&did=12383>
- FEMA 273 (1997). NEHRP Guidelines for the seismic rehabilitation of buildings, Washington, USA. http://www.fema.gov/media-library-data/20130726-1913-25045-6071/final_national_prevention_framework_20130501.pdf
- Fiksel J (2006). Sustainability and resilience: toward a systems approach. *Sustainability: Science Practice and Policy* 2006;2(2):14–21.
- Folke, C. (2006). Resilience: The emergence of a perspective for social–ecological systems analyses. *Global environmental change*, 16(3), 253-267.
- Folke, Carl, Crawford S. Holling, and Charles Perrings (1996). Biological diversity, ecosystems, and the human scale." *Ecological Applications* 6.4, 1018-1024.
- Franchin, P., & Cavalieri, F. (2015). Probabilistic assessment of civil infrastructure resilience to earthquakes. *Computer-Aided Civil and Infrastructure Engineering*, 30(7), 583-600.
- Franchin, P. & Cavalieri, F. (2013), Seismic vulnerability analysis of a complex interconnected civil infrastructure, in S.Tesfamariam and K. Goda (eds.). *Handbook of Seismic Risk Analysis and Management of Civil Infrastructure Systems*, Woodhead Publishing Limited, Cambridge, UK.
- Francis, R., & Bekera, B. (2014). A metric and frameworks for resilience analysis of engineered and infrastructure systems. *Reliability Engineering & System Safety*, 121, 90-103.
- Frangopol DM, Bocchini P. (2011). Resilience as optimization criterion for the rehabilitation of bridges belonging to a transportation network subject to earthquake. *Proceedings of the ASCE 2011 Structures Congress SEI 2011*, Ames D, Droessler TL, Hoit M (eds). Las Vegas, NV, 2044–2055.
- Frazier, T. G., Thompson, C. M., Dezzani, R. J., & Butsick, D. (2013). Spatial and temporal quantification of resilience at the community scale. *Applied Geography*, 42, 95-107.
- Frazier, A., Arendt, L., Cimellaro, G. P., Reinhorn, A. M., & Bruneau, M. (2010). A framework for defining and measuring resilience at the community scale: the PEOPLES resilience framework (pp. 10-0006). Buffalo: MCEER.
- Fujita Y. (2006) Systems are ever-changing. In: Hollnagel E, Woods DD, Leveson N, editors. *Resilience engineering: concepts and precepts*, 3. Hampshire, UK: Ashgate; 2006. p. 20–33.
- Garmezy N (1991). Resilience in children's adaptation to negative life events and stressed environments. *Pediatrics*. 1991;20:459–466.

- Garmezzy, N. (1973). Competence and adaptation in adult schizophrenic patients and children at risk. In: S.R. Dean (Ed.), *Schizophrenia: the First ten Dean Award lectures* (pp. 163-204), New York: MSS Information.
- Geis DE (2000). By design: the disaster resistant and quality-of-life community. *Nat Hazards Rev* 1(3):106–120.
- Goda K & Atkinson GM (2010). Intraevent spatial correlation of ground-motion parameters using SK-net data. *Bulletin of the Seismological Society of America*, 100(6), 3055-3067.
- Goda K & Atkinson G M (2009). Interperiod dependence of ground-motion prediction equations: A copula perspective. *Bulletin of the Seismological Society of America*, 99(2A), 922-927.
- Goda K & Hong HP (2008). Estimation of seismic loss for spatially distributed buildings. *Earthquake Spectra*, 24(4), 889-910.
- Goda K & Hong HP (2008). Spatial correlation of peak ground motions and response spectra. *Bulletin of the Seismological Society of America*, 98(1), 354-365.
- Godschalk, D. (2003). "Urban Hazard Mitigation: Creating Resilient Cities." *Nat. Hazards Rev.*, 10.1061/(ASCE)1527-6988(2003)4:3(136), 136-143.
- González, A. D., Dueñas-Osorio, L., Sánchez-Silva, M., & Medaglia, A. L. (2015). The Interdependent Network Design Problem for Optimal Infrastructure System Restoration. *Computer-Aided Civil and Infrastructure Engineering*.
- Gorochoowski, T.E., Di Bernardo, M. and Grierson C.S. (2011). *Evolving Dynamical Networks: A Formalism For Describing Complex Systems, Complexity*, Wiley Periodicals, Inc., Vol. 17, No. 3.
- Gotangco, C. K., See, J., Dalupang, J. P., Ortiz, M., Porio, E., Narisma, G., ... & Dator-Bercilla, J. (2016). Quantifying resilience to flooding among households and local government units using system dynamics: a case study in Metro Manila. *Journal of Flood Risk Management*.
- Goulet CA, Haselton CB, Mitrani-Reiser J, Beck JL, Deierlein GG, Porter KA & Stewart JP (2007). Evaluation of the seismic performance of a code-conforming reinforced concrete frame building—from seismic hazard to collapse safety and economic losses. *Earthquake Engineering & Structural Dynamics*, 36(13), 1973-1997.
- Granovetter, M. S. (1973). The strength of weak ties. *American journal of sociology*: 1360-1380.
- Grote G. (2006). Rules management as source for loose coupling in high-risk systems. In: *Proceedings of the second resilience engineering symposium*; p. 116–24.
- Gruppo di lavoro CPTI Catalogo Parametrico dei Terremoti Italiani, versione 2004 (CPTI04). INGV, Bologna 2004 DOI: 106092/INGVIT-CPTI04 (Available from: <http://emidiusmiingvit/CPTI04/>)
- Gunderson L, Holling CS, Pritchard L, Peterson G. (2002). Resilience. In: Mooney H, Canadell J, editors. *Encyclopedia of global environmental change*, 2. Scientific Committee on Problems of the Environment; p. 530–1.
- Gunderson LH and Holling CS. (Eds.) (2002). *Panarchy: Understanding Transformations in Human and Natural Systems*. Island Press, Washington, DC.
- Haimes YY. (2009). On the definition of resilience in systems. *Risk Analysis* 29(4):498–501.

- Hale A, Heijer T. (2006). Defining resilience. In: Hollnagel E, Woods DD, Leveson N, editors. Resilience engineering: concepts and precepts, 3. Hampshire, UK: Ashgate; p. 35–40.
- Hammer, Monica, Robert Costanza, and A. Jansson (1994). Investing in Natural Capital: Why, What and How?. Beijer International Institute of Ecological Economics.
- Henry, D., & Ramirez-Marquez, J. E. (2012). Generic metrics and quantitative approaches for system resilience as a function of time. *Reliability Engineering & System Safety*, 99, 114-122.
- Highland, L. (2004), Landslide types and processes, (No. 2004-3072).
- Hodge, G. (1991). Planning Canadian Communities: An Introduction to the Principles, Practice, and Participants, Second Edition, Nelson, Toronto, ON.
- Holling CS (2001). Understanding the complexity of economic, ecological, and social system. *Ecosystems* (N Y, Print) 4:390–405.
- Holling, C. S. (1996). Engineering resilience versus ecological resilience. *Engineering within ecological constraints*, 31, 32.
- Holling, C. S. (1994). Simplifying the complex: the paradigms of ecological function and structure. *Futures*, 26(6), 598-609.
- Holling CS (1986). The resilience of terrestrial ecosystems: local surprise and global change. In: Clark WC, Munn RE (eds) Sustainable development of the biosphere. Cambridge University Press, Cambridge, pp 292–317.
- Holling CS (1973). Resilience and stability of ecological systems. *Annu Rev Ecol Syst* 4:1–23.
- Hong HP, Zhang Y & Goda K (2009). Effect of spatial correlation on estimated ground-motion prediction equations. *Bulletin of the Seismological Society of America*, 99(2A), 928-934.
- Hong HP (2000). Distribution of structural collapses and optimum reliability for infrequent environmental loads. *Structural safety*, 22(4), 297-311.
- Home JF, Orr JE Assessing behaviours that create resilient organizations. *Employ Relat Today*, 24(4):29–39, 1998.
- Howard, R.A., Matheson, J.E. (Eds.) (1983). Readings on the Principles and Applications of Decision Analysis. Strategic Decisions Group, Menlo Park, CA.
- IFRC (2008). A Framework for community safety and resilience: In the face of disaster risk, IFRC.
- IFRC (2004). World Disasters Report 2004: Focus on community resilience (Geneva: IFRC)
- Inter-American Development Bank (IDB) (2010). Indicators of disaster risk and risk management, Program for Latin America and the Caribbean, Barbados, Environmental, Rural Development and Disaster Risk Management Division (INE/RND), Technical Notes, No. IDB-TN-169.
- IPCC 2014. Climate Change 2014: Synthesis Report. Contribution of Working Groups I, II and III to the Fifth Assessment Report of the Intergovernmental Panel on Climate Change. In: CORE WRITING TEAM, R. K. P., L.A. MEYER (ed.). Geneva.
- ISTAT - Istituto nazionale di statistica (2011). 14° Censimento generale della popolazione e delle abitazioni (Available from: <http://dawinciistatit/MD/dawinciMDjsp>).
- Jaiswal K and Wald DJ (2013). Estimating economic losses from earthquakes using an empirical approach. *Earthquake Spectra* 29(1), 309-324.

- Kang B, Lee SJ, Kang DH, Kim YO (2007). A flood risk projection for Yongdam dam against future climate change. *J Hydro-Environ Res* 1(2):118–125.
- Kappos AJ, Panagopoulos G, Panagiotopoulos C, Penelis G (2006). A hybrid method for the vulnerability assessment of R/C and URM buildings. *Bulletin of Earthquake Engineering*, 4, 391-413.
- Kappos AJ, Panagiotopoulos C, Panagopoulos G, Papadopoulos EI (2003). WP4 – Reinforce Concrete Buildings (Level 1 and Level 2 analysis). RISK-UE.
- Kates, R. W., & Parris, T. M. (2003). Long-term trends and a sustainability transition. *Proceedings of the National Academy of Sciences*, 100(14), 8062-8067.
- Kendra JM, Wachtendorf T. (2003). Elements of resilience after the World Trade Center disaster: reconstituting New York City's emergency operations centre. *Disasters* 2003;27(1):37–53.
- Kesete Y, Peng J, Gao Y, Shan X, Davidson R A, Nozick L K, & Kruse J (2014). Modeling Insurer-Homeowner Interactions in Managing Natural Disaster Risk. *Risk analysis*, 34(6), 1040-1055.
- Kimhi S, Shamai M (2004) Community resilience and the impact of stress: adult response to Israel's withdrawal from Lebanon. *J Community Psychol* 32(4):439–451, 2004.
- Kinzig AP, Ryan P, Etienne M, Allison H, Elmqvist T, Walker BH. (2006). Resilience and regime shifts: assessing cascading effects. *Ecology and Society* 2006;11 (1):20–42.
- Kostov M, Vaseva E, Kaneva A, Koleva N, Varbanov G, Stefanov D, Darvarova E, Solakov D, Simeonova S & Cristoskov L (2004). Application to Sofia. RISK-UE WP13.
- Kunreuther, H. (1996). Mitigating disaster losses through insurance. *Journal of risk and Uncertainty*, 12(2-3), 171-187.
- Kwon OS, Elnashai A (2006). The effect of material and ground motion uncertainty on the seismic vulnerability curves of RC structure. *Engineering Structures*; 28(2):289–303.
- Lagomarsino S & Giovinazzi S (2006). Macroseismic and mechanical models for the vulnerability and damage assessment of current buildings. *Bulletin of Earthquake Engineering* 4(4), 415-443.
- Latora, V., & Marchiori, M. (2001), Efficient behavior of small-world networks, *Physical review letters*, 87(19), 198701.
- legge 2 febbraio 1974, n. 64, “Provvedimenti per le costruzioni con particolari prescrizioni per le zone sismiche”, 1974.
- Leu, G., Abbass, H., & Curtis, N. (2010). Resilience of ground transportation networks: A case study on Melbourne.
- Li, Y., & Lence, B. J. (2007). Estimating resilience for water resources systems. *Water Resources Research*, 43(7).
- Lobo J, Bettencourt LM, Strumsky D, & West GB (2013). Urban scaling and the production function for cities. *PloS one*, 8(3), e58407.
- Loss events worldwide 1980 – 2014 (2015). 10 costliest events ordered by overall losses. 2015 Münchener Rückversicherungs-Gesellschaft, *Geo Risks Research*, Munich Re, NatCatSERVICE.
- Lotka AJ (1924). *Elements of Physical Biology*. Williams & Wilkins, Baltimore, (Reprinted in 1956 as ‘*Elements of Mathematical Biology*’. Dover, New York.)

- Maguire B, Hagan P (2007). Disasters and communities: understanding social resilience. *Aust J Emerg Manage* 22(2):16–20.
- Mallak L (1998). Resilience in the healthcare industry. Paper presented at the seventh annual engineering research conference, Banff, Alberta, Canada, 9–10 May.
- Marchini A., Facchinetti T., Mistri M. (2009). F-IND: A framework to design fuzzy indices of environmental conditions, *Ecological Indicators* 9, 485-496.
- Maslow, A. H. (1943). A theory of human motivation. *Psychological review*,50(4), 370.
- Mayer A.L. (2008). Strengths and weaknesses of common sustainability indices for multidimensional systems, *Environment International* 34, 277–291.
- Mc Mahon S.K., The development of quality of life indicators—a case study from the City of Bristol, UK, *Ecological Indicators* 2, 177–185, 2002.
- McCarthy JA. (2007). From protection to resilience: injecting ‘Moxie’ into the infrastructure security continuum. Arlington, VA: Critical Infrastructure Protection Program at George Mason University School of Law.
- McDaniels, T., Chang, S., Cole, D., Mikawoz, J., & Longstaff, H. (2008). Fostering resilience to extreme events within infrastructure systems: Characterizing decision contexts for mitigation and adaptation. *Global Environmental Change*, 18(2), 310-318.
- Mensah, A. F. (2015). Resilience Assessment of Electric Grids and Distributed Wind Generation under Hurricane Hazards.
- Mensah, A. F., & Dueñas-Osorio, L. (2015). Efficient Resilience Assessment Framework for Electric Power Systems Affected by Hurricane Events. *Journal of Structural Engineering*, C4015013.
- Miles, S. B. (2015). Foundations of community disaster resilience: well-being, identity, services, and capitals. *Environmental Hazards*, 14(2), 103-121.
- Miles, S. B., & Chang, S. E. (2006). A simulation model of urban disaster recovery and resilience: Implementation for the 1994 Northridge earthquake.
- Miletti D (1999). *Disasters by design: a reassessment of natural hazards in the United States*. Joseph Henry Press, Washington.
- Milgram, S. (1967). The small world problem. *Psychology today*, 2(1), 60-67.
- Milgram, S. (1974). The experience of living in cities. *Crowding and behavior*,167, 41.
- Miller-Hooks, E., Zhang, X., & Faturechi, R. (2012). Measuring and maximizing resilience of freight transportation networks. *Computers & Operations Research*, 39(7), 1633-1643.
- MINISTRO DEI LL.PP. DI CONCERTO CON IL MINISTRO DELL’INTERNO DECRETO MINISTERIALE 19 GIUGNO 1984, “Norme tecniche relative alle costruzioni in zone sismiche”, 1984.
- Mitsch, W. J., & Jørgensen, S. E. (2004). *Ecological engineering and ecosystem restoration*. John Wiley & Sons.
- Mitsch, William J. (1999). *Ecological engineering*. Springer Netherlands.
- Mitsch, William J., and Sven Erik Jørgensen (1989). *Ecological engineering*. A Wiley-Interscience Publication John Wiley & Sons, 1-130.
- Morris AEJ (1979). *History of urban form before industrial revolutions*, London: George Godwin.

- Munda, G., Nijkamp, P., Rietveld, P. (1995). Qualitative multicriteria methods for fuzzy evaluation problems: an illustration of economic-ecological evaluation. *Eur. J. Oper. Res.* 82, 79–97.
- Murray-Tuite, P. M. (2006, December). A comparison of transportation network resilience under simulated system optimum and user equilibrium conditions. In *Simulation Conference, 2006. WSC 06. Proceedings of the Winter* (pp. 1398-1405). IEEE.
- NATHAN World Map of Natural Hazards, version 2011 (2011). Münchener Rückversicherungs-Gesellschaft Königinstrasse 107, 80802 München, Germany.
- National Oceanic and Atmospheric Administration (NOAA 2015) US Climate Resilience Toolkit, National Oceanographic and Atmospheric Administration, Washington, D.C., <https://toolkit.climate.gov/>.
- National Preparedness Goal (2011), <https://www.fema.gov/pdf/prepared/npg.pdf>
- Nejat, A. & Damnjanovic, I. (2012), Agent-based modeling of behavioral housing recovery following disasters, *Computer-Aided Civil and Infrastructure Engineering*, 27(10), 748–63.
- Newman, M.E.J. (2003). The Structure and Function of Complex Networks, *SIAM REVIEW* Vol. 45, No. 2, pp . 167–256.
- Newman, W. L. (1997). *Social Research Methods: qualitative and quantitative approaches*, Alyn and Bacon, Boston.
- NIAC, National Infrastructure Advisory Council—a framework for establishing critical infrastructure resilience goals final report and recommendations; 2009.
- NIST (2015). "Disaster Resilience Framework: 75% Draft for San Diego, CA Workshop." National Institute of Standards and Technology (NIST), http://www.nist.gov/el/building_materials/resilience/framework.cfm Retrieved on 04/09/2015.
- NIST Special Publication 1190, Community Resilience Planning Guide for Buildings and Infrastructure Systems, Volume I (October 2015). <http://dx.doi.org/10.6028/NIST.SP.1190v2>
- Noll, H. (2002). Social indicators and quality of life research: background, achievements and current trend, Genov, Nicolai Ed., *Advances in Sociological Knowledge over Half a Century*, Paris: International Social Science Council.
- O'Rourke T. D. (2007). Critical infrastructure, interdependencies, and resilience. *The Bridge*, vol. 37, no. 1, pp. 22–29.
- Olick, K.J., Robbins, J., (1998). Social memory studies: from collective memory to the historical sociology of mnemonic practices. *Annual Review of Sociology* 24, 105–140.
- Omer, M., Nilchiani, R., & Mostashari, A. (2009). Measuring the resilience of the trans-oceanic telecommunication cable system. *Systems Journal, IEEE*,3(3), 295-303.
- O'Neill, R. V. (1986). *A hierarchical concept of ecosystems* (Vol. 23). Princeton University Press.
- OPCM 3519 del 28 aprile 2006. All 1b Pericolosità sismica di riferimento per il territorio nazionale 2006 (Available from: <http://zonesismichemiingvit/>)
- Opricovic, S. & Tzeng, G. H. (2002), Multicriteria planning of post-earthquake sustainable reconstruction, *Computer-Aided Civil and Infrastructure Engineering*, 17(3), 211–20.
- Ordinanza PCM 3519 del 28/04/2006. Criteri generali per l'individuazione delle zone sismiche e per la formazione e l'aggiornamento degli elenchi delle medesime zone, G.U. n.108 del 11/05/2006.

- Oregon Seismic Safety Policy Advisory Commission (OSSPAC 2013) The Oregon Resilience Plan: Reducing Risk and Improving Recovery for the Next Cascadia Earthquake and Tsunami, Salem, OR, February, http://www.oregon.gov/OMD/OEM/osspace/docs/Oregon_Resilience_Plan_Final.pdf.
- Ortiz, O., Castells, F., Sonnemann, G. (2009). Sustainability in the construction industry: a review of recent developments based on LCA, *Construction and Building Materials* 23, 28–39.
- Ouyang, M., Zhao, L., Pan, Z., and Hong, L. (2014). Comparisons of complex network based models and direct current power flow model to analyze power grid vulnerability under intentional attacks. *Physica A: Statistical Mechanics and its Applications*, 403(0), 45-53.
- Ouyang, M., and Dueñas-Osorio, L. (2014). Multi-dimensional hurricane resilience assessment of electric power systems. *Structural Safety*, 48(0), 15-24.
- Ouyang, M., and Duenas-Osorio, L. (2012). Time-dependent resilience assessment and improvement of urban infrastructure systems. *Chaos: An Interdisciplinary Journal of Nonlinear Science*, 22(3), 033122-033111.
- Ouyang, M., Dueñas-Osorio, L., & Min, X. (2012). A three-stage resilience analysis framework for urban infrastructure systems. *Structural Safety*, 36, 23-31.
- Ozmen HB, Inel M, Meral E and Bucakli M (2010). Vulnerability of Low and Mid-Rise Reinforced Concrete Buildings in Turkey. 14ECEE, Ohrid, Turkey.
- Palm, RI, Hodgson, ME, Blanchard, RD, Lyons, DI (1990). *Earthquake Insurance in California: Environmental Policy and Individual Decision-Making*. Westview press, 5500 central ave., boulder, co 80301 (USA).
- Paredes, R., & Dueñas-Osorio, L. (2015). A time-dependent seismic resilience analysis approach for networked lifelines.
- Parisi, F., Sabella, G. & Galasso C. (2015), Fragility of reinforced concrete framed structures to flow-type landslides, in 12th International Conference on Applications of Statistics and Probability in Civil Engineering, Vancouver, Canada.
- Paton D, Smith L, Violanti J. (2000). Disasters response: risk, vulnerabilities and resilience. *Disaster Prev Manage* 9(3):173–179.
- Pelling M. (2003). *The vulnerability of cities: natural disasters and social resilience*. Earthscan, London.
- Perrings C. (2006). Resilience and sustainable development. *Environment and Development Economics* 2006;11(4):417.
- Pfefferbaum, R.; B. Pfefferbaum; R.L. Van Horn; R.W. Klomp; F.H. Norris; and D.B. Reissman (2013) —The Communities Advancing Resilience Toolkit (CART): An Intervention to Build Community Resilience to Disasters, *Journal of Public Health Management & Practice*, May/June 2013, Vol. 19, Issue 3, p 250–258.
- Pfeiffer, K. (1929). *Untersuchungen über die Resilienz der durch die Prothesen beanspruchten Gewebe und ihre Bedeutung für die Okklusion der Prothesen* (Doctoral dissertation).
- Pimm, S. (1984), The complexity and stability of ecosystems, *Nature*, vol. 307, pp. 321-326.
- Pimm, S. L. (1991). *The balance of nature?: ecological issues in the conservation of species and communities*. University of Chicago Press.
- Pimm, S. L. (1994). Biodiversity and the balance of nature. In *Biodiversity and ecosystem function* (pp. 347-359). Springer Berlin Heidelberg.

Pitilakis, K., Crowley, H., & Kaynia, A. (2014). SYNER-G: typology definition and fragility functions for physical elements at seismic risk. *Geotechnical, Geological and Earthquake Engineering*, 27.

Population Division of the Department of Economic and Social Affairs of the United Nations Secretariat (2004). *World Urbanization Prospects: The 2003 Revision*. United Nations, New York

Presidential Policy Directive, PPD-21, The White House, March 30, 2011. <http://www.whitehouse.gov/the-press-office/2013/02/12/presidential-policy-directive-critical-398-infrastructure-security-and-resil>

Presidential Policy Directive, PPD-8 – National Preparedness, <http://www.dhs.gov/presidential-policy-directive-8-nationalpreparedness>.

PreventionWeb (2010). "HFA Mid-Term Review." Retrieved June 1st, 2010, from <http://www.preventionweb.net/english/hyogo/hfa-mtr/>.

Reed, D. A., Kapur, K. C., & Christie, R. D. (2009). Methodology for assessing the resilience of networked infrastructure. *Systems Journal, IEEE*, 3(2), 174-180.

Regione Molise – Struttura Commissariale 2010, "Il percorso della ricostruzione", in Italian, <http://www.regione.molise.it/web/grm/sis.nsf>

Renschler, C. S., Frazier, A. E., Arendt, L. A., Cimellaro, G. P., Reinhorn, A. M., & Bruneau, M. (2010, July). Developing the 'PEOPLES' resilience framework for defining and measuring disaster resilience at the community scale. In *Proceedings of the 9th US national and 10th Canadian conference on earthquake engineering (9USN/10CCEE)*, Toronto (pp. 25-29).

Revellino, P., Hungr, O., Guadagno, F. M., & Evans, S. G. (2004), Velocity and runout simulation of destructive debris flows and debris avalanches in pyroclastic deposits, Campania region, Italy, *Environmental Geology*, 45(3), 295-311.

Rockstrom J. (2003). Resilience building and water demand management for drought mitigation. *Phys Chem Earth* 28:869–877.

Rose, A. (2015). *Measuring Economic Resilience: Recent Advances and Future Priorities*.

Rose, A., & Krausmann, E. (2013). An economic framework for the development of a resilience index for business recovery. *International Journal of Disaster Risk Reduction*, 5, 73-83.

Rose, A. Z. (2009). *Economic resilience to disasters*.

Rose A. (2007). Economic resilience to natural and man-made disasters: multidisciplinary origins and contextual dimensions. *Environ Hazards* 7:383–398.

Rose A. (2004). Defining and measuring economic resilience to disasters. *Disaster Prev Manage* 13:307–314.

Rota M, Penna A, Magenes G (2010). A methodology for deriving analytical fragility curves for masonry buildings based on stochastic nonlinear analyses. *Engineering Structures* 32, 1312-1323.

Rota M, Penna A, Strobbia CL (2008). Processing Italian damage data to derive typological fragility curves. *Soil Dynamics and Earthquake Engineering* 28(10-11), 933-947.

Ruitenbeek, H. J. (1996). Distribution of ecological entitlements: implications for economic security and population movement. *Ecological Economics* 17, 49-64.

Sabetta F. e Pugliese A. (1996). Estimation of response spectra and simulation of nonstationary earthquake ground motions. *Bull. Seism. Soc. Am.*, 86, 2, 337-352.

Salski, A., Franzle, O., Kandzia, P. (1996). Introduction to Special Issue 'Fuzzy Logic in Ecological Modelling'. *Ecol. Model.* 85, 1–2.

San Francisco Planning and Urban Research Association (SPUR 2009) —When is a Building Safe Enough? San Francisco Urban Research Association, Issue 479, February 2009, 654 Mission Street, San Francisco, CA, <http://www.spur.org>, http://www.spur.org/sites/default/files/publications_pdfs/SPUR_Seismic_Mitigation_Policies.pdf.

Scawthorn, C., Kunreuther, H., and Roth Jr, R. (2003). Insurance and financial risk transfer, In: W.-F Chen. and C. Scawthorn (eds.), *Earthquake Engineering Handbook*, CRC Press, Chapter 32.

Schläpfer M, Bettencourt LM, Grauwin S, Raschke M, Claxton R, Smoreda Z, West GB & Ratti C (2014). The scaling of human interactions with city size. *Journal of The Royal Society Interface*, 11(98), 20130789.

Sen, A. (2008). *Capabilities and Happiness*, Edited by Luigino Bruni, Flavio Comim, Maurizio Pugno, Oxford University Press, pp. 16-28.

Sen, A. (1993). Capability and Well-Being, The Quality of Life. In: M.C. Nussbaum, A. Sen. Eds. Oxford: Clarendon Press, pp. 30-53.

Sharp A. (1999). Centre for the Study of Living Standards, A Survey of Indicators of Economic and Social Well-being, second draft, Paper prepared for Canadian Policy Research Networks, July 22.

Spence R (2007). Earthquake disaster scenario predictions and loss modelling for urban areas. In *LESSLOSS Report 7*, Pavia, Italy: IUSS Press.

Sperling F., Szekely F. (2005). *Disaster risk management in a changing climate*, Vulnerability and Adaptation Resource Group.

Steven, L. (1992). The earthquake and war damage commission – a look forward (and a look back), *Bull. N. Z. Nat. Soc. Earthquake Eng.*, 25, 52–55.

Subcommittee on Disaster Reduction (2005). Committee on Environment and Natural Resources, National Science and Technology Council, Grand challenges for disaster reduction. Washington, DC.

Tamvakis, P., & Xenidis, Y. (2013). Comparative evaluation of resilience quantification methods for infrastructure systems. *Procedia-Social and Behavioral Sciences*, 74, 339-348.

Tanguay, G.A., Rajaonson, J., Lefebvre, J., Lanoie, P. (2010). Measuring the sustainability of cities: An analysis of the use of local indicators, *Ecological Indicators* 10, 407–418.

Tapsell S., McCarthy S., Faulkner H., Alexander M., Steinführer A., Kuhlicke C., Brown C., Walker G., Pellizzoni L., Scolobig A., De Marchi B., Bianchizza C., Supramaniam M., Kallis G. (2010). Social vulnerability to natural hazards, Research Report”, Del. 4.1., CapHaz-Net Social capacity building for natural hazards – Toward more resilient societies, European Commission 7th Framework Programme. 86 pp.

Teodorescu H.-N. L. (2015). Defining resilience using probabilistic event trees. *Environment Systems and Decisions*, 35(2), 279-290.

Thomas, W.I., Thomas, D.S. (1928). *The Child in America: Behavior Problems and Programs*, New York: Alfred A. Knopf.

- Timmerman P. (1981). *Vulnerability. Resilience and the collapse of society: A review of models and possible climatic applications*. Environmental Monograph, Institute for Environmental Studies, University of Toronto, 1.
- Todini, E. (2000). Looped water distribution networks design using a resilience index based heuristic approach. *Urban water*, 2(2), 115-122.
- Tokgoz, B. E., & Gheorghe, A. V. (2013). Resilience quantification and its application to a residential building subject to hurricane winds. *International Journal of Disaster Risk Science*, 4(3), 105-114.
- Tsionis G, Papailia A, Fardis MN (2011). Analytical fragility functions for reinforced concrete and masonry buildings aggregates of euro-mediterranean regions – UPAT methodology Internal report, Syner-G Project, 2009/2012.
- Twigg, J. (2009). Identifying partnership needs and opportunities. Disaster studies working paper 18, Aon Benfield UCL Hazard Research Centre.
- Tyler, S., & Moench, M. (2012). A framework for urban climate resilience. *Climate and Development*, 4(4), 311-326.
- UN/ISDR (2005). *Hyogo Framework for Action 2005-2015: Building the Resilience of Nations and Communities to Disasters*.
- UN (1997), *Kyoto protocol to the United Nations framework convention on climate change*, Kyoto, Japan.
- UN, *Rio Declaration on Environment and Development*, United Nations Conference on Environment and Development, Rio de Janeiro, Brazil, 1992.
- UNEP 2013. *City-Level Decoupling: Urban resource flows and the governance of infrastructure transitions*. A Report of the Working Group on Cities of the International Resource Panel. In: SWILLINGVM., R. B., MARVIN S., HODSON M. (ed.). Nairobi.
- UNEP FI (2015). *Appel pour le climat / Appeal on climate change | 27/11/2015*, http://www.unepfi.org/psi/wp-content/uploads/2015/11/2015Appeal_on_climate_change.pdf
- UNEP-DTIE 2013. *Cities and Buildings*. Paris: UNEP.
- UNEP FI (2009). *The global state of sustainable insurance – Understanding and integrating environmental, social and governance factors in insurance*.
- UNEP FI (2007). *Insuring for sustainability – Why and how the leaders are doing it*.
- UNISDR (2015). *Making Development Sustainable: The Future of Disaster Risk Management*. Global Assessment Report on Disaster Risk Reduction. Geneva, Switzerland: United Nations Office for Disaster Risk Reduction (UNISDR).
- United Nations - Department of Economic and Social Affairs, 2014, *World Urbanization Prospects: The 2014 Revision*.
- UNITED NATIONS 2015a. *Durban Platform for Enhanced Action (decision 1/CP.17)*. Adoption of a protocol, another legal instrument, or an agreed outcome with legal force under the Convention applicable to all Parties. *ADOPTION OF THE PARIS AGREEMENT*. Paris: UNFCCC.
- UNITED NATIONS 2015b. *General Assembly Resolution 69/283. Sendai Framework for Disaster Risk Reduction 2015–2030*. New York: United Nations.
- UNITED NATIONS 2015c. *Resolution adopted by the General Assembly on 25 September 2015. Transforming our world: the 2030 Agenda for Sustainable Development*. New York: UN.

UNITED NATIONS 2015d. World Humanitarian Summit secretariat, *Restoring Humanity: Synthesis of the Consultation Process for the World Humanitarian Summit* (New York).

United Nations International Strategy for Disaster Reduction (UNISDR). *Global Assessment Report on Disaster Risk Reduction: Risk and Poverty in a Changing Climate*. UNISDR: Geneva. 2009.

United Nations Office for Disaster Risk Reduction (UNISDR 2014) *Disaster Resilience Scorecard for Cities, Based on the —Ten Essentials— defined by the United Nations International Strategy for Disaster Risk Reduction (UNISDR) for Making Cities Resilient*, Developed for The United Nations Office for Disaster Risk Reduction (UNISDR) by IBM and AECOM, Version 1.5, March 10, <http://www.unisdr.org/2014/campaign-cities/Resilience%20Scorecard%20V1.5.pdf>

United Nations, Department of Economic and Social Affairs, Population Division (2015). *World Urbanization Prospects: The 2014 Revision*, (ST/ESA/SER.A/366).

US/IOTWS (2008). *Review of lessons learned, U.S. Indian Ocean Tsunami Warning System Program*.

Vragović, I., Louis, E., & Díaz-Guilera, A. (2005). Efficiency of informational transfer in regular and complex networks. *Physical Review E*, 71(3), 036122.

Vugrin, E. D., Warren, D. E., & Ehlen, M. A. (2011). A resilience assessment framework for infrastructure and economic systems: Quantitative and qualitative resilience analysis of petrochemical supply chains to a hurricane. *Process Safety Progress*, 30(3), 280-290.

Vugrin, E. D., Warren, D. E., Ehlen, M. A., & Camphouse, R. C. (2010). A framework for assessing the resilience of infrastructure and economic systems. In *Sustainable and resilient critical infrastructure systems* (pp. 77-116). Springer Berlin Heidelberg.

Watts DJ and Strogatz SH (1998). Collective dynamics of “small-world” networks, *Nature*, 393 (1998), pp. 440–442.

Watts, D. J., & Strogatz, S. H. (1998). Collective dynamics of ‘small-world’ networks. *nature*, 393(6684), 440-442.

WCED (World Commission on Environment and Development). *Our Common Future*. The Brundtland Report. London: Oxford University Press, 1987.

Werner E, Smith R (1982). *Vulnerable but invincible: A study of resilient children*. McGraw-Hill; New York: 1982.

Werner E.E. (1971). *The children of Kauai: A longitudinal study from the prenatal period to age ten*. University of Hawaii Press, Honolulu, HI.

Wildavsky, A. (1991). *Searching for Safety*. Transaction, New Brunswick.

Woods D, Cook R (2006). Incidents-markers of resilience or brittleness. In: Hollnagel E, Woods DD, Leveson N, editors. *Resilience Engineering: Concepts and Precepts*. Hampshire, UK: Ashgate; 2006. p. 69–79.

Woods DHE (2006). *Resilience-the challenge of the unstable*. Burlington: Ashgate Publishing Company; 1–16.

World Bank, 2006. *Mexico at a glance*. World Bank, Washington, DC.

World Bank, Guy Carpenter & Co. Inc., EQECAT, & IIASA, 2000. *Managing the financial impacts of natural disaster losses in Mexico*. Report prepared for the Government of Mexico. World Bank, Washington, DC.

World Bank, Social indicators of development 1991-1992, Johns Hopkins University Press, Baltimore, 1992.

Yoshikawa H & Goda K (2013). Financial Seismic Risk Analysis of Building Portfolios. *Natural Hazards Review*, 15(2), 112-120.

Yucemen M. S. (2005). Probabilistic Assessment of Earthquake Insurance Rates for Turkey, *Natural Hazards*, 35: 291–313.

Zhou, H., Wang, J. a., Wan, J., and Jia, H. (2010). Resilience to natural hazards: a geographic perspective. *Natural Hazards*, 53(1), 21-41.